



**Susana Isabel Lopes
Gomes**

**Avaliação de efeitos de toxicidade de
nanopartículas no compartimento terrestre**

**Effect assessment of nanoparticles toxicity in the
terrestrial compartment**



**Susana Isabel Lopes
Gomes**

**Avaliação de efeitos de toxicidade de nanopartículas
no compartimento terrestre**

**Effect assessment of nanoparticles toxicity in the
terrestrial compartment**

Dissertação apresentada à Universidade de Aveiro para cumprimento dos requisitos necessários à obtenção do grau de Doutor em Biologia, realizada sob a orientação científica da Doutora Mónica João de Barros Amorim, (Investigadora Auxiliar da Universidade de Aveiro), e coorientação do Doutor Janeck James Scott-Fordsmand (Investigador Sénior da Universidade de Aarhus, Dinamarca) e do Doutor Nicola Pinna (Professor da Universidade de Humboldt-Berlim, Alemanha).

Apoio financeiro da FCT e do FSE no âmbito do III Quadro Comunitário de Apoio, através de uma bolsa de Doutoramento atribuída a Susana Isabel Lopes Gomes (SFRH/BD/63261/2010); do Fundo Europeu do Desenvolvimento Regional (FEDER) através do programa COMPETE e da FCT no âmbito do projeto NANOKA FCOMP-01-0124-FEDER-008944 (Ref. FCT PTDC/BIA-BEC/103716/2008); e do projeto MARINA (EU-FP7 Ref. 263215).

o júri

presidente

Prof. Doutor Casimiro Adrião Pio

professor catedrático do Departamento de Ambiente e Ordenamento da Universidade de Aveiro

Prof. Doutora Lúcia Maria Candeias Guilhermino

professora catedrática do Instituto de Ciências Biomédicas Abel Salazar (ICBAS) da Universidade do Porto

Prof. Doutor Amadeu Mortágua Velho da Maia Soares

professor catedrático do Departamento de Biologia da Universidade de Aveiro

Prof. Doutora Fernanda Maria Fraga Mimoso Gouveia e Cássio

professora associada com agregação do Departamento de Biologia da Universidade do Minho

Prof. Doutor Tito da Silva Trindade

professor associado com agregação do Departamento de Química da Universidade de Aveiro

Prof. Doutora Maria Cláudia Gonçalves da Cunha Pascoal

professora auxiliar do Departamento de Biologia da Universidade de Aveiro

Doutor Carlos Pérez Roca

investigador sénior do Laboratório de Investigação BioCenit do Departamento de Engenharia Química da Universidade Rovira i Virgili

Doutora Mónica João de Barros Amorim (orientadora)

Investigadora auxiliar do Departamento de Biologia e Centro de Estudos do Ambiente e do Mar (CESAM) da Universidade de Aveiro

agradecimentos

Aos meus orientadores, em particular à Doutora Mónica Amorim por todo o acompanhamento, compreensão e força transmitidos e ao Doutor Janeck Scott-Fordsmand pelo acompanhamento e por me ter recebido no laboratório de Biociências em Silkeborg (Dinamarca).

Ao Departamento de Biologia e CESAM que proporcionaram as condições para a realização da maior parte do meu trabalho laboratorial.

A todos os colegas com quem partilhei mais do que o espaço de trabalho, e em especial ao Abel que torna a nossa vida um pouco menos difícil pelo laboratório.

Às minhas mais do que colegas ;) por tudo

Aos meus pais a quem devo quase tudo e à minha irmã. E finalmente ao companheiro de todas as horas, Nuno...

palavras-chave

nanopartículas, avaliação de efeito, solo, mecanismos de resposta, vias metabólicas adversas, ferramentas de elevado varrimento, expressão genética, biomarcadores, stress oxidativo, sobrevivência, reprodução, cobre, prata, dióxido de titânio, dióxido de zircónio, Oligochaeta

resumo

Em 2012 foram produzidas mais de 11 milhões de toneladas de nanomateriais (NMs) e as perspectivas apontam para um aumento na produção. Apesar das previsões e o uso extensivo em produtos de consumo e indústria, o conhecimento é praticamente inexistente no que diz respeito ao potencial impacto destes materiais no ambiente. O principal objetivo desta tese é compreender o impacto de um grupo de NMs selecionados (NMs de base metálica) em invertebrados de solo, com especial incidência nos mecanismos de resposta. Uma vez que a avaliação de risco ambiental feita caso-a-caso para todos os contaminantes emergentes (particularmente NMs) é impossível, devido, entre outros fatores, ao tempo e custos necessário, a compreensão dos mecanismos de ação é muito importante para alcançar paradigmas comuns. A compreensão dos modos de ação fornece os caracteres com valor preditivo para a extrapolação entre partículas. Além disso, também fornece informação para a produção de novos materiais sustentáveis.

Em suma, os efeitos dos NMs selecionados (Cobre e Prata, Óxido de Titânio e Zircónio) e do respetivo sal, foram investigados ao nível dos genes (utilizando a ferramentas de alto varrimento, tecnologia de “microarrays” e PCR em tempo real), bioquímico (utilizando ensaios enzimáticos para a análise de marcadores de stress oxidativo) e do organismo (sobrevivência e reprodução, tal como nos protocolos OCDE), utilizando espécies modelo ecotoxicológicas (*Enchytraeus albidus*, *Enchytraeus crypticus*, *Eisenia fetida*).

A análise da expressão de genes forneceu informação importante sobre os mecanismos afetados por cada um dos NMs testados. Os perfis de expressão genéticos evidenciaram uma assinatura do (nano)material e o efeito do tempo de exposição. A análise funcional integrada com os dados bioquímicos e de organismo revelou um bom poder de entendimento. As respostas dos parâmetros bioquímicos (relacionados com stress oxidativo) foram distintas entre os materiais testados e também influenciados pelo tempo de exposição e concentrações testadas. As respostas padronizadas ao nível do organismo foram as que mostraram menor diferenciação entre os vários materiais testados.

De um modo geral, e neste contexto de avaliação de efeitos de NMs, a expressão de genes e ensaios enzimáticos, apresentaram um papel muito importante no preenchimento de lacunas que não poderia ter sido alcançado através dos efeitos no organismo isoladamente.

Um assunto recorrente relativo a alguns NMs de base metálica tem a ver com a possível dissolução e subsequente libertação de iões que *a posteriori* causam toxicidade, p.e. Cu-NPs ou Ag-NPs libertam Cu^{2+} ou Ag^+ . O estado de oxidação das partículas foi investigado, apesar deste não ser o foco da tese. O estudo do destino, p.e. dissolução de NPs, está ainda apenas no seu início e as técnicas apropriadas estão presentemente a ser desenvolvidas. Os resultados mostraram um efeito específico das nanopartículas. A exposição UV com o dióxido de titânio aumentou o seu efeito.

keywords

nanomaterials, nanoparticles, effect assessment, soil, mechanisms of response, adverse outcome pathways, high-throughput tools, gene expression, biomarkers, oxidative stress, survival, reproduction, copper, silver, titanium dioxide, zirconium dioxide, Oligochaeta

abstract

Over 11 million tons of nanomaterials (NMs) have been produced in 2012 and predictions point the increase in production. Despite predictions and extended usage via consumer products and industry, the understanding of the potential impact of these materials on the environment is virtually absent. The main aim of this thesis is to understand how a selected group of nanomaterials (metal based particles) may impact soil invertebrates, with special focus on the mechanisms of response. Since a case-by-case Environmental Risk Assessment (ERA) of all the emerging contaminants (particularly NMs) is impossible, among others due to time and cost reasons, to gain understanding on the mechanism of action and response is very important to reach a common paradigm. Understanding the modes of action provides predictive characters in cross particle extrapolation. Besides, it also provides insight for the production of new and sustainable materials.

Overall, the effects of the selected NMs (Copper and Silver, Titanium and Zirconium oxides) and the respective salt forms, were investigated at the gene expression (using high-throughput tools, microarray and qPCR technology), biochemical (using enzymatic assays for analysis of oxidative stress markers) and organism (survival and reproduction as in OECD test guidelines) levels, this using standard soil species (*Enchytraeus albidus*, *Enchytraeus crypticus*, *Eisenia fetida*).

Gene expression analysis provided valuable information on the mechanisms affected by each of the NMs. The gene expression profile highlighted a (nano)material signature and the effect of the duration of exposure. The functional analyses integrated with the biochemical and organism data, revealed a good understanding power. The biochemical parameters (oxidative stress related) were distinct across the materials and also influenced by duration of exposure and concentration. The standardized organismal responses differed the least between the various materials.

The overall outcome is that, in this context of NMs effect assessment, gene expression and enzymatic assays introduced a very important knowledge gap, which could not had been achieved by the standard organismal effects alone. A reoccurring issue with some metal based NMs is the possible dissolution and subsequent release of ions that then causes toxicity e.g. Cu-NPs or Ag-NPs release Cu^{2+} or Ag^+ . The oxidation state of the particles was investigated, although this was not the focus of the thesis. The study of fate, e.g. dissolution of NPs, is also only in its beginning and the appropriate techniques are currently being developed. The results showed a specific nanoparticle effect. The UV exposure with titanium dioxide nanoparticles increased its effect.

Index

I –Introduction.....	3
1. Nanotechnology and Nanomaterials.....	4
2. Test (nano)materials	5
3. Characterization.....	7
4. Environmental Hazard of NMs/NPs.....	9
5. Biological endpoints	12
6. Test organisms.....	18
7. Aim and outline of the thesis.....	19
References	21
II - Effect of Cu-nanoparticles versus one Cu-salt: Analysis of stress biomarkers response in <i>Enchytraeus albidus</i> (Oligochaeta).....	31
Abstract.....	31
1. Introduction	32
2. Materials and methods.....	35
3. Results	39
4. Discussion.....	45
5. Conclusions	48
References	49
III - Effect of Cu-nanoparticles versus Cu-salt in <i>Enchytraeus albidus</i> (Oligochaeta): Differential gene expression through microarray analysis	59
Abstract.....	59
1. Introduction	60
2. Materials and methods.....	62
3. Results	69
4. Discussion.....	76
5. Conclusions	82
References	83
Supplementary material.....	89

IV - Cu-Nanoparticles Ecotoxicity – Explored and explained	99
Abstract.....	99
1. Introduction	100
2. Materials and Methods	102
3. Results	107
4. Discussion.....	111
References	117
Supplementary material.....	120
V - Exposure to different copper forms – nanoparticles, nanowires, salt and field aged: gene expression profiling in <i>Enchytraeus crypticus</i>	125
Abstract.....	125
1. Introduction	126
2. Materials and Methods	128
3. Results	133
4. Discussion.....	142
5. Conclusions	148
References	149
Supplementary material.....	155
VI - Mechanisms of response to silver nanoparticles on <i>Enchytraeus albidus</i> (Oligochaeta): survival, reproduction and gene expression profile.....	167
Abstract.....	167
1. Introduction	168
2. Materials and methods.....	171
3. Results	176
4. Discussion.....	183
5. Conclusions	190
References	191
Supplementary material.....	197

VII - Effects of silver nanoparticles to soil invertebrates: oxidative stress biomarkers in <i>Eisenia fetida</i>	207
Abstract.....	207
1. Introduction	208
2. Materials and methods.....	209
3. Results	214
4. Discussion.....	218
5. Conclusions	221
References	222
VIII - Exposure to different silver nanoparticles forms and silver salt: gene expression profile in <i>Enchytraeus crypticus</i>	229
Abstract.....	229
1. Introduction	230
2. Materials and Methods	231
3. Results	236
4. Discussion.....	242
5. Conclusions	246
References	246
Supplementary material.....	251
IX - Effect of 10 different TiO₂ and ZrO₂ (nano)particles on the soil invertebrate <i>Enchytraeus crypticus</i>	265
Abstract.....	265
1. Introduction	266
2. Materials and methods.....	268
3. Results	273
4. Discussion.....	280
5. Conclusions	284
References	284
Supplementary material	
X – General discussion	293

Chapter I

General Introduction

I –Introduction

The present thesis focuses on the identification of the biological responses to nanomaterials (NMs), in order to provide a foundation for understanding the risks in the terrestrial environment.

Although there are well-established environmental risk assessment procedures for chemicals in Europe (as within REACH - Registration, Evaluation, Authorisation and Restriction of Chemicals), it is currently discussed whether the underlying exposure and effect-methods are sufficient, and whether the current risk paradigm covers NMs. Since, NMs are one of the most rapidly introduced materials in the market, it is of outmost importance to investigate the suitability of current test methods. Moreover, to identify mechanisms of response that are NMs-specific is very important, as this will aid rapid predictions of effects. In the present thesis I focus on identifying the mechanisms of response which precede the assessed phenotypical effects.

This introductory chapter is intended to briefly explain the main items within the thesis context, in the following order:

1. Nanotechnology and Nanomaterials
2. Test (nano)materials
3. Characterization
4. Environmental Hazard of NMs/NPs
5. Biological endpoints
6. Test organisms

Finally, the aim and outline of the thesis will be summarized.

1. Nanotechnology and Nanomaterials

The definition of nanomaterial(s) (NMs), as recommended by The European Commission (EU, 2011), is as follows:

“Nanomaterial means a natural, incidental or manufactured material containing particles, in an unbound state or as an aggregate or as an agglomerate and where, for 50 % or more of the particles in the number size distribution, one or more external dimensions is in the size range 1 nm-100 nm. In specific cases and where warranted by concerns for the environment, health, safety or competitiveness the number size distribution threshold of 50 % may be replaced by a threshold between 1 and 50 %.”

Further, particle, aggregate and agglomerate are also defined (see also Figure 1):

“‘particle’ means a minute piece of matter with defined physical boundaries; ‘agglomerate’ means a collection of weakly bound particles or aggregates where the resulting external surface area is similar to the sum of the surface areas of the individual components; ‘aggregate’ means a particle comprising of strongly bound or fused particles.”

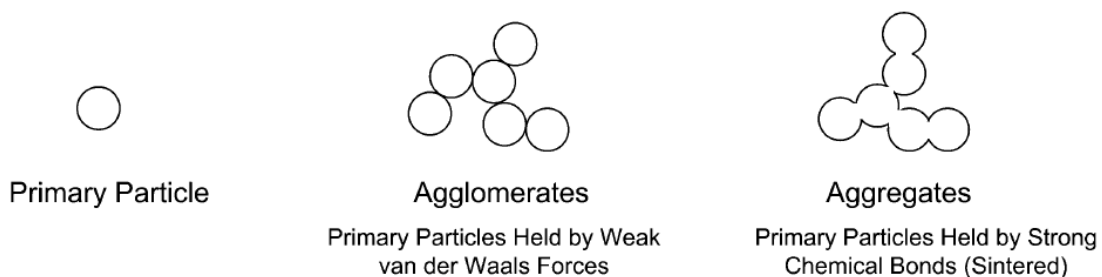


Figure 1: Schematic representation of nanoparticle (primary particle), agglomerates and aggregates (adapted from Jiang et al., 2009).

Although not specified within the European Commission definition, it is generally well accepted that a nanoparticle (NP) is a NM with the three dimensions at the nanoscale; when two dimensions are at the nanoscale we have structures like nanotubes or nanorods, and NMs with one dimension at the nanoscale results in nanolayers, such as coatings (The Royal Society, 2004).

Nanotechnology is the ability to engineer (develop and produce) materials at the nanoscale (ICCA, 2010; Bleeker et al., 2013), the so called engineered nanomaterials (ENM). It has been estimated that by 2011 there were more than 1300 nanotechnology-based consumer products, with a continuous rapid increase (<http://www.nanotechproject.org/>). Lövestam et al. (2010) identified a wide list of product areas containing NMs, e.g. with almost one third of the products belonging to sun lotions and cosmetics category. Hence, NMs are used in everyday life and exposure in environment is expected, however the potential impact of these materials on the environment is still poorly understood.

2. Test (nano)materials

In the present thesis, four NMs have been tested: copper (Cu), silver (Ag), titanium dioxide (TiO₂) and zirconium dioxide (ZrO₂). The selection of these materials was based on their relevance and as study models as explained bellow.

Cu-NMs can be synthesized in different morphologies (e.g. spherical NPs (Wu and Chen, 2004), wires (Chang et al., 2005)). Cu-NMs applications are related with electronics and catalysis (Lee et al., 2008; Wang et al., 2004). The replacement of copper-salt based wood preservatives by nano-copper based products (Evans et al.,

2008) represents a high production (about 39500 tons/year) of Cu-NMs and consequently increased risk to human health and the environment.

Silver is one of the most used NMs, the median production of Ag-NMs worldwide is around 55tons/year, ranging from 5 to 1000 tons/year according to industry manufacturers and downstream users (Piccinno et al., 2012). Their applications range from disinfecting agents (e.g. for cloths and medical devices), water treatment, bio-sensing and imaging. Ag-NMs can be synthesized in different sizes and morphologies, for instance spherical NPs (e.g. Panáček et al., 2006), nanowires (Sun and Xia, 2002), nanoplates (Washio et al., 2006) and the diversified range of applications in industry greatly increase the variety of Ag-NMs produced (Fauss, 2008). The most explored properties of nano-Ag are conductivity and anti-microbial activity (Piccinno et al., 2012).

Nano-TiO₂ is among the most used NMs worldwide, with a global production reported by the manufactures and downstream users ranging from 550 to 5500 tons/year (Piccinno et al., 2012). The largest proportion of produced TiO₂-NMs are used in cosmetic industry (including sunscreens) and then less than 20% is used in coatings, cleaning agents and paints (Fries and Simkó, 2012; Piccinno et al., 2012). TiO₂ occurs in three crystal forms (anatase, rutile and brookite). Both anatase and rutile absorbs UV radiation (i.e., are photoactive (Carp et al., 2004)), a characteristic for which is used in sunscreens and paints. What the nano metrics brings of new in terms of TiO₂ applications is the transparency (as opposed to white opacity of bulk TiO₂) (Smijs and Pavel, 2011) which increases its potential in cosmetic industry. Brookite has currently no commercial significance (Fries and Simkó, 2012).

Zirconium dioxide (ZrO_2) nanoparticles applications are mostly related with optical and electronic applications (Channu et al., 2011). More recently, it has been shown that the adding of ZrO_2 -NPs to concrete past improves its structure (Negahdary et al., 2013), which opens a new window of large scale application of ZrO_2 -NPs.

3. Characterization

Characterization of materials as pristine and as in exposure is an important issue for hazard (and risk) assessment, also when testing NMs. However, although there is a consensus regarding the need of proper characterization method both for pristine and for NMs in media there is lack of quantitative methods (Aschberger et al., 2011; Hasselov et al., 2008). Besides this, for the methods that are available at present (see a selection represented in Table 1 for a summary), the lack of standardized protocols has generated difficulties for interpretation of the results (Hasselov et al., 2008; Jiang et al., 2009; Warheit, 2008).

Table 1: List of physical properties/metrics and chemical composition/analytes of nanomaterials and respective associated instruments and methods (adapted from Hasselov et al., 2008).

Physical properties/metrics	<i>Instruments and methods</i>
Diameter	Electron microscopy (EM), Atomic Force Microscopy (AFM), Flow-Field-Flow Fractionation (FFF), Dynamic Light Scattering (DLS)
Volume	Sedimentation (Sed)-FFF
Area	EM, AFM
Mass	Liquid Chromatography-Electrospray Mass Spectrometry (LC-ESMS)
Surface charge	z-Potential, electrophoretic mobility
Crystal structure, Aspect ratio or other shape factor	X-Ray Diffraction (XRD), TEM-XRD (Selected area electron diffraction (SAED))

Chemical composition/analytes	
Elemental composition	Bulk: Inductively Coupled Plasma-Mass Spectrometry (ICP-MS), Inductively Coupled Plasma-Optical Emission Spectrometry (ICP-OES)
	single nanoparticle: TEM-Energy Dispersive X-Ray (EDX),
	particle population: FFF-ICP-MS
Fluorophores	Fluorescence spectroscopy
Fullerene (“molecules”)	Ultraviolet–Visible Spectroscopy (UV-vis), Infrared Spectroscopy (IR), Nuclear Magnetic Resonance Spectroscopy (NMR), Mass Spectrometry (MS), High Performance Liquid Chromatography(HPLC)
Total organic carbon	High temp chemical oxidation
Other properties not falling within the above classes	
Aggregation state	DLS, AFM, ESEM, etc.
Hydrophobicity	Liquid–liquid extraction chromatography
Dissolution rate	Dialysis or voltammetry or spectrometry
Surface chemistry, coating composition, # of proton exchanging surface sites	Optical or X-ray spectroscopic methods, acid–base titrations

But efforts and progresses in terms of analytical methods are also at a continuous rate and scientists discuss new ways: e.g., a new method consists in a development for ICP-MS that allows analysing one single particle at a time. Not only new methods are under development, and such tables are merely indicative, but also a number of specific requirements will vary with test media, e.g. measurements for materials in soils are virtually absent. Methods have been developed mainly for pristine material and not for materials in complex matrixes (Farre et al., 2011). The most important message has been that a combination of methods needs to be employed for the best possible characterization of materials. The discussions in terms of establishing a list of the minimum information for physicochemical characterisation for NMs is a requirement for regulatory compliance (Pettitt and Lead, 2013).

Such regulatory and by-law limitations should not be mistaken with the level that scientists aim for.

The current definition of NM by The European Commission (EU, 2011) is based on size, however it is generally agreed that size is not the only characteristic that is important since it is not determining the NMs behaviour/toxicity alone see e.g. the review by Luyts and co-authors (2013). Additional properties that should be studied include surface area, surface charge, shape, crystal structure, coating/corona, aggregation/agglomeration and solubility/dissolution. In the present thesis some characterization has been performed, however this was not done in full, partly because it was not the focus on the thesis partly because the methods were not present at the time.

4. Environmental Hazard of NMs/NPs

Over the last decade there has been a considerable increase in the number of reported NMs effects in environmental species. Data available for several aquatic organisms and bacteria, indicate that several NPs can be classified as from “very toxic” to “harmful”, e.g. single- and multi-walled carbon nanotubes, C60, TiO₂, Ag, ZnO and CuO. Compared to the aquatic species much less is known for soil dwelling organisms (e.g. Klaine et al., 2008; Tourinho et al., 2012).

The majority of the available data consists of a collection of “traditional” population endpoints (e.g. survival, reproduction, growth), probably because standardized or well-established protocols are available. Although such data are very important for hazard assessment, it has also been recognized that there is a requirement to adapt the guidelines so they cover NM specific issues. At this stage the importance of alternative tools, such as those that cover mechanisms of response comes strengthened since they are of more predictive nature.

It has been long known that changes at molecular level (e.g. genes) which precedes manifestations of toxicity on cell or organisms (De Coen et al., 2000) can be used to understand and predict effects. The specificity, sensitivity, and rapidity of gene response compared to responses at organism level, make these responses a very appealing foundation for development of tools in the field of ecotoxicology (van Straalen and Roelofs, 2008). The importance of “omics” (genomics, proteomics, metabolomics) tools to identify mechanisms/pathways of toxic responses is well recognized (e.g. Singh et al., 2010) and promises are that its inclusion would benefit regulatory decision-making (Kahru and Dubourguier, 2010) although the ways are still in its infancy.

One of the problems lays in the translation of the information from known molecular events (e.g. the up/down regulation of genes or the excess production of a certain enzyme) onto a quantifiable value that could be weighed on hazard and then risk assessment. It is worth mentioning an approach that is based on linking starting events to adverse outcomes – Adverse Outcome Pathways (AOPs) – in which data collected at different levels of biological organization can be integrated (see e.g. Ankley et al., 2010; Villeneuve and Garcia-Reyero, 2011).

Conceptual adverse outcome pathway (AOP)

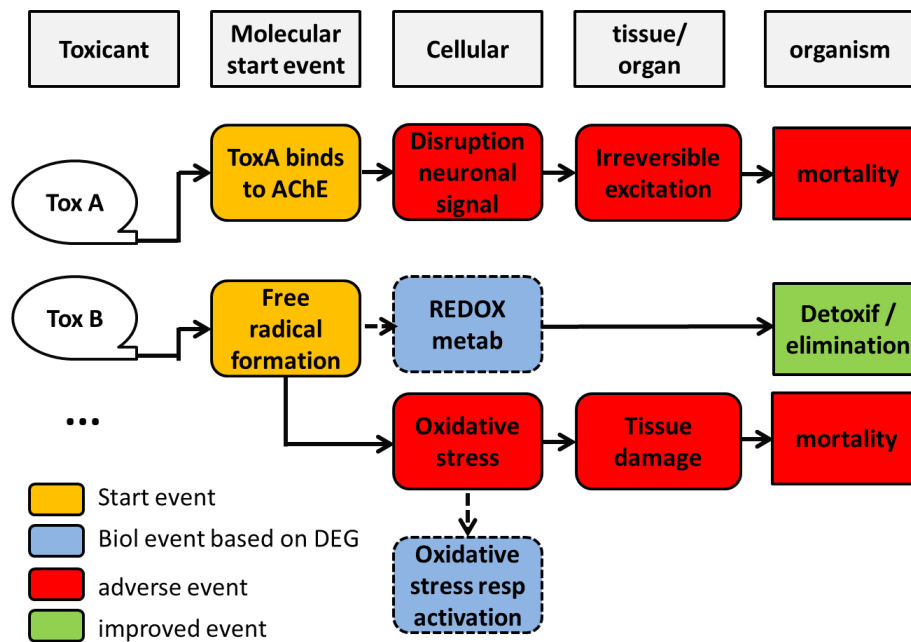


Figure 2: Conceptual Adverse Outcome Pathway (AOP) (adapted from Warner et al.(2012)).

Conceptualization of hypothetical responses to toxicants (Tox) exposure in a model organism based on transcript-expression data. Multiple adverse outcomes are integrated in this conceptualization where the various end-states are influenced by the relative tolerance and/or effectiveness of tox-detoxification strategies of each species. A key for module colors: green = improved state, orange = molecular initiating event, red = adverse event, blue = biological processes indicated to be in operation based on transcript expression. Square boxes represent final states for the organism, whereas rounded boxes represent intermediate states. Solid lines indicate relationships previously observed, whereas dashed lines represent relationships hypothesized in this study.

This approach may require further case studies and evidences to become fully in use; nevertheless, it reflects a way forward in terms of the inclusion of mechanistic information on risk assessment.

5. Biological endpoints

When we consider a final biological event like growth, this is preceded by series of cellular events which start at genomic level. Traditional ecotoxicological endpoints such as survival, reproduction or growth focus on the final events, which are of surmount importance to screen the toxicity of polluted sites, however, they provide little insight into how the organism deals with the stress. By investigating the responses at lower levels of biological organization, i.e. cellular and gene level we can obtain information about the mechanisms underlying toxicity and ultimately, by integrating the responses at different levels of biological organization (Fig. 3), to use molecular tools in a predictive context.

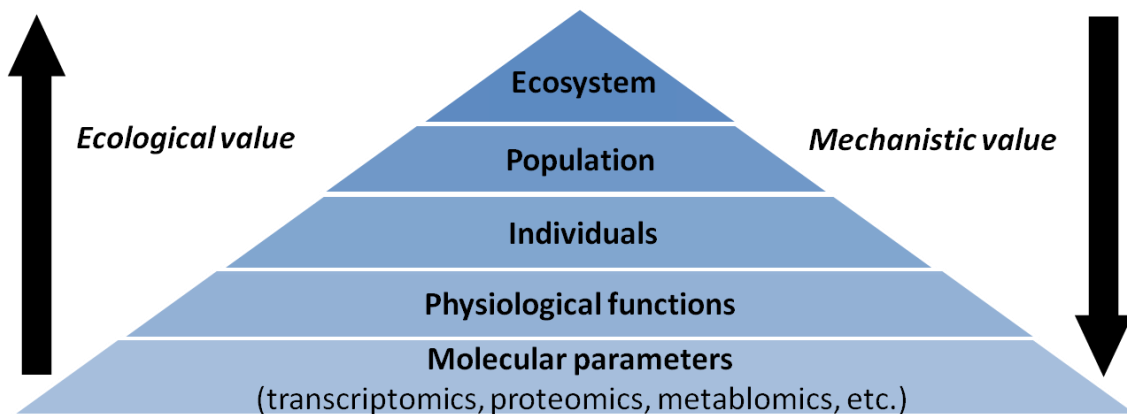


Figure 3: From molecules to population: conceptual framework for ecotoxicogenomics (Snape et al., 2004).

The two main endpoint levels will be further detailed ahead:

5.1. End points at individual/population level: survival and reproduction

For soil Oligochaetes, standardized ecotoxicity guidelines have been developed such as the ISO (International Organization for Standardization) and OECD (Organization for

Economic Cooperation and Development) to assess survival and/or reproduction (ISO, 1993, 1998, 2005; OECD, 1984; OECD, 2004a, b). These tests range from acute (assessment of survival, in short periods of exposure to highly toxic concentrations) to chronic (e.g. assessment of reproduction, bioaccumulation, etc., via longer exposure periods to sub-lethal concentrations).

5.2. Endpoints at cellular and sub-cellular (molecular) level

i. Biochemical responses: oxidative stress parameters

Oxidative stress refers to a disturbance in the pro oxidant-antioxidant balance in favour of the pro-oxidants, leading to the formation of ROS (reactive oxygen species) and potential damage (Sies, 1991). ROS are partially reduced forms of molecular oxygen (O_2) (Fig. 4) which are normal products of cellular metabolism and can also be produced by cells as a protective mechanism (Apel and Hirt, 2004) or in response to stress (e.g. xenobiotics (Turrens, 2003)). Normal cells can remove ROS by antioxidant defences, however larger increases in ROS production can unbalance the equilibrium between pro-oxidants and antioxidant defences leading to oxidative stress.

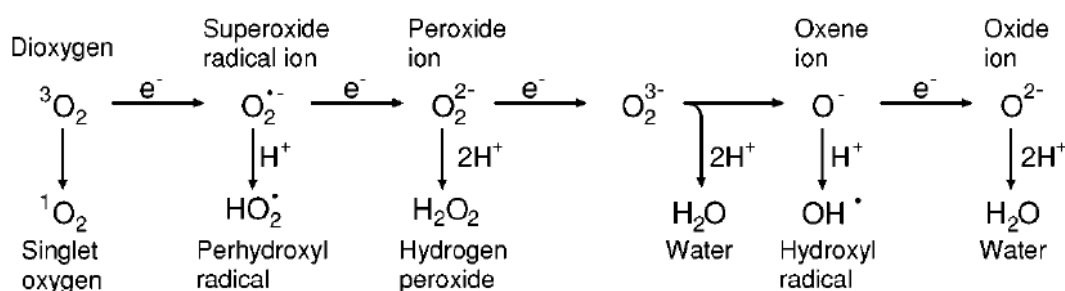


Figure 4: Generation of different ROS (reactive oxygen species) by energy transfer or sequential univalent reduction of ground state triplet oxygen. Adapted from Apel and Hirt (2004).

The study of antioxidant defence mechanisms and oxidative damage become a topic of significant interest for environmental toxicology studies as it represents a tool to assess toxic effects in response to stressors. The antioxidant defence mechanisms comprise enzymatic and non-enzymatic antioxidants. Enzymatic antioxidants include SOD (superoxide dismutase), CAT (catalase), GPx (glutathione peroxidase) and GSTs (glutathione-S-transferases). SOD acts as a first line defence mechanism, by converting O_2^- into H_2O_2 which is then detoxified onto H_2O by CAT and GPx. Detoxifying of H_2O_2 to H_2O by GPx involves the use of GSH (reduced glutathione) as reducing agent which is oxidized to GSSG; the GPx cycle is closed by the re-conversion of GSSG into GSH by GR (glutathione reductase) (Apel and Hirt, 2004). GSTs are a complex family of enzymes which catalyse the conjugation of GSH with several xenobiotics (including lipid peroxidation products) (Hermes-Lima, 2005). Glutathione is a non-enzymatic antioxidant which participates in defence mechanisms against ROS and xenobiotics in several ways: 1) by linking directly to prooxidants (like transition metals or sulphidryl groups), 2) by being the substrate for GPx, 3) by conjugating electrophilic xenobiotics during GST activities and 4) by participating in other antioxidants regeneration (i.e. ascorbate and tocopherol) (Saint-Denis et al., 1998). In Figure 5 the inter-relation between the antioxidant defence mechanisms was attempted. Related to the oxidative stress is the induction of Metallothioneins (MTs). MTs are metal binding proteins which protect cells from metal toxicity by acting as chelating agent of the excess of toxic metals, and also provide protection against oxidative stress as effective scavenger of hydroxyl radicals (Andrews, 2000).

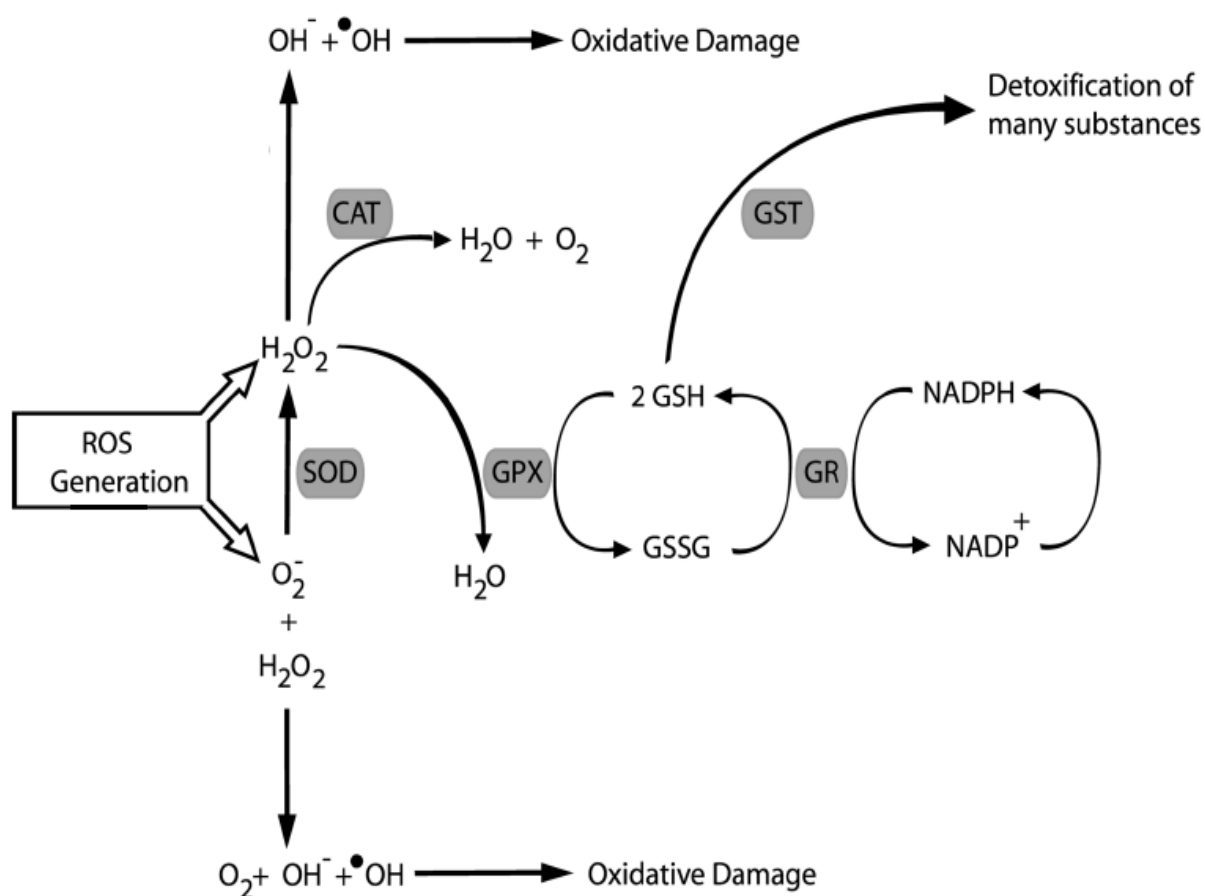


Figure 5: Schematic representation of the antioxidant defence mechanisms of the cells (adapted from Hermes-Lima, 2005). ROS (reactive oxygen species), SOD (superoxide dismutase), CAT (catalase), GPx (glutathione peroxidase), GST (glutathione-S-transferase), GR (glutathione reductase), GSH (reduced glutathione) and GSSG (oxidized glutathione).

ii. Gene expression - transcriptomics

Ubiquitous in their nature, gene responses provides a valuable tool to understand mechanisms of response in organisms exposed to toxins. In 2004, Snape et al. introduced the term ecotoxicogenomics as the integration of genomics (genomics, transcriptomics and metabolomics) into ecotoxicology (Snape et al., 2004). Transcriptomics refers to the expressed genes (portion of the genome which is transcribed onto RNA) in response to a certain stimulus. The application of

transcriptomics in ecotoxicology aims to provide mechanistic information about toxicants modes of action and optimally, to identify toxicants' genomic signatures. This information has the potential to improve the risk assessment of toxicants, however the narrow genomic information for many of the ecotoxicological model organisms limits its range (Robbens et al., 2007).

Among the tools to evaluate transcriptomic responses, microarrays and quantitative real-time polymerase chain reaction (qPCR) are the most used. Microarrays hold great potential in (eco)toxicology since it allows the (semi)quantification of the expression of thousands of genes in a single run (Rockett and Dix, 1999). With this technology it is possible to compare transcriptomic profiles (compare several treatments versus control) and identify if the differently expressed genes are up- or down-regulated. Thus it provides a powerful tool to study the multiple pathways/mechanisms being affected by a stressor and investigate/identify possible markers of exposure. Figure 6 provides an overview of the stepwise methodology involved in microarray analysis, for a two-color hybridization design. For a single-color experiment, only one biological sample (e.g. mRNA 1) is hybridized on each array.

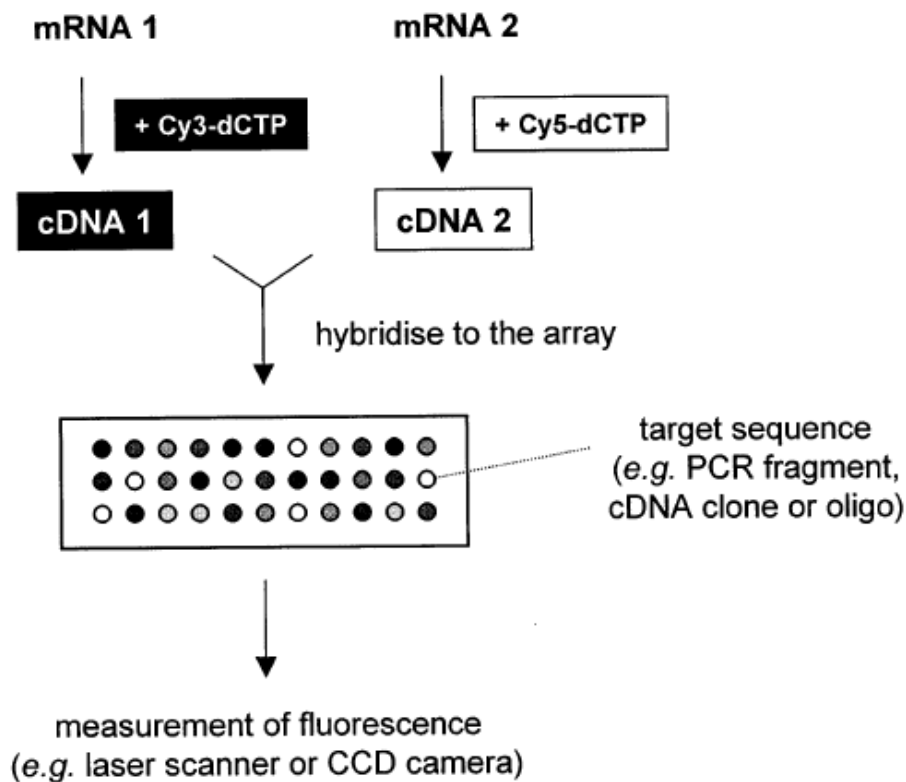


Figure 6: The principle of gene expression analysis by DNA microarray technology: mRNA samples are reverse transcribed to cDNA while fluorescently labelled nucleotides are incorporated (van Hal et al., 2000) to signal hybridization level on the microarray.

Quantitative real-time PCR can be used to quantify gene expression. This technique is often used associated with validation of microarray results or to investigate the expression of specific genes/biomarkers of exposure (genes expected to respond, by up- or down-regulation to a certain stressor). qPCR combines amplification (through polymerase chain reaction - PCR) and detection (based on fluorescent chemistries) in one step. The principle of quantification is simple: the more copies of DNA target there are at the beginning of the assay, the fewer cycles of amplification are required to generate the amount of PCR product that can be detected (Bustin et al., 2005). Thus, fewer amplification cycles are required for the fluorescence to reach the threshold level of detection (C_T) (Fig. 7).

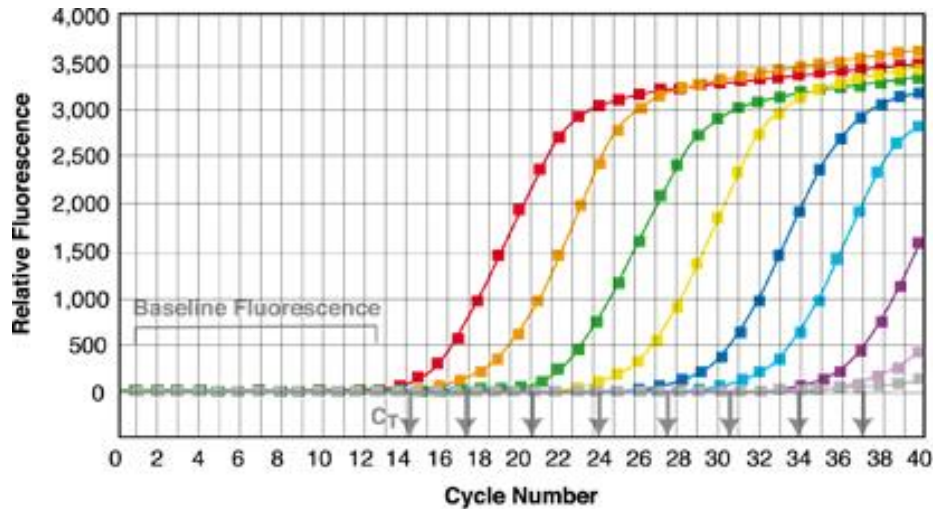


Figure 7: Schematic representation of qPCR amplification plot (adapted from: <http://www.thermoscientific.de/com/cda/article/general/1,,20636,00.html>)

6. Test organisms

The biological responses are of course species specific and the range of differences can be very different. In the present work, three different species of soil dwelling oligochaetes were used: the earthworm *Eisenia fetida* (Savigny, 1826) and the enchytraeid species *Enchytraeus albidus* (Henle, 1837) and *Enchytraeus crypticus* (Westheide and Graefe, 1992).

Earthworms (Annelida: Oligochaeta) are abundant in many soils where they greatly contribute for its quality via 2 main traits: their burrowing activity is very important in terms of soil structure and aeration, and their feeding activity plays a major role in organic matter decomposition and nutrients cycling (Lavelle, 1988). *Eisenia fetida* (and *Eisenia andrei*) are representative of soil fauna and have been used as models in ecotoxicological studies since more than three decades (OECD, 1984; OECD, 2004b).

Enchytraeids (Annelida: Oligochaeta) belong to the saprophagous mesofauna of the litter layer and the upper mineral soil (Römbke et al., 2009), they are found in several soils worldwide, where they contribute to the degradation of organic matter and

improve the pore structure of the soil (Amorim et al., 2005). The two enchytraeids species have been used as model species in terrestrial ecotoxicology studies (Castro-Ferreira et al., 2012; Rombke, 2003) and are included in the standardized protocol (OECD, 2004a). Additionally, since 2011 for *E. albidus* and 2013 for *E. crypticus* both species have transcriptomic information available (Amorim et al., 2011; Castro-Ferreira et al., 2013), allowing the performance of genomic studies.

7. Aim and outline of the thesis

The effects of metallic (Cu and Ag) and metal-oxide (TiO₂ and ZrO₂) nanoparticles were assessed at various endpoints: survival, reproduction, oxidative stress biomarkers and gene expression. With this multiple-endpoint approach we aimed to assess the toxicity of the selected NPs and to understand the mechanisms underlying the toxic responses.

The results obtained are organised in eight chapters (Chapter II to Chapter IX) in the format of journal publications, followed by an integrated overview of the main results (Chapter X), as follows:

In **Chapter II**: “Effect of Cu-nanoparticles versus one Cu-salt: analysis of stress and neuromuscular biomarkers response in *Enchytraeus albidus* (Oligochaeta)” several oxidative stress biomarkers and cholinesterases (neuromuscular parameter) were used to assess and compare the effects of copper nanoparticles with copper chloride in *E. albidus*.

In **Chapter III**: “Effect of Cu-nanoparticles versus Cu-salt in *Enchytraeus albidus* (Oligochaeta): Differential gene expression through microarray analysis” the gene

expression profile of *E. albidus*, in response to copper nanoparticles and copper chloride, was investigated and compared.

In **Chapter IV**: “Cu-Nanoparticles Ecotoxicity – Explored and explained”, the effects of several forms of copper were assessed in *Enchytraeus crypticus*: copper nanoparticles, copper nitrate (freshly added to the soil) and copper sulfate (from 80 years old soil contamination) at survival and reproduction levels.

In **Chapter V**: “Exposure to different copper shapes and forms: gene expression profile in *Enchytraeus crypticus*” the effects of several forms of copper: two types of nanomaterials (spherical NPs and nanowires), copper nitrate (freshly added to the soil) and copper sulfate (from 80 years old soil contamination) on the gene expression profile of *E. crypticus*, were investigated and compared.

In **Chapter VI**: “Mechanisms of response to silver nanoparticles on *Enchytraeus albidus* (Oligochaeta): Survival, reproduction and gene expression profile”, the effects of silver nanoparticles was assessed on survival and reproduction of the enchytraeids and compared with the effects caused by silver nitrate. The gene expression profile in response to the two forms of silver was investigated to compare and understand the mechanisms underlying toxicity.

In **Chapter VII**: “Effects of silver nanoparticles to soil invertebrates: oxidative stress biomarkers in *Eisenia fetida*” the effects of silver nanoparticles (in comparison with silver nitrate) on oxidative stress biomarkers of the earthworm *E. fetida* were investigated. The factor time of exposure on biomarkers response was also assessed.

In **Chapter VIII**: “Exposure to different silver nanoparticles forms and silver salt: gene expression profile in *Enchytraeus crypticus*” microarray technology was used to evaluate the gene expression profile of *E. crypticus* triggered by exposure to three types of silver nanoparticles and silver nitrate.

In **Chapter IX**: “Effect of 10 different TiO₂ and ZrO₂ (nano)particles on the soil invertebrate *Enchytraeus crypticus*” the effects of a set of TiO₂-NPs (in comparison with bulk TiO₂) and ZrO₂ materials on *E. crypticus* survival and reproduction were assessed. Effects were assessed in 3 increasing complexity media. The effects of UV (ultra violet) radiation on TiO₂ toxicity were also investigated.

In **Chapter X**: “General discussion” the results of the preceding chapters are discussed within an integrated perspective.

References

- Amorim, M.J.B., Novais, S.C., Van der Ven, K., Vandenbrouck, T., Soares, A.M.V.M., De Coen, W., 2011. Development of a microarray in *Enchytraeus albidus* (Oligochaeta): preliminary tool with diverse applications. *Environmental Toxicology and Chemistry* 30, 1395-1402.
- Amorim, M.J.B., Rombke, J., Soares, A.M.V.M., 2005. Avoidance behaviour of *Enchytraeus albidus*: Effects of Benomyl, Carbendazim, phenmedipham and different soil types. *Chemosphere* 59, 501-510.
- Andrews, G.K., 2000. Regulation of metallothionein gene expression by oxidative stress and metal ions. *Biochemical Pharmacology* 59, 95-104.

- Ankley, G.T., Bennett, R.S., Erickson, R.J., Hoff, D.J., Hornung, M.W., Johnson, R.D., Mount, D.R., Nichols, J.W., Russom, C.L., Schmieder, P.K., Serrano, J.A., Tietge, J.E., Villeneuve, D.L., 2010. Adverse outcome pathways: A conceptual framework to support ecotoxicology research and risk assessment. *Environmental Toxicology and Chemistry* 29, 730-741.
- Apel, K., Hirt, H., 2004. Reactive oxygen species: Metabolism, oxidative stress, and signal transduction. *Annual Review of Plant Biology* 55, 373-399.
- Aschberger, K., Micheletti, C., Sokull-Kluttgen, B., Christensen, F.M., 2011. Analysis of currently available data for characterising the risk of engineered nanomaterials to the environment and human health - Lessons learned from four case studies. *Environment International* 37, 1143-1156.
- Bleeker, E.A.J., de Jong, W.H., Geertsma, R.E., Groenewold, M., Heugens, E.H.W., Koers-Jacquemijns, M., van de Meent, D., Popma, J.R., Rietveld, A.G., Wijnhoven, S.W.P., Cassee, F.R., Oomen, A.G., 2013. Considerations on the EU definition of a nanomaterial: Science to support policy making. *Regulatory Toxicology and Pharmacology* 65, 119-125.
- Bustin, S.A., Benes, V., Nolan, T., Pfaffl, M.W., 2005. Quantitative real-time RT-PCR - a perspective. *Journal of Molecular Endocrinology* 34, 597-601.
- Carp, O., Huisman, C.L., Reller, A., 2004. Photoinduced reactivity of titanium dioxide. *Progress in Solid State Chemistry* 32, 33-177.
- Castro-Ferreira, M.P., de Boer, T.E., Colbourne, J.K., Vooijs, R., van Gestel, C.A.M., van Straalen, N.M., Soares, A.M.V.M., Amorim, M.J.B., Roelofs, D., 2013. Transcriptome assembly and microarray construction for *Enchytraeus crypticus*, a model oligochaete to assess stress response mechanisms and soil quality. *Submitted*.
- Castro-Ferreira, M.P., Roelofs, D., van Gestel, C.A.M., Verweij, R.A., Soares, A.M.V.M., Amorim, M.J.B., 2012. *Enchytraeus crypticus* as model species in soil ecotoxicology. *Chemosphere* 87, 1222–1227.

- Chang, Y., Lye, M.L., Zeng, H.C., 2005. Large-Scale Synthesis of High-Quality Ultralong Copper Nanowires. *Langmuir* 21, 3746-3748.
- Channu, V.S.R., Kalluru, R.R., Schlesinger, M., Mehring, M., Holze, R., 2011. Synthesis and characterization of ZrO₂ nanoparticles for optical and electrochemical applications. *Colloids and Surfaces a-Physicochemical and Engineering Aspects* 386, 151-157.
- De Coen, W.M., Janssen, C.R., Giesy, J.P., 2000. Biomarker applications in ecotoxicology: bridging the gap between toxicology and ecology. *New Microbiotests for Routine Toxicity Screening and Biomonitoring*, 550, 13-25.
- EU, 2011. Commission recommendation of 18 October 2011 on the definition of nanomaterial (2011/696/EU). *Official Journal of the European Union L275*, 38-40.
- Evans, P., Matsunaga, H., Kiguchi, M., 2008. Large-scale application of nanotechnology for wood protection. *Nature Nanotechnology* 3, 577-577.
- Farre, M., Sanchis, J., Barcelo, D., 2011. Analysis and assessment of the occurrence, the fate and the behavior of nanomaterials in the environment. *Trac-Trends in Analytical Chemistry* 30, 517-527.
- Fauss, E., 2008. The silver nanotechnology commercial inventory, Washington, DC
- Fries, R., Simkó, M., 2012. (Nano-)Titanium dioxide (Part I): Basics, Production, Applications. NanoTrust-Dossier No. 033en.
- Hasselov, M., Readman, J.W., Ranville, J.F., Tiede, K., 2008. Nanoparticle analysis and characterization methodologies in environmental risk assessment of engineered nanoparticles. *Ecotoxicology* 17, 344-361.
- Henle, F.G.J., 1837. Ueber Enchytraeus, eine neue Anneliden-Gattung. *Archiv für Anatomie, Physiologie und wissenschaftliche Medicin*, 74-90.
- Hermes-Lima, M., 2005. Oxygen in Biology and Biochemistry: Role of Free Radicals, Functional Metabolism. John Wiley & Sons, Inc., pp. 319-368.
- ICCA Core Elements of a Regulatory Definition of Manufactured Nanomaterials. 2010. 7p.

- ISO, 1993. Soil quality -- Effects of pollutants on earthworms (*Eisenia fetida*) -- Part 1: Determination of acute toxicity using artificial soil substrate. Guideline n°11268-1, ISO (International Organization for Standardization). Geneve, Switzerland.
- ISO, 1998. Soil quality -- Effects of pollutants on earthworms (*Eisenia fetida*) -- Part 2: Determination of effects on reproduction. Guideline n°11268-2, ISO (International Organization for Standardization). Geneve, Switzerland.
- ISO, 2005. Soil Quality - Effects of pollutants on Enchytraeidae (*Enchytraeus sp.*). Determination of effects on reproduction and survival. Guideline 16387. International Organization for Standardization, Geneva, Switzerland.
- Jiang, J.K., Oberdorster, G., Biswas, P., 2009. Characterization of size, surface charge, and agglomeration state of nanoparticle dispersions for toxicological studies. *Journal of Nanoparticle Research* 11, 77-89.
- Kahru, A., Dubourgier, H.C., 2010. From ecotoxicology to nanoecotoxicology. *Toxicology* 269, 105-119.
- Klaine, S.J., Alvarez, P.J.J., Batley, G.E., Fernandes, T.F., Handy, R.D., Lyon, D.Y., Mahendra, S., McLaughlin, M.J., Lead, J.R., 2008. Nanomaterials in the environment: Behavior, fate, bioavailability, and effects. *Environmental Toxicology and Chemistry* 27, 1825-1851.
- Lavelle, P., 1988. Earthworm Activities and the Soil System. *Biology and Fertility of Soils* 6, 237-251.
- Lee, Y., Choi, J.R., Lee, K.J., Stott, N.E., Kim, D., 2008. Large-scale synthesis of copper nanoparticles by chemically controlled reduction for applications of inkjet-printed electronics. *Nanotechnology* 19, (7pp).
- Lövestam, G., Rauscher, H., Roebben, G., Klüttgen, B.S., Gibson, N., Putaud, J.-P., Stamm, H., 2010. Considerations on a Definition of Nanomaterial for Regulatory Purposes. Joint Research Centre of the European Commission, Italy, p. 40.

- Luyts, K., Napierska, D., Nemery, B., Hoet, P.H.M., 2013. How physico-chemical characteristics of nanoparticles cause their toxicity: complex and unresolved interrelations. *Environmental Science: Processes & Impacts*.
- Negahdary, M., Habibi-Tamijani, A., Asadi, A., Ayati, S., 2013. Synthesis of Zirconia Nanoparticles and Their Ameliorative Roles as Additives Concrete Structures. *Journal of Chemistry*.
- OECD, 1984. Guideline for Testing Chemicals. Earthworm, acute toxicity tests, No.207, OCDE (Organization for Economic Cooperation and Development). Paris, France.
- OECD, 2004a. Guidelines for the testing of chemicals No. 220. Enchytraeid Reproduction Test. Organization for Economic Cooperation and Development. Paris.
- OECD, 2004b. Guidelines for the testing of chemicals No. 222. Earthworm Reproduction Test (*Eisenia fetida/ Eisenia andrei*). Organization for Economic Cooperation and Development. Paris.
- Panáček, A., Kvítek, L., Pucek, R., Kolář, M., Večeřová, R., Pizúrová, N., Sharma, V.K., Nevěčná, T.j., Zbořil, R., 2006. Silver Colloid Nanoparticles: Synthesis, Characterization, and Their Antibacterial Activity. *The Journal of Physical Chemistry B* 110, 16248-16253.
- Pettitt, M.E., Lead, J.R., 2013. Minimum physicochemical characterisation requirements for nanomaterial regulation. *Environment International* 52, 41-50.
- Piccinno, F., Gottschalk, F., Seeger, S., Nowack, B., 2012. Industrial production quantities and uses of ten engineered nanomaterials in Europe and the world. *Journal of Nanoparticle Research* 14.
- Robbens, J., van der Ven, K., Maras, M., Blust, R., De Coen, W., 2007. Ecotoxicological risk assessment using DNA chips and cellular reporters. *Trends in Biotechnology* 25, 460-466.
- Rockett, J.C., Dix, D.J., 1999. Application of DNA arrays to toxicology. *Environmental Health Perspectives* 107, 681-685.

- Rombke, J., 2003. Ecotoxicological laboratory tests with enchytraeids: A review. *Pedobiologia* 47, 607-616.
- Römbke, J., Schmelz, R.M., Knaebe, S., 2009. Field studies for the assessment of pesticides with soil mesofauna, in particular enchytraeids, mites and nematodes: Design and first results. *Soil Organisms* 81, 237-264.
- Saint-Denis, M., Labrot, F., Narbonne, J.F., Ribera, D., 1998. Glutathione, glutathione-related enzymes, and catalase activities in the earthworm *Eisenia fetida andrei*. *Archives of Environmental Contamination and Toxicology* 35, 602-614.
- Sies, H., 1991. Role of Reactive Oxygen Species in Biological Processes. *Klinische Wochenschrift* 69, 965-968.
- Singh, S., Singhal, N.K., Srivastava, G., Singh, M.P., 2010. Omics in mechanistic and predictive toxicology. *Toxicology Mechanisms and Methods* 20, 355-362.
- Smijs, T.G., Pavel, S., 2011. Titanium dioxide and zinc oxide nanoparticles in sunscreens: focus on their safety and effectiveness. *Nanotechnology, Science and Applications*, 95-112.
- Snape, J.R., Maund, S.J., Pickford, D.B., Hutchinson, T.H., 2004. Ecotoxicogenomics: the challenge of integrating genomics into aquatic and terrestrial ecotoxicology. *Aquatic Toxicology* 67, 143-154.
- Sun, Y., Xia, Y., 2002. Large-Scale Synthesis of Uniform Silver Nanowires Through a Soft, Self-Seeding, Polyol Process. *Advanced Materials* 14, 833-837.
- The Royal Society & The Royal Academy of Engineering. 2004. Nanoscience and nanotechnologies: opportunities and uncertainties, p. 127.
- Tourinho, P.S., van Gestel, C.A.M., Lofts, S., Svendsen, C., Soares, A.M.V.M., Loureiro, S., 2012. Metal-based nanoparticles in soil: Fate, behavior, and effects on soil invertebrates. *Environmental Toxicology and Chemistry* 31, 1679-1692.
- Turrens, J.F., 2003. Mitochondrial formation of reactive oxygen species. *The Journal of Physiology* 552, 335-344.

- van Hal, N.L.W., Vorst, O., van Houwelingen, A.M.M.L., Kok, E.J., Peijnenburg, A., Aharoni, A., van Tunen, A.J., Keijer, J., 2000. The application of DNA microarrays in gene expression analysis. *Journal of Biotechnology* 78, 271-280.
- van Straalen, N.M., Roelofs, D., 2008. Genomics technology for assessing soil pollution. *Journal of Biology* 7, 19.
- Villeneuve, D.L., Garcia-Reyero, N., 2011. Vision & strategy: Predictive ecotoxicology in the 21st century. *Environmental Toxicology and Chemistry* 30, 1-8.
- Wang, H.Y., Huang, Y.G., Tan, Z., Hu, X.Y., 2004. Fabrication and characterization of copper nanoparticle thin-films and the electrocatalytic behavior. *Analytica Chimica Acta* 526, 13-17.
- Warheit, D.B., 2008. How meaningful are the results of nanotoxicity studies in the absence of adequate material characterization? *Toxicological Sciences* 101, 183-185.
- Warner, C.M., Gust, K.A., Stanley, J.K., Habib, T., Wilbanks, M.S., Garcia-Reyero, N., Perkins, E.J., 2012. A Systems Toxicology Approach to Elucidate the Mechanisms Involved in RDX Species-Specific Sensitivity. *Environmental Science & Technology* 46, 7790-7798.
- Washio, I., Xiong, Y., Yin, Y., Xia, Y., 2006. Reduction by the End Groups of Poly(vinyl pyrrolidone): A New and Versatile Route to the Kinetically Controlled Synthesis of Ag Triangular Nanoplates. *Advanced Materials* 18, 1745-1749.
- Westheide, W., Graefe, U., 1992. Two new terrestrial *Enchytraeus* species (Oligochaeta, Annelida). *Journal of Natural History* 26, 479-488.
- Wu, S.-H., Chen, D.-H., 2004. Synthesis of high-concentration Cu nanoparticles in aqueous CTAB solutions. *Journal of Colloid and Interface Science* 273, 165-169.

Chapter II

Effect of Cu-nanoparticles versus one Cu-salt:
Analysis of stress biomarkers response in
Enchytraeus albidus (Oligochaeta)

II - Effect of Cu-nanoparticles versus one Cu-salt: Analysis of stress biomarkers response in *Enchytraeus albidus* (Oligochaeta)

Susana I.L. Gomes^a, Sara C. Novais^a, Carlos Gravato^b, Lúcia Guilhermino^b, Janeck J. Scott-Fordsmand^c, Amadeu M.V.M. Soares^a and Mónica J.B. Amorim^a

^aCESAM & Department of Biology, University of Aveiro, Aveiro, Portugal

^bUniversity of Porto: CIMAR-LA/CIIMAR & ICBAS – Centro Interdisciplinar de Investigação Marinha e Ambiental, Laboratório de Ecotoxicologia, Porto, and ICBAS – Instituto de Ciências Biomédicas de Abel Salazar, Laboratório de Ecotoxicologia, Universidade do Porto, Porto, Portugal

^cDepartment of Terrestrial Ecology, National Environmental Research Institute, Aarhus University, Vejlsøvej, Denmark

Published in Nanotoxicology, 2012 Mar;6(2):134-43.

doi: 10.3109/17435390.2011.562327.

Abstract

In the present study, the main goal was to compare the effects of ionic copper versus copper nanoparticles in *Enchytraeus albidus* assessing the effect at the biomarker level, testing different concentrations and exposure times. Measured parameters were lipid peroxidation (LPO), total, reduced and oxidized glutathione content (TG, GSH and GSSG), the enzymatic activity of superoxide dismutase (SOD), catalase (CAT), glutathione reductase (GR), glutathione peroxidase (GPx), glutathione S-transferases (GSTs) and cholinesterases (ChEs). Results showed that both salt- and nano-copper caused oxidative stress and damage to *E. albidus*, as confirmed by LPO levels, and

effects could be discriminated between the copper forms. Nevertheless and despite the visible discrimination between nano and the salt form (time and exposure dependent), there was no single or a set of biomarkers that provided the best discrimination.

Keywords: Oxidative stress, enzymatic and non-enzymatic antioxidants, copper nanoparticles, copper, Enchytraeids

1. Introduction

Copper nanoparticles (Cu NPs) are being given considerable attention due to their properties (e.g., high electrical and thermal conductivities) and therefore practical applications. Copper NPs are used in modern electronic circuits, e.g., chip-package interconnections (Tummala et al. 2006) and conductive inks for printing electronic components (Lee et al. 2008b), metallurgy, catalysis (Dhas et al. 1998; Samim et al. 2007) and sensors (Athanassiou et al. 2006). Increased use of nanomaterials will lead to their distribution in the environment, including the potential to contaminate soil, migrate into surface and groundwater, and interact with biota (Klaine et al. 2008). Despite the increased interest and recent investigation in this area, very little is known about the environmental effects and behaviour of nanoparticles especially for terrestrial ecosystems (Klaine et al. 2008). For example, no studies have been reported for Enchytraeids (Oligochaeta), which are important members of the soil fauna that have been used in ecotoxicological laboratory tests for more than 30 years (Rombke and Moser 2002) and have a standard guideline (International Organization for Standardization [ISO] 2003). They are ecologically relevant, being abundant in many

soils contributing to the improvement of the pore structure of the soil and, indirectly, to the degradation of the organic matter.

The available information about the ecotoxicology of nanoparticles includes mainly studies in organisms of the aquatic compartment (Oberdörster 2004; Fortner et al. 2005; Hund-Rinke and Simon 2006; Lovern and Klaper 2006; Griffitt et al. 2007; Lovern et al. 2007; Velzeboer et al. 2008; Zhu et al. 2006, 2008; Heinlaan et al. 2008), with very few studies on soil organisms (Tong et al. 2007; Johansen et al. 2008; Lee et al. 2008a; Scott-Fordsmand et al. 2008a, 2008b).

Despite the fact that copper is an essential element for most living organisms its toxicity is also very well documented, e.g., to the enchytraeid *Enchytraeus albidus* (Amorim et al. 2005, 2008; Howcroft et al. 2009). Copper is known to cause oxidative damage, catalysing the formation of hydroxyl radicals via the Haber-Weiss reaction (Bremner 1998): $O_2^{\cdot -} + Cu^{2+} \rightarrow O_2 + Cu^+$; $Cu^+ + H_2O_2 \rightarrow Cu^{2+} + OH^- + OH^\cdot$. Organisms are continuously exposed to oxidative stress in nature and have developed antioxidant pathways, present in all aerobic organisms, including antioxidant enzymes (superoxide dismutase [SOD], catalase [CAT], glutathione peroxidases [GPx] and glutathione reductase [GR]) and free radical scavengers (vitamins C and E, carotenoids, glutathione) whose function is to remove reactive oxygen species (ROS) (Doyotte et al. 1997). Enzymatic and nonenzymatic antioxidants play a crucial role in maintaining cell homeostasis. Therefore, the balance between prooxidant endogenous and exogenous factors and antioxidant defences can be used to assess toxic effects in biological systems under stressful environmental conditions (Howcroft et al. 2009).

Comparatively, very little is known about the effects of copper nanoparticles. Studies reporting acute toxicity comparing ionic copper with copper nanoparticles show that the first was more toxic to mice (LD50 of 110 and 413 mg/kg, respectively (Chen et al.

2006, 2007; Meng et al. 2007) and zebrafish (EC50 of 0.25 mg/L and 1.6 mg/L, respectively (Griffitt et al. 2007). Microarray experiments (Griffitt et al. 2007) showed that the 48 h exposure to sub-lethal concentrations of nanocopper resulted in 82 genes significantly differently expressed, and that the transcriptional response induced by nanocopper was different from the one generated by the soluble copper, suggesting that the effects caused by nanocopper were not only due to solubility. Recently, two studies have reported toxicity following Cu nanoparticles exposure; Heckmann et al. (2011) employed a limit test design with *Eisenia fetida* and observed that Cu-salts were more toxic in a standard test than Cu-nanoparticles, when measuring survival and reproduction. Unrine et al. (2010) found no mortality or reproductive effect at exposure concentration up to 65 mg Cu/kg (using two particles, average 37 and 102 nm), but a metallothionein induction at around 10–20 mg Cu/kg exposure. In the present study we wished to study the biological identity and effect of two copper forms in *Enchytraeus albidus*, copper-salt and nanosized copper. Effects were assessed in terms of oxidative stress, namely through the determination of lipid peroxidation (LPO), the activities of the enzymes SOD, CAT, GPx, GR and GSTs (glutathione S-transferases). In addition, neuro-muscular effects were evaluated by determining the activity of ChEs. As molecular responses generally change over time (Connors and Ringwood 2000; Saint-Denis 2001; Vlahogianni and Valavandis 2007) three different exposure times (2, 4 and 8 days) and two exposure concentrations of copper and nanocopper were analyzed.

2. Materials and methods

2.1. Test organism

The test organism used was *Enchytraeus albidus*, Henle 1837. Individuals were maintained in laboratory cultures under controlled conditions, e.g., the photoperiod was 16:8 h light:dark and a temperature of 18°C. Details of culturing are given in Rombke and Moser (2002).

2.2. Test soil

The test soil used was from a natural site in Hygum, Denmark. Soil was homogenized and sterilized. The general physico-chemical characteristics of the soil from the Hygum-site were as follows: 20–32% coarse sand (>200 μm), 20–25% fine sand (63–200 μm), 11–20% coarse silt (20–63 μm), 12–20% silt (20–20 μm), 12–16% clay (<2 μm), 3.6–5.5% humus, 2.1–3.2% organic carbon and 6.8 cmolc/kg dry weight CEC. The soil was sampled to a depth of 20 cm. To exclude existing soil fauna, the soil was dried at 80°C for 24 h in an oven (Memmert, Type UL40, Braunschweig, Germany) and then sieved through a 2-mm mesh to remove larger particles. Chemical substances The Cu nanoparticles (Supplier American Elements) had a mean diameter of 80 nm, (PW-XRD < 74 nm (primary particle size), in demineralized water the DLS = 419 ± 1 nm (indicating agglomeration of particles), Zeta = 15.3 ± 0.3 and a purity of 99.5% (see Heckmann et al. 2011). The nanoparticles were added to the soil following transfer to deionised water and ultrasonic-steering for 15 min (as in Heckmann et al. 2011). The Cu-salt was obtained from CuCl_2 solubilized in water. The concentrations used were 450 and 750 mg/kg of copper and nanosized copper.

To estimate the activity of free unbound Cu^{2+} released from the nanoparticles a ion-selective electrode (ISE25Cu, Radiometer) in combination with the reference electrode (REF251, Radiometer) equipped with a double salt bridge was used. The inner salt

bridge contained saturated KCl and the outer salt bridge contained 0.1 M KNO₃. A standard curve was made using Cu(NO₃)₂, detection limit of the ion selective electrode is 362 nM. The free ion activity was measured on a solution of 100 mg Cu-NP/L deionized water (same as stem solution) after an 8-day period (as in bioassay) using three replicates. In a concurrent experiment, the activity of Cu²⁺ in solution was below the detection limit/ limit of quantification and hence not possible to detect. This is equivalent to that less than 4.6 mg Cu/kg (less than 0.005% of the total Cu²⁺) was active in the soil solution as measured by the electrode. Other methods to estimate dissolution – filtration, DGT or soil solution sampling followed by AAS/ICP were not performed due to the uncertainties with these methods in regard to nanoparticles. Possibly the only alternative is ultracentrifugation followed by centrifugation (but this was not attempted).

2.3. Test procedure

After manual mixing (homogeneity was not checked, but previous measures with radio-labelled Ag nanoparticles showed a good dispersion using this mixing technique), sub-samples of the batch of soil were introduced into the test vessels (Ø 5.5 cm, 250 mL volume). Fifteen adult worms with well developed clitellum and similar size were introduced in each test vessel, each containing 25 g moist soil (40–60% of the maximum water holding capacity -WHC). The vessel was covered with a lid (containing small holes) and the worms were exposed for two, four and eight days (in the absence of food), at 20°C and a 16:8 h photoperiod. Seven replicates per treatment (including controls) were used. At test end, animals of each replicate (n = 15) were carefully removed, rinsed in deionised water, pooled, weighed and frozen in liquid Nitrogen. Samples were stored at -80°C until further analysis.

2.4. Biochemical analysis

Biochemical analyses were performed after 2, 4 and 8 days; the sampling days are based on previous experiments (Novais et al. 2009). Each sample containing 15 organisms was homogenized in 1500 mL K-Phosphate 0.1M buffer, pH 7.4. Part of the tissue homogenate (300 mL) was separated into a microtube with 5 mL BHT (2,6-dieter-butyl-4-metylphenol) 4% in methanol to prevent tissue oxidation for posterior lipid peroxidation (LPO) determination. The remaining tissue homogenate (1200 mL) of each sample was centrifuged at 10,000 g for 20 min at 4°C, to isolate the Post-Mitochondrial Supernatant (PMS). The PMS was divided into eight microtubes, stored at -80°C, for posterior analysis of biomarkers and protein quantification. Reaction blanks were made for all the parameters, determined using the homogenization buffer (K-Phosphate 0.1M, pH 7.4) instead of the sample. Superoxide dismutase (SOD), cholinesterases (ChEs) and protein content were measured in the microplate spectrophotometer reader Bio TEK Power Wave 340, for all the other a Jasco V-630 UV/VIS spectrophotometer was used.

2.4.1. Determination of lipid peroxidation

The extent of LPO was measured as thiobarbituric acid-reactive substances (TBARS) at 535 nm (Ohkawa et al. 1979; Bird and Draper 1984).

2.4.2. Quantification of enzymatic and nonenzymatic antioxidants

Superoxide Dismutase (SOD) activity was determined based on the reduction of cytochrome c by superoxide radicals generated by the xanthine-xanthine oxidase system. Measurements were recorded at 550 nm (McCord and Fridovich 1969) adapted to microplate. Catalase (CAT) activity was measured following the decrease in absorbance at 240 nm due to H₂O₂ (substrate) decomposition (Clairborne 1985). Glutathione Peroxidase (GPx) activity was determined following the oxidation of

NADPH, at 340 nm, when GSSG is reduced back to GSH by glutathione reductase, using H₂O₂ as substrate (Mohandas et al. 1984). Glutathione Reductase (GR) activity was measured assessing the decrease of NADPH level, at 340 nm (Cribb et al. 1989). Glutathione S-Transferase (GST) activity was measured at 340 nm, following the conjugation of GSH with CDNB (the substrate with the broadest range of GST isozymes delectability) (Habig et al. 1974). For more details see Howcroft et al. (2009). Total glutathione (TG, GSH + GSSG) and oxidized glutathione (GSSG) were measured at 412 nm, using the recycling reaction of reduced glutathione (GSH) with DTNB in the presence of GR excess (Tietze 1969; Baker et al. 1990). 2-Vinyl-pyridine was used to conjugate GSH for the GSSG determination (Griffith 1980). The GSH content was calculated by subtraction of GSSG from the total glutathione.

2.4.3. Quantification of cholinesterases activity

ChEs activity was measured using the Ellman method (Ellman et al. 1961) adapted to microplate (Guilhermino et al. 1996). ChE activity was determined in the PMS, using 50 mL of sample and 250 mL of reaction buffer (30 mL K-phosphate buffer 0.1 M pH 7.2, 1 mL DTNB 10 mM in K-phosphate buffer with 7.5 mg NaHCO₃ and 0.2 mL acetylthiocholine 0.075 M solution as the substrate). The absorbance was measured at 414 nm.

2.4.4. Protein quantification

Protein concentration was assayed using the Bradford method (Bradford 1976), adapted from BioRad's Bradford microassay set up in a 96-well flat bottom plate, using bovine g-globuline as a standard.

2.5. Statistical and data analysis

The main aim of this experiment was to analyze differences between response induction in the salt form (CuCl₂) and the nano form (Cu-NP). Correspondence Analysis – CA (multivariate analysis) was performed to identify correspondence between the biomarker expression and the exposure condition, using standardized data (Proc Corresp, SAS 9.1.3). Univariate statistical analysis was performed (SPSS 1997): one-way ANOVA (Dunnett's) was used to compare differences between control and treatments, for each individual exposure time, t-test was used to compare differences between Cu versus Cu-NP within the same concentration and different concentration of the same compound, one-way ANOVA (Holm-Sidak) was used to compare differences due to different times of exposure. All the univariate statistical analysis was performed with and without outliers, being the outliers calculated as the mean \pm 3 times standard error.

3. Results

3.1. Free ion activity

The solubility (free ion activity/concentration) of the Cu nanoparticles, studied by ion-selective electrode (ISE25CU), was in the range of 3–4% when dissolved in demineralized water. In the soil solution the Cu activity was less than 4.6 mg Cu/kg (concurrent experiment).

3.2. Multivariate analysis

Correspondence Analysis (CA) showed that on an overall basis 89% of the variation was associated with the first dimension, and that the response clearly corresponded to days (Figure 1A). When analyzing at the level of days it was observed that at Day 2 the Cu-salt samples correlated with expression of GSSG, which changed so that at Day 8 it

was mainly the nanoparticles samples that corresponded with the GSSG (Figure 1B, 1C). Day 4, showed an intermediate response (not shown). The same pattern but clearer was observed when analysing on an individual exposure concentration level, i.e., 450 mg Cu/kg (Figure 1D–F), with a clear separation between salt and nanoparticle exposure. Given this, data were subsequently analysed in accordance to the test treatments (days and concentrations). Hence, there seem in general to be a shift over time for each exposure type, where the GSSG shows the highest correspondence with the Cu-salt in the start and later with Cu-NP exposure.

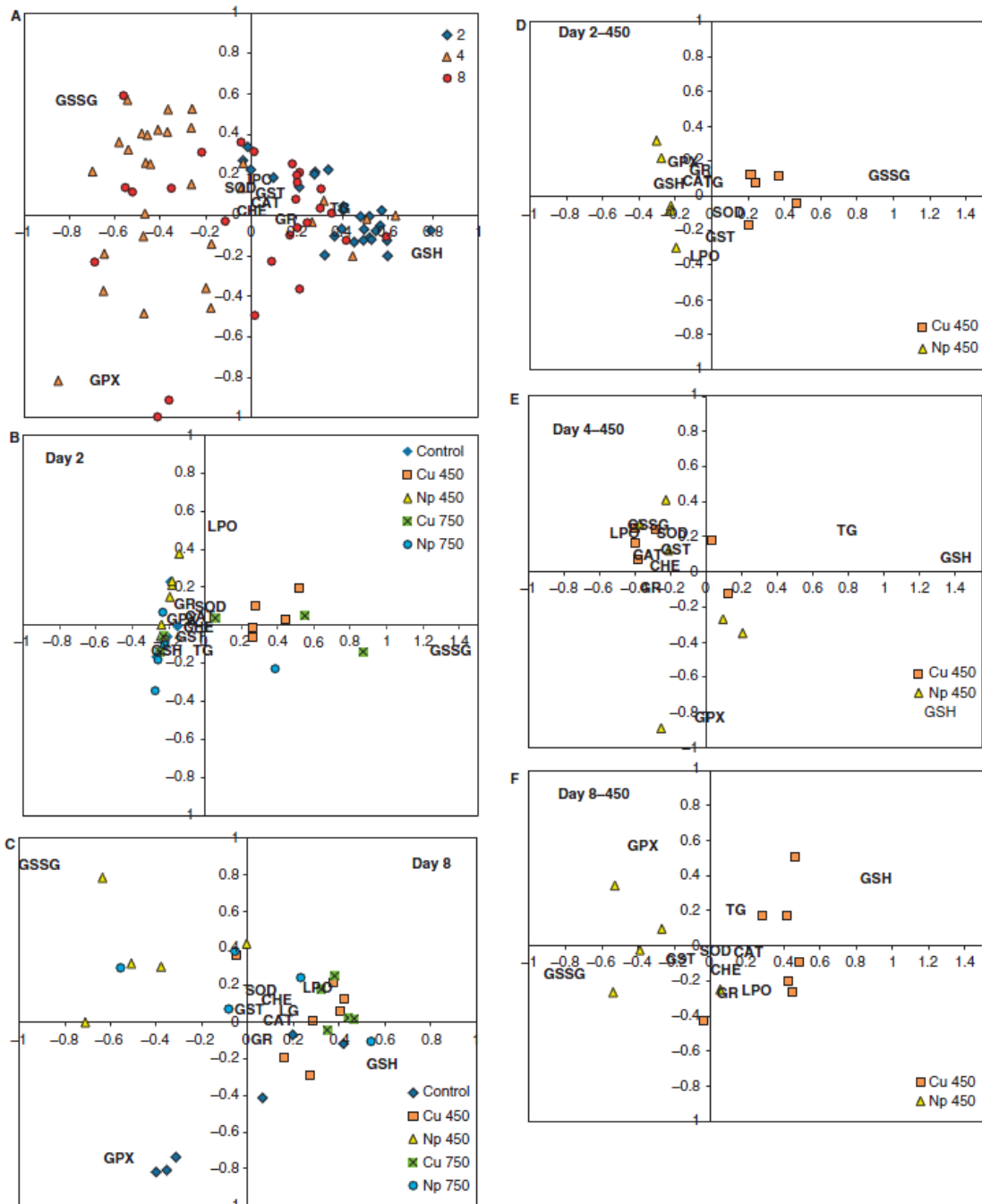


Figure 1: Correspondence Analysis (CA) of *E. albidus* biomarkers, including lipid peroxidation (LPO), superoxide dismutase (SOD), catalase (CAT), glutathione peroxidase (GPx), Glutathione reductase (GR), reduced glutathione (GSH), oxidized glutathione (GSSG), total glutathione (TG), glutathione-S-transferase (GST) and cholinesterases (ChE). (A) All data – all exposure concentrations and days; (B, C) All data – all concentrations for day 2 and day 8, separately; (D-F) All data – the 450 mg Cu/kg concentration and exposure duration 2, 4 and 8 days separately.

3.3. Univariate analysis

3.3.1. Effect of the test chemicals (Cu and Cu-NP) and different concentrations (450/750 mg/kg) on the enzymatic activity.

As also seen in the correspondence analysis, the individual results (Figure 2) show significant differences in the majority of biomarkers, due to exposure to both Cu-salt and Cu-NP. Significant changes were observed in terms of increase in LPO levels (Figure 2J) after 8 days of exposure caused by Cu-salt. Also at 8 days exposure, GSSG (Figure 2B) was stimulated by Cu-NP. At 4 days exposure, GPx activity increases with concentration increase and is higher for all NP versions. Similarly GSSG activity increases in both concentrations of both chemicals, while GSH activity decreases in the higher concentration of Cu-NP when the outliers are excluded (Figure 2A). At 2 days of exposure GSSG activity was stimulated by Cu-salt treatments while GR decreases (Figure 2F).

3.3.2. Effects of ionic copper versus nanosized copper.

Especially GSSG, GSH and CAT showed different responses depending on the chemical form applied (Cu-salt or Cu-NP) (Figure 2). At 2 days of exposure, GSH activity (Figure 2A) was more inhibited by Cu than by Cu-NP (in the lower concentration), while the GSSG activity (Figure 2B) was increased by both Cu-salt treatments and not affected by Cu-NP. The activity of CAT at 4 days of exposure (Figure 2H) was increased by Cu-NP 750, which was significantly different from Cu-salt 750. The same response, at 4 days of exposure, was observed for the biomarkers GR, SOD and ChE, being the activities significantly smaller when exposed at Cu-salt 750 when compared to Cu-NP 750.

3.3.3. Effects of concentration (450 vs. 750 mg/kg).

The two exposure concentration used caused different biomarker responses. SOD, CAT and ChE activities at 4 days exposure, were significantly reduced in Cu-salt 750 in comparison to Cu-salt 450. Also at 4 days of exposure, GR and GSSG activities were increased in Cu-NP 750 in comparison to Cu-NP 450. After 8 days of exposure LPO levels were significantly higher for Cu-salt 750 when compared to Cu-salt 450.

3.3.4. Effects of exposure time on biomarkers response.

As mentioned before, CA analysis showed an exposure time-related enzymatic response. Univariate analysis also confirmed that biomarkers responses varied with the time of exposure: GPx activity on controls was significantly different between the three exposure times. GR, GSH and TG activity decreased on controls at 4 and 8 days of exposure. Cu-salt 450 caused a dissimilar GSSG activity between the three times of exposure, LPO levels were elevated at 8 days and SOD, GSH and TG also varies over time. When exposed to Cu-NP 450, GSSG activity was different between all exposure times. In Cu-salt 750 CAT activity changed in all times of exposure, SOD, LPO, ChE and GPx were up (the first three at 8 days and the last at 4 days). Exposure to Cu-NP 750 caused a GSH and TG response that was different between all the times of exposure, GSSG and LPO decreased at 2 days.

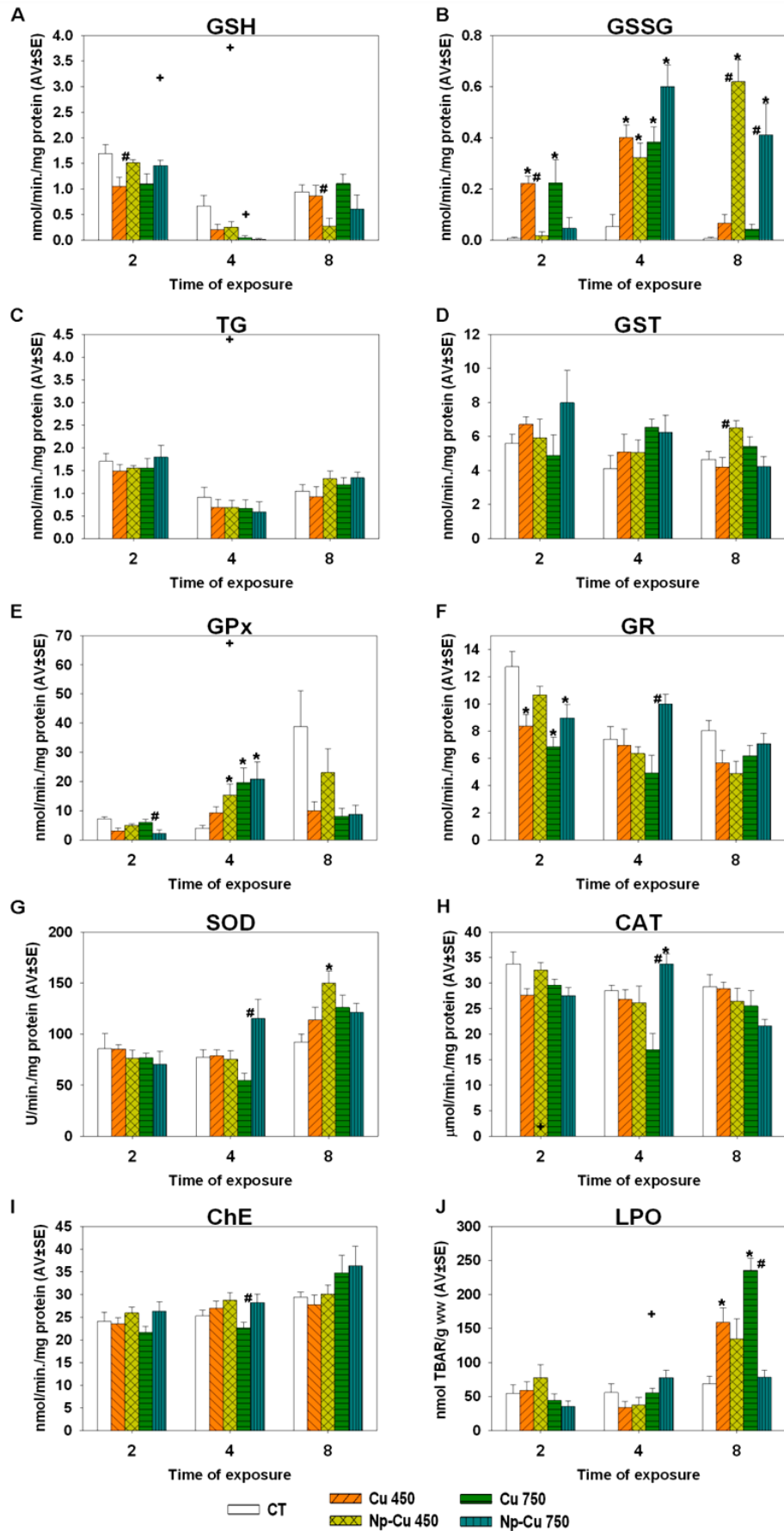


Figure 2: Reduced glutathione (GSH), oxidized glutathione (GSSG), total glutathione (TG), glutathione-S-transferase (GST), glutathione peroxidase (GPx), glutathione reductase (GR), catalase (CAT), superoxide dismutase (SOD), colinesterases (ChE) and lipid peroxidation (LPO) expressed as mean values \pm standard error ($Av \pm SE$) for *E. albidus* exposed to 450 and 750mg/kg of ionic and nanosized copper, during 2, 4 and 8 days. *Statistical significant differences compared to control, Holm-Sydak $p < 0.05$; #statistical significant differences between Cu salt and Cu-NP within the same concentration; + indicates outliers.

4. Discussion

It is assumed that the effects present in the Cu-NP exposed organisms are partially or fully caused by nanocopper and not due to the dissolved Cu. However, it must be realised that this may not be the case, but at present there is no method to verify and quantify this in situ. Despite that, dissolution experiments support our assumption since ion-selective electrode measurement showed a 3–4% free ion activity following 8 days, and in a concurrent study with the same particles we observed that less than 0.005% of soil introduced Cu-NP was active (as measured with electrode) in soil solution, which corresponds to less than 4.6 mg active Cu/kg.

The results presented indicate candidate responses that, combined with other markers (see, e.g. Unrine et al. 2010), should be further studied to discriminate between Cu-salt and Cu-NP, in order to obtain a biological identity. Both copper-salt and nano-copper caused changes in all evaluated parameters which differed with duration of exposure, revealing that organisms are facing an oxidative stress status that is changing over time. In fact, the biomarker response showing the best discrimination between the nano and the salt form changed with exposure duration and concentration.

Our results show that SOD activity increased after 8 days of exposure to Cu-NP 450. SOD is an antioxidant enzyme that protects tissues against superoxide anion radical,

catalysing its conversion in H₂O₂, which is detoxified by CAT and GPx. Increased SOD activity as a response to metals, including copper, has already been observed in several organisms (Jing et al. 2006; Drazkiewicz et al. 2007; Sampaio et al. 2008). A previous study where *E. albidus* was exposed to Cu (320 mg/kg) (Howcroft et al. 2009) showed no differences in SOD activity, after 2 days and 3 weeks' exposure. The differences found between the present results and those in Howcroft et al. (2009) could be explained by the difference in bioavailability of Cu in the used soil type. Besides, in control animals there was a time-dependent change in the GPx, GR, GSH and TG response similar to what was observed in other studies (see Introduction), which shows the importance of having controls for all sampling times. Hence, responses were compared to controls from the same sampling time (see Figure 1).

Upon exposure the LPO levels at the 8th day of exposure indicated that the organisms are suffering oxidative damage caused by copper-salt (Cu) (more pronounced at the highest concentration tested), while for Cu-NP an increase (despite not significant) is observed for 450, but not for 750 mg/kg. Previous work with LUFA 2.2 soil (Howcroft et al. 2009) showed that the antioxidant defence processes in *E. albidus* were able to prevent oxidative damage (LPO) on short exposures to copper (2 days), but not after 3 weeks. Our data suggests that 8 days of exposure at a sub-lethal concentration of copper (450 mg/kg) is already causing oxidative damage.

At 4 days exposure, GPx increased as GSH decreased: attending to the fact that GPx activity increases as an attempt to the detoxification of H₂O₂ (and other organic hydroperoxides) using GSH as substrate (and producing GSSG which is then regenerated into GSH by GR) (Thomas et al. 1990), the decrease in GSH activity observed at 4 days of exposure can result from its use as substrate by GPx in its antioxidant activity. This can be supported by the fact that at this time of exposure no

significant changes were observed in TG and GST. The results also suggest that the depletion of GSH is not being compensated since the activity of GR did not significantly increase, resulting in the increase of GSSG observed. In fact, GSH can directly bind to some metals (Scragg and Bonnett 2002; Helbig et al. 2008). Consumption of GSH can also occur due to conjugation activity, although our results did not show any increase of GST that would justify GSH depletion.

No significant changes occurred in ChEs, at any treatment or time of exposure. ChEs are a group of enzymes related with neuronal functions and in recent decades some studies have been published regarding the effect of metals in Acetyl cholinesterases (AChE) activity (the main cholinesterase present in six earthworms' whole body (Rault et al. 2007)), but results are contradictory possibly related with different species used as test organisms and/or distinct experimental conditions (e.g., Romani et al. 2003; Frasco et al. 2005, Varo et al. 2007, Vieira et al. 2009). However, it is also pointed that the interaction of the metals with the technique can contribute to artifacts in the measurement of AChE (Frasco et al. 2005; Varo et al. 2007) and that enzymatic characterization is often a prerequisite to the use of cholinesterase activity as effect criteria in laboratory studies. Thus, despite characterized in *E. albidus* (Howcroft et al., 2011), investigation is needed to allow better interpretation of this type of results.

Regarding the different concentrations tested, Cu-salt showed a dose effect, with the highest concentration causing more effects than the lower concentration. For Cu-NP, LPO levels were higher for 450mg/kg (Cu-NP 750 did not cause lipid peroxidation). This could be indicative of a bell-shape response which was already observed for other stress biomarkers (Dagnino et al. 2007; Dazy et al. 2009); nevertheless, this should be confirmed by testing more concentrations.

In general, the results seem to indicate that after 2 days of exposure the organisms start to respond to the oxidative stress imposed by copper-salt and copper nanoparticles. At 4 days of exposure GPx was the main defence against oxidative damage, for which *E. albidus* could not compensate for at 8 days of exposure, resulting in LPO increase.

At 4 days of exposure to 750 mg/kg differences between Cu-salt and Cu-NP are very pronounced, while those observed between the concentrations of 450 mg/kg at 2 days of exposure do not persist with increasing exposure time. Cu-salt exposure caused lower values of CAT compared to Cu-NP; considering that copper can bind directly to CAT, as suggested by Atli et al. (2006), to the enzymes –SH groups, which could mean that copper binding is higher for Cu-salt than for Cu-NP. Reduced activity of CAT results in the accumulation of hydroperoxides, which can be removed by GPx until a saturation point hence leading ultimately to the higher LPO levels observed at 8 days. Conversely, higher values of CAT and GR at Cu-NP in comparison to Cu-salt, associated with the activity of GPx, seem to have avoided the ultimate cellular damage, LPO.

5. Conclusions

Both salt- and nano-copper caused oxidative stress damage to *E. albidus*, and effects could be discriminated between the two copper forms. Nevertheless and despite the visible discrimination between nano and the salt form (time and exposure dependent), no individual or a set of biomarkers could be identified as providing the best discrimination. In general, effects of Cu-salt were more pronounced especially at LPO level. GPx seemed to be the main antioxidant acting against the stress imposed, and associated with GSH and GSSG were the biomarkers with more robust response. The selected time intervals were adequate to follow the evolution of the stress response until oxidative damage. The study highlight that the biological identity of Cu-NP exposure

can be a possible way forward, even much more studies are needed. To better characterize these responses a broader range of concentrations should be tested and more organism groups. Further research is needed to link these effects with higher levels of biological organization.

Declaration of interest: The project was financial support by the Danish Strategic Research Council through the NABIIT project 2006-06-0015 “SUNANO – Risk assessment of free nanoparticles” and by the NANOkA project (PTDC/BIA-BEC/103716/2008). The authors report no conflict of interest. The authors alone are responsible for the content and writing of the paper.

References

- Amorim MJB, Novais S, Rombke J, Soares AMVM. 2008. *Enchytraeus albidus* (Enchytraeidae): A test organism in a standardized avoidance test? Effects of different chemical substances. *Environ Int* 34:363–371.
- Amorim MJB, Rombke J, Schallna HJ, Soares AMVM. 2005. Effect of soil properties and aging on the toxicity of copper for *Enchytraeus albidus*, *Enchytraeus luxuriosus*, and *Folsomia candida*. *Environ Toxicol Chem* 24:1875–1885.
- Athanassiou EK, Grass RN, Stark WJ. 2006. Large-scale production of carbon-coated copper nanoparticles for sensor applications. *Nanotechnology* 17:1668–1673.
- Atli G, Alptekin O, Tukul S, Canli M. 2006. Response of catalase activity to Ag⁺, Cd²⁺, Cr⁶⁺, Cu²⁺ and Zn²⁺ in five tissues of freshwater fish *Oreochromis niloticus*. *Comparat Biochem Physiol C - Toxicol Pharmacol* 143:218–224.
- Baker MA, Cerniglia GJ, Zaman A. 1990. Microtiter plate assay for the measurement of glutathione and glutathione disulfide in large numbers of biological samples. *Analyt Biochem* 190:360–365.

- Bird RP, Draper HH. 1984. Comparative studies on different methods of malonaldehyde determination. *Meth Enzymol* 105:299–305.
- Bradford MM. 1976. Rapid and sensitive method for quantitation of microgram quantities of protein utilizing principle of proteindye binding. *Analyt Biochem* 72:248–254.
- Bremner I. 1998. Manifestations of copper excess. *Am J Clin Nutr* 67:1069s–1073s.
- Chen Z, Meng H, Yuan H, Xing GM, Chen CY, Zhao F, et al. 2007. Identification of target organs of copper nanoparticles with ICP-MS technique. *J Radioanalyt Nuclear Chem* 272: 599–603.7.
- Chen Z, Meng HA, Xing GM, Chen CY, Zhao YL, Jia GA, et al. 2006. Acute toxicological effects of copper nanoparticles in vivo. *Toxicol Lett* 163:109–120.
- Clairborne A. 1985. Catalase activity. In: Greenwald RA, editor.
- CRC handbook of methods in oxygen radical research: Boca Raton, FL: CRC Press.
- Connors DE, Ringwood AH. 2000. Effects of glutathione depletion on copper cytotoxicity in oysters (*Crassostrea virginica*). *Aquatic Toxicology* 50:341–349.
- Cribb AE, Leeder JS, Spielberg SP. 1989. Use of a microplate reader in an assay of glutathione-reductase using 5,5'-Dithiobis (2-Nitrobenzoic Acid). *Analyt Biochem* 183:195–196.
- Dagnino A, Allen JI, Moore MN, Broeg K, Canesi L, Viarengo A. 2007. Development of an expert system for the integration of biomarker responses in mussels into an animal health index. *Biomarkers* 12:155–172.
- Dazy M, Masfaraud JF, Ferard JF. 2009. Induction of oxidative stress biomarkers associated with heavy metal stress in *Fontinalis antipyretica* Hedw. *Chemosphere* 75:297–302.
- Dhas NA, Raj CP, Gedanken A. 1998. Synthesis, characterization, and properties of metallic copper nanoparticles. *Chem of Materials* 10:1446–1452.
- Doyotte A, Cossu C, Jacquin MC, Babut M, Vasseur P. 1997. Antioxidant enzymes, glutathione and lipid peroxidation as relevant biomarkers of experimental or field exposure in the gills and the digestive gland of the freshwater bivalve *Unio tumidus*. *Aquatic Toxicol* 39:93–110.

- Drazkiewicz M, Skorzynska-Polit E, Krupa Z. 2007. The redox state and activity of superoxide dismutase classes in *Arabidopsis thaliana* under cadmium or copper stress. *Chemosphere* 67: 188–193.
- Ellman GL, Courtney KD, Andres V, Featherstone RM. 1961. A new and rapid colorimetric determination of acetylcholinesterase activity. *Biochem Pharmacol* 7:88-95.
- Fortner JD, Lyon DY, Sayes CM, Boyd AM, Falkner JC, Hotze EM, et al. 2005. C-60 in water: Nanocrystal formation and microbial response. *Environ Sci Technol* 39:4307–4316.
- Frasco MF, Fournier D, Carvalho F, Guilhermino L. 2005. Do metals inhibit acetylcholinesterase (AChE)? Implementation of assay conditions for the use of AChE activity as a biomarker of metal toxicity. *Biomarkers* 10:360–375.
- Griffith OW. 1980. Determination of glutathione and glutathione disulfide using glutathione-reductase and 2-vinylpyridine. *Analyt Biochem* 106:207–212.
- Griffitt RJ, Weil R, Hyndman KA, Denslow ND, Powers K, Taylor D, et al. 2007. Exposure to copper nanoparticles causes gill injury and acute lethality in zebrafish (*Danio rerio*). *Environ Sci Technol* 41:8178–8186.
- Guilhermino L, Lopes MC, Carvalho AP, Soares AMVM. 1996. Inhibition of acetylcholinesterase activity as effect criterion in acute tests with juvenile *Daphnia magna*. *Chemosphere* 32:727–738.
- Habig WH, Pabst MJ, Jakoby WB. 1974. Glutathione S-transferases – first enzymatic step in mercapturic acid formation. *J Biological Chem* 249:7130–7139.
- Heckmann L, Hovgaard MB, Sutherland D, Autrup H, Besenbacher F, Scott-Fordsmand JJ. 2011. Limit-test toxicity screening of selected inorganic nanoparticles to the earthworm *Eisenia fetida*. *Ecotoxicology* 20:226–233.
- Heinlaan M, Ivask A, Blinova I, Dubourguier H-C, Kahru A. 2008. Toxicity of nanosized and bulk ZnO, CuO and TiO₂ to bacteria *Vibrio fischeri* and crustaceans *Daphnia magna* and *Thamnocephalus platyurus*. *Chemosphere* 71:1308–1316.

- Helbig K, Bleuel C, Krauss GJ, Nies DH. 2008. Glutathione and transition-metal homeostasis in *Escherichia coli*. *J Bacteriol* 190:5431–5438.
- Howcroft CF, Amorim MJB, Gravato C, Guilhermino L, Soares AMVM. 2009. Effects of natural and chemical stressors on *Enchytraeus albidus*: Can oxidative stress parameters be used as fast screening tools for the assessment of different stress impacts in soils? *Environ Int* 35: 318–324.
- Howcroft CF, Gravato C, Amorim MJB, Novais S, Soares AMVM, Guilhermino L. 2011. Biochemical characterization of cholinesterases in *Enchytraeus albidus* and assessment of in vivo and in vitro effects of different soil properties, copper and phenmedipham. *Ecotoxicology*. 20:119–130.
- Hund-Rinke K, Simon M. 2006. Ecotoxic effect of photocatalytic active nanoparticles TiO₂ on algae and daphnids. *Environ Sci Pollut Res* 13:225–232.
- International Organization for Standardization (ISO). 2003. Soil quality – effects of pollutants on Enchytraeidae (*Enchytraeus sp.*) – determination of effects on reproduction and survival. Guideline no. 16387. Genève: ISO.
- Jing G, Li Y, Xie LP, Zhang RQ. 2006. Metal accumulation and enzyme activities in gills and digestive gland of pearl oyster (*Pinctada fucata*) exposed to copper. *Comparat Biochem Physiol C – Toxicol Pharmacol* 144:184–190.
- Johansen A, Pedersen AL, Jensen KA, Karlson U, Hansen BM, Scott-Fordsmand JJ, et al. 2008. Effects of C-60 fullerene nanoparticles on soil bacteria and protozoans. *Environ Toxicol Chem* 27:1895–1903.
- Klaine SJ, Alvarez PJJ, Batley GE, Fernandes TF, Handy RD, Lyon DY, et al. 2008. Nanomaterials in the environment: Behavior, fate, bioavailability, and effects. *Environ Toxicol Chem* 27:1825–1851.
- Lee WM, An YJ, Yoon H, Kweon HS. 2008a. Toxicity and bioavailability of copper nanoparticles to the terrestrial plants mung bean (*Phaseolus radiatus*) and wheat

- (*Triticum aestivum*): Plant agar test for water-insoluble nanoparticles. *Environ Toxicol Chem* 27:1915–1921.
- Lee Y, Choi JR, Lee KJ, Stott NE, Kim D. 2008b. Large-scale synthesis of copper nanoparticles by chemically controlled reduction for applications of inkjet-printed electronics. *Nanotechnology* 19:7.
- Lovern SB, Klaper R. 2006. *Daphnia magna* mortality when exposed to titanium dioxide and fullerene (C-60) nanoparticles. *Environ Toxicol Chem* 25:1132–1137.
- Lovern SB, Strickler JR, Klaper R. 2007. Behavioral and physiological changes in *Daphnia magna* when exposed to nanoparticles suspensions (titanium dioxide, nano-C-60, and C(60)HxC(70) Hx). *Environ Sci Technol* 41:4465–4470.
- McCord JM, Fridovich I. 1969. Superoxide dismutase: An enzymic function for erythrocyte hemocuprein. *J Biological Chem* 244:6049–6055.
- Meng H, Chen Z, Xing GM, Yuan H, Chen CY, Zhao F, et al. 2007. Ultrahigh reactivity and grave nanotoxicity of copper nanoparticles. *J Radioanalyt Nuclear Chem* 272:595–598.
- Mohandas J, Marshall JJ, Duggin GG, Horvath JS, Tiller DJ. 1984. Differential distribution of glutathione and glutathione-related enzymes in rabbit kidney – possible implications in analgesic nephropathy. *Biochem Pharmacol* 33:1801–1807.
- Novais S, Gravato C, Amorim MJB, Guilhermino L, Soares AMVM, De Coen W. 2009. Ecological relevance of oxidative stress biomarkers in *Enchytraeus albidus* (Oligochaeta): effects of zinc and cadmium. 19th Annual Meeting of SETAC Europe; Göteborg, Sweden.
- Oberdörster E. 2004. Manufactured nanomaterials (Fullerenes, C-60) induce oxidative stress in the brain of juvenile largemouth bass. *Environ Health Perspect* 112:1058–1062.
- Ohkawa H, Ohishi N, Yagi K. 1979. Assay for lipid peroxides in animal-tissues by thiobarbituric acid reaction. *Analyt Biochem* 95:351–358.

- Rault M, Mazzia C, Capowiez Y. 2007. Tissue distribution and characterization of cholinesterase activity in six earthworm species. *Comparat BiochemPhysiolB–BiochemMolecBiol* 147:340–346.
- Romani R, Antognelli C, Baldracchini F, De Santis A, Isani G, Giovannini E, et al. 2003. Increased acetylcholinesterase activities in specimens of *Sparus auratus* exposed to sublethal copper concentrations. *Chemico-Biolog Interact* 145:321–329.
- Rombke J, Moser T. 2002. Validating the enchytraeid reproduction test: Organisation and results of an international ringtest. *Chemosphere*. 46:1117–1140.
- Saint-Denis M, Narbonne, JF, Arnaud C, Ribera D. 2001. Biochemical responses of the earthworm *Eisenia fetida andrei* exposed to contaminated artificial soil: effects of lead acetate. *Soil Biology & Biochemistry* 33:395–404.
- Samim M, Kaushik NK, Maitra A. 2007. Effect of size of copper nanoparticles on its catalytic behaviour in Ullman reaction. *Bull Materials Sci* 30:535–540.
- Sampaio FG, Boijink CDL, Oba ET, dos Santos LRB, Kalinin AL, Rantin FT. 2008. Antioxidant defenses and biochemical changes in pacu (*Piaractus mesopotamicus*) in response to single and combined copper and hypoxia exposure. *Comparat Biochem Physiol C – Toxicol Pharmacol* 147:43–51.
- Scott-Fordsmand JJ, Krogh PH, Lead JR. 2008a. Nanomaterials in ecotoxicology. *Integrated Environ Assess Manage* 4:126–128.
- Scott-Fordsmand JJ, Krogh PH, Schaefer M, Johansen A. 2008b. The toxicity testing of double-walled nanotubes-contaminated food to *Eisenia veneta* earthworms. *Ecotoxicol Environ Safety* 616–9.
- SPSS. 1997. SigmaStat for windows version 3.5. SPSS Inc., Chicago.
- Scragg AH, Bonnett C. 2002. Inhibition of microalgal growth by silver nitrate. *Biotechnol Lett* 24:169–172.
- Thomas JP, Maiorino M, Ursini F, Girotti AW. 1990. Protective action of phospholipid hydroperoxide glutathione-peroxidase against membrane-damaging lipid-peroxidation –

- in situ reduction of phospholipid and cholesterol hydroperoxides. *J Biological Chem* 265:454–461.
- Tietze F. 1969. Enzymic method for quantitative determination of nanogram amounts of total and oxidized glutathione – applications to mammalian blood and other tissues. *Analyt Biochem* 27:502–522.
- Tong ZH, Bischoff M, Nies L, Applegate B, Turco RF. 2007. Impact of fullerene (C-60) on a soil microbial community. *Environ Sci Technol* 41:2985–2991.
- Tummala RR, Raj PM, Aggarwal A, Mehrotra G, Koh SW, Bansal S, et al.. 2006. Copper interconnections for high performance and fine pitch flipchip digital applications and ultra-miniaturized RF module applications. 56th Electronic Components & Technology Conference. Vol. 1 and 2, Proceedings 102–111.
- Unrine JM, Tsyusko OV, Hunyadi SE, Judy JD, Bertsch PM. 2010. Effects of particle size on chemical speciation and bioavailability of copper to earthworms (*Eisenia fetida*) exposed to Copper nanoparticles. *J Environ Qual* 39: 1942–1953.
- Varo I, Nunes B, Amat F, Torreblanca A, Guilhermino L, Navarro JC. 2007. Effect of sublethal concentrations of copper sulphate on seabream *Sparus aurata* fingerlings. *Aquatic Living Resources* 20:263–270.
- Velzeboer I, Hendriks AJ, Ragas AMJ, Van de Meent D. 2008. Aquatic ecotoxicity tests of some nanomaterials. *Environ Toxicol Chem* 27:1942–1947.
- Vieira LR, Gravato C, Soares AM, Morgado F, Guilhermino L. 2009. Acute effects of copper and mercury on the estuarine fish *Pomatoschistus microps*: Linking biomarkers to behaviour. *Chemosphere* 76:1416–1427.
- Vlahogianni TH, Valavanidis A. 2007. Heavy-metal effects on lipid peroxidation and antioxidant defence enzymes in mussels *Mytilus galloprovincialis*. *Chemistry and Ecology* 23: 361–371.
- Zhu SQ, Oberdörster E, Haasch ML. 2006. Toxicity of an engineered nanoparticle (fullerene, C-60) in two aquatic species, *Daphnia* and *Fathead minnow*. *Marine Environ Res* 62: S5–9.

Zhu XS, Zhu L, Lang YP, Chen YS. 2008. Oxidative stress and growth inhibition in the freshwater fish *Carassius auratus* induced by chronic exposure to sublethal fullerene aggregates. *Environ Toxicol Chem* 27:1979–1985.

Chapter III

**Effects of Cu-nanoparticles versus Cu-salt in
Enchytraeus albidus (Oligochaeta): Differential gene
expression through microarray analysis**

III - Effect of Cu-nanoparticles versus Cu-salt in *Enchytraeus albidus* (Oligochaeta): Differential gene expression through microarray analysis

Susana I.L. Gomes^a, Sara C. Novais^a, Janeck J. Scott-Fordsmand^b, Wim De Coen^c,
Amadeu M.V.M. Soares^a and Mónica J.B. Amorim^a

^aDepartment of Biology & CESAM, University of Aveiro, 3810–193 Aveiro, Portugal

^bDepartment of Bioscience, Aarhus University, Denmark

^cEcophysiology, Biochemistry and Toxicology group, Department of Biology, University of Antwerp, Campus Groenenborger, Groenenborgerlaan 171, B-2020 Antwerp, Belgium

Published in Comparative Biochemistry and Physiology., C (2011),

doi:10.1016/j.cbpc.2011.08.008

Abstract

Despite increased utilization of copper (Cu) nanoparticles, their behaviour and effect in the environment is largely unknown. Enchytraeids are extensively used in studies of soil ecotoxicology. Ecotoxicogenomic tools have shown to be valuable in nanotoxicity interpretation. A cDNA microarray for *Enchytraeus albidus* has recently been developed, which was used in this study. We compared the gene expression profiles of *E. albidus* when exposed to Cu-salt (CuCl₂) and Cu-nanoparticles (Cu-NP) spiked soil. Exposure time was 48 h with a concentration range of 400 to 1000 mg Cu/kg. There were more down-regulated than up-regulated genes. The number of differently expressed genes (DEG) decreased with increasing concentration for CuCl₂ exposure, whereas for Cu-NP, the number did not change. The number of common DEG decreased with increasing concentration. Differences were mainly related to transcripts involved in energy metabolism (e.g. monosaccharide transporting ATPase, NADH

dehydrogenase subunit 1, cytochrome c). Overall, our results indicated that Cu-salt and Cu-NP exposure induced different gene responses. Indirect estimates of Cu-NP related ion-release indicated little or no free Cu²⁺ activity in soil solutions. Hence, it was concluded that the Cu-NP effects were probably caused by the nanoparticles themselves and not by released ions.

Keywords: Toxicogenomics, Gene expression profile, Copper salt, Copper nanoparticles, Oligochaeta

1. Introduction

Copper nanoparticles (Cu-NP) have been given considerable attention due to their properties, e.g. high electrical and thermic conductivities, which make them very useful in modern electronics, metallurgy and catalysis (Dhas et al., 1998; Tummala et al., 2006; Samim et al., 2007; Lee et al., 2008b). In organisms, copper (Cu) is known to cause oxidative damage via the Haber -Weiss reaction, catalyzing the formation of the powerful oxidant hydroxyl radical (OH[•]) (Bremner, 1998). For example, a recent investigation suggests that Cu exposure at sub-lethal concentrations affects mitochondrial function, with a clear alteration of energy metabolism with a switch to metabolism of stored carbohydrates (Bundy et al., 2008). The environmental effects of Cu-NP are still poorly known. When compared to soluble Cu, Cu-NP were less toxic to ICR mice (LD₅₀ of 110 and 413 mg/kg respectively) (Chen et al., 2006, 2007; Meng et al., 2007) and *Danio rerio* (EC₅₀ of 0.25 mg/L and 1.6 mg/L respectively) (Griffitt et al., 2007). Results obtained by Griffitt et al. suggest that the transcriptional response induced by Cu-NP was different from the response induced by the dissolved Cu salts, indicating that the effects of Cu-NP were not caused by the Cu ions alone (Griffitt et al.,

2007, 2009). Poynton et al. (2011) reached similar conclusions when studying the effects of zinc oxide NPs (ZnO-NP) and zinc sulfate (ZnSO₄) in *Daphnia magna* gene expression. They concluded that the gene expressions profile (unique to each of the Zn forms tested) indicated that Zn-NPs and ZnSO₄ caused effects through distinct mechanisms. It has also been observed that exposure to nanoparticles (Ag and Cu) induced a higher number of differentially expressed genes than the comparative salt form (Griffitt et al., 2009). Comparing the effects of silver (Ag) NPs with Ag ions in *Saccharomyces cerevisiae*, Gu et al. (2011) observed that longer exposure to Ag NPs (210min.) caused an expression pattern similar to that caused by exposure to Ag ions, however, unique patterns were observed at shorter periods of exposure (120 min.). These studies, as well as (Henry et al., 2007; Griffitt et al., 2009; Roh et al., 2009), all reported that a distinct gene expression profile occurred due to nano and non-nano forms. Hence, toxicogenomic studies have indicated different mechanisms of action and highlighted their relevance to study nanotoxicology, differentiating between NP and ionic exposure.

Besides this very limited number of toxicogenomic studies with nano particle exposed organisms, limited information is currently also available regarding the general effects of nano materials in terrestrial ecosystems (Tong et al., 2007; Johansen et al., 2008; Lee et al., 2008a; Scott-Fordsmand et al., 2008a,b; Lapied et al., 2010; Unrine et al., 2010a,b).

The terrestrial ecosystem contains a wide number of species. Among those used in ecotoxicology, enchytraeids (Oligochaeta) are some of the most important members of the soil fauna (Rombke and Moser, 2002). They are abundant in many soils, contributing to the improvement of the pore structure of the soil and, indirectly, to the degradation of organic matter (Amorim et al., 2005b). Traditionally, effect assessment

is made at the population level (ISO, 2005), evaluating e.g. survival and reproduction. Recently, a cDNA microarray for the enchytraeid *Enchytraeus albidus* has been developed, which allows toxicogenomic studies for this species (Amorim et al., 2011). DNA microarrays provide a powerful tool for analyzing gene responses in organisms exposed to stressors present in the environment. Through the quantification of the expression of thousands of genes in a single experiment (Rockett and Dix, 1999; Lettieri, 2006), it is possible to identify a cellular mechanism that may be altered/damaged during the stress exposure. The measurement of these responses can elucidate the mechanisms of action and also serve as a signal/marker for potential effects at the population level. Hence, as seen from the few toxicogenomic studies (see previous paragraph) with nano materials performed in other species, there is a clear indication that employing microarray studies on enchytraeids will also provide useful information in regard to cellular stress.

Therefore, in the present study, the main objective was to compare the effect of Cu salt (CuCl_2) versus Cu-NP at the gene level in *E. albidus*. The worms were exposed to a range of Cu-salt and Cu-NP concentrations for which the worm gene expression profile was analyzed using a cDNA microarray supported by qPCR. The responses were subsequently compared.

2. Materials and methods

2.1. Experimental procedure

For this experiment, nine treatments, each with four replicates, were employed. The treatments were one control (no added Cu), four CuCl_2 treatments (400, 600, 800 and 1000 mg Cu/kg) and four Cu-NP treatments (400, 600, 800 and 1000 mg Cu/kg). The CuCl_2 and Cu-NP (in aqueous solution) were added directly to individual replicates. For

each replicate, the stock solution was homogeneously mixed into the soil, each replicate containing 25 g moist soil (40 to 60% of the maximum Water Holding Capacity-WHC). The soil was introduced into the test vessel, and fifteen adult worms with well developed clitellum were introduced in each vessel (replicate). The vessels were covered with a lid (containing small holes) and the worms were exposed for 48 h at 20 °C with a 16:8 h photoperiod. At test end, all the animals were carefully removed, rinsed in deionised water, stored in RNA later (Ambion, USA) and frozen in liquid Nitrogen. The animals were not depurated, as this has no influence on the measures. Samples were stored at –80 °C.

2.2. Test organisms

Enchytraeus albidus, Henle 1837 were used; they were maintained in laboratory cultures under controlled conditions, e.g. photoperiod 16:8 h light:dark and a temperature of 18 °C. Details of culturing are given in Rombke and Moser (2002).

2.3. Test soil

The test soil used was a field collected soil from Hygum, Denmark. The general physico-chemical characteristics of the soil were as follows: 20–32% coarse sand (N200 µm), 20–25% fine sand (63–200 µm), 11–20% coarse silt (20–63 µm), 12–20% silt (20–20 µm), 12–16% clay (<2 µm) and 3.6–5.5% humus. The soil was sampled to a depth of 20 cm. To exclude soil fauna, the soil was sterilized by drying at 80 °C for 24 h in an oven (Memmert, Type UL40, Braunschweig, Germany) and then sieved through a 2 mm mesh to remove larger particles. The “background” Cu concentration for the Hygum soil was 30mg Cu/kg dry soil.

2.4. Chemical substance and spiking

The nanoparticles were made of Cu with a mean diameter of 80 nm, (PW-XRD<74 nm, DLS=419±1 nm, Zeta=15.3±0.3) and a purity of 99.5% (Heckmann et al., 2011). The nanoparticles were added to the soil following transfer to deionised water and ultrasonic steering for 15min. This Cu-NP solution was then added immediately to the soil, one for each replicate, with the soil being thoroughly (by appearance) mixed with a spatula. The authors are aware of the issues that NP may settle fast in solutions, hence, it was ensured that the entire volume was transferred to the soil. Filtering or dialysis was not performed, as once the NPs are in the soil the conditions change and any possible dissolution will be different than in stock solution (as discussed by (Scott-Fordsmand et al., 2008a)).

The Cu-salt was CuCl₂ (Sigma-Aldrich, Brøndby, Denmark) which was dissolved in water. The concentrations were selected based on previous toxicity test results at population level (survival, reproduction and avoidance) with Cu-salt (Amorim et al., 2005a, 2008). Concentrations used were 400, 600, 800 and 1000 mg/kg of Cu-salt and Cu-NP, representing concentration–response series around the 50% effect on the reproduction (EC₅₀).

The total Cu was verified by flame Atomic Absorption Spectrometry (Perkin Elmer 4100, Ueberlingen, Germany) using 7 N HNO₃ and heating up to 110 °C (as described by Scott-Fordsmand et al.(2000)). To estimate the activity of free unbound Cu²⁺ from the nanoparticles, an ion selective electrode (ISE25Cu, Radiometer) in combination with the reference electrode (REF251, Radiometer) equipped with a double salt bridge was used. The inner salt bridge contained saturated KCl, and the outer salt bridge contained 0.1 M KNO₃. A standard curve was made using Cu(NO₃)₂, detection limit of the ion selective electrode was 362.4 nM. The free ion activity was measured on a

solution of 100 mg Cu-NP/L deionised water (same as stock solution) after up to an 8 day period using three replicates, all measures were below detection limit. In a concurrent experiment, the activity of Cu²⁺ for the Cu-NP was measured partly in a water solution with the same ionic strength as in the soil (measured in the Hygum soil solution) and partly in a full soil solution (1 soil:5 water), both the measures were below the detection limit/limit of quantification. This is equivalent to less than 4.6 µg Cu/kg (less than 0.005% of the total Cu²⁺) being active in the soil solution, as measured by the electrode.

2.5. RNA extraction

Total RNA was isolated through TRIzol extraction method (Invitrogen, Belgium), followed by a DNase treatment (Fermentas, Germany). The quantity and purity of the isolated RNA were measured spectrophotometrically with nanodrop (NanoDrop ND-1000 Spectrophotometer), and its quality was checked on a denaturing formaldehyde agarose gel electrophoresis. Total RNA was extracted from four biological replicates per treatment and pooled in equal amounts per replicate (20 µg RNA). From this pool, 7 µg of RNA was used to synthesize cDNA, as described in the next section. Pooling of RNA samples offers a strategy to reduce microarray data-noise from biological sample variability, reducing sample-to-sample variability (Wang et al., 2008). This is even more important when the goal is to identify markers or expression patterns across individuals (as in the present study) and is not focused on individuals. One of the disadvantages of pooling is the inability to estimate within population variation (Kendzierski et al., 2005), but for purposes of identification of differentially expressed genes, pooling has shown no disadvantage when the number of pooled individuals was high (as in our case=15×4) and technical replicates were performed (Kendzierski et al., 2005).

2.6. cDNA synthesis and Aminoallyl labeling

Briefly, 7 µg of total RNA (pool from the four replicates) and Lucidea control mRNA spike mix (GE Healthcare, Amersham) was reverse-transcribed using 200 U/µL Superscript II (Invitrogen), random hexamer primers (Invitrogen) and the aminoallyl-dNTPs mix (containing a 2:3 ratio of aminoallyl-dUTP (Invitrogen)). Unincorporated aminoallyl dUTPs were removed using modified Qiagen PCR spin column protocol. Aminoallyl labeled cDNA was covalently bound to appropriate NSH-esters Cy Dyes (Amersham). Cy3 was coupled with control and Cy5 with treatments. Uncoupled dyes were removed using the QIAquick PCR purification kit (Qiagen). The efficiency of labeling reaction was measured spectrophotometrically with Nanodrop. The samples with a FOI (Frequency Of Incorporated dye) between 20 and 50 were selected for hybridization and 150 pmol labeled cDNA was vacuum dried.

2.7. Hybridization of microarrays

E. albidus cDNA microarray used in this study was developed by Amorim et al. (2011). Triplicates of each cDNA fragment were spotted onto Generoma microarray slides (Asper Biotech, Estonia) using the spotter MicroGrid Compact (Biorobotics). In addition, a set of artificial control genes (Lucidea Universal Scorecard, GE Healthcare, UK), containing calibration, ratio and negative control genes, was spotted over the arrays in 15 replicates to ensure evaluation of the dynamic range, sensitivity and non-specific hybridization. After rehydration and drying, the slides were cross-linked by UV-radiation at 300 mJ (UV Stratalinker 2400; Stratagene, USA). Before the hybridization, arrays were incubated in pre-hybridization buffer, consisting of 50% formamide, 5×SSC, 0.1% SDS and 0.1 BSA, at 42 °C for 60 min. After that, the arrays were washed by immersion in ultra-pure water followed by immersion in isopropanol and immediately dried with compressed N₂. The vacuum dried samples were resolved in

hybridization solution consisting of 50% formamide, 5×SSC, 0.1% SDS and 0.1 mg of salmon sperm, a nucleic-acid blocker. The probe solutions (result of the combination of Cy3 and Cy5 labeling probes), incubated at 95 °C for 5 min, were then applied on the arrays. The arrays were placed in Genetix hybridization chamber at 42 °C overnight. After hybridization, the arrays were immersed in four wash solutions containing decreasing concentrations of SSC and SDS, in MilliQ water and in isopropanol and immediately dried in compressed N₂. Three array replicates per treatment were performed, hybridizing each treatment sample versus the control sample.

2.8. Scanning and analysis of microarray data

Scanning was performed using an Agilent Microarray Scanner (Agilent Technologies) at 532 and 635 nm for Cy3 and Cy5, respectively. The images acquired were assessed using QuantArray (Packard Biochip Technologies) for spot identification and quantification of fluorescent signal intensities; similar values were selected for quality control. Subsequently, data was statistically analyzed using limmaGUI package (based on limma (Smyth, 2005)) in the R (2.8.0) software environment (<http://www.R-project.org>). After being submitted to local background subtraction, microarrays were normalized using global loess method (Yang et al., 2002). Quality control was done by making MA-plots and box plots of each array. Based on these quality criteria, one replicate was excluded from the final analysis of Cu-NP 600 and Cu-NP 1000. Differential expression was assessed using linear models and Benjamini–Hochberg's (BH) method to correct for multiple testing (Benjamini and Hochberg, 1995) (adjusted $p < 0.05$ was considered significant). Assessment of differential expression of genes was done for each treatment separately and resulted in a mean log₂ expression ratio (treated/untreated) and a p-value for each probe on the array. All cDNA fragments correspondent to differentially expressed genes (adjusted $p < 0.05$) and for which the

sequences were known (GenBank accession numbers: GT066377 to GT066724) were searched for homology to sequences in the National Center for Biotechnology Information (NCBI) database, as determined by the Basic Local Alignment Search Tool (BLAST). Both nucleotide-nucleotide and nucleotide-protein homology searches were done to identify the isolated clones (BLASTN and BLASTX). The MIAME compliant data from this experiment were submitted to the Gene Expression Omnibus (GEO) at the NCBI website (platform: GPL11360; series: GSE26331). Clustering analysis was performed using MultiExperiment Viewer (MeV, TIGR).

2.9. *Quantitative PCR*

Total RNA (500 ng) from the samples used for microarrays was converted into cDNA through a reverse transcription reaction using the SuperScript First-Strand Synthesis System for RT-PCR (Invitrogen). Quantitative (real time) PCR was carried out on 7500 Real-Time PCR System (Applied Biosystems), using Platinum SYBR Green qPCR SuperMix-UDG (Invitrogen). Primer sets were designed for 5 target genes and one endogenous control gene (Table 1) with the software Oligo Explorer™ (version 1.1.0). Determination of PCR efficiency and specificity was done by observing the obtained standard and melting curves, respectively, for all primer sets. The cDNA was 4× diluted and 2 µL were used in 20 µL PCR reaction volumes containing 2 µL of forward and 2 µL of reverse primers (2 µM), 10 µL of Platinum SYBR Green qPCR SuperMix-UDG (Invitrogen) and 4 µL of DEPC water. qPCR was performed in triplicate for each sample, on a 96-well optical plate (GeneAmp®, Applied Biosystems). Reaction conditions consisted of one initial cycle at 50 °C for 2 min, followed by one denaturation step at 95 °C for 2 min, 40 cycles at 95 °C for 10 s, and a dissociation step consisting of 15 s at 95 °C, 1 min at 60 °C, and 15 s at 95 °C. A mean normalized expression value was calculated from the obtained Ct values with Relative Expression

Software Tool (REST-MSC), using β -actin as a reference gene for normalization of input cDNA. Spearman's Rho nonparametric correlation was performed on log₂ transformed ratios using SAS software (2003) to compare microarray with qPCR data.

Table 1: Primer sequences used for qPCR gene quantification

	Accession number	5' – 3' Forward primer	5' – 3' Reverse primer
actine	-	CAGGGAAAAGATGACCCAAA	AAACCCAGTAGAAAAGGGAC
SOD	GT066724	TCAACCAAAGAGCGGC	CGCGTGAATCACAATCG
CaDPK	GT066419	AAAGGGTCGGCAGAATTGG	AAGGCGCGGAACCTCTATCC
TransFact	GT066480	AGTTTTCTCAAATCATCAAA	AGACTTCACCAACCTATTGCG
Cyt c	GT066613	CGGAAGGTGATGCTGAGAAG	CGTCTCCTTCGTCCATTG
HSPA8	GT066659	TG TTCAGGTTCTTTAACC	GTTTTCTTTTATTGCACC

3. Results

The total Cu concentration was confirmed, with less than 5-7% variation on all concentrations. For both Cu exposure forms, the Cu activity in soil solution was less than 4.6 μ g Cu/kg soil, as measured by ion-selective electrode (ISE25CU). As Cu-NPs were clearly visible in the stock solution, they entered the soil as full (or partial) particles.

It is well known (and observed) that CuCl₂ will be fully dissolved in the stock solution and once in soil strongly bound to soil constituents. All animals survived in all exposure concentrations and replicates. Using linear models and empirical Bayes methods (Smyth, 2005), a total of 208 in 480 gene fragments were identified as differentially expressed (BH adjusted $p < 0.05$) in at least one of the treatments. Fig. 1 shows an

overview of the differentially expressed genes for the various treatments. Cu-salt treatments caused 109, 26, 15 and 7 significant transcripts and Cu-NP 63, 3, 68 and 46, for the concentrations of 400, 600, 800 and 1000 mg/kg, respectively. No additional fold-change cutoff was used to identify differentially expressed genes, since slight changes in gene expression could also result in major physiological effects (Nota et al., 2008). All the differentially expressed genes with respective GO annotation can be found in Table S1 of the Supplementary data.

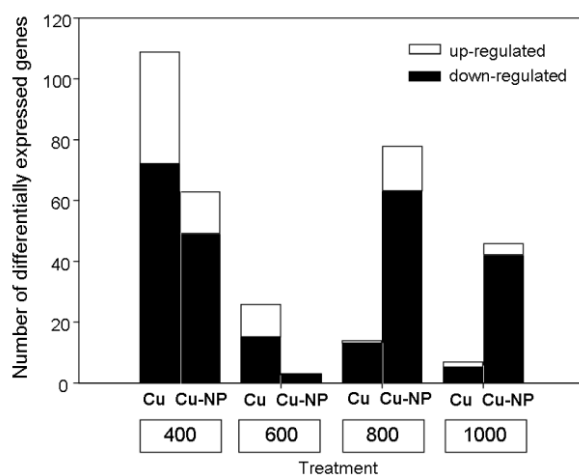


Figure 1: Number of differentially expressed genes after exposure to different concentrations (400, 600, 800 and 1000 mg/Kg) of Cu-salt (Cu) and Cu-NP.

Overall, there are more down than up-regulated genes. For Cu-salt treatment, there is a decrease in the number of differentially expressed genes with concentration increase, whereas for Cu-NP this pattern is not observed.

All the differentially expressed transcripts have previously been sequenced (Amorim et al., 2011) and were subjected to recent BLAST homology search. Only 55 of the 208 differentially expressed gene fragments had homology to sequences in public databases.

From these 55 sequences, 8 had unknown or uncategorized functions, and the remaining 47 could be classified in functional categories (% of total number of genes with homology): transcription and translation (29.1%), energy metabolism (21.8%), immune and stress response (9.1%), development (5.4%), signal transduction (7.3%), carbohydrate and fat metabolism (5.4%), protein metabolism (5.4%), and cell structure and cytoskeletal organization (1.8%) (Fig. 2).

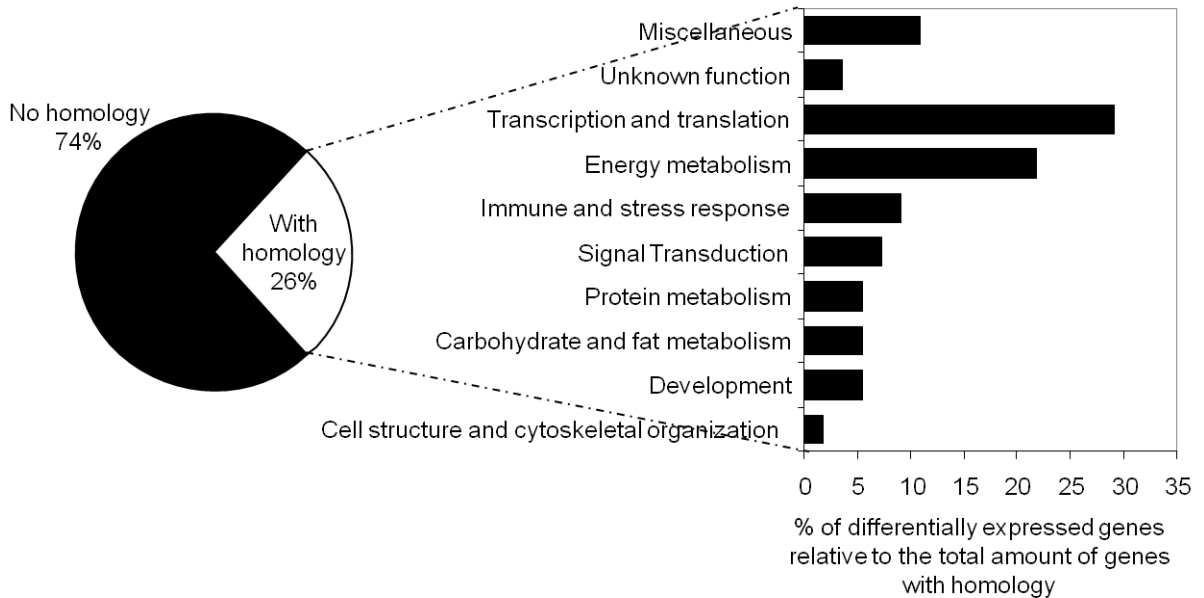


Figure 2: Schematic representation of all unique and known differentially expressed genes subdivided into functional classes according to their GO annotation.

To compare the response of each treatment (Cu-salt and Cu-NP) and the different concentrations tested, results can be depicted in the Venn diagrams in Fig. 3 representing the genes affected uniquely by one treatment and the overlapping genes (genes affected by more than one treatment).

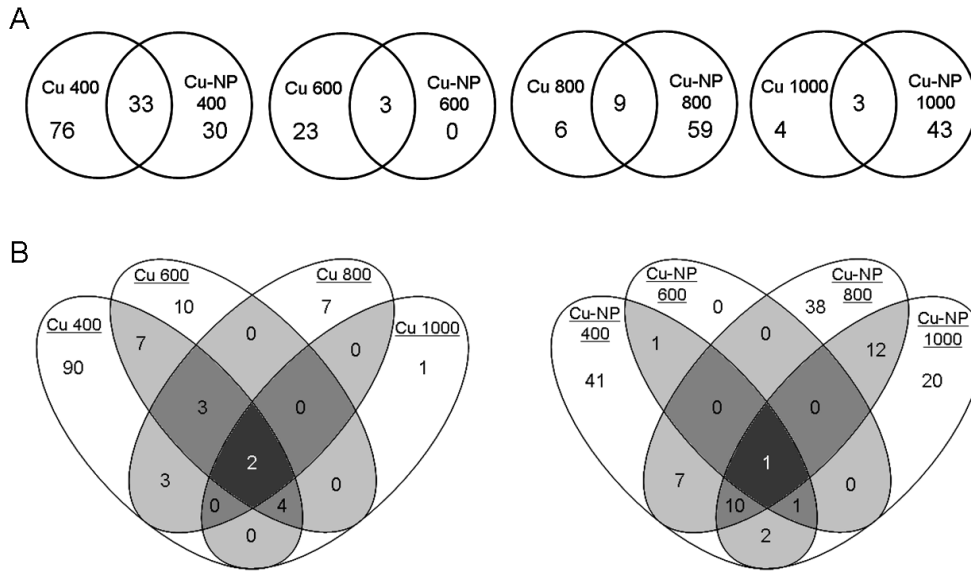


Figure 3: Venn diagram representation of the number of differentially expressed genes (BH adjusted, $p < 0.05$) shared by equal concentrations (400, 600, 800 and 1000 mg/Kg) of the different treatments (A), and shared by the different concentrations in each treatment (B) Cu-salt (Cu) and Cu-NP.

When comparing similar concentrations between the two Cu forms (Fig. 3A), the number of overlapping genes (indicative of a common response) is higher at low concentrations than at high concentrations. When focusing on each individual treatment (Fig. 3B), for both Cu-salt and Cu-NP a different set of genes is triggered at various concentrations, although with no homology to known function.

Based on the differentially expressed genes (BH adjusted, $p < 0.05$), a cluster analysis (Pearson's uncentered with average linkage) was performed, including both genes and treatments. The cluster analysis of genes did not group according to function (GO homology), lack of clarity may be due to high number of genes without known function (data not shown). Cluster between treatments is shown in Fig. 4.

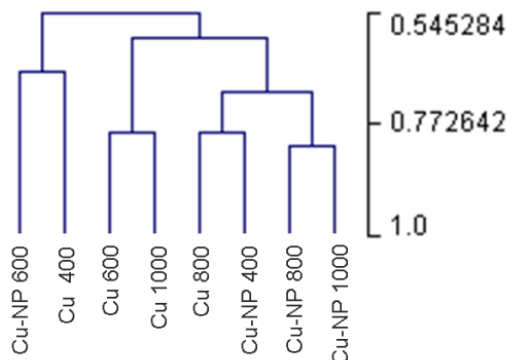


Figure 4: Hierarchical cluster of samples (Perarson's uncentered), based on differentially expressed genes (BH adjusted, $p < 0.05$).

Cluster analysis of treatments shows evidence of grouping of the two different Cu forms. Additionally, it is observed that Cu 400 and Cu-NP 600 are distant from the rest. If excluding Cu-NP 600 from the analysis as an outlier [which is an intermediate exposure concentration with very few genes expressed (see Fig. 1)], there are no changes in the clustering of the other treatments (figure not shown). The clustering position of the Cu-NP 600 is, possibly, due to the much lower number of differentially expressed genes in this intermediate treatment (Fig. 1) rather than a change in gene expression profile. A K-means clustering analysis (based on all differently expressed genes, see Table S1 of the Supplementary data) was performed to identify groups of possibly co-regulated genes and to see how their regulation changes over treatments (Fig. 5).

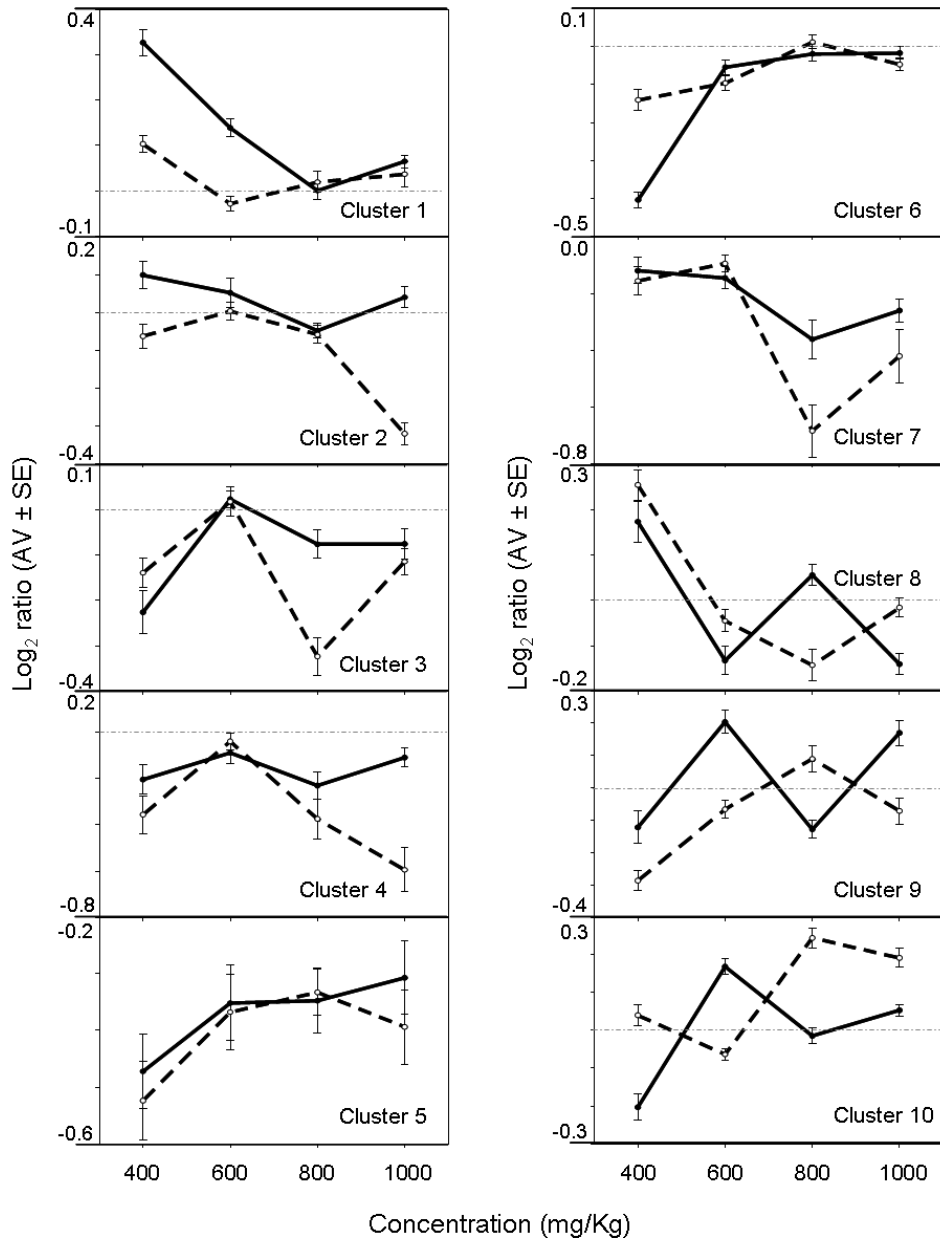


Figure 5: K-means clustering of the differentially expressed genes after exposure to Cu-salt (continuous line) and Cu-NP (dashed line).

K-means clustering analysis shows that there are clusters (groups of genes) where the expression trend is similar for both Cu forms and there are clusters where the trend is different. All the genes included in each cluster can be found in Table S2 of the Supplementary data.

Different expression trends were mainly visible in clusters 9 and 10 (Fig. 5). In these two clusters are included several genes involved in energy metabolism (e.g. cytochrome c, short-chain dehydrogenase and NADH dehydrogenase Fe–S protein 4) and fewer involved in transcription and translation (e.g. ribosomal protein L7A). In the rest of the clusters (Fig. 5), the gene expression patterns are similar between the two Cu forms. It should be noted that despite the overall pattern being similar, there are differences in gene expression intensity, for example, in cluster 1, Cu-salt causes more up-regulation than Cu-NP, while in clusters 4 and 7, Cu-NP causes more down-regulation compared with Cu-salt.

In the present study, five genes were qPCR quantified for all tested treatments, making a total of 40 confirmations (4 concentrations/2 treatments/ 5 genes). Genes to be confirmed were selected based on the following criteria 1) microarray differential expression; 2) homologous to known and different function. Selected genes were superoxide dismutase (SOD), calcium dependent protein kinase (CaDPK), heat shock protein 8 (HSPA8), cytochrome c (Cyt c) and transcription factor (TransFact). In 70% of the genes, the expression pattern was confirmed by qPCR and a significant correlation was obtained (Spearman's Rho): $r^2=0.40$, $n=40$ and $p=0.0108$. Fig. 6 shows the expression values obtained by microarray and qPCR analysis for two selected concentrations, 400 and 800 mg/kg. Further gene confirmation has been performed in previous studies and overall results showed a significant correlation (Spearman's Rho): $r^2=0.69$, $n=12$ and $p=0.0126$ (Amorim et al., 2011).

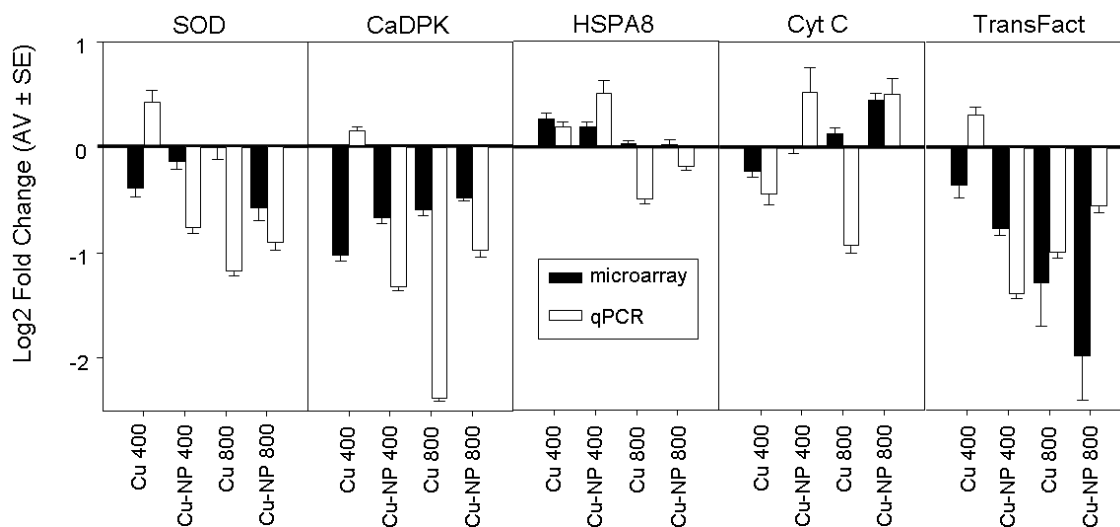


Figure 6: Graphic representation of log₂ fold change obtained for the genes superoxide dismutase (SOD), calcium-dependent protein kinase (CaDPK), heat shock 8 (HSPA8), cytochrome c (Cyt c) and transcription factor (TransFact) in microarrays (black) and qPCR (white) after exposure of *Enchytraeus albidus* to Cu-salt (Cu) and Cu-NP at concentrations 400 and 800 mg/Kg.

4. Discussion

The Cu-salt and Cu-NP exposures caused changes in the gene expression profile of *E. albidus* within the tested range of concentrations. The main difference in terms of total differently expressed gene number is related to its distribution along concentrations. For Cu-salt exposure, a negative concentration–response relationship was observed, i.e. a decrease in the number of differentially expressed genes with increasing concentration. For Cu-NP exposure, there were a similar number of differentially expressed genes at all concentrations. For Cu-salt, this seems to correspond to the results obtained at the population level (survival, reproduction and avoidance), where exposure to 10-1000 mg Cu-salt/kg showed a gradual increase in effects (Amorim et al., 2005a, 2008). It has been previously observed that lower exposure concentration causes higher number of differentially expressed genes than higher concentrations. Nota et al. (2009) observed this in the soil-dwelling *Folsomia candida* in response to phenanthrene. Authors suggest

that this may be the result of a reallocation of animals' energy to the production of biotransformation enzymes (to cope with phenanthrene toxicity) in detriment of less essential cellular processes. In the present experiment, organisms were exposed to 800 and 1000 mg Cu-salt/kg, which was 8-10 times higher than the 42 days reproduction EC_{50} (97 mg/kg) (Amorim et al., 2005a). Although no organism died, the decrease in gene response could be indicative of a “death” effect. The fact that Cu-NP does not show a concentration–response pattern in total gene expression may be due to a slower (or lower) effect of Cu-NPs.

For Cu-salt (Fig. 3B) exposure, it was observed that the majority of the genes affected by the two highest concentrations were shared with other concentrations. As suggested by other authors, this could be due to the decrease in the specificity of gene responses to higher toxic concentrations (Poynton et al., 2008), probably because the prevalent genes are related to general stress and cell death (Gou et al., 2010). The same pattern was not so clear with Cu-NPs.

Working with metal NPs, a partial (or full) ionization of the NPs may take place, which could explain the induction of similar genes for Cu-NP and Cu-salt. However, we observed that the Cu-NP induced a specific response (Fig. 3A). Hence, although it is indicated that the effects present in the Cu-NP exposed organisms are partially or fully caused by nanoparticles, it must be realised that release of ions (from NP) may play a significant role. At present, there is no method to verify and quantify this release directly in situ. Unrine et al. (2010b) observed that Cu-NPs remained as particles both in soil and in earthworm tissue following Cu-NPs exposure. Our dissolution experiments indirectly support the theory that it is the Cu-NPs causing effects, since the Cu-activity was near or below detection limits in the solutions. For the soil-solution, the NPs could, of course, have a full dissolution not detected due to a complete binding of

ions to dissolved organic matter. This is in accordance with the results mentioned by Griffitt et al. (2007), who observed that effects of Cu-NP were not caused by the Cu soluble fraction alone.

As shown in the Venn diagram for Cu-NP versus Cu-salt, there were 3–9 common genes at high exposure concentrations and 33 at lower exposure concentrations. Additionally, different concentrations triggered different sets of genes. Nota et al. (2009) also observed that few genes were shared between the two tested concentrations of phenanthrene compared to the total of the differentially expressed genes. However, they observed that many of the transcripts responding to each individual concentration shared similar putative functions.

Our results indicate the same, but many of the genes have no homology to known functions, therefore is not possible to fully corroborate this conclusion. Overall there is an indication that there are different underlying mechanisms of toxicity for Cu-salt and Cu-NP, mainly depicted by the different set of differently expressed genes at higher tested doses.

Cluster analysis indicated a grouping between Cu-salt and Cu-NP. This analysis also shows the separation of Cu-NP 600 and Cu-salt 400 from the other concentrations, both mainly due to having a very different number of differently expressed genes when compared to the other treatments. Cu-NP 600 had a very low number, and Cu-salt had a very high number. We are unaware of an explanation for the very low number of differentially expressed transcripts observed at 600 mg/kg Cu-NP. We cannot find a technical reason, since the MA-plots of the slides met the quality criteria.

Given that *E. albidus* is a non genome-model organism in which the gene-library is small and the function of many of the genes is unknown, this may be the reason for the lower discrimination power between Cu forms.

In the next paragraphs, we will discuss the gene expression profile, keeping in mind that microarrays alone are semi-quantitative. In particular, if the expression differences are only of a few orders of magnitude, such expressions are less likely to be relevant (or confirmed by qPCR), as acknowledged by many studies.

In terms of differences in gene expression profile between Cu-NP and Cu-salt, the most noticeable was in the transcripts involved in the energetic metabolism of *E. albidus*. Earthworm (*Lumbricus rubellus*) gene expression changes associated with mitochondrial electron transport due to Cu exposure, as also reported by Bundy et al. (2008). Our data showed that Cu-NP exposed *E. albidus* had down-regulation of ATP synthase E chain and NADH dehydrogenase subunit 1, but an up-regulation of cytochrome c (confirmed by qPCR, Fig. 6) and NADH-dehydrogenase Fe-S protein 4 (all mitochondrial proteins). On the other hand, Cu-salt exposed *E. albidus* had down-regulation of cytochrome c (confirmed by qPCR, Fig. 6) and short-chain dehydrogenase, but an up-regulation of ATP synthase E chain, cytochrome c subunit VI c and NADH-ubiquinone oxidoreductase. Hence, both Cu forms seem to affect the mitochondrial electron transport system, which is similar to Bundy's results (Bundy et al., 2008). Interestingly, organisms exposed to the two Cu forms triggered different genes from same GO category. It is also suggested that mitochondrial dysfunction leads to a switch to metabolism of stored carbohydrates after Cu exposure leading to the up-regulation of transcripts involved in carbohydrate metabolism (Bundy et al., 2008). These changes in energy metabolism accompanied by a decrease in lysosomal integrity are indicative of membrane damage (Bundy et al., 2008). This effect is a well-known Cu effect, which was also verified in *E. albidus* in a previous study where Cu exposure caused increased lipid peroxidation (Gomes et al. 2011). In addition, an up-regulation of the carbohydrate and fat metabolism related transcripts was observed, i.e.

monosaccharide transporting ATPase by Cu-NP and beta-1,3-glucase by Cu-salt. Related to transcription and translation processes, the differences between Cu-salt and Cu-NP are mainly in the up-regulated genes, i.e. for Cu-salt zinc finger transcription factor (snail 2 gene), eukaryotic translation termination factor 1, and for Cu-NP ribosomal protein L26. Independent of its specific function (translation termination, initiation or splicing), all of these transcripts are involved in cell division, development and differentiation. Regarding the up-regulation of ribosomal protein L26, which is associated with the 60S subunit of the ribosome, it is known that the ratio of rRNAs to ribosomal proteins is tightly regulated within the cell, and an excess or reduction in either component can disrupt ribosome assembly (Nusspaumer et al., 2000). Ribosome biogenesis and stability within the cell is associated with proliferation, cell growth and stress response, with the last most likely being the cause for the up-regulation of the ribosomal protein L26.

In regard to similarities, several genes encoding transcription/translation related proteins were down-regulated following both Cu-salt and Cu-NP exposure. These transcripts include: transcription factor, ribosomal protein (L34A-isoform A), pre-mRNA processing factor 8, small nuclear ribonucleoprotein D2, poly (ADP-ribose) polymerase member 14, and elongation factor-1 α (EF-1 α). This suggests that Cu is causing a serious impairment in translational processes. For example, the poly ADP-ribose polymerase member 14 (PARP14) is a multifunctional protein involved in many cellular functions. These PARP proteins are important components in the cellular responses to various kinds of DNA insults, including oxidative DNA damage, telomere erosion, or improper segregation of chromosomes. The observed down regulation of EF-1 α , an actin binding protein involved in the shuttling of aa-tRNA, was also observed in fathead minnow larvae when exposed to Cu (Lewis and Keller, 2009), and in recent investigations, its

down-regulation has been related with cell death (Byun et al., 2009; Kobayashi and Yonehara, 2009). Some transcripts involved in protein metabolism were regulated similarly by both Cu forms; the calcium dependent protein kinase and 20S proteasome (20S P) alpha subunit were both down-regulated (except for Cu-salt 400, where qPCR shows a slight up-regulation of CaDPK). The protein kinases play a role in a multitude of cellular processes, including division, proliferation, apoptosis and differentiation, which could be affected by the down-regulation of genes coding for these proteins. The down-regulation of 20S proteasome alpha subunit indicates the impairment of a very specific function, given proteasome subunits are responsible for cleavage of peptide bonds with high specificity. In the lower concentration tested (400 mg/kg), both forms of Cu caused the up-regulation of the heat shock protein 8 (HSPA8) (confirmed by qPCR, Fig. 6). The gene HSPA8 encodes a heat shock cognate protein (that belongs to the heat shock protein 70 family) which binds to emerging polypeptides to facilitate correct folding. The up-regulation of transcripts encoding heat shock proteins has already been observed in response to metals (Nota et al., 2008). As suggested for cadmium (Nota et al., 2008), Cu ions probably disturb the normal folding of proteins or cause indirect damage to proteins, e.g. through the generation of reactive oxygen species (ROS). Copper is also known to cause oxidative damage through the formation of hydroxyl radicals (Bremner, 1998), thus, the up-regulation of genes coding for antioxidant defence-related proteins would be expected. However, the transcript encoding SOD was found down-regulated (in both forms of Cu and confirmed by qPCR with exception for Cu-salt 400, Fig. 6). A previous study (Gomes et al., 2011) with *E. albidus* exposed to Cu-salt and Cu-NP for 2, 4 and 8 days also showed no changes in the enzymatic activity of SOD, even there was oxidative damage at 8 days exposure, indicating the impairment of the anti-oxidant defences of *E. albidus*.

5. Conclusions

Common genes were observed, indicating a common response mechanism, particularly at lower concentrations, but clearly Cu-NP exposed worms showed NP specific genes. The main difference in terms of total number of differently expressed genes is related with its distribution along concentrations: for Cu-salt exposure, a negative concentration–response relationship was observed, with a decrease in the number of differentially expressed genes with increasing concentration. In general the Cu-NP exposure showed a similar number of differentially expressed genes at all concentrations. These NP specific transcripts are mainly involved in the worms energy metabolism (e.g. monosaccharide transporting ATPase, ATP synthase E chain, NADH dehydrogenase subunit 1, cytochrome c, NADH-dehydrogenase Fe–S protein 4), are also stress related (SOD) and involved in transcription and translation (e.g. ribosomal protein L26). However, further studies are needed to get more quantitative measures of gene-expression, e.g. extensive qPCR of the identified responsive genes. In addition, studies on the exact toxico-kinetics for Cu-NP are needed, i.e. how particles behave (e.g. remain/dissolve) in the cells and bind to the target site.

Supplementary materials related to this article can be found online at doi:
10.1016/j.cbpc.2011.08.008.

Acknowledgments

The authors would like to acknowledge all the support provided by Patricia Pereira during the qPCR analysis. The project was financially supported by the Nordic NKG through the “Nordic group regarding health and environmental risk of nano materials” and by the funding FEDER through COMPETE-Programa Operacional Factores de

Competitividade, and by National funding through FCT-Fundação para a Ciência e Tecnologia, within the research project NANOkA FCOMP-01-0124-FEDER-008944 (Ref^a. FCT PTDC/BIA-BEC/103716/2008).

References

- Amorim, M.J.B., Novais, S., Römbke, J., Soares, A.M.V.M., 2008. *Enchytraeus albidus* (Enchytraeidae): A test organism in a standardised avoidance test? Effects of different chemical substances. *Environ Int* 34, 363-371.
- Amorim, M.J.B., Novais, S.C., Van der Ven, K., Vandenbrouck, T., Soares, A.M.V.M., De Coen, W., 2011. Development of a microarray in *Enchytraeus albidus* (Oligochaeta): preliminary tool with diverse applications. *Environ Toxicol Chem* 30, 1395-1402.
- Amorim, M.J.B., Rombke, J., Schallna, H.J., Soares, A.M.V.M., 2005a. Effect of soil properties and aging on the toxicity of copper for *Enchytraeus albidus*, *Enchytraeus luxuriosus*, and *Folsomia candida*. *Environ Toxicol Chem* 24, 1875-1885.
- Amorim, M.J.B., Römbke, J., Scheffczyk, A., Soares, A.M.V.M., 2005b. Effect of different soil types on the enchytraeids *Enchytraeus albidus* and *Enchytraeus luxuriosus* using the herbicide Phenmedipham. *Chemosphere* 61, 1102-1114.
- Amorim, M.J.B., Rombke, J., Soares, A.M.V.M., 2005c. Avoidance behaviour of *Enchytraeus albidus*: Effects of Benomyl, Carbendazim, phenmedipham and different soil types. *Chemosphere* 59, 501-510.
- Benjamini, Y., Hochberg, Y., 1995. Controlling the False Discovery Rate: A Practical and Powerful Approach to Multiple Testing. *J R Stat Soc Series B Stat Methodol* 57, 289-300.
- Bremner, I., 1998. Manifestations of copper excess. *Am J Clin Nutr* 67, 1069s-1073s.
- Bundy, J.G., Sidhu, J.K., Rana, F., Spurgeon, D.J., Svendsen, C., Wren, J.F., Sturzenbaum, S.R., Morgan, A.J., Kille, P., 2008. 'Systems toxicology' approach identifies coordinated

metabolic responses to copper in a terrestrial non-model invertebrate, the earthworm *Lumbricus rubellus*. *Bmc Biology* 6:25.

Byun, H.O., Han, N.K., Lee, H.J., Kim, K.B., Ko, Y.G., Yoon, G., Lee, Y.S., Hong, S.I., Lee, J.S., 2009. Cathepsin d and eukaryotic translation elongation factor 1 as promising markers of cellular senescence. *Cancer research* 69, 4638-4647.

Chen, Z., Meng, H., Yuan, H., Xing, G.M., Chen, C.Y., Zhao, F., Wang, Y., Zhang, C.C., Zhao, Y.L., 2007. Identification of target organs of copper nanoparticles with ICP-MS technique. *J Radioanal Nucl Chem* 272, 599-603.

Chen, Z., Meng, H.A., Xing, G.M., Chen, C.Y., Zhao, Y.L., Jia, G.A., Wang, T.C., Yuan, H., Ye, C., Zhao, F., Chai, Z.F., Zhu, C.F., Fang, X.H., Ma, B.C., Wan, L.J., 2006. Acute toxicological effects of copper nanoparticles in vivo. *Toxicol Lett* 163, 109-120.

Dhas, N.A., Raj, C.P., Gedanken, A., 1998. Synthesis, characterization, and properties of metallic copper nanoparticles. *Chem Mater* 10, 1446-1452.

Gomes, S.I.L., Novais, S.C., Gravato, C., Guilhermino, L., Scott-Fordsmand, J.J., Soares, A.M.V.M., Amorim, M.J.B., 2011. Effect of Cu-nanoparticles versus one Cu-salt: analysis of stress and neuromuscular biomarkers response in *Enchytraeus albidus* (Oligochaeta). *in press* in *Nanotoxicology* 10.3109/17435390.2011.562327

Gou, N., Onnis-Hayden, A., Gu, A.Z., 2010. Mechanistic Toxicity Assessment of Nanomaterials by Whole-Cell-Array Stress Genes Expression Analysis. *Environ Sci Technol* 44, 5964-5970.

Griffitt, R.J., Weil, R., Hyndman, K.A., Denslow, N.D., Powers, K., Taylor, D., Barber, D.S., 2007. Exposure to copper nanoparticles causes gill injury and acute lethality in zebrafish (*Danio rerio*). *Environ Sci Technol* 41, 8178-8186.

Gu, M.B., Niazi, J.H., Sang, B.I., Kim, Y.S., 2011. Global Gene Response in *Saccharomyces cerevisiae* Exposed to Silver Nanoparticles. *Appl Biochem Biotech* 164, 1278-1291.

- Heckmann, L.-H., Hovgaard, M.B., Sutherland, D.S., Autrup, H., Besenbacher, F., Scott-Fordsmand, J.J., 2011. Limit-test toxicity screening of selected inorganic nanoparticles to the earthworm *Eisenia fetida*. *Ecotoxicology* 20(1), 226-233.
- ISO, 2005. Soil Quality - Effects of pollutants on Enchytraeidae (*Enchytraeus* sp.). Determination of effects on reproduction and survival. Guideline 16387. International Organization for Standardization, Geneva, Switzerland.
- Johansen, A., Pedersen, A.L., Jensen, K.A., Karlson, U., Hansen, B.M., Scott-Fordsmand, J.J., Winding, A., 2008. Effects of C-60 fullerene nanoparticles on soil bacteria and protozoans. *Environ Toxicol Chem* 27, 1895-1903.
- Kendzioriski, C., Irizarry, R.A., Chen, K.S., Haag, J.D., Gould, M.N., 2005. On the utility of pooling biological samples in microarray experiments. *P Natl Acad Sci USA* 102, 4252-4257.
- Kobayashi, Y., Yonehara, S., 2009. Novel cell death by downregulation of eEF1A1 expression in tetraploids. *Cell death and differentiation* 16, 139-150.
- Lapied, E., Moudilou, E., Exbrayat, J.M., Oughton, D.H., Joner, E.J., 2010. Silver nanoparticle exposure causes apoptotic response in the earthworm *Lumbricus terrestris* (Oligochaeta). *Nanomedicine-Uk* 5, 975-984.
- Lee, W.M., An, Y.J., Yoon, H., Kweon, H.S., 2008a. Toxicity and bioavailability of copper nanoparticles to the terrestrial plants mung bean (*Phaseolus radiatus*) and wheat (*Triticum aestivum*): Plant agar test for water-insoluble nanoparticles. *Environ Toxicol Chem* 27, 1915-1921.
- Lee, Y., Choi, J.R., Lee, K.J., Stott, N.E., Kim, D., 2008b. Large-scale synthesis of copper nanoparticles by chemically controlled reduction for applications of inkjet-printed electronics. *Nanotechnology* 19, (7pp).
- Lettieri, T., 2006. Recent applications of DNA microarray technology to toxicology and ecotoxicology. *Environ Health Perspect* 114, 4-9.

- Lewis, S.S., Keller, S.J., 2009. Identification of copper-responsive genes in an early life stage of the fathead minnow *Pimephales promelas*. *Ecotoxicology* 18, 281-292.
- Meng, H., Chen, Z., Xing, G.M., Yuan, H., Chen, C.Y., Zhao, F., Zhang, C.C., Wang, Y., Zhao, Y.L., 2007. Ultrahigh reactivity and grave nanotoxicity of copper nanoparticles. *J Radioanal Nucl Chem* 272, 595-598.
- Nota, B., Bosse, M., Ylstra, B., van Straalen, N.M., Roelofs, D., 2009. Transcriptomics reveals extensive inducible biotransformation in the soil-dwelling invertebrate *Folsomia candida* exposed to phenanthrene. *Bmc Genomics* 10:236.
- Nota, B., Timmermans, M.J.T.N., Franken, C., Montagne-Wajer, K., Marien, J., De Boer, M.E., De Boer, T.E., Ylstra, B., Van Straalen, N.M., Roelofs, D., 2008. Gene Expression Analysis of Collembola in Cadmium Containing Soil. *Environ Sci Technol* 42, 8152-8157.
- Poynton, H.C., Lazorchak, J.M., Impellitteri, C.A., Smith, M.E., Rogers, K., Patra, M., Hammer, K.A., Allen, H.J., Vulpe, C.D., 2011. Differential Gene Expression in *Daphnia magna* Suggests Distinct Modes of Action and Bioavailability for ZnO Nanoparticles and Zn Ions. *Environ Sci Technol* 45, 762-768.
- Poynton, H.C., Loguinov, A.V., Varshavsky, J.R., Chan, S., Perkins, E.I., Vulpe, C.D., 2008. Gene expression profiling in *Daphnia magna* part I: Concentration-dependent profiles provide support for the No Observed Transcriptional Effect Level. *Environ Sci Technol* 42, 6250-6256.
- Rockett, J.C., Dix, D.J., 1999. Application of DNA arrays to toxicology. *Environ Health Perspect* 107, 681-685.
- Rombke, J., Moser, T., 2002. Validating the enchytraeid reproduction test: organisation and results of an international ringtest. *Chemosphere* 46, 1117-1140.
- Samim, M., Kaushik, N.K., Maitra, A., 2007. Effect of size of copper nanoparticles on its catalytic behaviour in Ullman reaction. *Bull Mater Sci* 30, 535-540.

- Scott-Fordsmand, J.J., Krogh, P.H., Lead, J.R., 2008a. Nanomaterials in ecotoxicology. *Integr Environ Assess Manag* 4, 126-128.
- Scott-Fordsmand, J.J., Krogh, P.H., Schaefer, M., Johansen, A., 2008b. The toxicity testing of double-walled nanotubes-contaminated food to *Eisenia veneta* earthworms. *Ecotox Environ Saf* 616– 619.
- Smyth, G.K., 2005. Limma: Linear Models for Microarray Data, in: R. Gentleman, Carey, V., Dudoit, S., Irizarry, R., Huber, W., Eds. (Ed.), *Bioinformatics and Computational Biology Solutions Using R and Bioconductor*. Springer, New York, 397-420.
- Tong, Z.H., Bischoff, M., Nies, L., Applegate, B., Turco, R.F., 2007. Impact of fullerene (C-60) on a soil microbial community. *Environ Sci Technol* 41, 2985-2991.
- Tummala, R.R., Raj, P.M., Aggarwal, A., Mehrotra, G., Koh, S.W., Bansal, S., Tiong, T.T., Ong, C.K., Chew, J., Vaidyanathan, K., Rao, V.S., 2006. Copper interconnections for high performance and fine pitch flipchip digital applications and ultra-miniaturized RF module applications. *56th Electronic Components & Technology Conference 2006, Vol 1 and 2, Proceedings*, 102-111.
- Unrine, J.M., Hunyadi, S.E., Tsyusko, O.V., Rao, W., Shoults-Wilson, W.A., Bertsch, P.M., 2010. Evidence for Bioavailability of Au Nanoparticles from Soil and Biodistribution within Earthworms (*Eisenia fetida*). *Environ Sci Technol* 44, 8308-8313.
- Wang, R.L., Bencic, D., Biales, A., Lattier, D., Kostich, M., Villeneuve, D., Ankley, G.T., Lazorchak, J., Toth, G., 2008. DNA microarray-based ecotoxicological biomarker discovery in a small fish model species. *Environ Toxicol Chem* 27, 664-675.
- Yang, Y.H., Dudoit, S., Luu, P., Lin, D.M., Peng, V., Ngai, J., Speed, T.P., 2002. Normalization for cDNA microarray data: a robust composite method addressing single and multiple slide systematic variation. *Nucleic Acids Res* 30, e15.

Supplementary material

Table S1: List of all the differentially expressed genes (BH adjusted, $p < 0.05$) with the adjusted p value for each treatment and the GO annotation (and E value) for each gene.

Unique ID	Acc Number	E-value	GO Category	Adjusted P value per Treatment								GeneName(homology)
				Cu 400	Cu 600	Cu 800	Cu 1000	Cu-NP 400	Cu-NP 600	Cu-NP 800	Cu-NP 1000	
EBT_SF_P1_A1				0.0121	0.8121	0.9044	0.9979	0.6818	0.9975	0.8193	0.9470	
EBT_SF_P1_A10	GT066377			0.0000	0.8909	0.9663	0.9979	0.2023	0.9975	0.9057	0.1192	
EBT_SF_P1_A11	GT066378	4.16E-17	Transcription and translation	0.0065	0.8909	0.9980	0.9979	0.4533	0.9975	0.5365	0.9370	replication protein a3
EBT_SF_P1_A12				0.0138	0.6127	0.9296	0.9979	0.1063	0.9975	0.6624	0.8597	
EBT_SF_P1_A14	GT066539			0.0080	0.9680	0.6700	0.9979	0.1516	0.9975	0.7256	0.4575	
EBT_SF_P1_A15	GT066395			0.0068	0.3172	0.9791	0.9979	0.5096	0.9975	0.1051	0.9720	
EBT_SF_P1_A16				0.0429	0.5900	0.9040	0.9979	0.8116	0.9975	0.7554	0.9635	
EBT_SF_P1_A18	GT066396			0.0284	0.9799	0.9663	0.9979	0.1887	0.9975	0.5261	0.5109	
EBT_SF_P1_A19	GT066397			0.2873	0.6650	0.7830	0.9342	0.3116	0.5497	0.0114	0.2615	
EBT_SF_P1_A2	GT066482	4.27E-09	immune and stress response	0.0090	0.9925	0.9616	0.9979	0.4636	0.9975	0.5919	0.9903	mannose C type 1-like 1
EBT_SF_P1_A20	GT066398			0.0000	0.0000	0.0000	0.0001	0.0000	0.0000	0.1208	0.0000	
EBT_SF_P1_A21	GT066540			0.1896	0.6342	0.1760	0.5687	0.2605	0.9975	0.0006	0.0421	
EBT_SF_P1_A24	GT066537			0.0269	0.5346	0.9791	0.9932	0.0305	0.5363	0.2168	0.5167	
EBT_SF_P1_A3	GT066483			0.0027	0.9913	0.9319	0.9979	0.2783	0.9975	0.8406	0.9226	
EBT_SF_P1_A4	GT066379			0.0062	0.1424	0.9791	0.9979	0.8002	0.9975	0.0005	0.1422	
EBT_SF_P1_A6	GT066484			0.0108	0.2769	0.7430	0.9979	0.0466	0.9975	0.2125	0.3900	
EBT_SF_P1_A8	GT066486	1.03E-30	Energy metabolism	0.0251	0.8121	0.9253	0.9342	0.4959	0.9975	0.3964	0.6531	short-chain dehydrogenase
EBT_SF_P1_A9	GT066380	3.47E-04	Development	0.0000	0.8797	0.9791	0.9979	0.2480	0.9975	0.8618	0.7206	regeneration-upregulated protein
EBT_SF_P1_B1	GT066381			0.9073	0.0231	0.1297	0.1183	0.2034	0.9975	0.0172	0.0456	
EBT_SF_P1_B20	GT066545	3.22E-21	Transcription and translation	0.0066	0.8134	0.0004	0.2853	0.0006	0.9975	0.8595	0.0116	pre-mrna processing factor 8
EBT_SF_P1_B21	GT066401			0.7388	0.3207	0.3551	0.6518	0.0166	0.9975	0.4664	0.9720	
EBT_SF_P1_B22	GT066399			0.2378	0.7283	0.9040	0.9133	0.8556	0.9975	0.0139	0.0310	
EBT_SF_P1_B5	GT066479			0.0481	0.0069	0.7849	0.9342	0.9262	0.9975	0.5919	0.8104	
EBT_SF_P1_B6	GT066491			0.3874	0.2259	0.9791	0.9979	0.0004	0.9975	0.6215	0.5401	

Supplementary material – Chapter III

EBT_SF_P1_B8	GT066493			0.1790	0.0515	0.9850	0.8018	0.1650	0.9975	0.0010	0.1353	
EBT_SF_P1_B9	GT066494			0.8110	0.5495	0.8104	0.7624	0.0183	0.9975	0.8239	0.9223	
EBT_SF_P1_C1				0.0008	0.9913	0.8104	0.9979	0.5659	0.9975	0.5919	0.7587	
EBT_SF_P1_C10				0.8503	0.9925	0.9616	0.9979	0.7158	0.9975	0.0053	0.9635	
EBT_SF_P1_C13	GT066548	4.74E-24	Carbohydrate and fat metabolism	0.0102	0.4792	0.6700	0.9979	0.6273	0.9975	0.0649	0.8597	maltase 1
EBT_SF_P1_C18	GT066404			0.4861	0.7865	0.9040	0.9932	0.0132	0.9975	0.1974	0.4856	
EBT_SF_P1_C22	GT066546	2.79E-56	Unknown function	0.9478	0.4981	0.9453	0.9979	0.1567	0.9975	0.8406	0.0394	transmembrane and coiled-coil domains 1
EBT_SF_P1_C5	GT066385			0.0633	0.7283	0.7906	0.9979	0.1887	0.9975	0.0057	0.0819	
EBT_SF_P1_C9	GT066497			0.4757	0.6118	0.9791	0.9979	0.0483	0.9975	0.0053	0.0310	
EBT_SF_P1_D1				0.2949	0.1183	0.9791	0.7705	0.9616	0.9975	0.3803	0.0310	
EBT_SF_P1_D13	GT066408			0.5799	0.9138	0.6700	0.9979	0.8030	0.9975	0.8137	0.0423	
EBT_SF_P1_D20	GT066555			0.1604	0.2034	0.9791	0.9979	0.8767	0.9975	0.7241	0.0488	
EBT_SF_P1_D22				0.3682	0.5182	0.9040	0.9932	0.3852	0.9975	0.5261	0.0116	
EBT_SF_P1_D4				0.0019	0.4981	0.7133	0.9979	0.8687	0.9975	0.9703	0.9728	
EBT_SF_P1_D5	GT066480	2.94E-05	Transcription and translation	0.3276	0.6160	0.0006	0.1551	0.0369	0.9975	0.0000	0.0009	transcription factor
EBT_SF_P1_E1	GT066388	1.22E-04	Unknown function	0.0196	0.3693	0.9253	0.9979	0.2719	0.9975	0.9938	0.7401	uncharacterized protein c1orf189 homolog
EBT_SF_P1_E10	GT066502			0.0000	0.0355	0.9996	0.9979	0.7158	0.9975	0.1471	0.9936	
EBT_SF_P1_E12	GT066504	2.19E-66	Transcription and translation	0.7775	0.4658	0.8239	0.7221	0.0380	0.9975	0.8406	0.6940	ribosomal protein l26
EBT_SF_P1_E13	GT066558	3.66E-27	Transcription and translation	0.3611	0.9354	0.9791	0.9979	0.0183	0.9975	0.7298	0.6160	mitochondrial ribosomal
EBT_SF_P1_E16	GT066560			0.0262	0.6650	0.9040	0.9979	0.4647	0.9975	0.2588	0.5109	
EBT_SF_P1_E18	GT066410			0.0136	0.7634	0.8737	0.9979	0.2986	0.9975	0.6624	0.9720	
EBT_SF_P1_E19	GT066561	6.22E-32	Transcription and translation	0.0518	0.7142	0.7830	0.9979	0.7158	0.9975	0.8406	0.8597	ribosomal protein s7
EBT_SF_P1_E2	GT066389			0.0132	0.3970	0.9872	0.9979	0.6173	0.9975	0.6346	0.9527	
EBT_SF_P1_E3	GT066505	4.55E-72	Signal Transduction	0.1857	0.1709	0.9981	0.9979	0.1619	0.9975	0.0029	0.4739	protein tyrosine phosphatase 4a2 of regenerating liver
EBT_SF_P1_E4	GT066506	6.04E-15	Miscellaneous	0.0007	0.0239	0.9850	0.9979	0.9615	0.9975	0.0286	0.0839	leukocyte receptor cluster member 1
EBT_SF_P1_E6	GT066507			0.0163	0.4613	0.9453	0.9979	0.9925	0.9975	0.4418	0.9370	
EBT_SF_P1_E7	GT066508	1.96E-20	Cell structure and cytoskeletal organization	0.0103	0.9680	0.9453	0.9979	0.6785	0.9975	0.7641	0.7892	microtubule-associated protein tau
EBT_SF_P1_E8				0.0015	0.0563	0.9791	0.3099	0.6173	0.9975	0.6998	0.8118	
EBT_SF_P1_E9	GT066390			0.0005	0.7097	0.7735	0.9979	0.0278	0.9975	0.9809	0.5000	
EBT_SF_P1_F1				0.0268	0.6601	0.9512	0.9342	0.5484	0.9975	0.6015	0.9226	

Supplementary material – Chapter III

EBT_SF_P1_F10	GT066509			0.0245	0.7572	0.8847	0.9979	0.7970	0.9975	0.1078	0.9257	
EBT_SF_P1_F12	GT066391	1.00E-09	Unknown function	0.0665	0.3041	0.9850	0.9979	0.0891	0.9975	0.0050	0.0970	similar to CG41389, partial
EBT_SF_P1_F18	GT066567			0.0442	0.0018	0.9453	0.9979	0.1228	0.9975	0.0090	0.2453	
EBT_SF_P1_F2	GT066510			0.0226	0.9913	0.9850	0.9932	0.8687	0.9975	0.1033	0.9936	
EBT_SF_P1_F20	GT066568			0.1491	0.4630	0.8147	0.9932	0.0496	0.9975	0.0845	0.6531	
EBT_SF_P1_F6	GT066512	8.80E-10	Transcription and translation	0.0008	0.0420	0.1978	0.0320	0.0026	0.9975	0.3035	0.2864	ribosomal protein l7a
EBT_SF_P1_F9	GT066515			0.0905	0.1585	0.7397	0.6711	0.0860	0.9975	0.0070	0.1344	
EBT_SF_P1_G1	GT066517			0.5064	0.0089	0.9616	0.6518	0.6273	0.9975	0.7597	0.7584	
EBT_SF_P1_G11	GT066516			0.9478	0.9292	0.4598	0.6518	0.6761	0.9975	0.0196	0.9728	
EBT_SF_P1_G13	GT066413			0.0007	0.0630	0.8147	0.9979	0.8032	0.9975	0.9919	0.3426	
EBT_SF_P1_G16				0.5852	0.0348	0.7732	0.9442	0.5484	0.9975	0.0031	0.0091	
EBT_SF_P1_G17				0.0022	0.7420	0.9850	0.9979	0.7158	0.9975	0.7955	0.3335	
EBT_SF_P1_G2	GT066518			0.9715	0.0020	0.9616	0.1183	0.2783	0.9975	0.0689	0.9936	
EBT_SF_P1_G23	GT066570	6.00E-23	Transcription and translation	0.0007	0.3020	0.0450	0.9932	0.0016	0.9975	0.8097	0.9720	DEAD/DEAH box helicase
EBT_SF_P1_G3	GT066519			0.9016	0.8421	0.0329	0.9979	0.9068	0.9975	0.9057	0.1911	
EBT_SF_P1_G6	GT066521	1.00E-04	Transcription and translation	0.1857	0.0608	0.6214	0.0781	0.0166	0.9975	0.0649	0.9226	16s ribosomal rna partial sequence
EBT_SF_P1_G7	GT066522	2.18E-44	Energy metabolism	0.4968	0.3712	0.8474	0.9442	0.9193	0.9975	0.0488	0.2210	nadh dehydrogenase fe-s protein 4
EBT_SF_P1_G9	GT066720			0.0000	0.0008	0.0795	0.0320	0.0006	0.9975	0.0139	0.0116	
EBT_SF_P1_H1	GT066394			0.0284	0.2230	0.7732	0.7568	0.2783	0.9975	0.1208	0.9370	
EBT_SF_P1_H10				0.5372	0.7097	0.6700	0.9979	0.6964	0.9975	0.0307	0.6262	
EBT_SF_P1_H11	GT066524			0.2466	0.0055	0.9616	0.2345	0.1111	0.9975	0.0475	0.9430	
EBT_SF_P1_H12	GT066525			0.0738	0.9925	0.5037	0.6123	0.1180	0.9975	0.0150	0.8118	
EBT_SF_P1_H18	GT066416			0.4718	0.1229	0.7397	0.2543	0.0212	0.9975	0.2099	0.9904	
EBT_SF_P1_H19	GT066579			0.3682	0.7634	0.8402	0.9979	0.2667	0.9975	0.5941	0.0310	
EBT_SF_P1_H20	GT066580			0.9250	0.6042	0.9296	0.9932	0.1357	0.9975	0.8402	0.0416	
EBT_SF_P1_H21	GT066417			0.2380	0.9325	0.2146	0.9979	0.2834	0.9975	0.0642	0.0167	
EBT_SF_P1_H24				0.6513	0.8909	0.5665	0.9979	0.2043	0.9975	0.0499	0.0011	
EBT_SF_P1_H5				0.7121	0.9925	0.3972	0.9979	0.8687	0.9975	0.4771	0.0310	
EBT_SF_P1_I1	GT066418	1.00E-04	Protein metabolism	0.0007	0.9680	0.9841	0.9979	0.9262	0.9975	0.9928	0.7344	calmodulin-domain protein kinase
EBT_SF_P1_I10				0.0027	0.3207	0.7732	0.9342	0.0000	0.9975	0.7032	0.9719	
EBT_SF_P1_I11	GT066585			0.0322	0.6735	0.4731	0.9934	0.3226	0.9975	0.2773	0.0883	
EBT_SF_P1_I12				0.0001	0.2769	0.3028	0.7717	0.1228	0.2080	0.1309	0.8258	

Supplementary material – Chapter III

EBT_SF_P1_I16				0.0595	0.7097	0.6023	0.9979	0.2986	0.9975	0.0014	0.1344	
EBT_SF_P1_I2				0.0109	0.4899	0.7397	0.9979	0.1619	0.9975	0.8595	0.9635	
EBT_SF_P1_I20				0.0372	0.8231	0.8215	0.9979	0.5911	0.9975	0.2614	0.9085	
EBT_SF_P1_I21	GT066435			0.8798	0.0355	0.6540	0.1375	0.0212	0.9975	0.4580	0.1605	
EBT_SF_P1_I22	GT066432			0.0024	0.9775	0.9616	0.9979	0.0293	0.9975	0.9119	0.9527	
EBT_SF_P1_I24	GT066718			0.0665	0.3207	0.0829	0.3099	0.2715	0.8368	0.0227	0.0065	
EBT_SF_P1_I3	GT066586			0.0101	0.5778	0.1076	0.3648	0.6761	0.9477	0.0001	0.1943	
EBT_SF_P1_I4				0.0041	0.0906	0.9166	0.6853	0.3481	0.9975	0.0623	0.0781	
EBT_SF_P1_I5	GT066723	3.15E-06	Unknown function	0.7341	0.9680	0.9850	0.9979	0.0466	0.9975	0.9905	0.9241	diuretic hormone 34
EBT_SF_P1_I7				0.0442	0.9780	0.9981	0.9979	0.8032	0.9975	0.8193	0.7755	
EBT_SF_P1_I8				0.0001	0.4426	0.9040	0.9979	0.0322	0.9975	0.3572	0.8675	
EBT_SF_P1_I9	GT066419	3.60E-09	Protein metabolism	0.0000	0.0012	0.1572	0.0000	0.0072	0.0002	0.3464	0.5006	calcium-dependent protein kinase
EBT_SF_P1_J1	GT066420			0.3799	0.8018	0.7732	0.9979	0.5202	0.9975	0.0150	0.6355	
EBT_SF_P1_J10				0.0007	0.0812	0.9980	0.9342	0.1653	0.9975	0.7187	0.8597	
EBT_SF_P1_J11	GT066588			0.0132	0.2949	0.9253	0.9979	0.0369	0.9975	0.0706	0.0137	
EBT_SF_P1_J19	GT066437	9.85E-12	Energy metabolism	0.0122	0.2066	0.9850	0.9979	0.5150	0.9975	0.6363	0.9226	cytochrome c oxidase subunit vic
EBT_SF_P1_J24	GT066436			0.3851	0.5182	0.3205	0.9979	0.0026	0.9975	0.0075	0.0503	
EBT_SF_P1_J8	GT066592	1.16E-08	Energy metabolism	0.8378	0.5723	0.9319	0.9979	0.1982	0.9975	0.1054	0.0256	adipokinetic hormone akh2
EBT_SF_P1_K1	GT066422			0.2006	0.7468	0.4149	0.9979	0.7195	0.9975	0.0056	0.3263	
EBT_SF_P1_K10				0.0325	0.0915	0.9791	0.9979	0.2976	0.9975	0.7862	0.2635	
EBT_SF_P1_K13	GT066643			0.0016	0.4888	0.9296	0.9979	0.2438	0.9975	0.9498	0.8675	
EBT_SF_P1_K17				0.4757	0.8587	0.9196	0.9979	0.8798	0.9975	0.4174	0.0455	
EBT_SF_P1_K19	GT066439	8.38E-12	Energy metabolism	0.0062	0.6889	0.9616	0.9932	0.3900	0.9975	0.9928	0.4856	nadh-ubiquinone oxidoreductase subunit
EBT_SF_P1_K23	GT066642			0.0980	0.1311	0.4801	0.9932	0.0006	0.9975	0.0148	0.2097	
EBT_SF_P1_K24				0.7125	0.7622	0.9196	0.9979	0.0322	0.9975	0.2168	0.4739	
EBT_SF_P1_K6	GT066598	6.45E-08	Unknown function	0.9657	0.7115	0.2146	0.9979	0.8796	0.9975	0.0008	0.8597	diuretic hormone dh34
EBT_SF_P1_L11	GT066603	3.93E-19	Transcription and translation	0.1513	0.4658	0.0008	0.5482	0.0001	0.9975	0.0001	0.4856	small nuclear ribonucleoprotein d2
EBT_SF_P1_L13				0.7125	0.4496	0.7745	0.9979	0.2986	0.9975	0.5941	0.0442	
EBT_SF_P1_L14	GT066442	1.00E-06	Unknown function	0.0009	0.9799	0.6700	0.9932	0.0496	0.9975	0.3572	0.9370	ltu24570 lumbricus terrestris complete genome
EBT_SF_P1_L15	GT066647			0.5183	0.5900	0.3551	0.9979	0.3462	0.9975	0.0139	0.9728	
EBT_SF_P1_L17	GT066631			0.0241	0.4071	0.6700	0.9979	0.4679	0.9975	0.7544	0.2839	

Supplementary material – Chapter III

EBT_SF_P1_L19				0.5372	0.8033	0.9981	0.9979	0.9895	0.9975	0.3599	0.0279	
EBT_SF_P1_L21				0.0012	0.0000	0.0009	0.0074	0.0000	0.0079	0.0001	0.0000	
EBT_SF_P1_L22	GT066441			0.4139	0.7919	0.8847	0.9979	0.5973	0.9975	0.2672	0.0116	
EBT_SF_P1_L23	GT066645			0.2585	0.6537	0.8402	0.9979	0.0272	0.9975	0.0042	0.0009	
EBT_SF_P1_L24	GT066646			0.0929	0.8909	0.4439	0.6518	0.0043	0.9975	0.0267	0.0047	
EBT_SF_P1_L5	GT066582	1.52E-07	immune and stress response	0.1554	0.4496	0.8457	0.9934	0.8883	0.9975	0.8406	0.0442	heat shock 70kDa protein 5
EBT_SF_P1_L7	GT066608	3.48E-04	Energy metabolism	0.9073	0.0462	0.9616	0.9979	0.6421	0.9975	0.7502	0.9370	adipokinetic hormone akh2
EBT_SF_P1_M10				0.2031	0.9690	0.1484	0.8630	0.9930	0.9975	0.0002	0.3454	
EBT_SF_P1_M12				0.0268	0.8372	0.9981	0.9979	0.9531	0.9975	0.8934	0.6939	
EBT_SF_P1_M14	GT066651	2.40E-06	Signal Transduction	0.9780	0.8797	0.9319	0.6518	0.0498	0.9975	0.0767	0.3263	pseudo-response regulator 95
EBT_SF_P1_M15	GT066652			0.4621	0.0948	0.9616	0.9979	0.8737	0.9975	0.0056	0.2839	
EBT_SF_P1_M16	GT066724	5.16E-31	immune and stress response	0.0048	0.9925	0.9981	0.5576	0.4130	0.9975	0.0001	0.8652	superoxide dismutase
EBT_SF_P1_M18	GT066653	4.94E-09	Development	0.0526	0.1171	0.8457	0.0068	0.7939	0.9975	0.5982	0.8160	GDF11
EBT_SF_P1_M2				0.0000	0.0069	0.0027	0.1551	0.0000	0.4059	0.1001	0.2210	
EBT_SF_P1_M21	GT066655	7.53E-08	Carbohydrate and fat metabolism	0.0221	0.1229	0.6023	0.9979	0.9386	0.9477	0.1051	0.9720	beta-1,3-glucanase
EBT_SF_P1_M22	GT066444			0.0062	0.9604	0.3551	0.9979	0.5065	0.5930	0.5207	0.5717	
EBT_SF_P1_M3	GT066611	5.70E-09	Transcription and translation	0.0251	0.5063	0.7921	0.9979	0.8645	0.9975	0.6719	0.8104	mrna for transcription
EBT_SF_P1_M4				0.0834	0.3532	0.9791	0.9740	0.2976	0.9975	0.0172	0.2731	
EBT_SF_P1_M7	GT066612	4.15E-52	Carbohydrate and fat metabolism	0.8071	0.9138	0.9453	0.9979	0.0212	0.9975	0.0029	0.9157	monosaccharide-transporting ATPase
EBT_SF_P1_M8	GT066613	5.95E-39	Energy metabolism	0.0311	0.8516	0.6103	0.9979	0.9616	0.9975	0.0000	0.0239	cytochrome c
EBT_SF_P1_N1				0.0000	0.8797	0.9791	0.9979	0.7056	0.9975	0.3487	0.9370	
EBT_SF_P1_N10				0.0404	0.9680	0.5175	0.9979	0.0032	0.9975	0.0267	0.7344	
EBT_SF_P1_N14				0.8913	0.9680	0.9040	0.9932	0.7021	0.9975	0.0031	0.8104	
EBT_SF_P1_N19	GT066658			0.0088	0.8797	0.5175	0.9979	0.2894	0.9975	0.6478	0.9635	
EBT_SF_P1_N20	GT066659	2.84E-08	immune and stress response	0.0024	0.5634	0.9253	0.9979	0.0466	0.9975	0.9057	0.9211	heat shock hspa8
EBT_SF_P1_N22	GT066656	4.44E-05	Development	0.0175	0.3020	0.9616	0.9979	0.5137	0.9975	0.6619	0.8597	pls_hallaame: full=perlustrin
EBT_SF_P1_N23				0.0152	0.0413	0.9253	0.6518	0.1448	0.9975	0.7137	0.7344	
EBT_SF_P1_N24				0.7125	0.9009	0.9980	0.9932	0.2272	0.9975	0.0307	0.9257	
EBT_SF_P1_N4	GT066617			0.7290	0.0045	0.9453	0.7717	0.3734	0.9975	0.0093	0.4193	
EBT_SF_P1_N6	GT066618	9.79E-09	Energy metabolism	0.4655	0.2454	0.6023	0.9979	0.8716	0.9975	0.0029	0.9085	atp synthase e chain

Supplementary material – Chapter III

EBT_SF_P1_N7				0.7926	0.7097	0.8717	0.9979	0.0169	0.9975	0.8406	0.9720	
EBT_SF_P1_N9	GT066427			0.0007	0.4648	0.1306	0.6518	0.0041	0.4486	0.0689	0.1297	
EBT_SF_P1_O1	GT066621			0.8496	0.4613	0.0047	0.2853	0.0913	0.9975	0.0000	0.0285	
EBT_SF_P1_O10	GT066722			0.3531	0.9680	0.9040	0.9979	0.3423	0.9975	0.0322	0.9728	
EBT_SF_P1_O13	GT066662			0.0012	0.4613	0.9791	0.7705	0.0273	0.9975	0.6274	0.9658	
EBT_SF_P1_O14	GT066663	6.80E-18	Transcription and translation	0.8087	0.0787	0.9196	0.4405	0.8716	0.9975	0.0005	0.9505	poly (adp-ribose) polymerase member 14
EBT_SF_P1_O17				0.7413	0.9087	0.9044	0.9979	0.4464	0.9975	0.5398	0.0481	
EBT_SF_P1_O18	GT066664			0.0245	0.9680	0.9040	0.9979	0.9471	0.9975	0.1311	0.2053	
EBT_SF_P1_O2	GT066622			0.0030	0.0874	0.3397	0.9740	0.1211	0.9975	0.9809	0.1593	
EBT_SF_P1_O20				0.0010	0.9292	0.0489	0.9979	0.0962	0.9975	0.6143	0.9915	
EBT_SF_P1_O21				0.0078	0.9925	0.9040	0.9979	0.1357	0.9975	0.7726	0.9925	
EBT_SF_P1_O23	GT066661			0.0018	0.8046	0.9946	0.9979	0.2408	0.9975	0.5451	0.6879	
EBT_SF_P1_O24				0.0140	0.5810	0.9791	0.9979	0.9193	0.9975	0.8406	0.9350	
EBT_SF_P1_O5	GT066584			0.0015	0.9680	0.4922	0.6711	0.0011	0.9975	0.0745	0.5575	
EBT_SF_P1_O7				0.1326	0.9680	0.9296	0.9979	0.1653	0.9975	0.0029	0.7061	
EBT_SF_P1_O9	GT066625	9.79E-09	Energy metabolism	0.0006	0.3207	0.9616	0.9979	0.2316	0.9975	0.7957	0.9527	atp synthase e chain
EBT_SF_P1_P1	GT066429			0.0833	0.4947	0.0031	0.2427	0.0212	0.9975	0.0000	0.0027	
EBT_SF_P1_P10				0.0122	0.5900	0.9296	0.9979	0.6908	0.9975	0.8425	0.7061	
EBT_SF_P1_P14				0.0284	0.1881	0.9791	0.6518	0.0212	0.9975	0.3733	0.9720	
EBT_SF_P1_P15				0.0595	0.3570	0.6540	0.9979	0.6273	0.9975	0.0427	0.9527	
EBT_SF_P1_P20	GT066667	8.55E-04	Transcription and translation	0.0284	0.5519	0.7397	0.9979	0.5973	0.9975	0.9057	0.8597	zinc finger transcription factor (snail2 gene)
EBT_SF_P1_P23				0.8071	0.8432	0.9791	0.9979	0.8378	0.9975	0.6143	0.0481	
EBT_SF_P1_P5				0.0102	0.0420	0.9253	0.0584	0.8140	0.9975	0.0000	0.0056	
EBT_SF_P1_P6				0.2937	0.9775	0.5958	0.9979	0.6785	0.9975	0.0196	0.5000	
EBT_SF_P1_P7				0.0483	0.6109	0.9319	0.9979	0.4579	0.9975	0.3017	0.2453	
EBT_SF_P1_P9	GT066431			0.0201	0.0151	0.2146	0.2822	0.0006	0.9477	0.7310	0.1665	
EBT_SF_P2_A1	GT066675	7.23E-38	Protein metabolism	0.0122	0.0000	0.0060	0.6518	0.0058	0.5930	0.0097	0.1531	20s proteasome alpha subunit
EBT_SF_P2_A5				0.0170	0.9680	0.2146	0.9979	0.0169	0.9975	0.1154	0.1892	
EBT_SF_P2_A6	GT066672			0.0012	0.5124	0.9253	0.9979	0.0039	0.9975	0.9119	0.9762	
EBT_SF_P2_B7	GT066710			0.2444	0.0012	0.8947	0.2822	0.3258	0.9975	0.0706	0.9881	
EBT_SF_P2_C8	GT066715			0.9029	0.4658	0.9319	0.9979	0.4820	0.9975	0.0051	0.2638	
EBT_SF_P2_D1	GT066676			0.6987	0.3207	0.8947	0.9979	0.0369	0.9975	0.9445	0.1943	
EBT_SF_P2_D2	GT066681			0.1857	0.4947	0.9196	0.9979	0.0278	0.9975	0.9057	0.2731	
EBT_SF_P2_D7	GT066711	1.98E-06	Signal Transduction	0.5633	0.0064	0.9040	0.5482	0.0964	0.9975	0.0280	0.0423	pseudo-response regulator 95

Supplementary material – Chapter III

EBT_SF_P2_D8	GT066716	2.09E-46	Transcription and translation	0.3825	0.1233	0.0035	0.0611	0.0483	0.9975	0.0000	0.0000	ribosomal protein l34a cg6090-isoform a
EBT_SF_P2_E2	GT066669	5.51E-07	Energy metabolism	0.7367	0.5634	0.9850	0.9979	0.4679	0.9975	0.0355	0.2638	hypertrehalosaemic hormone precursor (hrth gene)
EBT_SF_P2_E5	GT066699			0.2006	0.8815	0.1818	0.4405	0.9363	0.9975	0.0004	0.1804	
EBT_SF_P2_E7	GT066476			0.0024	0.1171	0.9981	0.5482	0.7804	0.9975	0.2648	0.9350	
EBT_SF_P2_E8	GT066717			0.0070	0.5634	0.6700	0.9979	0.0001	0.9975	0.0056	0.1297	
EBT_SF_P2_F2	GT066455	1.77E-54	Transcription and translation	0.0000	0.8634	0.9616	0.9979	0.6686	0.9975	0.8406	0.5006	eukaryotic translation termination factor 1
EBT_SF_P2_F3	GT066461	1.59E-08	immune and stress response	0.1301	0.3020	0.7732	0.3156	0.6686	0.5691	0.0172	0.2627	calmodulin (cam-1 gene)
EBT_SF_P2_F8	GT066712			0.8255	0.9925	0.0822	0.7999	0.5973	0.9975	0.0016	0.0310	
EBT_SF_P2_G1	GT066677			0.0122	0.0408	0.2193	0.0280	0.0039	0.9975	0.7281	0.9252	
EBT_SF_P2_G6				0.6193	0.7697	0.3397	0.9979	0.1863	0.9975	0.0492	0.0116	
EBT_SF_P2_H1	GT066678			0.6996	0.9925	0.7735	0.9442	0.0322	0.9975	0.4752	0.9915	
EBT_SF_P2_H2	GT066456			0.8071	0.9787	0.9453	0.9979	0.4647	0.9975	0.9625	0.0394	
EBT_SF_P2_H3				0.2695	0.9913	0.9040	0.9979	0.0305	0.9975	0.8650	0.7061	
EBT_SF_P2_H5	GT066693			0.1415	0.4947	0.0159	0.5335	0.0293	0.9975	0.0004	0.0002	
EBT_SF_P2_H6	GT066700	1.72E-07	Signal Transduction	0.0000	0.0261	0.0001	0.0793	0.0000	0.7150	0.0000	0.0000	neuropeptide F 2
EBT_SF_P2_I1	GT066452			0.0284	0.9292	0.9319	0.9979	0.1016	0.9975	0.7774	0.9521	
EBT_SF_P2_I2	GT066683	8.81E-75	Transcription and translation	0.0015	0.9780	0.9616	0.9979	0.0440	0.9975	0.2466	0.4856	elongation factor-1 alpha
EBT_SF_P2_I4	GT066692			0.0494	0.6363	0.7732	0.9979	0.5096	0.9975	0.8077	0.9350	
EBT_SF_P2_J1	GT066449			0.0012	0.3020	0.3551	0.3099	0.0272	0.9975	0.8402	0.8597	
EBT_SF_P2_J2	GT066679			0.0140	0.7097	0.9791	0.9979	0.0369	0.9975	0.8994	0.8597	
EBT_SF_P2_K1	GT066673	4.60E-09	Energy metabolism	0.0359	0.8550	0.9791	0.9979	0.1918	0.9975	0.6059	0.5909	adipokinetic hormone akh2
EBT_SF_P2_L2				0.2006	0.3207	0.7764	0.9979	0.2758	0.9975	0.0857	0.0036	
EBT_SF_P2_L4	GT066687	1.01E-13	Energy metabolism	0.0697	0.8660	0.3551	0.9979	0.0041	0.9975	0.0019	0.0411	nadh dehydrogenase subunit 1
EBT_SF_P2_M4				0.0122	0.8909	0.9237	0.9979	0.0007	0.9975	0.1643	0.8597	
EBT_SF_P2_N1	GT066695			0.0205	0.4849	0.8968	0.2427	0.6517	0.9975	0.6713	0.9521	
EBT_SF_P2_O3	GT066709	6.65E-05	Miscellaneous	0.0219	0.5634	0.9791	0.9442	0.9548	0.9975	0.9809	0.8104	btb poz domain-containing protein
EBT_SF_P2_P3				0.6480	0.9325	0.9980	0.9979	0.8796	0.9975	0.9959	0.0310	

Table S2: List of the differentially expressed genes with homology with known functions and respective GO categories, divided according to the clusters from K-means analysis (Fig.5).

Cluster	Gene name (homology)	GO category
1	maltase 1	Carbohydrate and fat metabolism
	cytochrome c oxidase subunit vic	Energy metabolism
	nadh-ubiquinone oxidoreductase subunit	Energy metabolism
	beta-1,3-glucanase	Carbohydrate and fat metabolism
	heat shock hspa8	immune and stress response
	perlustrin	Development
	atp synthase e chain	Energy metabolism
	zinc finger transcription factor (snail2 gene)	Transcription and translation
	eukaryotic translation termination factor 1	Transcription and translation
	btb poz domain-containing protein	Miscellaneous
2	transmembrane and coiled-coil domains 1	Unknown function
	heat shock 70kDa protein 5	immune and stress response
3	superoxide dismutase	immune and stress response
	adipokinetic hormone akh2	Energy metabolism
4	neuropeptide F 2	Signal Transduction
	nadh dehydrogenase subunit 1	Energy metabolism
5	pre-mrna processing factor 8	Transcription and translation
	calcium-dependent protein kinase	Protein metabolism
	small nuclear ribonucleoprotein d2	Transcription and translation
	adipokinetic hormone akh2	Energy metabolism
	20s proteasome alpha subunit	Protein metabolism
6	replication protein a3	Transcription and translation
	mannose C type 1-like 1	immune and stress response
	regeneration-upregulated protein	Development
	ribosomal protein s7	Transcription and translation
	microtubule-associated protein tau	Cell structure and cytoskeletal organization
	calmodulin-domain protein kinase	Protein metabolism
7	elongation factor-1 alpha	Transcription and translation
	transcription factor	Transcription and translation
	diuretic hormone dh34	Unknown function
	atp synthase e chain	Energy metabolism
	poly (adp-ribose) polymerase member 14	Transcription and translation
	pseudo-response regulator 95	Signal Transduction
8	ribosomal protein l34a cg6090-isoform a	Transcription and translation
	ribosomal protein l26	Transcription and translation
	DEAD/DEAH box helicase	Transcription and translation
	diuretic hormone 34	Unknown function
	pseudo-response regulator 95	Signal Transduction
9	GDF11	Development
	ribosomal protein l7a	Transcription and translation
10	16s ribosomal rna partial sequence	Transcription and translation
	short-chain dehydrogenase	Energy metabolism
	mitochondrial ribosomal	Transcription and translation
	protein tyrosine phosphatase 4a2 of regenerating liver	Signal Transduction
	leukocyte receptor cluster member 1	Miscellaneous
	nadh dehydrogenase fe-s protein 4	Energy metabolism
	adipokinetic hormone akh2	Energy metabolism
	mrna for transcription	Transcription and translation
	monosaccharide-transporting ATPase	Carbohydrate and fat metabolism
	cytochrome c	Energy metabolism
hypertrehalosaemic hormone precursor (hrth gene)	Energy metabolism	
calmodulin (cam-1 gene)	immune and stress response	

Chapter IV

Cu-Nanoparticles Ecotoxicity – Explored and explained

IV - Cu-Nanoparticles Ecotoxicity – Explored and explained

Susana I.L. Gomes^a, Michael Murphy^b, Margrethe T. Nielsen^c, Søren M. Kristiansen^c,

Mónica J.B. Amorim^a and Janeck J. Scott-Fordsmand^d

^aDepartment of Biology & CESAM, University of Aveiro, Aveiro, Portugal

^bHASYLAB, DESY, Nokestraße 85, 22607 Hamburg, Germany

^cDepartment of Geoscience, Aarhus University, Høegh-Guldbergs Gade 2, DK-8000

Aarhus C, Denmark

^dDepartment of Bioscience, Aarhus University, Vejlsøvej 25, DK-8600 Silkeborg,

Denmark

Submitted

Abstract

The nano-form of Cu (Cu-NPs) is already extensively used, e.g. as wood preservatives. In addition, Cu-NPs are likely to be further used in other areas, e.g. as nano-Cu based fertilisers. In this paper the toxic responses in *Enchytraeus crypticus* (Oligochaeta: Enchytraeidae) were assessed following exposure to different forms of Cu. The different copper-exposures were: (1) Cu-salt: freshly spiked soil with copper-nitrate, (2) Cu-NPs: freshly spiked soil with Cu nanoparticles (80 nm), and (3) Cu-field: historically contaminated soil (80 years ago). Characterization of *in situ*-exposure included identification of oxidation states with synchrotron generated X-ray absorption near-edge spectroscopy (XANES) analysis, activity of free Cu²⁺ in soil-solution (Ion Selective Electrode), and the relative distribution of the labile Cu-fractions (Sequential Extraction). Freshly spiked Cu-salt was the most toxic, followed by Cu-NPs and then Cu-field. Regarding the fate, XANES indicated only one oxidation state (II) in Cu-salt

and Cu-field soil, whereas three were present in the Cu-NPs soil (0, I and II). For the Cu-soil the outer layer of Cu-NPs (*in situ*) seemed to be oxidised, which may have caused a partial dissolution of the NPs and release of Cu^{2+} . The free Cu ion (Cu^{2+}) activity was below detection limit for all the Cu treatments, irrespectively of Cu form: the sequential extraction showed similar distribution of Cu between the various fractions (oxidisable etc.) for Cu-NPs and Cu-salt exposure, whereas the field Cu-contaminated soil showed a different pattern. In the latter, Cu was more tightly bound to soil constituents – hence only extracted in the later extractions. The toxicity of Cu-NPs could be explained by the dissolution of the particles, but could also be explained by and inherent toxicity of the particles, depending on the premises.

Keywords: copper nanoparticles, XANES, *Enchytraeus crypticus*

1. Introduction

The number of studies focusing on the ecotoxicology of nano-materials is growing; despite this there is still very little information available regarding the environmental fate and effects of these materials, especially on the terrestrial ecosystem (Klaine et al. 2008).

Some of these nano-materials are based on Copper (Cu). The nano-form of Cu is for example already extensively used as wood-preservatives (Evans et al. 2008). Evans et al. (2008) estimated that approximately 50% of the Cu containing wood-preservatives on the North American market contained Cu-NPs (Cu nanoparticles) rather than Cu-salts. The North America market was estimated to be 79.000 tonnes (valued at \$4.9 billion), which represents 50% of the global market. Additional future sources may be Cu-NPs containing fertilisers and food additives. Hence, based on this, direct exposure to soils is very likely.

Copper toxicity is well documented to soil-dwelling organisms, e.g. enchytraeids (Amorim et al. 2005; Maraldo et al. 2006; Amorim et al. 2008; Menezes-Oliveira et al. 2011). However, very little is known about Cu-NPs. So far, only five studies reported effects of Cu-NPs via soil-exposure. Heckmann et al. (2011) observed that Cu-salt was more toxic (survival and reproduction) than Cu-NPs to the earthworm *Eisenia fetida*. Unrine et al. (2010), also using *E. fetida*, observed metallothionein induction following exposure to Cu-NPs (34 nm and 102 nm, TEM estimation) contaminated soil. Gomes et al. (2012b; 2012a), using enchytraeids (*Enchytraeus albidus*), observed that both Cu-salt and Cu-NPs exposure caused oxidative stress and differential gene-expression, with different response-patterns for Cu-NPs and for Cu-salt. Finally, Amorim et al. (2012) , also using *Enchytraeus albidus*, observed no differences energy-reserves (lipids, proteins and carbohydrates) following exposure to Cu-salt or Cu-NPs.

In this study, our hypothesis is that there are no differences in toxicity to *E. crypticus* between various Cu exposure forms, i.e. Cu-NPs, Cu-salts and field Cu-contaminated soil (Cu-field)(Scott-Fordsmand et al. 2000a), both at the effect level and at the exposure level. Toxicity will be estimated by measuring changes in survival and reproductive-output. Exposure will be characterised by measuring (1) total Cu, estimating the labile concentration by measuring the Cu distribution between various soil fraction using (2) sequential extraction and the (3) free active Cu ions in soil solution (ion selective electrode), and by measuring the (4) oxidation state (*in situ*) of Cu (X-ray absorption near-edge spectroscopy, XANES).

E. crypticus was used as test species because it is an important member of the soil community, actively contributing to the acceleration of organic matter decomposition and nutrient recycling processes. Additionally, enchytraeids toxicity-tests are standardized (OECD 2004; ISO 2005), making comparison to other studies easier.

2. Materials and Methods

Overall, the study consists of laboratory experiments with the enchytraeid *Enchytraeus crypticus* exposed to three different Cu regimes: Cu-salt, Cu-NPs and Cu-field, all based on the same soil, collected at Hygum soil (Scott-Fordsmand et al. 2000a). Cu-salt: uncontaminated Hygum-soil spiked to different concentrations with copper-nitrate, Cu-NPs: uncontaminated Hygum-soil spiked to different concentrations with copper-nanoparticles, and Cu-Field: Field Copper-contaminated Hygum soil that was sampled at different Cu concentration (the field contamination is more than 80 years old). The experiments were conducted as conventional concentration-response experiments.

2.1. Test soil

Test soil was collected at Hygum, Jutland, Denmark. The general physico-chemical characteristics of the soil from the Hygum-site are as follows: 20-32% coarse sand (>200 μ m), 20-25% fine sand (63- 200 μ m), 11-20% coarse silt (20-63 μ m), 12-20% silt (20-20 μ m), 12-16% clay (<2 μ m), 3.6-5.5% organic matter, Cation Exchange Capacity 6.8-10 (cmolc/kg dw), N 0.25-0.31% and P 0.10-0.12%. The clay mineralogy analysed by X-ray diffraction were dominated by illite, kaolinite, chlorite and vermiculite.

Previous (more than 80 years ago), this site was a timber preservation site using copper sulphate to preserve; this caused a contamination of the soil. Hence, there is a known field contaminated gradient of Cu, ranging from the natural background levels of 30 to 2,900 mg Cu/kg dry soil (Scott-Fordsmand et al. 2000a).

For the experiments, soil was sampled in the field to a depth of 20 cm. To exclude existing soil animals, major stones and plant material, the soil was dried at 80°C for 24 h in an oven (Memmert, Type UL40, Braunschweig, Germany) and then sieved to < 2 mm. Besides the control soil (with background Cu levels), the field test soil included Cu concentrations of 525, 1155, 2880 and 3900 mg Cu/kg, as picked from different

locations along the field gradient and measured (AAS). The physical-chemical parameters (described above) vary little with increasing Cu concentrations; the only monotonic trend observed was for the organic matter, 3-6-5.5%.

In the experiment, the control soil was spiked with either Cu-salt or Cu-NPs, and the field soil with original concentrations. For the Cu-salt spiked soil the pH was regulated (with CaCl_2) to 6.5. During the experiment the soil pH was measured at the beginning (day 0) and at the end of the experiment (3 weeks).

2.2. Test chemicals and characterization

Cu-salt: copper (II) nitrate trihydrate ($\text{Cu}(\text{NO}_3)_2 \cdot 3\text{H}_2\text{O}$) ($\geq 99\%$ pure, Merck, Darmstadt, Germany). Cu-NPs: elemental Cu (reported particle size 80 nm) with no coating (American Elements). The particles were characterised (see(Heckmann et al. 2011)) by transmission electron microscopy - TEM (Phillips/FEI, Eindhoven, The Netherlands), scanning electron microscopy - SEM (FEI NOVA 600, FEI Company, Hillsboro USA), powder x-ray diffraction - PXRD (STOE STAPI PSTOE & Cie GmbH, Darmstadt, Germany) and dynamic light scattering - DLS (Malvern Zetasizer Nano, Malvern Instruments Ltd, Worcestershire, UK).

Oxidations states, of pure particles and in soil, were analysed by X-ray absorption near edge structure (XANES) measurements, performed at Beamlines C and X1 at DORIS (DESY, Hamburg, Germany) using a Si (111) crystal pair monochromator for the Cu energy range with a resolution $\Delta E/E$ of $< 10^{-4}$ ($< 1\text{eV}$). Powder Standards were mixed with cellulose and pressed into pellets 13mm in diameter with ~ 2 absorption lengths of material ensuring sufficient uniformity and thickness for transmission measurements. Soil samples (three replicates) were sealed in Kapton tape and measured in fluorescence mode using a Canberra 7 element solid state (Ge) detector to monitor the Cu $\text{K}\alpha$ fluorescence line. Spectra were normalized to the incoming flux and a uniform edge

step. Background subtraction, normalization and linear combination analysis of the spectra was performed using Athena (Ravel and Newville 2005). To enhance resolution the soil samples contained 3000 mg Cu/kg soil (spiked), similar spectra were obtained at lower soil Cu concentrations.

To verify exposure, the total soil Cu-concentrations were analysed by flame Atomic Absorption Spectrometry (AAS) (Perkin Elmer 4100, Ueberlingen, Germany). The AAS analyses were checked using a standard reference samples. The soil (1 g dry weight) was digested using 7N HNO₃ and heating up to 110 °C until all brown fumes were gone (Scott-Fordsmand et al. 2000b).

To estimate the labile Cu fraction two concurrent experiments were performed. For these experiments the labile Cu-fractions were estimated by measures of free active Cu²⁺ in soil-solution and estimating the distribution of Cu between the various soil fractions using sequential extraction of Cu from soil. The free Cu-activity (Cu²⁺) was measured on soil solutions using an ion-selective electrode (ISE25CU, Radiometer) see (Gomes et al. 2012b). The soil-solution extract was the supernatant of a (1:5) soil:water solution which was mixed for 5 min at 250 rpm (lab shaker) and then settled for 2 hours. This soil solution contained other elements that possibly could interfere with the ISE measures, hence to support the soil-water observations, the possible dissolution of the Cu-NPs was measured in a simpler solution, a modified-water solution. The modified-water solution was demineralised-water with the same ionic strength and pH as soil-solution extracts, the ion strength was made by adding KNO₃ to the demineralised water. The distribution between soil fraction was estimated by sequential extraction following the Rauret et al. (1999) modifications of the BCR-method. In short, 1st extraction: 0.11 M acetic acid [targeting carbonates], 2nd extraction: 0.5 M hydroxylammonium chloride [to dissolve Mn-and Fe-oxides], and the 3rd extraction: 8.8

M hydrogen-peroxide plus heating [to digest organic matter] followed by 1.0 M ammonium acetate [to complex re-adsorbed Cu]. The extraction analyses were performed on 1.3 g dry soil at the exposures scenario similar to that of the XANES analyses. The extracted fractions were analysed for Cu on AAS (as described above).

2.3. *Test organism*

The test organism used for this study belongs to the specie *Enchytraeus crypticus*, Westheide and Graefe 1992. Individuals were cultured in Petri dishes containing agar medium, consisting of a sterilized mixture of four different salt solutions (CaCl₂·2H₂O; MgSO₄; KCl; NaHCO₃) and a Bacti-Agar medium (Oxoid, Agar No. 1), kept at 20°C and fed on dried, ground oats.

2.4. *Spiking procedure*

Spiking of uncontaminated field collected soil was done according to OECD recommendations for the testing of non-soluble substances (OECD 2004). In short, the equivalent of 2.5 g of dry soil per test vessel (10 g per treatment) was mixed with the quantity of the test substances (Cu-salt or Cu-NPs), as dry powders, to obtain the desired final concentrations. This portion of contaminated soil was added to the remaining pre-moistened soil (20% of water) and mixed manually 10 min. The procedure was repeated for each test concentration and the soil was then divided into 4 replicates per treatment. The spiked concentrations used were 100, 200, 400, 600, 800, 1000 and 1500 mg Cu/kg for Cu-salt and 100, 400, 800, 1000 and 1500 mg/kg for Cu-NPs.

2.5. Test procedure

Test procedures followed the Enchytraeid Reproduction Test (ERT) (OECD 2004). In short ten adult organisms with well-developed clitellum and similar size were selected and introduced in each test vessel containing 25 g of moist soil and fed with 25 mg of finely ground and autoclaved rolled oats. The vessels were covered with a lid containing small holes and the test ran for 3 weeks, at 20°C and 16:8h photoperiod. Four replicates per treatment were used. Weekly, 12.5 mg of food was supplied and soil moisture was adjusted by replenishing weight loss with the proper amount of deionised water. At the test end enchytraeids were extracted by spreading the soil of each test vessel into plastic containers (200 ml volume and diameter of 7 cm), which were filled with demineralised water, gently shaken and left for 24 h at 5 °C for sedimentation to occur. After that, adult and juvenile enchytraeids appeared on the soil surface and were collected and counted under dissection microscope within 24 h to assess their survival and reproduction.

In regard to the biological responses, all the tests fulfilled the biological validity-criteria described in the OECD guideline 14, i.e. controls mortality < 20%, number of juveniles > 25 and coefficient of variation <50%. The soil pH was not significantly different between test conditions and did not significantly change during the test duration.

2.6. Statistics

Results were analysed through a one-way ANOVA (Dunnett's Method) (SigmaPlot11.0) to assess differences between control and treatments and to determine the No Observed Effect Concentration (NOEC) and the Lowest Observed Effect Concentration (LOEC) as the highest tested concentration with no statistically significant effect and the lowest tested concentration with a statistically significant effect, respectively. The reproduction effect concentrations (EC_x) and the lethal concentration to 50% of the organisms (LC_{50}),

were calculated using the Toxicity Relationship Analysis Program (TRAP). For the LC_{50} probit was used and for the EC_x determination a 2-parameters non-linear sigmoid threshold models were used [$X < X_0$: $Y = Y_0$; $X_0 < X < X_{50}$: $Y = Y_0(1 - \frac{1}{2}(1 + S(X - X_{50}))^2)$; $X_{50} < X < X_{100}$: $Y = Y_0(\frac{1}{2}(1 - S(X - X_{50}))^2)$; $X > X_{100}$: $Y = 0$].

3. Results

The concentration of Cu in the background was 30 mg Cu/kg. For all test-exposures the total concentration (measured by AAS) was within 5-7% of the “background” plus added Cu. The pH of the soil remained constant throughout the experiments.

3.1. Particle characterisation

The nanoparticles (American elements) used had a mean nominal diameter of 80 nm, purity of 99.5%. Measured by PXRD the primary particle size was ≥ 66 nm with a z-average of 419 ± 1 nm (measured by DLS) indicating agglomeration of particles, and a Zeta potential of 15.3 ± 0.3 mV (measured in demineralised water). Correspondence between the Cu and CuO crystallite sizes and the TEM and SEM images, tentatively suggest that the particle morphology was comprised by a Cu crystalline core with a Cu_xO_y (shell) surface oxidation (Heckmann et al. 2011), see supplementary material (Table S1, Fig. S1A/B, and S2). Hence, copper oxide crystallites were observed in addition to the specified Cu crystalline phase, which was confirmed with PXRD and XANES. A flower-like morphology of agglomerated particles was observed (see (Heckmann et al. 2011)). The XANES (using linear combination fit (LCF) in the program Athena) indicated that oxidation state distribution of Cu-NPs – before addition to soil - was approximately 86% Cu(0), 1% Cu(I) and 13% Cu(II) (see Table S1).

3.2. Exposure characterisation

The XANES (using linear combination fit (LCF) in the program Athena (Ravel and Newville, 2005)) showed that only the oxidation state Cu(II) could be observed in the Cu-salt and Cu-field soils. For the Cu-NPs spiked soil, oxidation state distribution was approximately 58-59% Cu(0), 10% Cu(I) and 32% Cu(II), based upon analysis of a soil containing 3000 mg Cu-NPs/kg soil (Fig. 1 and Table 1, see supplementary material). For Cu-NPs spiked soil the “background” soil Cu concentration (approx. 30 mg Cu/kg) explained 1% of the oxidation state. The XANES spectra indicate that the Cu(II) mainly exists as Cu-O bonds (although not possible to exclude N bound). For both the Cu-salt and the Cu-field the indications are also Cu bonds to oxygen (or nitrogen).

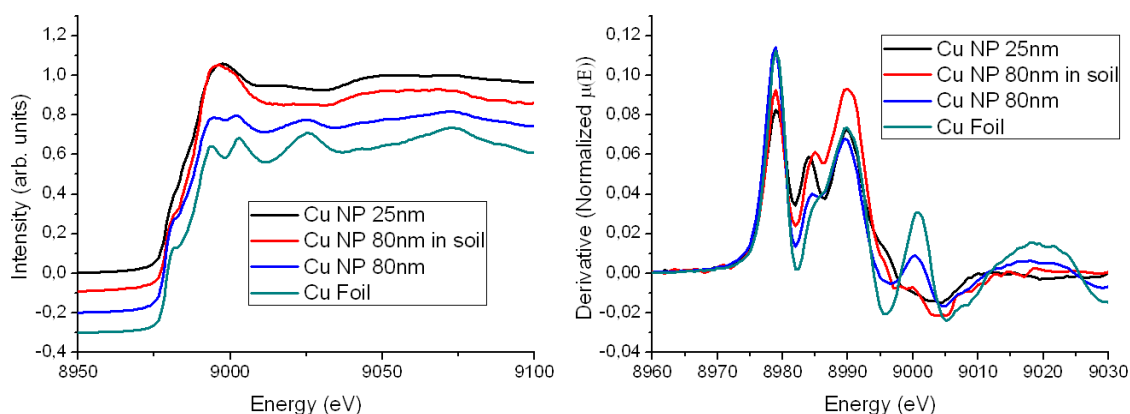


Figure 1: Left, normalized XANES spectra at the Cu K-edge. Right, 1st Derivative of the normalized XANES spectra.

The active Cu²⁺ fraction (as measured by Cu-ISE) in modified-water and the soil-solution extracts was below the detection limit and quantification (3×10^{-9} M Cu²⁺). The detection limit corresponded to that less than 5×10^{-7} % of the total-content could be detected.

The sequential extraction (see Fig. 2) showed similar extraction patterns for the Cu-NPs and the Cu-salt samples, with approximate values of 69% (Cu-NPs) and 77% (Cu-salt)

in the first extraction, 28% (Cu-NPs) and 22% (Cu-salt) in the second extraction, 3% (both) in the third extraction, and less than 1% (both) in the residues. For the field-contaminated soil the equivalent % were: 1st extraction 34%, 2nd extraction 40%, 3rd extraction 13% and 12% in the residual. Technically speaking, the 1st extraction targets exchangeable and acid soluble Cu, the 2nd extraction the reducible Cu, and the 3rd extraction targets the oxidisable Cu in the soil sample.

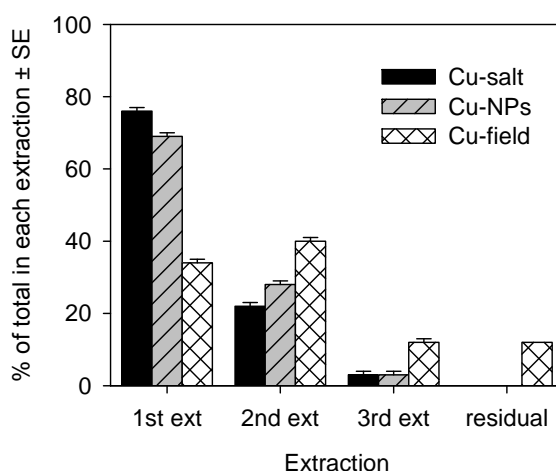


Figure 2: Relative distribution between fractions from sequential extraction of copper from Hygum-soil contaminated with 2000 mg/kg of $\text{Cu}(\text{NO}_3)_2$ (Cu-salt), copper nanoparticles (Cu-NPs) and CuSO_4 historical contamination (Cu-field).

3.3. Biological effects

Survival was affected by Cu-salt and Cu-field treatments, but not by Cu-NPs (Table 1, Figure 3). Freshly spiked Cu-salt caused an LC_{50} at 595 mg Cu/kg (adult-survival) and an EC_{50} at 361 mg Cu/kg (reproductive output). The Cu-NPs caused an EC_{50} at 1760 mg Cu/kg (reproductive output). For the historically Cu-contaminated field soil (Cu-field) the EC_{50} was at 2068 mg Cu/kg, with adult survival affected at 3900 mg Cu/kg (Table 1).

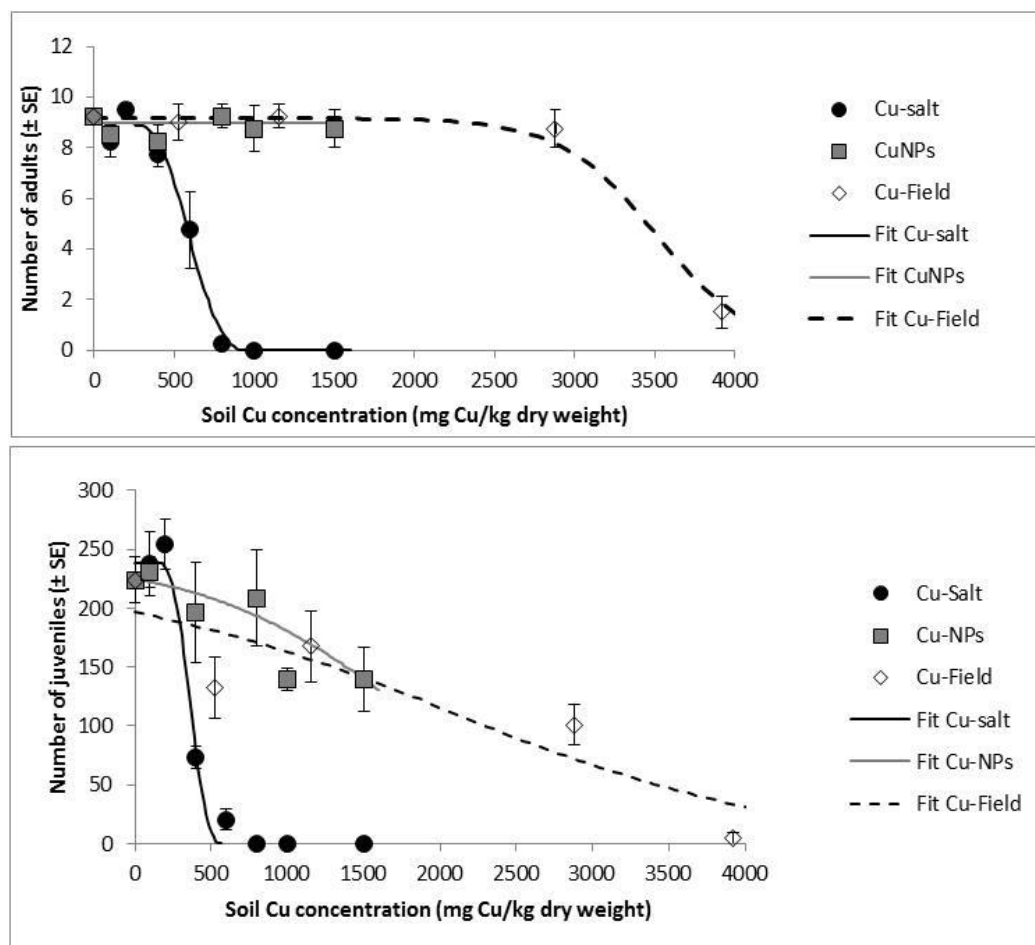


Figure 3: Effects of copper nitrate (Cu-salt), copper nanoparticles (Cu-NPs) and historically Cu-salt contaminated filed soil (Cu-field) on survival (up) and reproduction (down) of *Enchytraeus crypticus*. Results are expressed as average (AV) \pm standard error (SE); $n = 4$. The fitted lines are the models (threshold sigmoid) used to estimate EC_x values, see Table 1.

Table 1 Effect concentrations (EC_x), no observed effect concentrations (NOEC) and lowest observed effect concentrations (LOEC) for survival and reproduction of *Enchytraeus crypticus* exposed to $Cu(NO_3)_2$ (Cu-salt), copper nanoparticles (Cu-NPs) and historically Cu field contaminated soil (Cu-field).

	Survival		Reproduction				Steepness (SE) Y_0
	LC_{50}	NOEC/ LOEC	EC_{10}	EC_{20}	EC_{50}	NOEC/ LOEC	
Cu-salt	595 (555-653)	400/ 600	254 (150-358)	290 (211-369)	361 (326-398)	200/ 400	$5.1 \cdot 10^{-3}$ ($1.8 \cdot 10^{-3}$) 239
Cu-NPs	NE	>1500	590 (-29-1208)	982 (575-1389)	1760 (1038-2482)	>1500	$4.7 \cdot 10^{-4}$ ($2.1 \cdot 10^{-4}$) 227
Cu-field	3508 (3292-3726)	2880/ 3990	NE	564 (-352-1482)	2068 (1391-2747)	<525	$2.4 \cdot 10^{-4}$ ($0.6 \cdot 10^{-4}$) 224

LC_{50} =50% Lethal Concentration; EC_{10} =10% Effect Concentration; EC_{20} =20% Effect Concentration; EC_{50} =50% Effect Concentration; NOEC = No Observed Effect Concentration; LOEC = Lowest Observed Effect Concentration; 95% CL = 95% Confidence Limits; NE: no effect;

4. Discussion

This study showed that in a 21 day test the Cu toxicity to soil organisms *E. crypticus* depended on the Cu-form. The highest toxicity was caused by $CuNO_3$ exposure, followed by Cu nanoparticle (Cu-NPs) exposure and then by field Cu-contaminated soil (Cu-field). The Cu oxidation state in the soil was Cu(II) for the $CuNO_3$ spiked and the field contaminated soil, whereas all three oxidation states Cu(0), Cu(I) and Cu(II) were present in the Cu-NPs spiked soil. The relative Cu distribution between soil fractions (sequential extraction) was similar for $CuNO_3$ and Cu-NPs spiked soils, whereas the Cu-field soil had a larger fraction of Cu attached to the residual fraction. It was not

possible to detect Cu^{2+} in (1:5) soil solutions from any of the soils [Ion Selective Electrode].

A continuous discussion point in relation to Cu-NPs exposure of organisms is whether the particles remain particles or dissolve in the soil matrix. For the Cu-NPs exposures, two fate scenario's (or a combination of these) seem plausible based on observed (O, I, II) oxidations states [XANES observations]: (i) some of the particles are completely oxidised while others remain reduced, or (ii) the particles are more or less uniformly oxidized. However, since the Cu-NPs soil spectra resembles that of a non-soil 25 nm particle [more than the non-soil 80 nm spectra] this indicates (only indicate) the presence of a smaller and more oxidised particle within the soil rather than a mixture of larger particles and dissolved ions. Assuming a uniform oxidation of the particles (scenario ii above), the observed 42 % Cu oxidation (10% Cu(I) and 32% Cu(II)) in soil indicates that approximately 6-7 nm of the particle surface is oxidised, with the interior of the particle remaining as Cu(0) [calculated based on the spherical 80 nm diameter].

Using a particle density of 9 g/cm^3 , a cubic structure, and a van der Waals radius of 0.14 nm for Cu, this means that the core is Cu(0) followed by 24 Cu-atom layers oxidised to Cu(I) and 48 Cu-atom layers oxidised to Cu(II). [The equivalent numbers before addition to the soil are a core (Cu(0)) coated with 3 layers Cu(I) and 30 layers of Cu(II).]

It must be emphasized that this is a rough estimate to illustrate the possible scenario. The observation that particles are present in the soil corresponds with Unrine et al. (2010) who observed partial oxidation of Cu-particles (32 and 102 nm) in OECD soil. This indicates that there could be a release of Cu-ions from the nanoparticles within the soil-matrix, however there was no measurable Cu activity in the soil solution (measured with ion selective Cu-activity). The Cu-NPs may have released ions without this being

detected by the ISE-measures in soil-solution, as released Cu-ions may have been bound immediately to soil constituents. Such binding is evident in the Cu-salt soil-solution, where Cu-activity was also low despite the ready dissolution of CuNO₃. On the other hand, since there was no measurable Cu activity in the modified-water Cu-NPs solution, there may be a limited release of Cu from Cu-NPs. The modified water had the same ionic strength and pH as the soil-solution, and in this case the observation was free of the interference problems that may arise for ISE measures in the more complex solutions. Nevertheless, it should be kept in mind that soil-solution may contain other characteristics that could influence particle dissolution/ stabilisation. The sequential extraction showed that Cu from Cu-NPs and Cu-salt were present in approximately the same relative amounts (or percentages) in the three extracts and the residual. Combined with the above information on oxidation states this indicates that both Cu from Cu-NPs and Cu-salt are in relatively loosely bound fractions (first extraction), corresponding with a higher toxicity. The extraction probably covers Cu specifically sorbed on surfaces of clays, OM, Fe/Mn oxyhydroxides and to some degree silicates (Gleyzes et al. 2002), whereas the next extraction covers Cu bound in Fe- and Mn-oxides. The final oxidation step releases Cu bound in organic matter (Gleyzes et al. 2002). For the field contaminated soil, a larger fraction remained in the residual fraction (believed to be less accessible) which corresponded to a lower toxicity in this soil. It is recognised that the extraction procedure (sequential extraction) may influence dissolution of the Cu-NPs, however an increased dissolution is unlikely in the acetic acid solution (see e.g. Deng et al 2013), but may be the case in the latter two extractions. Hence, the exposure measures indicate that the organisms in the Cu-NPs exposure were partly exposed to Cu in the form of nanoparticles and less [in terms of total-concentration (weight)] to the released dissolved Cu²⁺ ions.

Among the different tested Cu forms, the Cu-salt exposure caused the most pronounced toxicity to *E. crypticus*, followed by Cu-field and Cu-NPs [the latter two at comparable levels]. Amorim and Scott-Fordsmand (2012) on the contrary observed, that for *E. albidus*, Cu-NPs was more toxic (reproduction) than CuCl₂ salt. We are not aware of the reason for such a difference between the two enchytraeid species, but this will be explored. The difference in toxicity for *E. crypticus* between the different Cu-forms is in agreement with a previous study using the earthworm *Eisenia fetida* (Heckmann et al. 2011). When comparing Cu-salt and historically contaminated soil (Cu-field), the results are in agreement with previous results obtained for the same species (Maraldo et al. 2006) and for other soil invertebrates (Scott-Fordsmand et al. 2000a; Scott-Fordsmand et al. 2000b). It is generally observed that aged contaminated soil causes less immediate toxicity. Here, the “aging” reflected that a larger Cu-fraction (of total) was present in the residual soil part (sequential extraction).

If we speculate that dissolved Cu²⁺ was responsible for the Cu-NPs toxicity, then the difference in toxicity (see Fig. 3) between the Cu-salt and Cu-NPs exposure should provide an indication of the amount of Cu²⁺-release from particles. Data (the Cu-salt/Cu-NPs reproduction-data, Fig. 3) suggest that with increasing numbers of Cu-NPs (i.e. increasing total mass) there is a lower relative release of Cu²⁺ (see Fig. 4). For example, the effect on reproduction at 400 mg Cu-NPs/kg exposure corresponds to the effect at approximately 250 mg Cu-salt/kg exposure, hence given our above assumption, there is approximately 62.5% Cu²⁺ release from the Cu-NPs. Performing a similar calculation for the 1500 mg Cu-NPs/kg exposure, the potential Cu release is 23% (note that this is close to the level of oxidation observed with the XANES), see in Fig. 4. We see that the possible release (toxicity difference) is not directly related to the surface area of the particles (Fig 4). The relative bioavailability of Cu-NPs seems to decrease

with increasing concentration and is not inversely related to the calculated total surface area.

Doing it the opposite way i.e. assuming a constant release of 32% (see XANES oxidation levels) then 32% of the total Cu-NPs concentrations is equivalent to the Cu(II) available. These calculations show a better overlap of the two concentration response curves, but the curve modified Cu-NPs concentration ($S=1,47 \cdot 10^{-3}$, with $EC_{10} = 188$ and $EC_{50} = 560$ mg Cu/kg) of response curve has a less steep slope again indicating relatively less release with increasing concentrations.

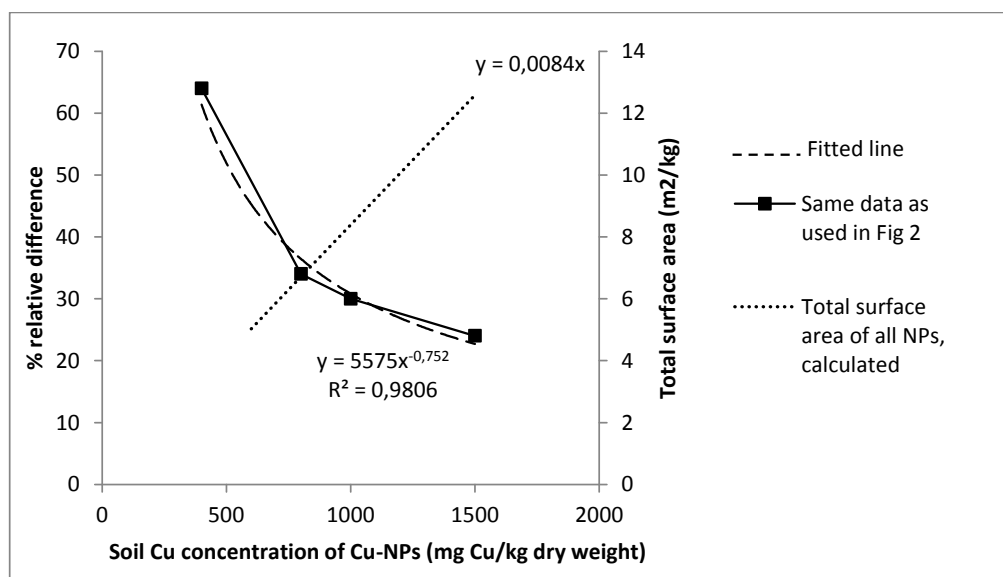


Figure 4: Estimated release of Cu ions from Cu-nanoparticles (Cu-NPs), assuming that Cu^{2+} is causing the toxicity.

It must be assumed that a relatively larger fraction of the total Cu^{2+} released from the lower exposure Cu-NPs concentration will bind to soil components, as relatively more soil sorption-sites per released Cu atom are present. However, at higher concentrations agglomeration and/or changes in partitioning may reduce the release of Cu from particles. It seems that the similar toxicity for the Cu-NPs and Cu-field should be

explained by two different mechanisms; (i) for the Cu-NPs exposure, the particles are present in soil-solution (various easily extractable fractions) and less as free ions, and (ii) in the Cu-field exposure, a smaller fraction of the Cu is present in the solution and more bound in the residual fraction (assumed less available). Whether dissolution of the particles influences the traditional concerns related to sequential extractions – the redistribution between fractions is unknown.

Finally, assuming that the particles are toxic *per se* [rather than the ions alone], then a slower uptake-rate could explain the observed toxicity differences. This would also fit with all the exposure measurements, i.e. primary oxidation state of 0 in the soil (with oxidation state I and II still associated with the particle), low Cu^{2+} activity in the soil solution and a similar distribution in the sequential extraction (the toxicity could be expressed based on the first extraction which would highlight the differences). Copper-NPs would simply be less immediate toxic (than free ions) in the duration of the test (3 weeks), but the toxicity may be expressed later or over longer time. This would also fit with that the toxicity pattern is similar to that of the field contaminated soil, but that it is not caused because the soil Cu is aged as we know that ageing does not happen immediately experiment.

Acknowledgments

Portions of this research were carried out at Beamlines X1 and C of the DORIS light source at DESY. DESY is a member of the Helmholtz Association (HGF). The project was financially supported by the funding FEDER through COMPETE-Programa Operacional Factores de Competitividade, by National funding through FCT-Fundação para a Ciência e Tecnologia, within the research project NANOkA FCOMP-01-0124-FEDER-008944 (Ref^a. FCT PTDC/BIA-BEC/103716/2008), and through an FCT PhD

grant to Susana Gomes (SFRH/BD/63261/2009)- FP7 project, MARINA (263215). The authors report no conflict of interest. The authors alone are responsible for the content and writing of the paper.

Supplementary material is available with calculations, derivations and additional graphs for XANES measurements (see relevance in main text).

References

- Amorim, M. and Scott-Fordsmand, J. 2012. Toxicity of Copper nanoparticles and CuCl₂ salt to *Enchytraeus albidus* worms: survival, reproduction and avoidance responses. *Environ Pollut* 164: 164-168.
- Amorim, M. J. B., Rombke, J., Schallna, H. J. and Soares, A. M. V. M. 2005. Effect of soil properties and aging on the toxicity of copper for *Enchytraeus albidus*, *Enchytraeus luxuriosus*, and *Folsomia candida*. *Environ. Toxicol. Chem.* 24(8): 1875-1885.
- Amorim, M. J. B., Novais, S., Rombke, J. and Soares, A. M. V. M. 2008. *Enchytraeus albidus* (Enchytraeidae): A test organism in a standardised avoidance test? Effects of different chemical substances. *Environ. Int.* 34(3): 363-371.
- Amorim, M. J. B., Gomes, S. I. L., Soares, A. M. V. M. and Scott-Fordsmand, J. J. 2012. Energy Basal Levels and Allocation among Lipids, Proteins, and Carbohydrates in *Enchytraeus albidus*: Changes Related to Exposure to Cu Salt and Cu Nanoparticles. *Water Air Soil Pollut.* 223(1): 477-482.
- Evans, P., Matsunaga, H. and Kiguchi, M. 2008. Large-scale application of nanotechnology for wood protection. *Nat. Nanotechnol.* 3(10): 577-577.
- Gleyzes, C., Tellier, S. and Astruc, M. 2002. Fractionation studies of trace elements in contaminated soils and sediments: a review of sequential extraction procedures. *Trac-Trend Anal Chem* 21(6-7): 451-467.

- Gomes, S. I. L., Novais, S. C., Scott-Fordsmand, J. J., Coen, W. D., Soares, A. M. V. M. and Amorim, M. J. B. 2012a. Effect of Cu-nanoparticles versus Cu-salt in *Enchytraeus albidus* (Oligochaeta): Differential gene expression through microarray analysis. *Comp Biochem Physiol, C* 155: 219-227.
- Gomes, S. I. L., Novais, S. C., Gravato, C., Guilhermino, L., Scott-Fordsmand, J. J., Soares, A. M. V. M. and Amorim, M. J. B. 2012b. Effect of Cu-nanoparticles versus one Cu-salt: analysis of stress and neuromuscular biomarkers response in *Enchytraeus albidus* (Oligochaeta). *Nanotoxicology* 6(2): 134-143.
- Heckmann, L.-H., Hovgaard, M. B., Sutherland, D. S., Autrup, H., Besenbacher, F. and Scott-Fordsmand, J. J. 2011. Limit-test toxicity screening of selected inorganic nanoparticles to the earthworm *Eisenia fetida*. *Ecotoxicology* 20(1): 226-233.
- ISO (2005). Soil Quality - Effects of pollutants on Enchytraeidae (*Enchytraeus* sp.). Determination of effects on reproduction and survival. Guideline 16387. International Organization for Standardization, Geneva,Switzerland.
- Klaine, S. J., Alvarez, P. J. J., Batley, G. E., Fernandes, T. F., Handy, R. D., Lyon, D. Y., Mahendra, S., McLaughlin, M. J. and Lead, J. R. 2008. Nanomaterials in the environment: Behavior, fate, bioavailability, and effects. *Environ Toxicol Chem* 27(9): 1825-1851.
- Maraldo, K., Christensen, B., Strandberg, B. and Holmstrup, M. 2006. Effects of copper on enchytraeids in the field under differing soil moisture regimes. *Environ Toxicol Chem* 25(2): 604-612.
- Menezes-Oliveira, V. B., Scott-Fordsmand, J. J., Rocco, A., Soares, A. M. V. M. and Amorim, M. J. B. 2011. Interaction between density and Cu toxicity for *Enchytraeus crypticus* and *Eisenia fetida* reflecting field scenarios. *Sci Total Environ* 409(18): 3370-3374.
- OECD 2004. Guidelines for the testing of chemicals No. 220. Enchytraeid Reproduction Test. Organization for Economic Cooperation and Development. Paris.

- Rauret, G., Lopez-Sanchez, J. F., Sahuquillo, A., Rubio, R., Davidson, C., Ure, A. and Quevauviller, P. 1999. Improvement of the BCR three step sequential extraction procedure prior to the certification of new sediment and soil reference materials. *J Environ Monit* 1(1): 57-61.
- Ravel, B. and Newville, M. 2005. ATHENA, ARTEMIS, HEPHAESTUS: data analysis for X-ray absorption spectroscopy using IFEFFIT. *J Synchrotron Radiat* 12: 537-541.
- Scott-Fordsmand, J. J., Krogh, P. H. and Weeks, J. M. 2000a. Responses of *Folsomia fimetaria* (Collembola : Isotomidae) to copper under different soil copper contamination histories in relation to risk assessment. *Environ Toxicol Chem* 19(5): 1297-1303.
- Scott-Fordsmand, J. J., Weeks, J. M. and Hopkin, S. P. 2000b. Importance of contamination history for understanding toxicity of copper to earthworm *Eisenia fetida* (Oligochaeta : Annelida), using neutral-red retention assay. *Environ Toxicol Chem* 19(7): 1774-1780.
- SigmaPlot11.0 Copyright © 2009 Systat Software Inc. Systat Software Inc.
- Unrine, J. M., Tsyusko, O. V., Hunyadi, S. E., Judy, J. D. and Bertsch, P. M. 2010. Effects of Particle Size on Chemical Speciation and Bioavailability of Copper to Earthworms (*Eisenia fetida*) Exposed to Copper Nanoparticles. *J Environ Qual* 39(6): 1942-1953.

Supplementary material

Table S1: Linear Combination Fitting (LCF) results using Cu Foil, Cu₂O, CuO standards.

Sample	Fit region (E0)	R-Factor	Chi-Square	Reduced Chi-Square	Cu foil		Cu ₂ O		CuO	
					Cu(0)	+/-	Cu(I)	+/-	Cu(II)	+/-
Cu NP 80nm	-20 to +50	0,047498	0,00575	0,0000417	86,0%	2,1%	1,4%	1,6%	12,5%	2,6%
Cu NP 80nm in soil	-20 to +50	0,051878	0,00796	0,0000632	58,7%	2,6%	9,7%	2,0%	31,7%	3,3%

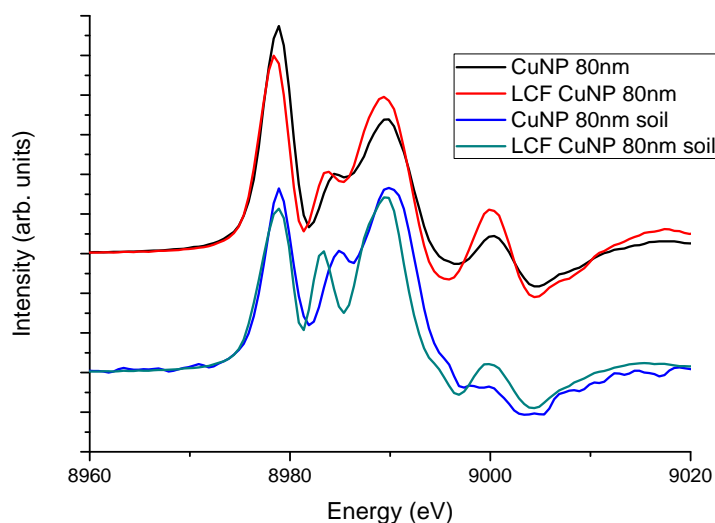


Figure S1: Fits of Cu NP 80nm and Cu NP 80nm in Soil (1st derivative of normalized spectra).

The discrepancy in the fits originates from the difference between bulk Cu and the Cu nanoparticle as seen in Figure 1. There is additionally a similar difference between the CuO and Cu₂O bulk powder used for the fittings and nano-Cu_xO_y layers surrounding the Cu nanoparticles. This difference between bulk and nano-samples is due to the increase in surface area to bulk ratio that results in more contribution of surface states in the nano-samples. The nano-samples also lack long range order compared to their bulk

counter parts as seen in the decrease of multiple scattering peak at 9000 eV (Figure 1) making this area difficult to fit in terms of peak intensity. Since the number of surface states (peak intensity) changes while peak position remains relatively unchanged for a given oxidation state (shifts to higher energy with increase oxidation state, see Figure S2) the fittings were performed on the derivative of the normalized spectra. It is impossible to know the exact compounds in the soil bound to the Cu NP 80nm and therefore the fit is only a rough approximation to determine the relative change in oxidation state for the Cu nanoparticles.

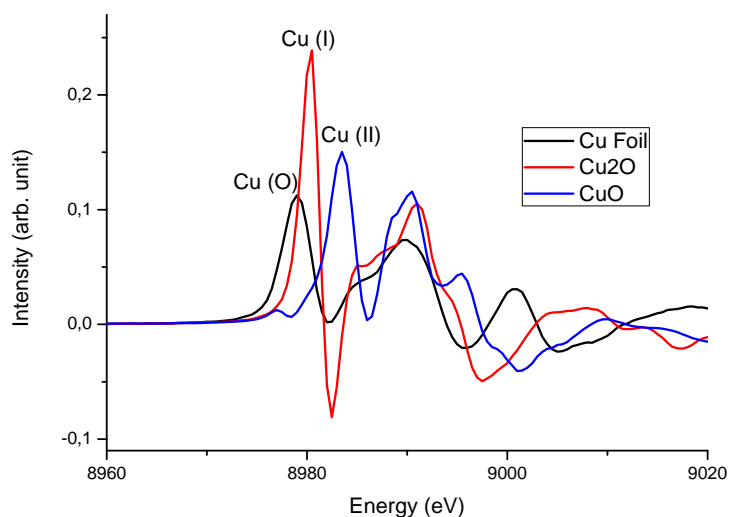


Figure S2: Oxidation states of copper (1st derivative of normalized spectra).

Chapter V

Exposure to different copper forms – nanoparticles,
nanowires, salt and field aged: gene expression profiling in

Enchytraeus crypticus

V - Exposure to different copper forms – nanoparticles, nanowires, salt and field aged: gene expression profiling in *Enchytraeus crypticus*

Susana I.L. Gomes^a, Natália Pegoraro^a, Tito Trindade^b, Janeck J. Scott-Fordsmand^c and
Mónica J.B. Amorim^a

^aDepartment of Biology & CESAM, University of Aveiro, 3810-193 Aveiro, Portugal

^bDepartment of Chemistry, CICECO, Aveiro Institute of Nanotechnology, University of Aveiro, 3810-193 Aveiro, Portugal

^cDepartment of Bioscience, Aarhus University, Vejlsovej 25, PO BOX 314, DK-8600 Silkeborg, Denmark

Abstract

The testing of NMs under the currently available standard toxicity tests does not cover many of the NMs specificities. One of the current recommended approaches forward lays on understanding the mechanisms of action as these can help predicting long term effects and safe-by-design production. Copper nanomaterials (Cu-NMs) usage has been highly increasing with the concern in terms of exposure, effect and associated risks. In the present study we used the high-throughput gene expression tool developed for *Enchytraeus crypticus* (44Kx4 Agilent microarray) to study to the effect of exposure to several copper forms. The copper treatments include two NMs (spherical and wires) and two copper-salt treatments (CuNO₃ spiked and Cu field historical contamination). Testing was done based on reproduction effect concentrations (EC₂₀, EC₅₀) using 3 and 7 days exposure periods. Gene expression profile showed a main separation between exposure times; Cu-Field/Cu-Nwires were separated from CuNO₃/Cu-NPs. The

functional analysis indicated NMs specific mechanisms of response. Cu-salt exposure affects mechanisms related with calcium homeostasis and activates the chemosensory system of the enchytraeids. The regulation of translation was affected by the salt and NMs. Energetic metabolism was affected differently depending on the copper forms; processes related with histone modifications and DNA repair were exclusively affected by NMs. Additionally, the different NMs (NPs and Nwires) affected different functions, indicating that the shape must play a role.

Keywords: nanoparticles; high-throughput; toxicogenomic; mechanisms of response; enchytraeids

1. Introduction

The testing of NMs under the currently available standard toxicity tests does not cover many of the NMs specificities. Much of the uncertainty is due the lack of knowledge on the interactions between NMs and the organisms/cells, the nano-bio interactions (Roca et al., 2012). One of the current recommended options lays on understanding the mechanisms of action as these can help predicting long term effects and safe-by-design production. High-throughput omic tools together with in depth bioinformatics can help understanding the mechanisms of toxic-mediated responses. Further, to establish the link between alterations in critical macromolecules (e.g. genes, proteins, metabolites) and their possible biological implications (Singh et al., 2010) represents one of the major milestones.

Applications for copper nanomaterials (Cu-NMs) started mainly with electronics and catalysis (Lee et al., 2008; Wang et al., 2004). The current replacement of copper-salt

based wood preservatives by nano-copper based products (Evans et al., 2008) represents a high production of Cu-NMs (about 39 500 tones/year). Copper NMs can be synthesized in different shapes, ranging from spherical (NPs) (Wu and Chen, 2004) to wires (Chang et al., 2005).

The shape of NMs is known to influence toxicity of such materials e.g. for Ni-NMs in zebrafish embryos (Ispas et al., 2009) or Ag-NMs on the bacteria *Escherichia coli* (Pal et al., 2007). For example, dendrimers of Ni-NPs were more toxic to zebrafish embryos than spherical Ni-NPs, with LC₁₀ of 21 and 180mg/L respectively (Ispas et al., 2009); truncated triangular Ag-NPs were more effective in reducing *E. coli* growth than spherical Ag-NPs, which were more effective than Ag-nanorods (Pal et al., 2007). Regarding Cu-NMs, to authors' knowledge this is the first study comparing the toxicity of different shapes of Cu-NMs.

Data on effects of “spherical” Cu-NPs to soil invertebrates showed that NPs are comparatively less toxic than Cu-salt for *E. crypticus* (EC₅₀(Cu-NPs)=1760mg/kg and EC₅₀(CuNO₃)=361mg/kg) (Gomes et al., 2013), more toxic for *E. albidus* (EC₅₀(Cu-NPs)=95mg/kg and EC₅₀(CuCl₂)=251mg/kg) (Amorim and Scott-Fordsmand, 2012) and cause no toxicity to *Eisenia fetida* up to 50mg/kg, in terms of survival and reproduction (Unrine et al., 2010). Data on molecular analysis (e.g. at gene level) can bring a valuable input in the understanding of the mechanisms underlying the toxic responses observed and in pointing the way forward. Mechanistic effects of Cu-NPs have been investigated in *E. albidus* showing that Cu affected antioxidant enzymatic response in the worms with Cu-salt causing lipid peroxidation (Gomes et al., 2012a). At transcriptomic level, e.g. genes involved in energy metabolism were discriminating between Cu-NPs and CuCl₂ (Gomes et al., 2012b). Griffitt et al. (2009) also showed that zebrafish exposed to Cu-NPs and Cu-salt produce a distinct gene expression profile.

In the present study the aim was to assess the response mechanisms due to exposure to different copper shapes and forms using the high-throughput tool developed for the standard ecotoxicity species *Enchytraeus crypticus* (OECD, 2004), a high density microarray (Castro-Ferreira et al., 2013) refined onto a 4x44K Agilent platform. The Cu materials included CuNO₃, Cu-NPs (spherical), Cu-nanowires (Cu-Nwires) and Cu-salt from an historically contaminated field; exposure was performed during 3 and 7 days to concentrations corresponding to the EC₂₀ and EC₅₀ (20 and 50% effect concentrations on reproduction) (Gomes et al., 2013).

The test species, *E. crypticus*, besides being a standard species for soil ecotoxicology (OECD, 2004), has information on much more gene sequences (ca. 44000 Expressed Sequence Tags (ESTs) in the present microarray) than for other soil oligochaete (*Lumbricus rubellus* has 17000 ESTs (Bundy et al., 2008), *Eisenia fetida* has 4032 ESTs (Pirooznia et al., 2007) and *Enchytraeus albidus* with 2100 ESTs (Novais et al., 2012)).

2. Materials and Methods

2.1. Test organism

The test species *Enchytraeus crypticus* (Westheide and Graefe, 1992) was used. Individuals were cultured in Petri dishes containing agar medium, consisting of a sterilized mixture of four different salt solutions (CaCl₂·2H₂O; MgSO₄; KCl; NaHCO₃) and a Bacti-Agar medium (Oxoid, Agar No. 1). The cultures were kept under controlled conditions, at 19°C and photoperiod 16:8 hours light:dark. Organisms were feed on ground and autoclaved oats twice a week.

2.2. Test chemicals and characterization

Copper nitrate ($\text{Cu}(\text{NO}_3)_2 \cdot 3\text{H}_2\text{O}$) was purchased from Sigma Aldrich.

Two Cu nanomaterials were tested: Cu-nanoparticles (Cu-NPs) and Cu-nanowires (Cu-Nwires). Cu-NPs were purchased from American elements, purity 99.8%, with a size between 20-30 nm and Cu-Nwires were synthesized following the procedure described by Chang and co-authors (2005) by reduction of copper (II) nitrate with hydrazine in alkaline medium. The Cu-NPs were characterized as described in Gomes et al. (2013). The Cu-Nwires were characterized by powder X-ray diffraction (XRD) using a Philips X'Pert instrument operating with Cu K_α radiation ($\lambda = 1.543178 \text{ \AA}$) at 40 kV and 50 mA and by scanning electron microscopy (SEM) using a Hitachi S4100 instrument.

2.3. Test soil and spiking procedure

Test soil was collected at Hygum, Jutland, Denmark. The general physico-chemical characteristics of the Hygum study-site soil are as follows: 20-32% coarse sand ($>200\mu\text{m}$), 20-25% fine sand (63- $200\mu\text{m}$), 11-20% coarse silt (20- $63\mu\text{m}$), 12-20% silt (20- $20\mu\text{m}$), 12-16% clay ($<2\mu\text{m}$), 3.6-5.5% organic matter, Cation Exchange Capacity 6.8-10 (cmolc/kg dw), pH=5, N 0.25-0.31% and P 0.10-0.12%. The clay mineralogy analysed by X-ray diffraction were dominated by illite, kaolinite, chlorite and vermiculite.

At Hygum site soil has been exposed to contamination with CuSO_4 due to activities of timber preservation, which ceased more than 80 years ago. There is a well known Cu gradient along the field, ranging from the natural background levels of 30 up to 2,900 mg Cu/kg dry soil (Scott-Fordsmand et al., 2000). Soil was sampled in the field to a depth of 20 cm. To exclude soil fauna, the soil was dried at 80 °C for 24 h in an oven

(Memmert, Type UL40, Braunschweig, Germany), and then sieved through a 2 mm mesh to remove larger particles.

Spiking was done in soil from control area. Procedures for the Cu nanomaterials followed the OECD recommendations for the testing of non-soluble substances (OECD, 2004). In short, the equivalent of 2 g of dry soil per test vessel was mixed with the quantity of the test materials, as dry powders, to obtain the corresponding concentration range. This portion of contaminated soil was added to the remaining pre-moistened soil and mixed manually during 10 min. After that, demineralised water was added until 50% of soil WHC. The procedure was repeated for each replicate individually.

2.4. Experimental procedure

2.4.1. Survival and reproduction - Cu-Nwires

The test followed the standard procedures in the Enchytraeid Reproduction Test (ERT) guideline (OCDE, 2004). The concentrations tested were 0-100-400-600-800-1000-1500 mg/kg. For further details see e.g. Gomes et al.(2013).

2.4.2. Gene expression - Microarrays

For the gene expression assay, exposure followed the same procedures as the standard ERT (OECD, 2004) with adaptations as follows: twenty adults with well-developed clitellum were placed in each test vessel, containing 20g of moist soil (control or contaminated). The organisms were exposed for 3 and 7 days under controlled conditions of photoperiod (16:8h light:dark) and temperature ($20\pm 1^{\circ}\text{C}$) without food. After the exposure period, the organisms were carefully removed from the soil, rinsed in distilled water and frozen in liquid nitrogen. The samples were stored at -80°C , until analysis.

The exposure concentrations besides the control soil included a selection based on previously obtained reproduction effect concentrations EC₂₀ and EC₅₀ (see Table 1).

The Cu concentration in the field test soil was measured using Atomic Adsorption Spectroscopy (Cu concentrations of 502 and 1398 mg Cu/kg), To test the range for effects of the 25 nm Cu-NPs a limit test was conducted for 980 and 1760 mg/kg and similar effects to the 80nm Cu-NPs (within a 95% confidence intervals) were observed.

Table 1: Exposure concentrations (values in mg/kg) used for gene expression studies, which reflect the reproduction effect concentrations (EC₂₀ and EC₅₀ within the confidence intervals (CI)).

	control	EC ₂₀ (mg/kg)	EC ₅₀ (mg/kg)
CuNO ₃ *	0	290	360
Cu-NPs*	0	980	1760
Cu-Nwires	0	850	1610
Cu-Field*	0	500	1400

*(Gomes et al., 2013)

2.4.2.1. RNA extraction, labelling and hybridizations

RNA was extracted from each replicate containing a pool of 20 animals. Three biological replicates per test treatment (including controls) were used. Total RNA was extracted using SV Total RNA Isolation System (Promega). The quantity and purity of the isolated RNA were measured spectrophotometrically with a nanodrop (NanoDrop ND-1000 Spectrophotometer) and its quality was checked on a denaturing formaldehyde agarose gel electrophoresis. A single-colour design was used. In brief, 500ng of total RNA was amplified and labelled with Agilent Low Input Quick Amp Labelling Kit (Agilent Technologies, Palo Alto, CA, USA). Positive controls were

added with the Agilent one-colour RNA Spike-In Kit (Agilent Technologies, Palo Alto, CA, USA). Purification of the amplified and labelled cRNA was performed with the RNeasy columns (Qiagen, Valencia, CA, USA).

The cRNA samples were hybridized on the Custom Gene Expression Agilent Microarray (4x44k format) developed for this species (Castro-Ferreira et al., 2013). Hybridizations were performed using the Agilent Gene Expression Hybridization Kit (Agilent Technologies, Palo Alto, CA, USA) and each biological replicate was individually hybridized on one array. The arrays were hybridized at 65°C with a rotation of 10 rpm, during 17h. After that the microarrays were washed using Agilent Gene Expression Wash Buffer Kit (Agilent Technologies, Palo Alto, CA, USA) and scanned with the Agilent DNA microarray scanner G2505B (Agilent Technologies).

2.4.2.2. Acquisition and microarray data analysis

Fluorescence intensity data was obtained with Feature Extraction Software (10.5.1.1, Agilent Technologies). Quality control was done by inspecting the reports on the Agilent Spike-in control probes and by making box plots of each array. Processing of the data and statistical analysis were performed using RobiNA (v 1.2.4) (Lohse et al., 2012; Lohse et al., 2010) in the R environment (<http://www.R-project.org>). After background subtraction, data was normalized between arrays using Quantile normalization. Differential expression between control and treated samples was assessed using linear models and Benjamini-Hochberg's (BH) method to correct for multiple testing (Benjamini and Hochberg, 1995) (adjusted $p < 0.05$ was considered significant). The Minimum Information About a Microarray Experiment (MIAME) compliant data from this experiment will be submitted to the Gene Expression Omnibus (GEO) at the National Center for Biotechnology Information (NCBI) website.

Cluster analysis on differentially expressed genes was performed using MultiExperiment Viewer (MeV, TIGR). The differentially expressed genes for each treatment were analysed separately for GO (Gene Ontology) term enrichment analysis (Alexa et al., 2006) using the Blast2GO software.

2.5. Survival and reproduction data analysis

Data were checked for normality and homogeneity of variances, and one-way ANOVA with Post Hoc Dunnett's test (SigmaPlot11.0) was used to assess differences between control and treatments and to determine the No Observed Effect Concentration (NOEC) and the Lowest Observed Effect Concentration (LOEC) as the highest tested concentration with no statistically significant effect and the lowest tested concentration with a statistically significant effect, respectively. The reproduction effect concentrations (EC_x) were calculated using the Toxicity Relationship Analysis Program (TRAP 1.21) fitting the 2-parameters Logistic model.

3. Results

3.1. Materials characterization

Two distinct types of Cu nanomaterials have been evaluated in this research; these include Cu spherical particles (20-30 nm diameter) of commercial origin and wires (400-500 nm in cross section with length superior to 10 μ m). The Cu-Nwires powder obtained was identified by X-ray diffraction as composed mainly of metallic copper with a small amount of copper oxides resulting from surface oxidation (ca. 20%). Figure 1 shows a typical SEM image of as prepared Cu-Nwires that were kept under nitrogen before analysis to limit the extent of surface oxidation.

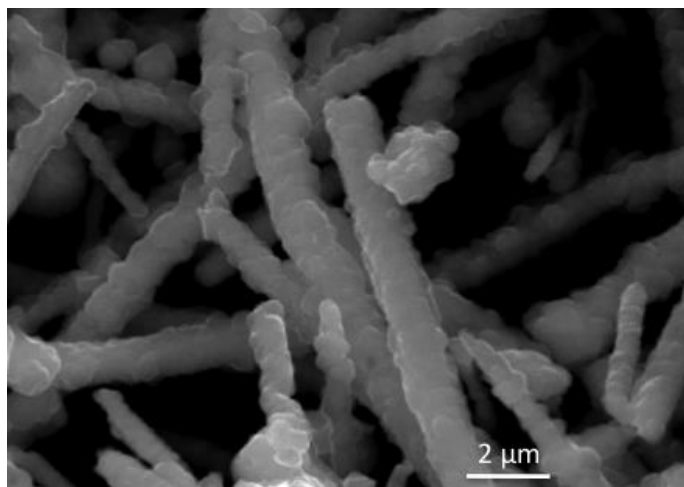


Figure 1: SEM image of Cu-Nwires prepared in aqueous medium.

3.2. Survival and reproduction - Cu-Nwires

The test fulfilled the validity criteria as within the OECD guideline (OECD, 2004) with controls' mortality lower than 20%, number of juveniles produced per replicate higher than 25, and coefficient of variation below 50%.

Cu-Nwires did not affect adults survival in the tested concentrations. Reproduction was significantly decreased at 1000 and 1600mg/kg ($p < 0.05$). The EC_{20} and EC_{50} were calculated based on a 2 parameters logistic model as 846.4 (680 < CI < 1013) mg/kg and 1613.3 (1372 < CI < 1855) mg/kg, respectively. The effects on reproduction can be depicted on figure 2.

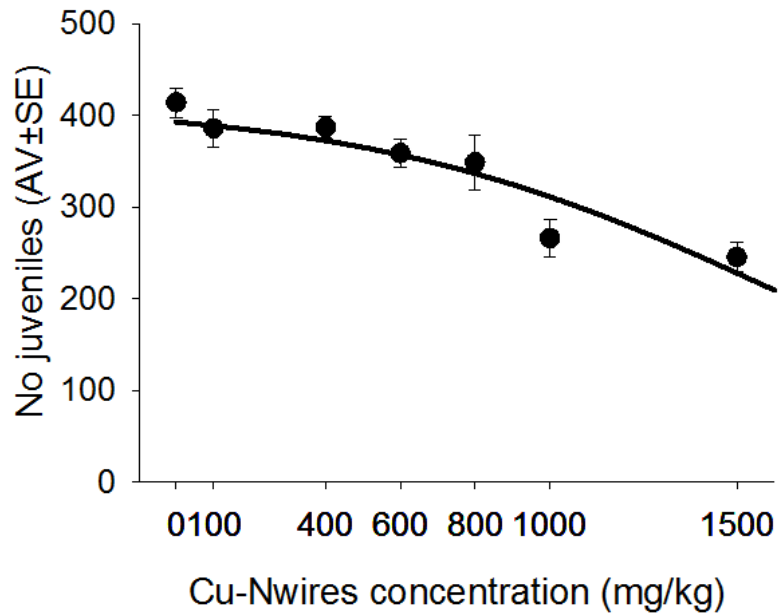


Figure 2: Results in terms of number of juveniles produced per 10 adult *Enchytraeus crypticus* exposed to copper-nano wires (Cu-Nwires). Data are presented as average \pm standard error (n=4). The model fitted to the data was a 2 parameters logistic.

3.3. Gene expression

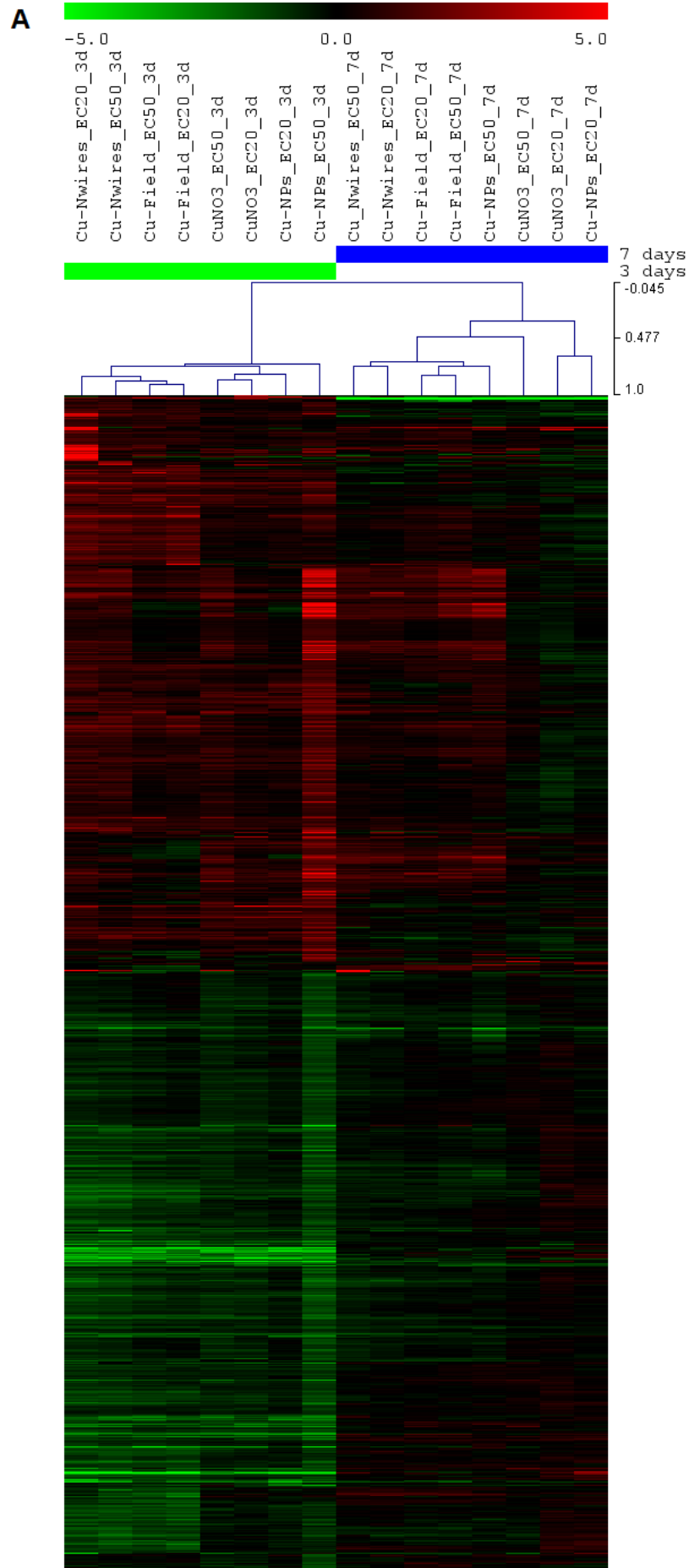
A total of 3494 transcripts (out of 43750) were significantly differentially expressed (adjusted $p < 0.05$) after 3 or 7 days of exposure to the different Cu treatments, in at least one condition. The number of DEGs affected by each test condition is shown on Table 2.

Table 2: Number of differentially expressed genes (adjusted $p < 0.05$) affected by exposure to the reproduction EC_{20} and EC_{50} for copper nitrate ($CuNO_3$), copper-nanoparticles (Cu-NPs), copper-nanowires (Cu-Nwires) and copper historical contamination (Cu-Field) for 3 and 7 days.

	time (days)	down- regulated	up- regulated
CuNO ₃ EC ₂₀	3	8	8
	7	3	5
CuNO ₃ EC ₅₀	3	7	8
	7	1	2
Cu-NPs EC ₂₀	3	16	8
	7	5	6
Cu-NPs EC ₅₀	3	1399	1173
	7	11	3
Cu-Nwires EC ₂₀	3	530	498
	7	0	0
Cu-Nwires EC ₅₀	3	397	173
	7	2	6
Cu-Field EC ₂₀	3	200	156
	7	0	0
Cu-Field EC ₅₀	3	74	56
	7	4	21

Results show that exposure for 3 days cause consistently a higher number of DEGs (differentially expressed genes) compared to 7 days (3446 and 63 total DEGs respectively). Comparing the different copper forms, $CuNO_3$ was the treatments affecting fewer transcripts, followed by Cu-Field, with the nanomaterials (Cu-NPs and Cu-Nwires) affecting a higher number of genes.

A clustering analysis (Pearson's uncentered with average linkage) was performed on genes and samples, based on all the DEGs (Fig. 3 A). Results show a clear separation by time of exposure, hence the analysis was redone for each time individually based on the 3446 and 63 DEGs affected at 3 and 7 days of exposure, respectively (Fig. 3 B and C).



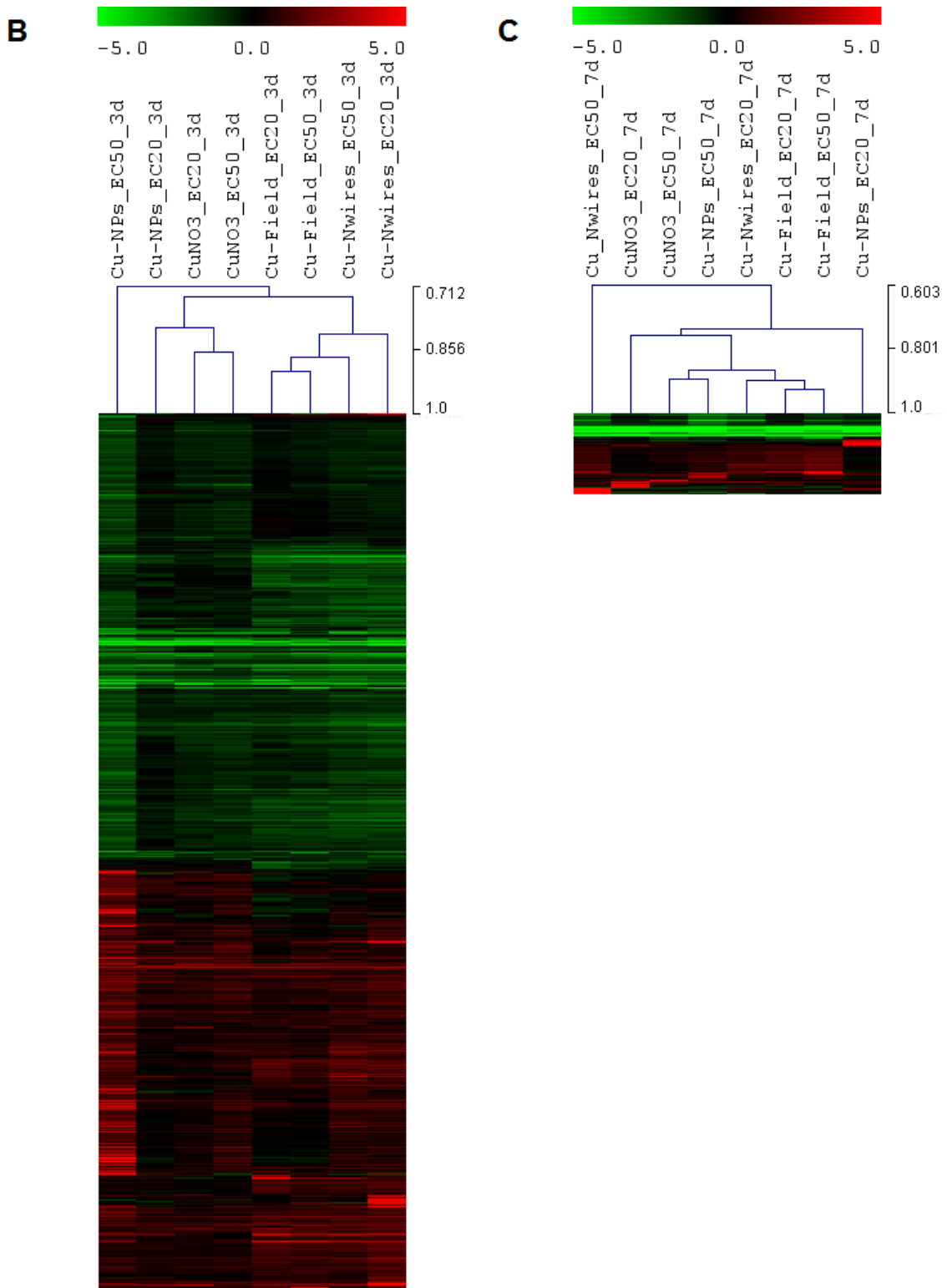
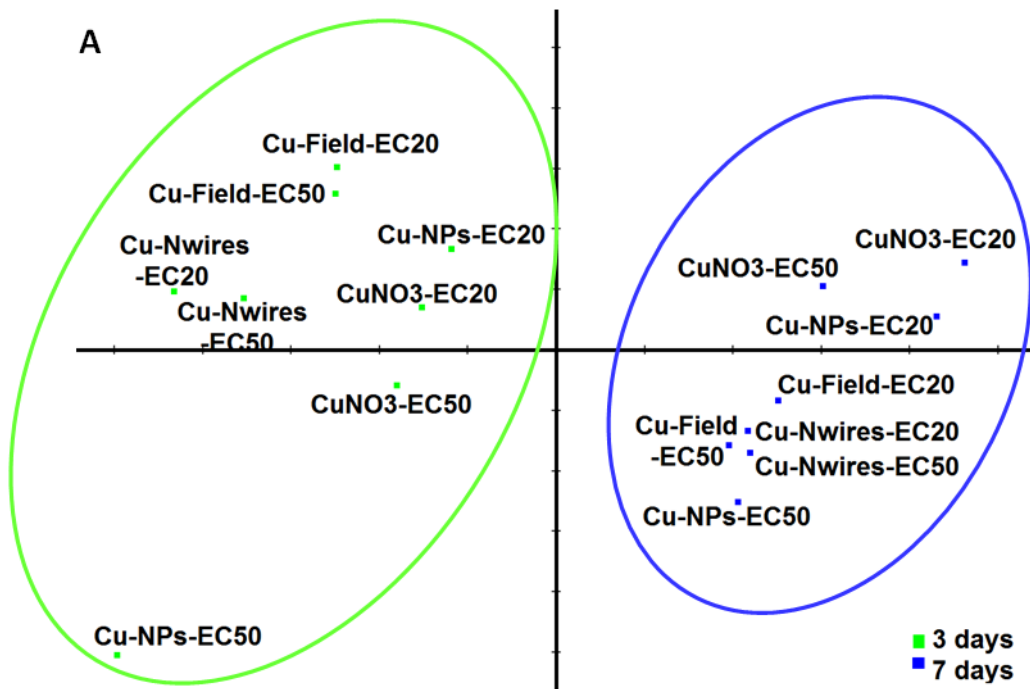


Figure 3: Expression heat map (green: down-regulation, red: up-regulation; black: not differentially expressed) of the 3494 differentially expressed genes (adjusted $p < 0.05$) after exposure to copper treatments, CuNO₃: copper nitrate, Cu-NPs: copper nanoparticles, Cu-Nwires: copper nanowires, Cu-Field: copper historical contamination, EC₂₀, EC₅₀: effect

concentration for 20% and 50% reproduction reduction. Genes and samples (treatments) are hierarchically clustered using Pearson' Uncentered and average linkage (dendrogram on genes not shown). (A) All treatments and exposure periods (3 and 7 days). (B) 3 days of exposure. (C) 7 days of exposure.

No clear separation by effect concentration (EC) could be observed (Fig. 3 B and C). For 3 days exposure there is a tendency for clustering by copper form, being clearer in the case of CuNO₃ and Cu-Field treatments. Similar trends were obtained after PCA analysis (Fig. 4)



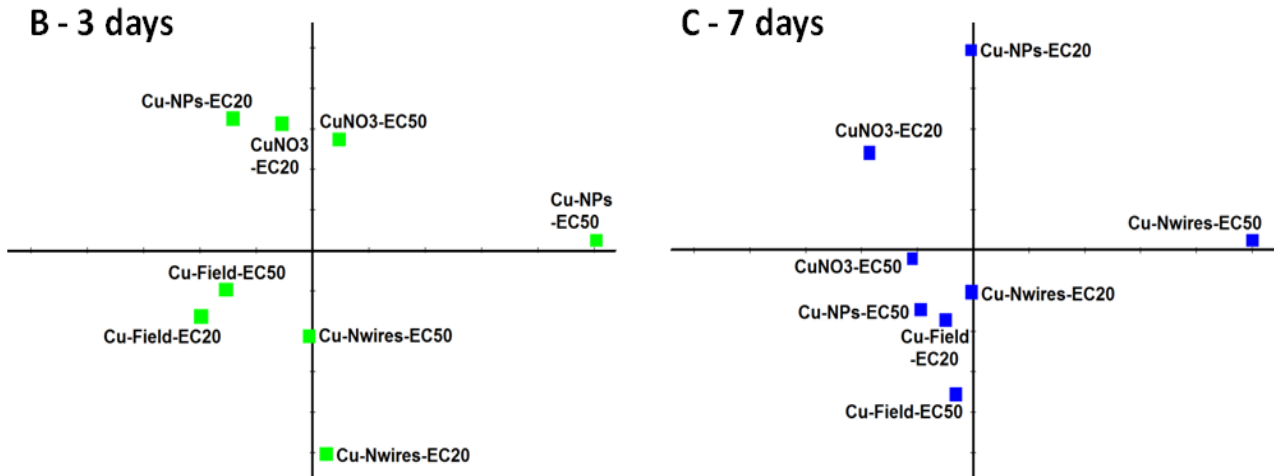


Figure 4: Principal component analysis of the samples (treatments) based on (A) all the DEGs (adjusted $p < 0.05$) for 3 and 7 days of exposure. The first two component presented explain 71.675% of the data variance (PC1-x axis = 51.342%, PC2-y axis = 16.332%). (B) 3446 DEGs for 3 days (PC1=45.106%; PC2=25.697%) (C) 63 DEGs for 7 days (PC1=41.879%, PC2=25.8%). CuNO₃: copper nitrate, Cu-NPs: copper nanoparticles, Cu-Nwires: copper nanowires, Cu-Field: copper historical contamination, EC₂₀, EC₅₀: reproduction effect concentration of 20%, 50%.

The overview in terms of number of genes affected by each copper form (independently of the tested concentration) and shared among the treatments per time of exposure, as well as the proportion of down- and up-regulated transcripts can be depicted in the Venn diagrams (Fig. 5).

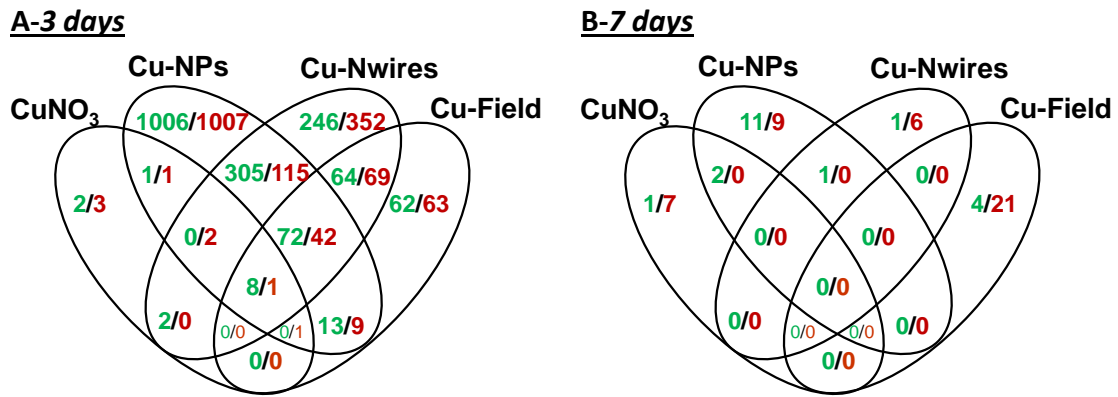


Figure 5: Venn diagram representation of the differentially expressed genes (adjusted $p < 0.05$) after exposure to the several copper treatments (CuNO₃: copper nitrate, Cu-NPs: copper nanoparticles, Cu-Nwires: copper nanowires, and Cu-Field: copper historical contamination) at 3 days (A) and 7 days of exposure (B). Number of genes is expressed as green for down-regulated and red for up-regulated.

Results show that after 3 days of exposure there is a high number of transcripts being commonly affected by Cu-NPs, Cu-Nwires and Cu-Field.

Gene set enrichment analysis on GO terms was performed to identify biological processes significantly affected. For that, 4 gene lists which include the annotated transcripts affected by each copper form (independently of the effect concentration – EC) were analysed versus the entire gene library (annotated transcripts present in the microarray). The list of biological processes affected by each copper form is shown on Table S1. The analysis was not performed for 7 days of exposure due to the low number of DEGs.

4. Discussion

4.1. Survival and reproduction – Cu-Nwires

Results show that there are no differences, in terms of survival and reproduction between the copper-nanowires and the 80nm previously tested copper-nanoparticles (Gomes et al., 2013). Similarly to Cu-NPs, Cu-Nwires starts oxidation in “normal” atmosphere. Further characterization will be included.

4.2. Differential gene expression

The total number of DEGs show that after 3 days of exposure was possible to capture a momentum of high regulatory activity in terms of transcripts whereas after 7 days this must have stabilised. Results for the same species in response to zinc chloride showed a variation between 250-2500-500 DEGs when exposed to 2-3-4 days respectively (data not published). Hence, results were reflected in the clustering by time of exposure and are also in agreement with previous studies reporting such time-dependency of gene regulation (e.g. (Nota et al., 2008; Novais et al., 2011)). The lower number of DEGs in response to CuNO₃ in comparison to the remaining treatments could be related with differences in assimilation rates - uptake of Cu from CuNO₃ will be faster than for the other Cu forms - probably the peak of gene regulation occurred after 1 or 2 days exposure. Copper bioaccumulation in *Eisenia fetida* follows a fast accumulation rate, reaching equilibrium within the first 7 days of exposure (Spurgeon and Hopkin, 1999). Unrine et al. (2010) found a linear relationships between Cu concentrations in *E. fetida* tissues and Cu-salt and Cu-NPs (20-40 nm) concentrations in soil media. Regarding the differences between the 4 Cu forms, there is a main separation between two sets: Cu-Field and Cu-Nwires versus CuNO₃ and Cu-NPs. In a previous study (Gomes et al., 2013) it was found that in the Cu-Field contaminated soil 40% of the copper was bound

to carbonates compared to ca. 70-80% for Cu-NPs and CuNO₃. The clustering could be partly related to this aspect the higher bioavailability of Cu from CuNO₃ and Cu-NPs in comparison to Cu-Field. This could be on the origin of the differences observed in terms of the high number of DEGs affected by Cu-NPs, Cu-Nwires and Cu-Field. If results would be due to Cu oxidation (i.e. associated with a gradual release of Cu²⁺ from the NMs, at least until the stabilization provided by the formed oxidation layer (Unrine et al., 2010)) that means that after 7 days the effect should be the equivalent to an increased exposure to Cu ions, hence higher effect. This does not seem to be the case, at least not directly.

Gene set enrichment analysis showed that Cu-NPs affected the most biological processes (CuNO₃ affected the least, but this is bound to the lowest amount of DEGs after 3 days).

Among the processes affected by CuNO₃ and Cu-field are the Wnt signaling pathway which regulates the calcium inside the cell. The up-regulation of transcripts involved in calcium regulation was observed in HepG2 cells exposed to copper sulfate (Song et al., 2009). Another affected function is related with cilium assembly. Cilia are present in virtually all eukaryotic organisms; the primary cilia (or non-motile cilia) are associated with the ability to sense chemical and physical environment. *C. elegans* has ciliated cells in the sensory neuron (Inglis et al., 2007) and abnormal cilia results in chemosensory defects. In *E. crypticus* the up regulation of cilium assembly can indicate the activation of the chemosensory system as a response to Cu. Enchytraeids are known to have chemoreceptors like and to be able to avoid various chemicals (Amorim et al., 2005) including Cu (Amorim et al., 2008). Autophagic vacuole assembly is being negatively affected by CuNO₃ exposure. Autophagy, or cellular self-digestion, is a

known conserved mechanism involved in the degradation of proteins and organelles in the cytoplasm. Excess or imbalance of autophagic flux can indicate cellular toxicity, and in mammals contributes to the development of pathological conditions (Liang, 2010). Autophagic cell death was induced after exposure of A549 cells to CuO-NPs (Sun et al., 2012). In our study, we did not find this function affected by NMs exposure, and exposure to CuNO₃ reduced autophagic processes. A possible explanation could be related with the tested concentrations, being an EC80 (75% reduction in cell viability) (Sun et al., 2012) versus an EC_{20/50} (20/50% reduction in reproduction).

Venn diagram analysis (Fig. 5A) show that Cu-NPs, Cu-Nwires and Cu-Field share 114 commonly affected genes, although comparatively less was common in terms of function. Among the commonly affected functions are the one related with translation processes, which is highly affected in Cu-NPs and Cu-Nwires (and to less extent in Cu-Field). Translation is affected by the up-regulation of several transcripts coding for elongation factors and ribosomal proteins. Similarly, Cu exposure also caused the up-regulation of several ribosomal proteins in mussel (Negri et al., 2013) and as suggested by the authors the increase in ribosome biosynthesis is to support cellular activities as protein translation, transcription activation and mRNA stabilization. A ribosomal protein L26 was also found up-regulated after Cu-NPs exposure in *E. albidus* (and not to CuCl₂) (Gomes et al., 2012b). Several transcription related processes were affected by Cu-NPs exposure (e.g. mRNA processing, transcription elongation from RNA polymerase II promoter) and one process is affected by Cu-Field (transcription initiation from RNA polymerase III promoter). In this case exposure to Cu is promoting and reducing transcription since genes coding for, for example DNA polymerase and endonuclease reverse transcriptase were found up-regulated, while splicing factors, transcription factors found down-regulated, additionally different protein kinases were

found up- or down-regulated and together that indicates that the regulation of transcription processes is being done depending on the organisms' requirement to keep Cu levels balanced. Also in other enchytraeid species, *E. albidus*, genes involved in transcription and translation had different patterns of response between Cu-NPs and Cu-salt (Gomes et al., 2012b). In our study, some differences in terms of transcriptional processes can be observed, for instance, more functions related with transcription are affected by Cu-NPs (note that this was not the case for Cu-Nwires) and less by Cu-Field.

Energetic metabolism is being affected by Cu-NPs, Cu-Nwires and Cu-Field but in different ways. For instance in the case of Cu-NPs genes involved in lipids production are up-regulated (triglyceride biosynthetic process, lipopolysaccharide biosynthetic process). For Cu-Field the transport and catabolism of fatty acids is being reduced due the down-regulation of the transcripts involved in medium-chain fatty acid transport and very long-chain fatty acid catabolic process. For Cu-Nwires and Cu-Filed the ATP synthetic processes were significantly enriched due to the up-regulation of several ATP synthases. Bundy and co-authors (2008) found that exposure of the earthworm *L. rubellus* to sub-lethal concentrations of Cu-salt induced mitochondrial dysfunction (several transcripts coding for ATP synthases up-regulated) as well as clear alteration of lipids metabolism. NADH related transcripts were also found up-regulated in response to Cu-Nwires and Cu-Field, although not considered a significant function after GSEA, indicating a switch to metabolism of stored carbohydrates in response to copper, as suggested for *L. rubellus* (Bundy et al., 2008) and also confirmed in *E. albidus* (Gomes et al., 2012b).

These results indicate that part of the mechanisms triggered by Cu-Nwires (in the case of energetic metabolism) and Cu-NPs (in the case transcriptional processes) are probably due to released ionic Cu. However, exposure to the NMs (NPs and Nwires) affected processes not found in any other treatments. For instance, NMs exposure induced several histone modifications (e.g. methylation, acetylation, dephosphorylation). Histones are a component of chromatin and its modifications are involved in the manipulation and expression of DNA, they play an important role in controlling transcription and marking damaged DNA for its removal. All the genes affecting histone modification were down-regulated in response to the NMs exposure which can indicate the blockage of these very important biological processes. One of the processes being negatively affected is DNA repair through the down-regulation of several transcripts. Alterations in DNA repair enzymes were reported by Bundy et al. (2008) conjugated with enzymes involved in cell cycle control (which we also found affected by exposure to Cu-NPs and Cu-Nwires) indicating DNA damage as one of the causes of Cu-salt toxicity. In our study DNA repair and cell cycle control related processes were only affected by NMs exposure. Mechanisms of DNA damage caused by exposure to CuO-NPs have been reported in cell lines and plants (Ahamed et al., 2010; Atha et al., 2012; Karlsson et al., 2008) often associated with oxidative damage. We found transcripts coding for SOD (superoxide-dismutase), GST (glutathione-S-transferase) and a HSP (heat shock protein), significantly up-regulated in response to Cu-Nwires, indicating that enchytraeids must be regulating oxidative stress mechanisms.

Among the functions uniquely affected by Cu-NPs exposure are ubiquitin related processes. Ubiquitination processes can interact with histone to regulate gene silencing (Bannister and Kouzarides, 2011) and can participate in apoptosis regulation (Lee and

Peter, 2003). Apoptotic signaling pathway is being affected by exposure to Cu-NPs through the up-regulation an apoptosis-regulator-bcl2-like gene. Oxidative stress induced apoptosis via mitochondrial dysfunction was reported in the renal tissue of mice exposed to Cu-NPs (Sarkar et al., 2011) and bcl2 protein was involved in the reduction of mitochondrial membrane potential. Often associated with this apoptotic process is the release of cytochrome c (Cyt C). Cu-NPs exposure caused the up-regulation of several Cyt C related transcripts, which can indicate that apoptosis is being activated.

Among the processes uniquely affected by Cu-Nwires exposure was the adult locomotory behaviour. Enchytraeids are able to avoid unfavorable environmental conditions, and were shown to avoid Cu-NPs contaminated soil (Amorim and Scott-Fordsmand, 2012) earlier than Cu-salt. If the locomotion behaviour is affected, consequences can go from inability to avoid chemical exposure to increased chances of predation.

In summary, results from *E. crypticus*' transcriptomic profile show that exposure to copper salt (CuNO₃ and Cu-Field) activates the calcium regulation and the chemosensory system of the organisms. The Cu-Field, Cu-NPs and Cu-Nwires treatments, which likely have slower uptake rate for Cu compared to CuNO₃, affected translation factors, which have implications on the actual Cu toxicity mediation or detoxification. Interestingly, the energetic metabolism is affected by Cu-NPs, Cu-Nwires and Cu-Field but in distinct ways, indicating varying mechanisms being triggered by the different copper forms. Exclusive to the nanomaterials (NPs and Nwires) are the effects on histone modifications and DNA repair related transcripts, which can be linked to an increase in DNA damage, a known mechanism of Cu-NPs

toxicity. It has been shown that Cu-NPs (4-5 nm) interact directly with DNA of cancer cells inducing DNA degradation in a dose-dependent way, and despite causing cytotoxicity, when CuSO₄ is incubated with DNA, no degradation was observed (Jose et al., 2011). Regarding each NM individually, the most notorious functions affected were apoptosis regulation (in part via ubiquitination processes) in response to Cu-NPs, and adult locomotory behaviour in response to Cu-Nwires.

5. Conclusions

The study of gene expression pointed differences in gene responses to the various Cu forms, information that is notoriously absent with the standard effects endpoints of survival/reproduction alone. A very important confirmation was the fact that NMs interfered with DNA repair, histone modifications and ubiquitination processes, on the contrary of Cu salt spiked or aged. This obviously has consequences in terms of risks for the animals, e.g. the already reported epigenetic affecting future generations (long-term effects).

Acknowledgements

This study was supported by funding FEDER through COMPETE Programa Operacional Factores de Competitividade, and by National funding through FCT-Fundação para a Ciência e Tecnologia, within the research project NANOkA FCOMP-01-0124- FEDER-008944 (Ref. FCT PTDC/BIA-BEC/103716/2008), through an FCT PhD grant to Susana Gomes (SFRH/BD/63261/2009) and by the EU-FP7 MARINA (Ref. 263215).

References

- Ahamed, M., Siddiqui, M.A., Akhtar, M.J., Ahmad, I., Pant, A.B., Alhadlaq, H.A., 2010. Genotoxic potential of copper oxide nanoparticles in human lung epithelial cells. *Biochemical and Biophysical Research Communications* 396, 578-583.
- Alexa, A., Rahnenfuhrer, J., Lengauer, T., 2006. Improved scoring of functional groups from gene expression data by decorrelating GO graph structure. *Bioinformatics* 22, 1600-1607.
- Amorim, M., Scott-Fordsmand, J., 2012. Toxicity of Copper nanoparticles and CuCl₂ salt to *Enchytraeus albidus* worms: survival, reproduction and avoidance responses. *Environmental Pollution* 164, 164-168.
- Amorim, M.J.B., Novais, S., Rombke, J., Soares, A.M.V.M., 2008. *Enchytraeus albidus* (Enchytraeidae): A test organism in a standardised avoidance test? Effects of different chemical substances. *Environment International* 34, 363-371.
- Amorim, M.J.B., Rombke, J., Soares, A.M.V.M., 2005. Avoidance behaviour of *Enchytraeus albidus*: Effects of Benomyl, Carbendazim, phenmedipham and different soil types. *Chemosphere* 59, 501-510.
- Atha, D.H., Wang, H.H., Petersen, E.J., Cleveland, D., Holbrook, R.D., Jaruga, P., Dizdaroglu, M., Xing, B.S., Nelson, B.C., 2012. Copper Oxide Nanoparticle Mediated DNA Damage in Terrestrial Plant Models. *Environmental Science & Technology* 46, 1819-1827.
- Bannister, A.J., Kouzarides, T., 2011. Regulation of chromatin by histone modifications. *Cell Research* 21, 381-395.
- Benjamini, Y., Hochberg, Y., 1995. Controlling the False Discovery Rate: A Practical and Powerful Approach to Multiple Testing. *Journal of the Royal Statistical Society* 57, 289-300.
- Bundy, J.G., Sidhu, J.K., Rana, F., Spurgeon, D.J., Svendsen, C., Wren, J.F., Sturzenbaum, S.R., Morgan, A.J., Kille, P., 2008. 'Systems toxicology' approach identifies coordinated metabolic responses to copper in a terrestrial non-model invertebrate, the earthworm *Lumbricus rubellus*. *Bmc Biology* 6:25.

- Castro-Ferreira, M.P., de Boer, T.E., Colbourne, J.K., Vooijs, R., van Gestel, C.A.M., van Straalen, N.M., Soares, A.M.V.M., Amorim, M.J.B., Roelofs, D., 2013. Transcriptome assembly and microarray construction for *Enchytraeus crypticus*, a model oligochaete to assess stress response mechanisms and soil quality. *Submitted*.
- Chang, Y., Lye, M.L., Zeng, H.C., 2005. Large-Scale Synthesis of High-Quality Ultralong Copper Nanowires. *Langmuir* 21, 3746-3748.
- Evans, P., Matsunaga, H., Kiguchi, M., 2008. Large-scale application of nanotechnology for wood protection. *Nature Nanotechnology* 3, 577-577.
- Gomes, S.I.L., Murphy, M., Nielsen, M.T., Kristiansen, S.M., Amorim, M.J.B., Scott-Fordsmand, J.J., 2013. Cu-Nanoparticles Ecotoxicity - Explored and Explained. *submitted*
- Gomes, S.I.L., Novais, S.C., Gravato, C., Guilhermino, L., Scott-Fordsmand, J.J., Soares, A.M.V.M., Amorim, M.J.B., 2012a. Effect of Cu-nanoparticles versus one Cu-salt: Analysis of stress biomarkers response in *Enchytraeus albidus* (Oligochaeta). *Nanotoxicology* 6, 134-143.
- Gomes, S.I.L., Novais, S.C., Scott-Fordsmand, J.J., Coen, W.D., Soares, A.M.V.M., Amorim, M.J.B., 2012b. Effect of Cu-nanoparticles versus Cu-salt in *Enchytraeus albidus* (Oligochaeta): Differential gene expression through microarray analysis. *Comparative Biochemistry and Physiology, Part C* 155, 219-227.
- Griffitt, R.J., Hyndman, K., Denslow, N.D., Barber, D.S., 2009. Comparison of Molecular and Histological Changes in Zebrafish Gills Exposed to Metallic Nanoparticles. *Toxicological Sciences* 107, 404-415.
- Inglis, P.N., Ou, G., Leroux, M.R., Scholey, J.M., 2007. The sensory cilia of *Caenorhabditis elegans*. *WormBook*, 1-22.
- Ispas, C., Andreescu, D., Patel, A., Goia, D.V., Andreescu, S., Wallace, K.N., 2009. Toxicity and Developmental Defects of Different Sizes and Shape Nickel Nanoparticles in Zebrafish. *Environmental Science & Technology* 43, 6349-6356.

- Jose, G., Santra, S., Mandal, S., Sengupta, T., 2011. Singlet oxygen mediated DNA degradation by copper nanoparticles: potential towards cytotoxic effect on cancer cells. *Journal of Nanobiotechnology* 9, 9.
- Karlsson, H.L., Cronholm, P., Gustafsson, J., Moller, L., 2008. Copper oxide nanoparticles are highly toxic: A comparison between metal oxide nanoparticles and carbon nanotubes. *Chemical Research in Toxicology* 21, 1726-1732.
- Lee, J.C., Peter, M.E., 2003. Regulation of apoptosis by ubiquitination. *Immunological Reviews* 193, 39-47.
- Lee, Y., Choi, J.R., Lee, K.J., Stott, N.E., Kim, D., 2008. Large-scale synthesis of copper nanoparticles by chemically controlled reduction for applications of inkjet-printed electronics. *Nanotechnology* 19, (7pp).
- Liang, C., 2010. Negative regulation of autophagy. *Cell Death Differ* 17, 1807-1815.
- Lohse, M., Bolger, A.M., Nagel, A., Fernie, A.R., Lunn, J.E., Stitt, M., Usadel, B., 2012. RobiNA: a user-friendly, integrated software solution for RNA-Seq-based transcriptomics. *Nucleic Acids Res* 40, W622-W627.
- Lohse, M., Nunes-Nesi, A., Kruger, P., Nagel, A., Hannemann, J., Giorgi, F.M., Childs, L., Osorio, S., Walther, D., Selbig, J., Sreenivasulu, N., Stitt, M., Fernie, A.R., Usadel, B., 2010. Robin: An Intuitive Wizard Application for R-Based Expression Microarray Quality Assessment and Analysis. *Plant Physiology* 153, 642-651.
- Negri, A., Oliveri, C., Sforzini, S., Mignione, F., Viarengo, A., Banni, M., 2013. Transcriptional Response of the Mussel *Mytilus galloprovincialis* (Lam.) following Exposure to Heat Stress and Copper. *Plos One* 8.
- Nota, B., Timmermans, M.J.T.N., Franken, C., Montagne-Wajer, K., Marien, J., De Boer, M.E., De Boer, T.E., Ylstra, B., Van Straalen, N.M., Roelofs, D., 2008. Gene Expression Analysis of Collembola in Cadmium Containing Soil. *Environmental Science & Technology* 42, 8152-8157.

- Novais, S.C., Arrais, J., Lopes, P., Vandenbrouck, T., De Coen, W., Roelofs, D., Soares, A.M.V.M., Amorim, M.J.B., 2012. *Enchytraeus albidus* Microarray: Enrichment, Design, Annotation and Database (EnchyBASE). Plos One 7.
- Novais, S.C., Howcroft, C.F., Carreto, L., Pereira, P.M., Santos, M.A., De Coen, W., Soares, A.M.V.M., Amorim, M.J.B., 2011. Differential gene expression analysis in *Enchytraeus albidus* exposed to natural and chemical stressors: effect of different exposure periods. *Ecotoxicology*, 213-224.
- OECD, 2004. Guidelines for the testing of chemicals No. 220. Enchytraeid Reproduction Test. Organization for Economic Cooperation and Development. Paris.
- Pal, S., Tak, Y.K., Song, J.M., 2007. Does the antibacterial activity of silver nanoparticles depend on the shape of the nanoparticle? A study of the gram-negative bacterium *Escherichia coli*. *Applied and Environmental Microbiology* 73, 1712-1720.
- Pirooznia, M., Gong, P., Guan, X., Inouye, L.S., Yang, K., Perkins, E.J., Deng, Y.P., 2007. Cloning, analysis and functional annotation of expressed sequence tags from the Earthworm *Eisenia fetida*. *Bmc Bioinformatics* 8.
- Roca, C.P., Rallo, R., Fernandez, A., Giralt, F., 2012. Chapter 6 Nanoinformatics for Safe-by-Design Engineered Nanomaterials, Towards Efficient Designing of Safe Nanomaterials: Innovative Merge of Computational Approaches and Experimental Techniques. The Royal Society of Chemistry, pp. 89-107.
- Sarkar, A., Das, J., Manna, P., Sil, P.C., 2011. Nano-copper induces oxidative stress and apoptosis in kidney via both extrinsic and intrinsic pathways. *Toxicology* 290, 208-217.
- Scott-Fordsmand, J.J., Krogh, P.H., Weeks, J.M., 2000. Responses of *Folsomia fimetaria* (Collembola : Isotomidae) to copper under different soil copper contamination histories in relation to risk assessment. *Environmental Toxicology and Chemistry* 19, 1297-1303.
- SigmaPlot11.0, Copyright © 2009 Systat Software Inc.
- Singh, S., Singhal, N.K., Srivastava, G., Singh, M.P., 2010. Omics in mechanistic and predictive toxicology. *Toxicology Mechanisms and Methods* 20, 355-362.

- Song, M.O., Li, J.Y., Freedman, J.H., 2009. Physiological and toxicological transcriptome changes in HepG2 cells exposed to copper. *Physiological Genomics* 38, 386-401.
- Spurgeon, D.J., Hopkin, S.P., 1999. Comparisons of metal accumulation and excretion kinetics in earthworms (*Eisenia fetida*) exposed to contaminated field and laboratory soils. *Applied Soil Ecology* 11, 227-243.
- Sun, T.T., Yan, Y.W., Zhao, Y., Guo, F., Jiang, C.Y., 2012. Copper Oxide Nanoparticles Induce Autophagic Cell Death in A549 Cells. *Plos One* 7.
- Unrine, J.M., Tsyusko, O.V., Hunyadi, S.E., Judy, J.D., Bertsch, P.M., 2010. Effects of Particle Size on Chemical Speciation and Bioavailability of Copper to Earthworms (*Eisenia fetida*) Exposed to Copper Nanoparticles. *Journal of Environmental Quality* 39, 1942-1953.
- Wang, H.Y., Huang, Y.G., Tan, Z., Hu, X.Y., 2004. Fabrication and characterization of copper nanoparticle thin-films and the electrocatalytic behavior. *Analytica Chimica Acta* 526, 13-17.
- Westheide, W., Graefe, U., 1992. Two new terrestrial *Enchytraeus* species (Oligochaeta, Annelida). *Journal of Natural History* 26, 479-488.
- Wu, S.-H., Chen, D.-H., 2004. Synthesis of high-concentration Cu nanoparticles in aqueous CTAB solutions. *Journal of Colloid and Interface Science* 273, 165-169.

Supplementary material

Table S1: List of Biological processes (GO terms) significantly affected by exposure to AgNO₃ and Ag-NPs: Coated, NC (non-coated) and 300K for 3 days. a: number of annotated transcripts in the gene library. b: number of genes found for this GO term in the significant gene list and c: P value calculated by the Fisher exact test.

CuNO₃					
GO-ID	Term	Annotated^a	Sig. Annotated^b	P-Value^c	TestSeqs
GO:0009236	cobalamin biosynthetic process	3	1	0.002177	contig09971
GO:0007223	Wnt receptor signaling pathway, calcium modulating pathway	5	1	0.003625	GYUW2K401DU4NT
GO:0000045	autophagic vacuole assembly	9	1	0.006517	contig17229
GO:0031018	endocrine pancreas development	9	1	0.006517	GYUW2K401DU4NT
GO:0060027	convergent extension involved in gastrulation	15	1	0.01084	GYUW2K401DU4NT
GO:0006662	glycerol ether metabolic process	16	1	0.011559	contig12937
GO:0009950	dorsal/ventral axis specification	17	1	0.012277	GYUW2K401DU4NT
GO:0042384	cilium assembly	30	1	0.021572	GYUW2K401DU4NT
GO:0001707	mesoderm formation	34	1	0.024416	GYUW2K401DU4NT
GO:0007368	determination of left/right symmetry	59	1	0.042019	GYUW2K401DU4NT

Cu-NPs					
GO-ID	Term	Annotated^a	Sig. Annotated^b	P-Value^c	TestSeqs
GO:0019432	triglyceride biosynthetic process	8	4	5.02E-04	contig14559, contig17117, GYUW2K402I6F10, GYUW2K401BMCT5
GO:0006414	translational elongation	119	16	6.81E-04	contig01380, contig01377, contig23953, contig19675, contig04726, contig24859, contig25900, contig18370, contig09557, contig24311, contig07334, contig13676, contig17200, contig20295, contig26330, contig14250
GO:0045603	positive regulation of endothelial cell differentiation	2	2	0.002929	contig11741, contig21353
GO:0001826	inner cell mass cell differentiation	2	2	0.002929	contig10540, GYUW2K402JIE4R
GO:0034755	iron ion transmembrane transport	2	2	0.002929	contig16337, GYUW2K402GX1FS
GO:0009103	lipopolysaccharide biosynthetic process	13	4	0.00412	contig09917, contig20364, GYUW2K402I6F10, GYUW2K401BMCT5
GO:0042254	ribosome biogenesis	393	34	0.004823	contig16748, contig20542, GYUW2K402JTB9I, contig07766, contig15466,

					contig27072, contig23953, contig19675, contig24582, contig17124, contig08676, contig24870, contig14611, contig17784, contig24859, contig09240, contig25900, contig22640, contig18370, contig09557, contig26084, contig23236, contig24311, contig24309, contig11164, contig13676, contig10859, contig15013, contig13191, contig26330, contig11455, contig09346, contig14250, contig15335
GO:0006278	RNA-dependent DNA replication	133	15	0.005583	contig01044, GYUW2K402FZO91, GYUW2K401BDUXS, contig25684, contig22065, GYUW2K401DTC0A, contig26216, contig24811, GYUW2K401DRJ8E, contig22953, contig15512, contig24949, contig01896, GYUW2K401DMX87, GYUW2K401CB4Y2
GO:0097190	apoptotic signaling pathway	41	7	0.005967	GYUW2K402JXBC2, GYUW2K402H35VW, GYUW2K401CWGVM, contig21553, GYUW2K402F1CQU, contig18616, GYUW2K402HP3PK
GO:0006446	regulation of translational initiation	110	13	0.006468	contig08588, GYUW2K401EG5VI, contig10981, contig08512, contig09472, contig10915, contig22529, GYUW2K401D9GEU, contig18042, contig03799, GYUW2K402FMGVC, contig09346, GYUW2K402I737P
GO:0045739	positive regulation of DNA repair	8	3	0.007218	contig12345, contig03492, contig15522
GO:0006397	mRNA processing	245	23	0.007321	GYUW2K402GNPZQ, contig12828, contig02487, contig05275, contig09941, GYUW2K401AFY3O, contig08806, contig18230, GYUW2K402JKJMB, contig21767, contig21764, contig03325, contig12904, contig14628, GYUW2K401AU6L9, contig10242, contig10562, contig08408, contig08403, contig07310, GYUW2K401C7F6V, contig09802, GYUW2K402HP3PK
GO:0051974	negative regulation of telomerase activity	3	2	0.008471	GYUW2K401EAXVI, contig02986
GO:0002071	glandular epithelial cell maturation	3	2	0.008471	GYUW2K402I6F10, GYUW2K401BMCT5
GO:0006422	aspartyl-tRNA aminoacylation	3	2	0.008471	contig08464, contig11921
GO:0000729	DNA double-strand break processing	3	2	0.008471	contig12345, contig15522
GO:0015904	tetracycline transport	3	2	0.008471	GYUW2K402I4KIB, GYUW2K402HO9A4
GO:0034969	histone arginine methylation	3	2	0.008471	GYUW2K401DMP11, contig08403
GO:0042501	serine phosphorylation of STAT protein	3	2	0.008471	GYUW2K402HQ25N, contig09039
GO:0006261	DNA-dependent DNA replication	79	10	0.010026	GYUW2K401BVUK2, contig16568, GYUW2K401A7MLU, GYUW2K401BBKHD, GYUW2K401EI5C8, contig10898, GYUW2K402I0ZY4, GYUW2K401DR3E1, contig11450, GYUW2K402IP5U3
GO:0051290	protein heterotetramerization	9	3	0.010394	contig03355, contig12141, GYUW2K401CEKCT
GO:0045931	positive regulation of mitotic cell cycle	9	3	0.010394	GYUW2K401CXCYW, GYUW2K401BX9RL, GYUW2K401A0E60
GO:0006338	chromatin remodeling	68	9	0.010746	contig12455, contig13093, contig08488, contig09090, contig21047, contig11926, contig20295, contig04016, contig02986
GO:0006368	transcription elongation from RNA polymerase II promoter	46	7	0.011251	contig26196, contig14809, contig22529, contig09777, contig11399, GYUW2K401BEZTU, contig20295
GO:0000097	sulfur amino acid biosynthetic process	26	5	0.01171	contig07491, GYUW2K401EKCCP, contig01812, GYUW2K401AQTJA, GYUW2K402HNGH2

Supplementary material – Chapter V

GO:0015994	chlorophyll metabolic process	27	5	0.013745	contig08390, GYUW2K402I4D5D, contig16950, contig12896, contig02987
GO:0032873	negative regulation of stress-activated MAPK cascade	10	3	0.014258	contig10951, contig08469, contig02986
GO:0009263	deoxyribonucleotide biosynthetic process	10	3	0.014258	contig03355, contig12141, GYUW2K401CEKCT
GO:0040014	regulation of multicellular organism growth	60	8	0.015094	contig08883, contig10951, contig14332, contig15769, contig09708, contig25117, GYUW2K402I6F10, GYUW2K401BMCT5
GO:0006656	phosphatidylcholine biosynthetic process	4	2	0.016334	GYUW2K402I6F10, GYUW2K401BMCT5
GO:0043060	meiotic metaphase I plate congression	4	2	0.016334	contig20093, GYUW2K402HP3PK
GO:0045823	positive regulation of heart contraction	4	2	0.016334	contig21964, contig19687
GO:0006297	nucleotide-excision repair, DNA gap filling	19	4	0.017247	contig16568, GYUW2K401A7MLU, contig11450, contig12896
GO:0071173	spindle assembly checkpoint	11	3	0.018827	contig18097, GYUW2K401BP13A, contig10004
GO:0016056	rhodopsin mediated signaling pathway	11	3	0.018827	contig20557, GYUW2K402FYBMB, GYUW2K402FPJ77
GO:0035017	cuticle pattern formation	11	3	0.018827	contig07266, GYUW2K402H07WS, GYUW2K402JORSQ
GO:0010149	senescence	12	3	0.024109	contig26196, GYUW2K402H35VW, contig08469
GO:0000209	protein polyubiquitination	31	5	0.024229	contig12345, contig14360, GYUW2K401CWGVM, contig08408, contig08248
GO:0045777	positive regulation of blood pressure	5	2	0.026252	contig07924, contig21964
GO:0001755	neural crest cell migration	5	2	0.026252	contig07310, contig09825
GO:0051865	protein autoubiquitination	5	2	0.026252	contig14360, contig03637
GO:0031639	plasminogen activation	5	2	0.026252	GYUW2K401EBYLT, contig13163
GO:0043497	regulation of protein heterodimerization activity	5	2	0.026252	GYUW2K401CWGVM, contig21553
GO:0030728	ovulation	5	2	0.026252	GYUW2K401CMPQ3, GYUW2K401ERWCZ
GO:0015811	L-cystine transport	5	2	0.026252	GYUW2K402H3IGK, GYUW2K402F03ET
GO:0046898	response to cycloheximide	5	2	0.026252	contig27072, contig17784
GO:0051443	positive regulation of ubiquitin-protein ligase activity	67	8	0.027714	contig09179, contig04952, contig03022, contig08669, contig20635, contig24528, contig15522, contig08728
GO:1901990	regulation of mitotic cell cycle phase transition	55	7	0.028125	contig15135, contig08804, contig08669, contig18097, GYUW2K401BP13A, GYUW2K401A0E60, contig04027
GO:0031145	anaphase-promoting complex-dependent proteasomal ubiquitin-dependent protein catabolic process	55	7	0.028125	contig09179, contig04952, contig03022, contig08669, contig20635, contig08728, contig10004
GO:0030218	erythrocyte differentiation	22	4	0.028637	contig08856, contig24859, contig03492, GYUW2K402GX1FS
GO:0021695	cerebellar cortex development	13	3	0.030106	GYUW2K402F9KNW, contig08904, GYUW2K402HQ25N
GO:0043968	histone H2A acetylation	13	3	0.030106	contig26773, contig10726, contig04016
GO:0000288	nuclear-transcribed mRNA catabolic process, deadenylation-dependent decay	13	3	0.030106	GYUW2K401EWHAM, contig17442, GYUW2K402HP3PK

Supplementary material – Chapter V

GO:0009186	deoxyribonucleoside diphosphate metabolic process	13	3	0.030106	contig03355, contig12141, GYUW2K401CEKCT
GO:0006547	histidine metabolic process	23	4	0.033224	GYUW2K401CQAGE, GYUW2K402GUZQY, contig09626, contig22639
GO:0008284	positive regulation of cell proliferation	151	14	0.034689	contig20557, GYUW2K401DMP11, contig16568, contig10106, contig19675, contig12141, GYUW2K402FUII9, GYUW2K401A0E60, contig08469, contig05155, contig01251, GYUW2K401E0G58, contig04027, GYUW2K401DG3W2
GO:0006367	transcription initiation from RNA polymerase II promoter	46	6	0.036622	contig14809, contig22529, contig09777, contig11399, contig18042, contig17577
GO:0046653	tetrahydrofolate metabolic process	14	3	0.03681	GYUW2K401EKCCP, GYUW2K402H1T03, contig22639
GO:0051439	regulation of ubiquitin-protein ligase activity involved in mitotic cell cycle	71	8	0.037516	contig09179, contig04952, contig03022, contig08669, contig20635, contig24528, contig08728, contig10004
GO:0007252	I-kappaB phosphorylation	6	2	0.03798	GYUW2K402ISG01, contig09039
GO:0007035	vacuolar acidification	6	2	0.03798	contig21922, contig26702
GO:0043496	regulation of protein homodimerization activity	6	2	0.03798	GYUW2K401CWGVM, contig21553
GO:0034381	plasma lipoprotein particle clearance	6	2	0.03798	contig17107, contig02050
GO:0043524	negative regulation of neuron apoptotic process	24	4	0.038215	contig12345, GYUW2K401CWGVM, contig08904, contig20400
GO:0007155	cell adhesion	317	25	0.038512	contig26196, contig07929, GYUW2K402ID8OQ, contig21964, contig19051, GYUW2K402IPCP9, contig22514, contig12484, GYUW2K402FUSAU, GYUW2K402HCZ07, GYUW2K401CWGVM, GYUW2K401CXCYW, GYUW2K401BX9RL, contig08911, contig04563, GYUW2K402HQ25N, contig07359, GYUW2K401B45VT, contig14429, GYUW2K401BTN27, contig14402, contig04507, GYUW2K401AMVEI, contig13166, GYUW2K401AYGYU
GO:0031397	negative regulation of protein ubiquitination	59	7	0.039347	contig09179, contig04952, contig03022, contig20635, GYUW2K402HQ25N, contig08728, contig10004
GO:0006941	striated muscle contraction	36	5	0.043145	contig24782, contig21964, GYUW2K402ISG01, contig19687, contig07266
GO:0030518	intracellular steroid hormone receptor signaling pathway	25	4	0.04361	GYUW2K401DMP11, contig11399, contig09599, contig11926
GO:0046677	response to antibiotic	25	4	0.04361	contig27072, contig17784, GYUW2K402I4KIB, GYUW2K402HO9A4
GO:0051789	response to protein stimulus	15	3	0.04421	contig08512, contig10106, contig03799
GO:0000718	nucleotide-excision repair, DNA damage removal	15	3	0.04421	contig14809, contig09777, contig11399
GO:0032042	mitochondrial DNA metabolic process	15	3	0.04421	GYUW2K401DHDMU, GYUW2K401EI5C8, GYUW2K402IP5U3
GO:0000226	microtubule cytoskeleton organization	231	19	0.046063	GYUW2K402ITFDE, GYUW2K401ESS6F, contig07913, contig15946, contig10951, contig16568, contig01647, GYUW2K402F8RX0, contig18097, contig19144, contig09599, contig01794, contig26084, contig01251, contig04068,

					GYUW2K401DIS3P, contig10004, GYUW2K402HP3PK, GYUW2K401CO7QO
GO:0008380	RNA splicing	277	22	0.046749	GYUW2K402GNPZQ, contig12828, contig02487, contig05275, contig09941, contig08806, contig18230, contig21767, contig21764, contig03325, contig08301, contig12904, contig14628, GYUW2K401AU6L9, contig12418, contig10242, contig10562, contig08408, contig08403, contig07310, contig09802, contig26330
GO:0050905	neuromuscular process	49	6	0.04778	contig12484, contig09708, GYUW2K402F9KNW, contig08904, contig21016, GYUW2K401DDZRR
GO:0021953	central nervous system neuron differentiation	49	6	0.04778	contig20557, contig16095, contig08686, contig09708, GYUW2K402F9KNW, GYUW2K402HQ25N

Cu-Nwires					
GO-ID	Term	Annotated ^a	Sig. Annotated ^b	P-Value ^c	TestSeqs
GO:0006933	negative regulation of cell adhesion involved in substrate-bound cell migration	2	2	7.40E-04	contig01486, contig01482
GO:0006450	regulation of translational fidelity	2	2	7.40E-04	contig05018, contig22854
GO:0000028	ribosomal small subunit assembly	3	2	0.002179	contig24859, contig10519
GO:0015991	ATP hydrolysis coupled proton transport	35	5	0.002421	contig24873, contig01486, contig01482, contig03955, contig06697
GO:0019730	antimicrobial humoral response	23	4	0.003183	GYUW2K402JKJ5T, contig26597, GYUW2K401APNIO, GYUW2K401DWI53
GO:0031062	positive regulation of histone methylation	4	2	0.004279	GYUW2K401B2QAX, contig02986
GO:0000060	protein import into nucleus, translocation	14	3	0.005835	contig09802, contig12280, GYUW2K401DWI53
GO:0015811	L-cystine transport	5	2	0.007004	GYUW2K402F03ET, GYUW2K402H3IGK
GO:0060027	convergent extension involved in gastrulation	15	3	0.007147	contig22237, GYUW2K401DU4NT, contig13523
GO:0042777	plasma membrane ATP synthesis coupled proton transport	15	3	0.007147	contig01486, contig01482, contig03955
GO:0006413	translational initiation	128	9	0.008356	GYUW2K402FTRGS, GYUW2K402HRO65, contig10519, GYUW2K401BRDJS, contig08588, contig14328, contig17118, contig22854, contig08870
GO:0045727	positive regulation of translation	34	4	0.013183	contig19675, contig14328, contig12955, GYUW2K401DWI53
GO:0019260	1,2-dichloroethane catabolic process	7	2	0.014185	contig10175, contig09626
GO:0042776	mitochondrial ATP synthesis coupled proton transport	8	2	0.018576	contig01486, contig01482
GO:0042771	intrinsic apoptotic signaling pathway in response to DNA damage by p53 class mediator	8	2	0.018576	GYUW2K401DWI53, GYUW2K402F1CQU
GO:0000910	cytokinesis	79	6	0.020623	contig26597, GYUW2K402HZK1J, contig02589, contig03607, GYUW2K401CWM4K, contig13523
GO:0030218	erythrocyte differentiation	22	3	0.021021	contig24859, contig24031, contig24387

Supplementary material – Chapter V

GO:0002237	response to molecule of bacterial origin	40	4	0.022882	contig02050, GYUW2K402JKJ5T, GYUW2K402HT2CP, contig10175
GO:0006264	mitochondrial DNA replication	9	2	0.023458	GYUW2K402IP5U3, GYUW2K401EI5C8
GO:0006172	ADP biosynthetic process	9	2	0.023458	contig01486, contig01482
GO:0021768	nucleus accumbens development	1	1	0.027227	contig09626
GO:0018960	4-nitrophenol metabolic process	1	1	0.027227	contig05083
GO:0060338	regulation of type I interferon-mediated signaling pathway	1	1	0.027227	contig03045
GO:0021551	central nervous system morphogenesis	1	1	0.027227	GYUW2K402HDS3M
GO:0060166	olfactory pit development	1	1	0.027227	contig09626
GO:0007042	lysosomal lumen acidification	1	1	0.027227	contig20400
GO:0002084	protein depalmitoylation	1	1	0.027227	contig20400
GO:0002072	optic cup morphogenesis involved in camera-type eye development	1	1	0.027227	contig09626
GO:0045163	clustering of voltage-gated potassium channels	1	1	0.027227	GYUW2K402G72B2
GO:0051615	histamine uptake	1	1	0.027227	contig00245
GO:0032429	regulation of phospholipase A2 activity	1	1	0.027227	contig20400
GO:0048549	positive regulation of pinocytosis	1	1	0.027227	contig20400
GO:0048386	positive regulation of retinoic acid receptor signaling pathway	1	1	0.027227	contig09626
GO:0043402	glucocorticoid mediated signaling pathway	1	1	0.027227	contig09711
GO:0000290	deadenylation-dependent decapping of nuclear-transcribed mRNA	1	1	0.027227	contig17442
GO:0016576	histone dephosphorylation	1	1	0.027227	GYUW2K401ETAQ5
GO:0015822	ornithine transport	1	1	0.027227	GYUW2K401EPXCE
GO:0015819	lysine transport	1	1	0.027227	GYUW2K401EPXCE
GO:0034970	histone H3-R2 methylation	1	1	0.027227	GYUW2K401DMP11
GO:0010971	positive regulation of G2/M transition of mitotic cell cycle	1	1	0.027227	GYUW2K401A0E60
GO:0016267	O-glycan processing, core 1	1	1	0.027227	GYUW2K402HDS3M
GO:0035284	brain segmentation	1	1	0.027227	contig24031
GO:0003146	heart jogging	1	1	0.027227	contig22237
GO:0016254	preassembly of GPI anchor in ER membrane	10	2	0.028801	GYUW2K402I28CB, contig26297
GO:0042035	regulation of cytokine biosynthetic process	10	2	0.028801	contig24782, GYUW2K401DWI53
GO:0009262	deoxyribonucleotide metabolic process	25	3	0.029574	GYUW2K402IP5U3, GYUW2K401EI5C8, contig12141
GO:0042445	hormone metabolic process	739	29	0.03128	GYUW2K402GKT0F, GYUW2K401D30WU, GYUW2K402FTRGS, contig01733,

Supplementary material – Chapter V

					GYUW2K401AX8UT, contig18292, contig09780, contig10175, contig24782, GYUW2K401EKK62, contig05083, contig19338, contig03361, GYUW2K402IOZY4, contig10546, contig04027, contig05788, GYUW2K402JSOYD, contig01486, contig01482, contig09626, GYUW2K401B92S9, GYUW2K401A0E60, GYUW2K402F1CQU, contig21016, GYUW2K402G2KS0, contig03955, contig08464, contig10726
GO:0001558	regulation of cell growth	89	6	0.034487	contig12034, GYUW2K401BKIMW, GYUW2K402JS38K, GYUW2K402JGNLR, contig09711, contig20400
GO:0035017	cuticle pattern formation	11	2	0.034576	GYUW2K402H07WS, contig03607
GO:0048168	regulation of neuronal synaptic plasticity	12	2	0.040757	GYUW2K401AFY3O, contig17495
GO:0046632	alpha-beta T cell differentiation	12	2	0.040757	contig05620, GYUW2K401DWI53
GO:0008344	adult locomotory behavior	48	4	0.041187	contig14379, contig15769, contig20400, contig21016
GO:0007286	spermatid development	29	3	0.043405	GYUW2K402JKJ5T, contig14379, contig03955
GO:0006555	methionine metabolic process	50	4	0.046754	contig23001, GYUW2K402HNGH2, GYUW2K401AR80D, GYUW2K401EKCCP
GO:0043968	histone H2A acetylation	13	2	0.047317	contig04016, contig10726
GO:0019852	L-ascorbic acid metabolic process	13	2	0.047317	contig10175, contig09626
GO:0097305	response to alcohol	97	6	0.049107	GYUW2K402HT2CP, contig10175, contig04027, GYUW2K401C7F6V, contig03607, contig06697

161

Cu-Field					
GO-ID	Term	Annotated ^a	Sig. Annotated ^b	P-Value ^c	TestSeqs
GO:0060027	convergent extension involved in gastrulation	15	3	3.20E-04	contig11044, contig13523, GYUW2K401DU4NT
GO:0007601	visual perception	44	3	0.007665	contig26682, GYUW2K401B9VZQ, contig16580
GO:0045724	positive regulation of cilium assembly	1	1	0.009197	contig11044
GO:0051877	pigment granule aggregation in cell center	1	1	0.009197	contig11044
GO:0032516	positive regulation of phosphoprotein phosphatase activity	1	1	0.009197	contig14540
GO:0032515	negative regulation of phosphoprotein phosphatase activity	1	1	0.009197	contig14540
GO:0050893	sensory processing	1	1	0.009197	contig11044
GO:0043402	glucocorticoid mediated signaling pathway	1	1	0.009197	contig09711
GO:0035307	positive regulation of protein dephosphorylation	1	1	0.009197	contig14540
GO:0034454	microtubule anchoring at centrosome	1	1	0.009197	contig11044
GO:0002119	nematode larval development	107	4	0.017093	GYUW2K402FP4GN, contig20631, contig07521, GYUW2K402JBILH

Supplementary material – Chapter V

GO:0051124	synaptic growth at neuromuscular junction	22	2	0.017205	contig22599, contig18292
GO:0006883	cellular sodium ion homeostasis	2	1	0.018309	contig09711
GO:0002315	marginal zone B cell differentiation	2	1	0.018309	GYUW2K401EZSI5
GO:0045415	negative regulation of interleukin-8 biosynthetic process	2	1	0.018309	GYUW2K401EZSI5
GO:0002268	follicular dendritic cell differentiation	2	1	0.018309	GYUW2K401EZSI5
GO:0001579	medium-chain fatty acid transport	2	1	0.018309	contig21490
GO:0032581	ER-dependent peroxisome organization	2	1	0.018309	contig15631
GO:0000338	protein deneddylation	2	1	0.018309	contig08588
GO:0042832	defense response to protozoan	2	1	0.018309	GYUW2K401EZSI5
GO:0031115	negative regulation of microtubule polymerization	2	1	0.018309	contig09711
GO:0042536	negative regulation of tumor necrosis factor biosynthetic process	2	1	0.018309	GYUW2K401EZSI5
GO:0035308	negative regulation of protein dephosphorylation	2	1	0.018309	contig14540
GO:0015986	ATP synthesis coupled proton transport	64	3	0.021116	contig07613, contig24873, GYUW2K402F9KNW
GO:0001947	heart looping	25	2	0.021947	contig08466, contig11044
GO:0009396	folic acid-containing compound biosynthetic process	27	2	0.025374	contig11510, contig25221
GO:0002467	germinal center formation	3	1	0.027338	GYUW2K401EZSI5
GO:0060296	regulation of cilium beat frequency involved in ciliary motility	3	1	0.027338	contig11044
GO:0032729	positive regulation of interferon-gamma production	3	1	0.027338	GYUW2K401EZSI5
GO:0006384	transcription initiation from RNA polymerase III promoter	3	1	0.027338	GYUW2K401C9X9H
GO:0045082	positive regulation of interleukin-10 biosynthetic process	3	1	0.027338	GYUW2K401EZSI5
GO:0045046	protein import into peroxisome membrane	3	1	0.027338	contig15631
GO:0016557	peroxisome membrane biogenesis	3	1	0.027338	contig15631
GO:0055113	epiboly involved in gastrulation with mouth forming second	3	1	0.027338	contig13523
GO:0009258	10-formyltetrahydrofolate catabolic process	3	1	0.027338	GYUW2K402H1T03
GO:0046548	retinal rod cell development	3	1	0.027338	contig11044
GO:0030147	natriuresis	3	1	0.027338	GYUW2K402JS38K
GO:0030146	diuresis	3	1	0.027338	GYUW2K402JS38K

Supplementary material – Chapter V

GO:0060707	trophoblast giant cell differentiation	3	1	0.027338	GYUW2K402HYO9Z
GO:0007283	spermatogenesis	124	4	0.027603	contig19854, contig22599, contig11044, GYUW2K402HJBIK
GO:0040035	hermaphrodite genitalia development	30	2	0.03089	GYUW2K402FP4GN, contig20631
GO:0010225	response to UV-C	4	1	0.036285	GYUW2K401EZSI5
GO:0021702	cerebellar Purkinje cell differentiation	4	1	0.036285	GYUW2K402F9KNW
GO:0002455	humoral immune response mediated by circulating immunoglobulin	4	1	0.036285	GYUW2K401EZSI5
GO:0045064	T-helper 2 cell differentiation	4	1	0.036285	GYUW2K401EZSI5
GO:0009737	response to abscisic acid stimulus	4	1	0.036285	GYUW2K401C7F6V
GO:0070306	lens fiber cell differentiation	4	1	0.036285	GYUW2K402GTRO5
GO:0048172	regulation of short-term neuronal synaptic plasticity	4	1	0.036285	contig17495
GO:0042760	very long-chain fatty acid catabolic process	4	1	0.036285	contig21490
GO:0043114	regulation of vascular permeability	4	1	0.036285	GYUW2K402JS38K
GO:0045947	negative regulation of translational initiation	4	1	0.036285	contig08870
GO:0000910	cytokinesis	79	3	0.036309	contig02589, contig11044, contig13523
GO:0007223	Wnt receptor signaling pathway, calcium modulating pathway	5	1	0.04515	GYUW2K401DU4NT
GO:0051457	maintenance of protein location in nucleus	5	1	0.04515	contig11044
GO:0035058	nonmotile primary cilium assembly	5	1	0.04515	contig11044
GO:0042088	T-helper 1 type immune response	5	1	0.04515	GYUW2K401EZSI5
GO:0045444	fat cell differentiation	39	2	0.049886	contig26682, contig11044

Chapter VI

**Mechanisms of response to silver nanoparticles on
Enchytraeus albidus (Oligochaeta): survival,
reproduction and gene expression profile**

**VI - Mechanisms of response to silver nanoparticles on
Enchytraeus albidus (Oligochaeta): survival, reproduction and gene
expression profile**

Susana I.L. Gomes^a, Amadeu M.V.M. Soares^a, Janeck J. Scott-Fordsmand^b

and Mónica J.B. Amorim^a

^aDepartment of Biology & CESAM, University of Aveiro, 3810-193 Aveiro, Portugal

^bDepartment of Bioscience, Aarhus University, Vejlsovej 25, PO BOX 314, DK-8600
Silkeborg, Denmark

Published in Journal of Hazardous Materials 254– 255 (2013) 336– 344

doi.org/10.1016/j.jhazmat.2013.04.005

Abstract

Silver has antimicrobial properties and silver nanoparticles (Ag-NPs) have been some of the most widely used NPs. Information regarding their effects is still insufficient, in particular for soil dwelling organisms. The standard soil Oligochaeta *Enchytraeus albidus* was used to study the effects of Ag in soils, using differential gene expression (microarray) and population (survival, reproduction) response to Ag-NPs (PVP coated) and AgNO₃. Results showed higher toxicity of AgNO₃ (EC₅₀<50mg/kg) compared to toxicity of Ag-NPs (EC₅₀=225mg/kg). Based on the biological and material identity, the difference in toxicity between Ag-NPs and AgNO₃ could possibly be explained by a release of Ag⁺ ions from the particles or by a slower uptake of Ag-NPs. The indications were that the responses to Ag-NPs reflect an effect of Ag ions and Ag-NPs given the

extent of similar/dissimilar genes activated. The particles characterization supports this deduction as there were limited free ions measured in soil extracts, maybe related to little oxidation and/or complexation in the soil matrix. The possibility that gene differences were due to different levels of biological impact (i.e. physiological responses) should not be excluded. Testing of Ag-NPs seem to require longer exposure period to be comparable in terms of effect/risk assessment with other chemicals.

Keywords: silver nanoparticles; silver nitrate; toxicity; gene expression; *Enchytraeus albidus*

1. Introduction

The use of Ag-NPs and their consequent release into the environment has been increasing over the last decade. For instance, in 2008 Mueller and Nowack [1] predicted that Ag-NPs concentrations in soil would be 0.02-0.1 µg/kg, whereas in 2009 [2] predictions show that in the U.S. up to 13µg/kg can reach the soil via sludge, i.e. not only a model refinement but also an indication of an actual assumed increase (130 times increase). Despite this, information is still insufficient regarding effects on non-target species, particularly in soil dwelling organisms.

Silver ions antibacterial activity is known to be related to the inhibition of several enzymatic functions (by denaturation) [3], to cause the generation of Reactive Oxygen Species (ROS) [3] and to trigger apoptotic responses [4, 5]. Similarly, Ag-NPs toxicity to bacteria has been proposed to be caused by 1) oxidative stress caused by ROS generation formed on the NPs surface and 2) interaction of released Ag ions with thiol groups of vital enzymes and proteins, affecting cellular processes, ultimately with cell death events [6]. The role of Ag⁺ release from Ag-NPs as the sole cause of Ag-NPs anti microorganisms' activity is still under debate. For example, Miao et al. [7] and Navarro

et al. [8] suggests that the toxicity caused by Ag-NPs in two species of unicellular algae is mediated by Ag ions, whereas Fabrega and co-authors [9] indicated that Ag-NPs itself caused toxicity to the bacteria *Pseudomonas fluorescens*. Sotiriou and Pratsinis [10] showed that the nano size plays a crucial role in Ag-NPs toxicity to *Escherichia coli*; smaller (<10nm) Ag-NPs release more Ag ions which became the major cause of toxicity, while for larger particles (> 10 nm) with low release of ions, the NPs themselves influenced the antibacterial activity. Several *in vitro* studies performed in mammalian cell lines confirm the generation of ROS, resulting from the impairment of antioxidant enzymes (e.g. glutathione) as one of the main causes for Ag-NPs cytotoxicity [11-13]. For worms, Hayashi and co-authors [14] found that *in vitro* exposure to Ag-NPs increased the ROS levels in *Eisenia fetida* coelomocytes. They also found that immune signalling was similarly affected in *E. fetida* coelomocytes and human THP1-cells (human acute monocytic leukemia cell line). Further, exposure to Ag-NPs causes apoptosis as shown both *in vitro* (in Human liver cells [13]) and *in vivo* (in *Drosophila melanogaster* [15] and in *Lumbricus terrestris* [16]).

Despite the obvious interest and importance to understand the causes of Ag-NPs toxicity, relatively few studies have focused on the molecular pathways/modes of action on a gene expression based approach [17-20]. From these studies, only one was performed on a “soil” organism (*Caenorhabditis elegans*), although the actual exposure was done in growth media rather than soil [18]. Overall, the results show that the expression patterns differ between silver nanoparticles and silver-salt (or ions) [17-19]. For instance, Gu and co-authors [19] found that at early growth stages (120 min. exposure) Ag-NPs cause the up-regulation of a large number of genes involved in cellular rescue and stress response, while Ag-ions induced down-regulation of

transcripts involved in several other biological processes (e.g. transcription, protein synthesis, cell growth/division).

Concerning survival and reproduction related Ag-NPs toxicity studies, the majority of the information available is covering the aquatic compartment (e.g. [21-24]). The relative Ag⁺/Ag-NPs sensitivity (based on mass) seem to differ between organisms, for example, *Daphnia magna* is more sensitive to AgNO₃ exposure (48h LC₅₀=2.5 µg/l) than to Ag-NPs exposure (no mortality up to 500 µg/l) [21]; on the other hand for the Japanese medaka (*Oryzias latipes*) Ag-NPs exposure resulted in similar sensitivity between the two forms (i.e. the 96h LVC₅₀ (50% loss in viability) being ca 36µg/l [23]. For soil dwelling organisms, Ag-NPs were less toxic than AgNO₃ to the earthworm (*Eisenia fetida*), i.e. effects on cocoon production were observed at 728 and 773 mg/kg of two differently coated Ag-NPs and at 94 mg/kg for AgNO₃ [25]. Nevertheless, the earthworms started to avoid Ag-NPs and AgNO₃ at the same concentration, 7mg Ag/kg soil [26]. Results of a limit-test on the same species [27] showed that a concentration of 1000mg/kg caused no mortality for Ag-NPs and 98% mortality for AgNO₃ exposure, while reproduction was completely inhibited for both forms of silver.

The main aim of this study was to assess the effects of Ag-NPs on soil organisms and further understand the possible mechanisms of response. For that the effects of Ag-NPs (PVP coated) and AgNO₃ were assessed on the enchytraeid *Enchytraeus albidus* (Oligochaeta) in terms of survival, reproduction and differential gene expression profile (microarray analysis). *E. albidus* is a standardized ecotoxicological species [28, 29], abundant in many soils contributing to important soil functions [30]. Further, it is an early stage development genomic model [31], so the effect caused on gene expression level was possible using the enriched gene library and microarray for this species [32].

2. Materials and methods

2.1. Test organisms

The test organism belongs to the species *Enchytraeus albidus* [33]. The individuals were maintained in laboratory cultures for several years in moist soil (mixture of LUFA 2.2 natural soil and Organisation for Economic Cooperation and Development - OECD artificial soil, in a proportion of 3:1) media under controlled conditions, photoperiod 16:8h light:dark, at 18°C. Animals were fed on roasted oats twice a week.

2.2. Test chemicals and characterization

The silver nanoparticles Ag-NPs (PVP coated 0.2%, NanoAmor US) had an initial reported mean diameter 30-50 nm with a 99.9% purity. PVP coated were used because it is a “common particle” and it is a known non-toxic way to stabilize individual particles. The characterisation of Ag-NPs revealed more precise information (see results section). Characterisation techniques included: Powder X-Ray diffraction (XRD), using a STOE STAPI P (STOE & Cie GmbH, Darmstadt, Germany) powder diffractometer; Transmission Electron Microscopy (TEM), using a Phillips CM20 (Phillips/FEI, Eindhoven, The Netherlands); Dynamic Light Scattering (DLS) and Zeta potential were performed on Malvern Zetasizer Nano (Malvern Instruments Ltd, Worcestershire, UK); and Ion Selective electrode (ISE 25S, Radiometer). For further details see [27]. The AgNO₃ (high-grade: 98.5-99.9% purity) was purchased from Sigma-Aldrich (Brøndby, Denmark).

In a concurrent experiment the Ag⁺ present in the water and soil-water was measured with an ion-selective electrode (ISE 25S, Radiometer) in combination with the reference electrode (REF251, radiometer) equipped with a double salt bridge. The inner salt bridge contained saturated KCl and the outer 0.1 M KNO₃.

Concurrent experimental design: The concentration of silver ions in the soil was measured in an aqueous extract from the soil (soil-water). The soil suspension was made by mixing 5 g of soil (dw) with 25 ml of demineralised water (corresponding to 1:5 soil to water weight ratio). The soil suspensions were prepared in 50 ml centrifuge tubes. The tubes were placed horizontally on a lab shaker (Köttermann 4020, Holm og Halby, DK) and agitated at 250 rpm for 5 minutes. The suspensions were subsequently centrifuged 20 minutes at 2000 rpm and hereafter left to rest for 10 minutes for most of the organic matter to float. A sub-fraction of the supernatant was pipetted to a plastic beaker used for measurements, flushing the pipette tip and walls of the beaker to minimize loss of silver ions due to adsorption before the final transfer. This sub-fraction was then discarded. 9 ml of the remaining supernatant were subsequently transferred to the rinsed plastic beaker and 1 ml of 1 M KNO₃ was added to regulate the ionic strength. This solution was used for the measurements within 20 minutes from time of preparation. The ISE was calibrated with Ag⁺ standards made by dissolution from a AgNO₃ stock solution in 0.1 M KNO₃.

2.3. Test soil and spiking procedure

The test soil used for this experiment was the artificial OECD soil [29] containing 7% of sphagnum peat, 20% kaolin clay and 73% of sand, pH was adjusted to 6 with CaCO₃. The OECD soil was prepared in the required amount for all the experiments initially containing half of the sand content (36.5%) and pre-moistened with approximately 10% (v/w) of water. Spiking was done into each individual replicate except for the 50 mg AgNO₃/kg where the 4 replicates were mixed together in order to optimise precision in weighing. Spiking was done for each replicate, adding the required amount of Ag-NPs or AgNO₃ as dry powder to the sand and mixed manually. The individual contamination of each replicate has previously been described as a better approach as this ensures

similar total soil concentration per replicate within a particular concentration [34]. The moisture content was adjusted in each replicate by adding water until 40-60% of the maximum Water Holding Capacity (WHC) of the soil. In a preliminary test the range 0-10-100-1000 mg/kg was used and survival was assessed in a 2 weeks test. The concentrations in the definitive test were 0-100-200-400-600-800-1000 mg Ag-NPs/kg soil and 0-50-100-200-300-400-600 mg AgNO₃/kg soil. For the gene expression 0-100-200-400-600 mg/kg range was used for both Ag forms.

2.4. Experimental procedure

2.4.1. Survival and reproduction

The test followed the procedures in the Enchytraeid Reproduction Test (ERT) guideline (OCDE, 2004). In short, ten adult worms with visible *clitellum* were introduced in each test vessel, each containing 25 g moist soil (40 to 60% of the maximum Water Holding Capacity – WHC) and fed with 50 mg of ground and autoclaved rolled oats. The vessels were covered with parafilm (containing small holes) and left for 6 weeks, at 20°C and a 16:8h photoperiod. Weekly, 25 mg of food was supplied and the soil moisture content was adjusted by replenishing the weight loss with the proper amount of deionised water. Four replicates per treatment were used. At the test end the organisms were fixated with ethanol and coloured with a few drops of Bengal red (1% in ethanol). After one hour, the soil solution was spread into a larger container where pink coloured adults and juveniles could be searched and counted under a binocular stereo microscope, assessing survival and reproduction.

2.4.2. Gene expression- Microarrays

The organisms were exposed following the exact same procedure as in the survival/reproduction test, except that exposure lasted 2 days and no food was added.

Four replicates per treatment, with 10 organisms were used. The gene expression was analysed for comparable treatments (where all organism survived) between Ag forms i.e. 0-100-200mg/kg. At test end, animals were carefully removed from soil, rinsed in deionised water, stored in RNA later (Ambion, USA) in criotubes and frozen in liquid Nitrogen. Samples were stored at -80°C till further analysis. Three biological replicates out of the four were used.

2.4.2.1. RNA extraction, labelling and hybridizations

RNA was extracted from each replicate containing 10 pooled animals. Three biological replicates per test treatment (including control) were used. Total RNA was extracted through TRIzol extraction method (Invitrogen, Belgium), followed by DNase treatment (Fermentas, Germany). The quantity and purity of the isolated RNA were measured spectrophotometrically with a nanodrop (NanoDrop ND-1000 Spectrophotometer) and its quality was checked on a denaturing formaldehyde agarose gel electrophoresis.

A single-colour design was used. In brief, 500 ng of total RNA was amplified and labelled with the Agilent Low Input Quick Amp Labelling Kit (Agilent Technologies, Palo Alto, CA, USA). Positive controls were added with the Agilent one-colour RNA Spike-In Kit (Agilent Technologies, Palo Alto, CA, USA). Purification of the amplified and labelled cRNA was performed with the RNeasy columns (Qiagen, Valencia, CA, USA).

The cRNA samples were hybridized on Custom Gene Expression Agilent Microarrays (8 x 15k format) developed for this species [32]. Hybridizations were performed using the Agilent Gene Expression Hybridization Kit (Agilent Technologies, Palo Alto, CA, USA) and each biological replicate was individually hybridized on one array. The arrays were hybridized at 65°C with a rotation of 10 rpm, during 17h. After that the

microarrays were washed using Agilent Gene Expression Wash Buffer Kit (Agilent Technologies, Palo Alto, CA, USA) and scanned with the Agilent DNA microarray scanner G2505B (Agilent Technologies).

2.4.2.2. Acquisition and microarray data analysis

Fluorescence intensity data was obtained with Feature Extraction (10.5.1.1) Software (Agilent Technologies). Quality control was done by inspecting the reports on the Agilent Spike-in control probes and by making box plots of each array. Processing of the data and statistical analysis were performed using BRB Array Tools version 4.2.1 Stable Release (<http://linus.nci.nih.gov/BRB-ArrayTools.html>). After background subtraction, the replicated spots within each array were averaged and the intensities were log₂ transformed (spots with intensity below 1 were excluded from the analysis). Data was then normalized using Quantile normalization. Statistical class comparison between groups of arrays was performed between each exposure condition and the control using a two-sample t-test and 95% of confidence level for the assessment of differentially expressed genes. The Minimum Information About a Microarray Experiment (MIAME) compliant data from this experiment was submitted to the Gene Expression Omnibus (GEO) at the National Center for Biotechnology Information (NCBI) website (platform: GPL14928; series: GSE42431).

All cDNA fragments that corresponded to differentially expressed genes ($p < 0.05$) and for which sequences were known were searched for homology to sequences in the NCBI database as determined by the Basic Local Alignment Search Tool (BLAST) for update. The sequences were submitted to Blast2GO [35] and were compared with peptide sequence databases using BLASTX analysis (with minimum 10^{-6} e-value). Clustering analysis was performed using MultiExperiment Viewer (MeV, TIGR). The

differentially expressed genes for each treatment were analysed separately for GO (Gene Ontology) term enrichment analysis [36] using the Blast2GO software; this analysis is a tool to identify over-represented GO terms from a list of interesting genes.

2.5. Survival and reproduction data analysis

The reproduction effect concentrations (EC_x) were calculated using Toxicity Relationship Analysis Program (TRAP 1.02) applying the 2-parameters Logistic model, logging exposure concentrations. Data was tested for normality and one-way ANOVA and Post-Hoc Dunnetts' test was used to identify the No Observed Effect Concentration (NOEC) and the Lowest Observed Effect Concentration (LOEC).

3. Results

3.1. Nanoparticles characterization and soil concentrations

Results of characterization are summarized on Table 1. For further details on the methods and characterisation see [27].

Table 1: Characteristics of tested Ag-NPs (n=294 particles; n=9 measurements; n=8 measurements).

	Size (nm)			Zeta potential (mV)	Surface area (m ² /g)	Coating	Crystal structure (XRD)
	Nominal (supplier)	TEM	DLS				
Ag-NPs	30-50	82±2 (n=294)	235±4 (n=9)	28.6±0.16 (n= 8)	5-10	PVP	Cubic

For all test-exposures the total concentration (measured by Atomic Absorption Spectroscopy - AAS) was within 10% of the “background” plus the added Ag (nominal). Given this, the biological results are related to the total nominal concentrations. In soil-water there was no measureable Ag^+ activity for Ag-NPs treatments, with the LOD (limit of detection) being 10^{-7}M Ag^+ and the LOQ (limit of quantification) 10^{-6}M Ag^+ . For AgNO_3 , at total (nominal) concentrations below 50 mg/kg soil there was no detectable Ag^+ in soil-water. At total concentration above 50 mg/kg there was up to 1% Ag^+ (of total added) in the soil-water after 1 day (24 hours), which decreased to below the detection limit after 4 days. Hence, for all the exposure concentrations for which surviving enchytraeids were found, there was no measureable Ag^+ in the soil-water. In a similar measurement, in demineralised water adjusted with KNO_3 to the same ionic-strength as soil-water, there was also no detectable Ag^+ following Ag-NPs addition up to 900 mg/kg.

3.2. Survival and reproduction

All tests fulfilled the validity criteria as within the standard guideline (OCDE, 2004) criteria, with controls' mortality lower than 20% and number of juveniles higher than 25 with respective coefficient of variation below 50%.

Results of the two week preliminary test showed 100% mortality for 1000 mg AgNO_3 /kg and approximately 100% survival in all other treatments.

Results of the reproduction tests (Figure 1) show the higher toxicity (mass based) of AgNO_3 compared to Ag-NPs, with $\text{LC}_{50} < 50$ mg/kg for AgNO_3 whereas Ag-NPs caused no significant effects on adult's survival.

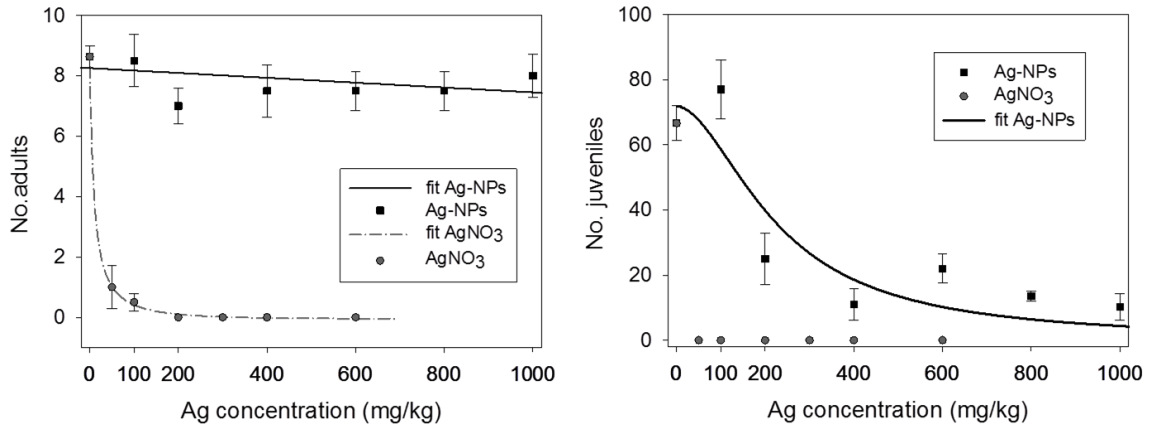


Figure 1: Effects of silver nanoparticles (Ag-NPs) and silver nitrate (AgNO₃) on survival (left) and reproduction (right) of *Enchytraeus albidus*. Results are expressed as average \pm standard error, n=4. The models fitted to the data were: polynomial linear to Ag-NPs survival, rational 4 parameters to AgNO₃ survival and 2 parameters logistic to Ag-NPs reproduction.

Regarding the reproduction, AgNO₃ caused 100% effect in all tested concentrations (Tab. 2); Ag-NPs caused a 50% reduction in the number of juveniles at around 225mg/kg. Results on effect concentrations are summarized in Table 2 and literature data is included for comparison.

Table 2: Reproduction effect concentrations for *Enchytraeus albidus* when exposed to Ag-NPs and AgNO₃. Literature data on *E. andrei* and *C. elegans* was added for comparison. Results are presented in mg/kg (mg/L for *C. elegans*) and 95% confidence intervals in brackets.

		EC ₅₀	EC ₂₀	EC ₁₀	NOEC	LOEC
<i>E. albidus</i>	Ag-NPs	225 [161-313]	106 [59-189]	70 [31-149]	100	200
	AgNO ₃	<50	<50	<50		
<i>Literature data on soil organisms</i>						
<i>E. andrei</i>	Ag-NPs	<1000 ^[27]			80 ^[25]	800 ^[25]
	AgNO ₃	<1000 ^[27]			8 ^[25]	80 ^[25]
<i>C. elegans</i>	Ag-NPs	>100 ^[37]			1 ^[37]	5 ^[37]
	AgNO ₃	>10 ^[37]			1 ^[37] /0.05 ^[18]	5 ^[37] /0.1 ^[18]

3.3. Gene expression profile

Results presented are relative to the control (M values were calculated by subtracting the control \log_2 intensity to the exposed \log_2 intensity).

Using class comparison statistical analysis (two-sample t-test, $p < 0.05$) a total of 170 transcripts was found differentially expressed in at least one of the treatments. Ag-NPs exposure caused 22 and 45 differentially expressed transcripts at 100 and 200 mg/kg respectively, while AgNO₃ caused 71 and 93 differentially expressed transcripts for the same concentrations. Figure 2A shows an overview of the number of differentially expressed transcripts, and the proportion of up and down-regulated transcripts in each condition. From the 170 transcripts, 66 are annotated. All the differentially expressed genes (DEGs), with respective GO annotations can be found in Table S1 of Supplementary data. The numbers of DEGs (two-sample t-test, $p < 0.05$) shared by the different treatment are represented in the Venn Diagrams (Figure 2B).

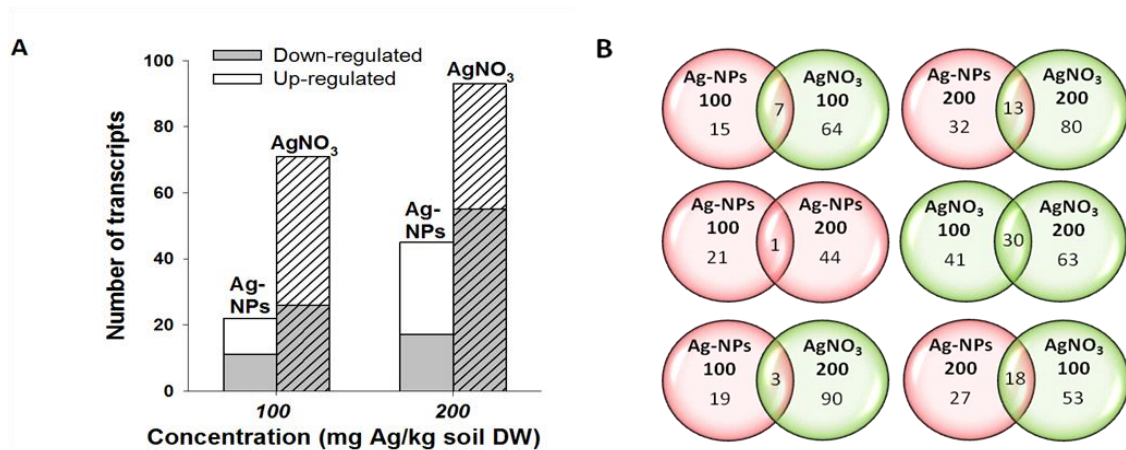


Figure 2: Number of significantly differentially expressed genes (two-sample T-test, $p < 0.05$) in *Enchytraeus albidus* after two days of exposure to 100 and 200 mg/kg of silver nitrate (AgNO₃) and silver-nanoparticles (Ag-NPs). (A) Total numbers of up- and down-regulated genes (B) Venn diagrams with the combinations indicating number of shared genes among treatments.

Overall, organisms exposed to AgNO₃ showed a higher number of DEGs compared to Ag-NPs. For both forms of Ag there was a concentration-related increase in the number of DEGs and higher number in AgNO₃ within the same concentration. As can be depicted from the Venn diagrams (Figure 2B), around one third of the genes triggered by 100 mg/kg of Ag-NPs and around one quarter of those triggered by 200 mg/kg are shared with the same concentration of AgNO₃. When comparing different concentrations of the same Ag form, only one DEG is shared between Ag-NPs, whereas AgNO₃ 100/200 share 30 DEGs. Interestingly, Ag-NPs 200 share more DEGs with AgNO₃ 100 than with the Ag-NPs 100 (same compound) or AgNO₃ 200 (same concentration). All the shared DEGs shown on Venn Diagrams have similar expression regulation (up or down) (see Table S1 Supplementary Data).

To compare the expression profiles between treatments, a hierarchical cluster analysis (Pearsons' uncentered, average linkage) was performed between genes and samples (treatments) (Figure 3A), based on all the differentially expressed transcripts ($p < 0.05$). The results show a separation of 200mg AgNO₃ /kg from all other exposures, whereas smaller differences occur among the others (100AgNO₃, 100Ag-NPs and 200Ag-NPs). If comparing each Ag form separately (Figure 3B and 3C) (isolates the differences due to concentration), we can see that with concentration increase the gene expression mostly changes in terms of intensity level to more or less expressed. However, there are also transcripts that were shut down or turned on e.g. differentially expressed at 100, but not at 200 mg/kg (all the genes included in each heat map are presented in Figure S1 and S2, Supplementary Data).

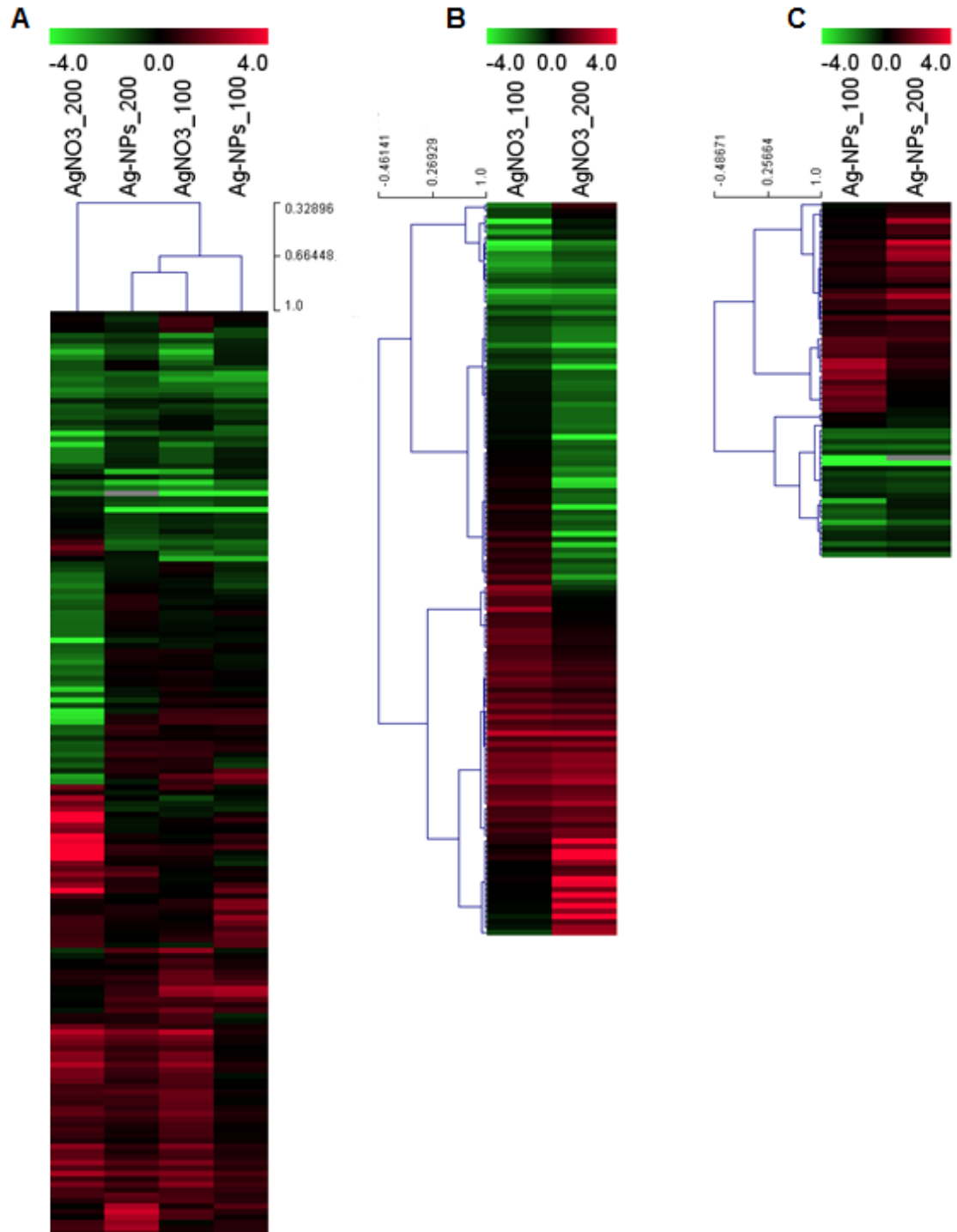


Figure 3: (A) Expression heat map of 170 differentially expressed transcripts ($p < 0.05$) of *Enchytraeus albidus* when exposed to 100 and 200 mg/kg of silver nitrate (AgNO₃) and silver nanoparticles (Ag-NPs) in comparison to control. Genes and samples (treatments) are hierarchically clustered using Pearson's Uncentered and average linkage. (B) Heat map of genes affected by AgNO₃ treatments. (C) Heat map of genes affected by Ag-NPs treatments.

To investigate the functions significantly affected by each treatment, gene set enrichment analysis of GO was performed [36]. The analysis was carried out on the differentially expressed transcripts (with GO annotation) induced by each condition (two-sample T-test, $p < 0.05$). For 100 mg/kg of Ag-NPs, no GO term was significantly represented (over or under) relatively to the whole gene library (which has a high number of non-annotated transcripts). Significantly affected GO terms are shown in Table 3.

Table 3: List of Biological processes (GO terms) affected by each treatment after gene set enrichment analysis.

Treatment	GO-ID	GO ancestor	GO term
Ag-NPs 200	GO:0045138	developmental process	tail tip morphogenesis
	GO:0040027	developmental process	negative regulation of vulval development
	GO:0040017	regulation of locomotion	positive regulation of locomotion
	GO:0042464	regulation of gene expression	dosage compensation, by hypoactivation of X chromosome
AgNO₃ 100	GO:0042517	signal transduction	positive regulation of tyrosine phosphorylation of Stat3 protein
	GO:0007140	reproduction	male meiosis
	GO:0008360	cell morphogenesis	regulation of cell shape
	GO:0051457	regulation of biological quality	maintenance of protein location in nucleus
AgNO₃ 200	GO:0040010	growth	positive regulation of growth rate
	GO:0007126	reproduction	Meiosis
	GO:0006094	carbohydrate metabolic process	Gluconeogenesis
	GO:0010557	metabolic process	positive regulation of macromolecule biosynthetic process
	GO:0006091	metabolic process	generation of precursor metabolites and energy
	GO:0009790	developmental process	embryonic development
	GO:0009791	developmental process	post-embryonic development
	GO:0010171	developmental process	body morphogenesis
	GO:0006325	cellular process	chromatin organization
	GO:0006323	cellular process	DNA packaging

4. Discussion

4.1. Survival and reproduction

Results in terms of survival and reproduction indicated higher toxic effect of AgNO₃ than Ag-NPs, based on mass. Such differences in toxicity have also been reported in other studies with earthworms, e.g. (i) a limit-test (1000mg/kg) with *E. fetida* where Ag-NPs did not affect survival and AgNO₃ caused ca. 100% mortality [27], (ii) a standard OECD reproduction study exhibited a NOEC (reproduction) of 8 mg for AgNO₃/kg and a NOEC of 80 mg for Ag-NPs/kg [25].

The difference in toxicity between Ag-NPs and AgNO₃ could possibly be explained by a release of Ag⁺ ions from the particles or by a slower uptake of Ag-NPs (which could be eventually detected in a prolonged test).

If we speculate that the toxicity of Ag-NPs is caused by the dissolved Ag⁺ fraction, then the difference in toxicity between the AgNO₃ and Ag-NPs exposure (see Fig. 1) should provide an indication of the amount of Ag⁺ released from particles. The survival data (Fig. 1A) suggests that less than 5% of Ag is released (as ions) from the Ag-NPs, since for AgNO₃ a near 100% mortality is observed at 50 mg/kg while for Ag-NPs there is 0% mortality at 1000 mg Ag-NPs/kg exposure. Hence, applying the 5% to the observed EC₅₀ of 225 mg/kg (reproduction) for Ag-NPs, we can predict that the EC₅₀ (reproduction) for AgNO₃ should be approximately 11.25 mg AgNO₃/kg. This is below our lowest tested AgNO₃ concentration, hence cannot be proved or disproved here. The above is of course under the assumption that the relative release (%) is the same independently of the Ag-NPs concentration, if this is not the case e.g. due to agglomeration, then we cannot derive the potential release. The ion selective electrode (ISE) measurements in soil-water do not support the 5% free ions in solution as no Ag⁺ was detected in the soil-water of Ag-NPs spiked soil containing 900 mg/kg soil (i.e. 5%

predicted is approx. 45mg Ag⁺ per 200 ml soil-water). The ISE measurements could “only” detect Ag⁺ in the 50 mg Ag/kg in soil-water following AgNO₃ spiking and “only” at day 1. Hence, if a release of Ag⁺ occurred then either less was released, or was slowly released, or released ions immediately precipitated. The apparent low amount of ions released from our particles (TEM = 82 nm) is in accordance with results from [10] who showed that particles > 10 nm release a low amount of Ag ions, compared to smaller Ag-NPs, although other NP characteristics may play a role for release e.g. the fact that our particles were PVP coated (at least initially).

Seemingly opposing findings are reported in the literature, e.g. Roh et al [18] observed that for *C. elegans* the reproductive output was more affected following Ag-NPs exposure than AgNO₃ exposure, hence this indicated that release of ions is not the full answer. On the other hand, Kim and co-authors [37] noted that Ag-NPs were less toxic than AgNO₃ for *C. elegans*, hence supporting the cause due to released ions. Yang et al [38] tested different Ag-NPs (in coating and size) in *C. elegans* reproduction and in general also found that the Ag-NPs were less toxic than AgNO₃, within the studied timeframe. Finally, studies on *Eisenia fetida* ([25] indicated that after 28 days exposure the 10-15% ionisation of Ag-NPs explained the toxicity in earthworms' reproduction.

Hence, the above speculations and physical-chemical measures are inconclusive in regard to the mechanism of the actual exposure and toxicity. Further, we know that at *E. fetida* and *E. albidus* ingest soil particles, hence once in the intestinal tract a different exposure scenario is displayed. Once internalised (in organism) a low pH and other cell factors can e.g. oxidise the particles to a larger extent or set in motion a series of reactions not occurring outside the organisms or cells, which could well explain toxicity.

Finally, as mentioned above exposure duration may be of importance and a longer-term study may reveal prolonged Ag-NPs related effects. In this context it is worth noting that we based our range finding experiments on a 2-week exposure, where no mortality was observed up to 100 mg/kg, neither for AgNO₃ nor for Ag-NPs exposures (100 mg/kg was however LC₁₀₀ after 3 weeks). Hence, effects occurred between weeks 2 and 3 in this case. This indicates that initial release of Ag⁺ is not directly related to toxicity, in fact toxicity may be related to a reaching bioaccumulation threshold with increased bioaccumulation over time – for which the latter is probably different for AgNO₃ and Ag-NPs exposure. Hence, it seems that the time of exposure for NPs may be crucial for effect assessment. Thus, testing of NPs such as Ag-NPs may require longer exposure periods for a comparable risk assessment with their respective salts i.e. short term exposures may be insufficient to fully understand and assess the hazard or risk of NPs in the environment. This is somewhat similar to what has been recommended in the past for metals standard testing [39], e.g. a minimum equilibration period after soil spiking (3-6 days) should be respected before test start, also to test NPs, and depending on further verification, such an equilibration period could be advisable. In McLaughlin et al. [39], there are in fact 3 approaches recommended for metals RA: testing should be conducted in soil after spiking: 1) 2-7 days; 2) 60 days ageing, and 3) Lixivate soil – soil leached 2-7 days after spiking, partly dried and stored during 60 days. Whether the observed differences between NPs and its salt are due to changes in fate or effect we cannot conclude with the present data.

4.2. Gene expression

Both Ag forms (nano and salt) showed a concentration related transcriptional response in terms of number of differentially expressed genes (DEGs), being in higher number with increasing concentration. Despite this apparent relationship, more DEGs do not necessarily correlate with higher stress level, see e.g. [40].

Perhaps of more interest is the interpretation of the *Venn* diagrams which show how much similarity/difference exists among particles and concentrations. As can be depicted, for AgNO₃ exposure at 100 and 200mg/kg the organisms responded using a large fraction of the same genes (30 common out of 104 DEGs, Fig. 2B); for Ag-NPs, the organisms used a different set of genes (1 common out of 65 DEGs). Such a difference in gene response could be related to the actual effect, i.e. similar mechanisms activated within acute (EC₁₀₀) levels of toxicity (100/200 AgNO₃) compared to a NOEC and EC₅₀ (100/200 Ag-NPs) levels. Still, the comparisons between Ag-NPs and AgNO₃ treatments show a degree of similarity, which probably reflect that general response to stress is also expected. The fact that 100-AgNO₃ and 200-Ag-NPs share more common genes, could corroborate the hypothesis that Ag ions are the main cause of toxicity. The degree to which the mechanisms between Ag-NPs and AgNO₃ toxicity differs is less straight forward to deduct i.e. although the same total concentrations are compared these represent different organismal effects level (and probably different uptake). In any case, 100mg of AgNO₃/kg shows a gene response that is more similar to Ag-NPs (0.66 correlation) than to the 200mg of AgNO₃/kg (Figure 3A). Despite the fact that differences were not discriminated between 100 and 200mg/kg AgNO₃ for survival and reproduction (6 weeks exposure-100% effect) at the gene level (2 days exposure) there was a clear difference between the two concentrations (see Figure 3 A). This is also in agreement with previous considerations on the importance of exposure time.

Gene set enrichment analysis revealed that 200 mg/kg of AgNO₃ is the treatment affecting a higher number of biological functions. Among these was energetic metabolism, clearly affected with up-regulation of several transcripts (glycine N-methyltransferase, phosphoglycerate kinase, NADH dehydrogenase subunit 5 and cytochrome oxidase subunit 1). Alterations in energy production related transcripts' expression was already observed in response to Cu and Cu-NPs [41], Cu [42], Zn and Cd [43] and dimethoate [44]. Despite the fact that several chemicals induce energy related transcripts this is not an indication of general stress related response, since the expression pattern has been found to be concentration and time dependent. In the present study, the energy related transcripts were consistently up-regulated. Knowing that the energy expenditure depends, among others, on the amount required to maintain homeostasis, the fact that organisms died after 6 weeks exposure to 200 mg/kg of AgNO₃ would fit with the previous activation of response mechanisms – energy costing - at 2 days exposure. Although, it would not explain why this was not significantly expressed at 100mg/kg of AgNO₃.

Often the result of a certain high energy cost process, e.g. detoxification, has a trade-off that results in using less energy in other processes. This has been reported by Novais et al. [43] who suggested that detoxifying mechanisms for Zn (up-regulation of energy metabolism related genes) occurred together with down-regulation for e.g. ribosomal protein synthesis. This same principle could be occurring here with associated effects on embryonic development, meiosis and macromolecule biosynthetic process (Table 3) related to the down-regulation of transcripts coding for sarcoplasmic calcium binding, 40s ribosomal protein s4 and histone.

AgNO₃ (200 and 100mg/kg) caused the down-regulation of histone transcript. Histones can undergo several post-translational modifications which act in different biological

functions (e.g. gene regulation, DNA repair, and spermatogenesis); in this case, histone down-regulation is affecting male meiosis and regulation of cell shape. The ADP-ribosylation factor-like protein 2-binding protein (ARL2BP gene) is involved (together with ADP-ribosylation factor-like 2) in the nuclear translocation, retention and transcriptional activity of STAT3, and is up-regulated in response to AgNO₃-100. STAT proteins are called transcription factors because they regulate the activity of specific genes (by turning them “on” or “off”). STAT3 regulates genes that are involved in cell growth and division, mobility and the self-destruction. It is not possible to know if any of these processes were induced by AgNO₃ exposure, since no other transcripts involved in the cascades related to STAT3 protein activation were differently expressed (maybe simply because the genes are not present in the library or they are non-annotated), but the transcript coding for ARL2BP was up-regulated and affecting positive regulation of tyrosine phosphorylation of STAT3 protein (see Table 3).

Exposure to 100 mg/kg of Ag-NPs cause changes in gene expression of 22 transcripts (Figure 2A), among the functions affected by these transcripts none were significant comparatively to the total gene library hence we will not discuss those. Exposure to 200 mg/kg of Ag-NPs affected the developmental processes (tail tip morphogenesis and vulval development), and regulation of locomotion and gene expression, (see Table 3), by the down-regulation of the gene coding for dpy-30-like protein. We are not clear about how to interpret these alterations, because some of the functions/organs mentioned are not present in the test species in such a form. In *C. elegans* the development of vulval abnormalities (and other phenotype alterations) were also observed after prolonged exposure to Mn [45].

Some studies have reported distinct gene expression patterns between nano and salt (or ionic) forms of Ag, when comparing similar total concentrations of both silver forms

[18] or by comparison of Ag-NPs with the amount of ions released from the particles as AgNO₃ [17]. Despite the indication that the Ag-form (nano versus salt) induces different expression patterns as observed in *Saccharomyces cerevisiae*, Gu and co-authors [19] suggest that after 210 min. of exposure (in comparison to 120 min.) the release of Ag ions from Ag-NPs is responsible for the similar response of some genes between Ag-NPs and Ag-NO₃ exposure. In our study, and as mentioned above, we could not fully support that the toxicity is caused by a release of ions from the particles, not based on measurements in soil solution (all below detection limit) nor by evaluation of organisms' response data. Our genomic data does not fully corroborate a distinct pattern between nano and salt for the reasons already discussed. The low explanatory power can be due to the relatively small genomic library base (also with a high number of non-annotated transcripts) and the basis for its development that did not include enrichment for Ag stress related genes.

Summarising, indications are that the responses to Ag-NPs reflect an effect of Ag ions and Ag nanoparticles given the extent of similar/dissimilar genes activated. Further, the particles characterization supports this conclusion due to the limited free ions measured in the soil water extracts. Because we used relatively large Ag-NPs the oxidation is not expected to be very high [10]. Further, being in the soil matrix, the released Ag ions would probably be complexed with organic matter (OM) or sulfide, slowing down the oxidation. Still, specific Ag-NPs effects also seem to occur since toxicity level could not be explained based on the Ag ions released from NPs, as based on the biological and materials ID.

5. Conclusions

Comparison between Ag salt and NPs revealed that AgNO₃ was more toxic (based on mass) to the soil worm *Enchytraeus albidus*, affecting its survival and reproduction in the lowest tested range (EC₅₀<50mg/kg), whereas for Ag-NPs the EC₅₀ was 225mg/kg. At the gene expression level, comparison between 100 and 200 mg/kg of both Ag forms showed that organisms responded most differently to 200 mg AgNO₃ (compared to other exposure concentrations), whereas the remaining exposures were less distinct. Differences in gene expression could partly be attributed to the probable differences in actual exposure despite exposure to the same total Ag concentration. We could not fully conclude upon whether Ag-NPs toxicity was caused mainly by particle-related effects or due to release (less than 5%) of Ag⁺ from the Ag-NPs. The time of exposure is important for effect assessment and testing of NPs such as Ag may require longer exposure periods for a comparable effect/risk assessment with other chemicals, and focus on the more subtle long term effects. Our gene expression analysis indicates similarities and differences in response to Ag-NPs and AgNO₃, although not conclusive because 1) the effect due to different EC_x exposures cannot be ruled out and, 2) if NPs toxicity is caused by Ag ions, the short exposure time and respective oxidation could be masking similarities, which could become apparent in a longer exposure period or ageing.

Acknowledgments

This work was supported by funding FEDER through COMPETE Programa Operacional Factores de Competitividade, and by National funding through FCT-Fundação para a Ciência e Tecnologia, within the research project NANOkA FCOMP-01-0124-FEDER-008944 (Ref. FCT PTDC/BIA-BEC/103716/2008), through an FCT

PhD grant to Susana Gomes (SFRH/BD/63261/2009) and by the EU-FP7 MARINA (Ref. 263215).

Supplementary data

Table S1: All differentially expressed genes, with M value and Parametric p value for each treatment. The genes are identified with cluster ID from Enchybase (<http://bioinformatics.ua.pt/enchybase/>) and sequence description (annotation).

Figure S1: Heat map of genes affected by AgNO₃ treatments, with gene annotation.

Figure S2: Heat map of genes affected by Ag-NPs treatments, with gene annotation.

References

- [1] N.C. Mueller, B. Nowack, Exposure Modeling of Engineered Nanoparticles in the Environment, *Environ Sci Technol*, 42 (2008) 4447-4453.
- [2] F. Gottschalk, T. Sonderer, R.W. Scholz, B. Nowack, Modeled Environmental Concentrations of Engineered Nanomaterials (TiO₂, ZnO, Ag, CNT, Fullerenes) for Different Regions, *Environ Sci Technol*, 43 (2009) 9216-9222.
- [3] H.J. Park, J.Y. Kim, J. Kim, J.H. Lee, J.S. Hahn, M.B. Gu, J. Yoon, Silver-ion-mediated reactive oxygen species generation affecting bactericidal activity, *Water Res*, 43 (2009) 1027-1032.
- [4] M. Sopjani, M. Foller, J. Haendeler, F. Gotz, F. Lang, Silver ion-induced suicidal erythrocyte death, *J Appl Toxicol*, 29 (2009) 531-536.
- [5] M.R. Almofti, T. Ichikawa, K. Yamashita, H. Terada, Y. Shinohara, Silver ion induces a cyclosporine A-insensitive permeability transition in rat liver mitochondria and release of apoptogenic cytochrome C, *J Biochem*, 134 (2003) 43-49.
- [6] C. Levard, E.M. Hotze, G.V. Lowry, G.E. Brown, Environmental Transformations of Silver Nanoparticles: Impact on Stability and Toxicity, *Environ Sci Technol*, 46 (2012) 6900-6914.

- [7] A.J. Miao, K.A. Schwehr, C. Xu, S.J. Zhang, Z. Luo, A. Quigg, P.H. Santschi, The algal toxicity of silver engineered nanoparticles and detoxification by exopolymeric substances, *Environ Pollut*, 157 (2009) 3034-3041.
- [8] E. Navarro, F. Piccapietra, B. Wagner, F. Marconi, R. Kaegi, N. Odzak, L. Sigg, R. Behra, Toxicity of Silver Nanoparticles to *Chlamydomonas reinhardtii*, *Environ Sci Technol*, 42 (2008) 8959-8964.
- [9] J. Fabrega, S.R. Fawcett, J.C. Renshaw, J.R. Lead, Silver nanoparticle impact on bacterial growth: effect of pH, concentration, and organic matter, 43 (2009) 7285-7290.
- [10] G.A. Sotiriou, S.E. Pratsinis, Antibacterial Activity of Nanosilver Ions and Particles, *Environ Sci Technol*, 44 (2010) 5649-5654.
- [11] S.M. Hussain, K.L. Hess, J.M. Gearhart, K.T. Geiss, J.J. Schlager, In vitro toxicity of nanoparticles in BRL 3A rat liver cells, *Toxicol in Vitro*, 19 (2005) 975-983.
- [12] C. Carlson, S.M. Hussain, A.M. Schrand, L.K. Braydich-Stolle, K.L. Hess, R.L. Jones, J.J. Schlager, Unique Cellular Interaction of Silver Nanoparticles: Size-Dependent Generation of Reactive Oxygen Species, *J Phys Chem B*, 112 (2008) 13608-13619.
- [13] M.J. Piao, K.A. Kang, I.K. Lee, H.S. Kim, S. Kim, J.Y. Choi, J. Choi, J.W. Hyun, Silver nanoparticles induce oxidative cell damage in human liver cells through inhibition of reduced glutathione and induction of mitochondria-involved apoptosis, *Toxicol Lett*, 201 (2011) 92-100.
- [14] Y. Hayashi, P. Engelmann, R. Foldbjerg, M. Szabo, I. Somogyi, E. Pollak, L. Molnar, H. Autrup, D.S. Sutherland, J. Scott-Fordsmand, L.H. Heckmann, Earthworms and Humans in Vitro: Characterizing Evolutionarily Conserved Stress and Immune Responses to Silver Nanoparticles, *Environ Sci Technol*, 46 (2012) 4166-4173.
- [15] M. Ahamed, R. Posgai, T.J. Gorey, M. Nielsen, S.M. Hussain, J.J. Rowe, Silver nanoparticles induced heat shock protein 70, oxidative stress and apoptosis in *Drosophila melanogaster*, *Toxicol Appl Pharm*, 242 (2010) 263-269.

- [16] E. Lapied, E. Moudilou, J.M. Exbrayat, D.H. Oughton, E.J. Joner, Silver nanoparticle exposure causes apoptotic response in the earthworm *Lumbricus terrestris* (Oligochaeta), *Nanomedicine-Uk*, 5 (2010) 975-984.
- [17] R.J. Griffitt, K. Hyndman, N.D. Denslow, D.S. Barber, Comparison of Molecular and Histological Changes in Zebrafish Gills Exposed to Metallic Nanoparticles, *Toxicol Sci*, 107 (2009) 404-415.
- [18] J.Y. Roh, S.J. Sim, J. Yi, K. Park, K.H. Chung, D.Y. Ryu, J. Choi, Ecotoxicity of Silver Nanoparticles on the Soil Nematode *Caenorhabditis elegans* Using Functional Ecotoxicogenomics, *Environ Sci Technol*, 43 (2009) 3933-3940.
- [19] M.B. Gu, J.H. Niazi, B.I. Sang, Y.S. Kim, Global Gene Response in *Saccharomyces cerevisiae* Exposed to Silver Nanoparticles, *Appl Biochem Biotech*, 164 (2011) 1278-1291.
- [20] N. Gou, A. Onnis-Hayden, A.Z. Gu, Mechanistic Toxicity Assessment of Nanomaterials by Whole-Cell-Array Stress Genes Expression Analysis, *Environ Sci Technol*, 44 (2010) 5964-5970.
- [21] C.M. Zhao, W.X. Wang, Comparison of Acute and Chronic Toxicity of Silver Nanoparticles and Silver Nitrate to *Daphnia Magna*, *Environ Toxicol Chem*, 30 (2011) 885-892.
- [22] P.V. Asharani, Y.L. Wu, Z.Y. Gong, S. Valiyaveetil, Toxicity of silver nanoparticles in zebrafish models, *Nanotechnology*, 19 (2008).
- [23] Y.J. Chae, C.H. Pham, J. Lee, E. Bae, J. Yi, M.B. Gu, Evaluation of the toxic impact of silver nanoparticles on Japanese medaka (*Oryzias latipes*), *Aquat Toxicol*, 94 (2009) 320-327.
- [24] T.M. Scown, E.M. Santos, B.D. Johnston, B. Gaiser, M. Baalousha, S. Mitov, J.R. Lead, V. Stone, T.F. Fernandes, M. Jepson, R. van Aerle, C.R. Tyler, Effects of Aqueous Exposure to Silver Nanoparticles of Different Sizes in Rainbow Trout, *Toxicol Sci*, 115 (2010) 521-534.
- [25] W.A. Shoults-Wilson, B.C. Reinsch, O.V. Tsyusko, P.M. Bertsch, G.V. Lowry, J.M. Unrine, Effect of silver nanoparticle surface coating on bioaccumulation and reproductive toxicity in earthworms (*Eisenia fetida*), *Nanotoxicology*, 5 (2011) 432-444.

- [26] W.A. Shoults-Wilson, O.I. Zhurbich, D.H. McNear, O.V. Tsyusko, P.M. Bertsch, J.M. Unrine, Evidence for avoidance of Ag nanoparticles by earthworms (*Eisenia fetida*), *Ecotoxicology*, 20 (2011) 385-396.
- [27] L.-H. Heckmann, M.B. Hovgaard, D.S. Sutherland, H. Autrup, F. Besenbacher, J.J. Scott-Fordsmand, Limit-test toxicity screening of selected inorganic nanoparticles to the earthworm *Eisenia fetida*, *Ecotoxicology*, 20(1) (2011) 226-233.
- [28] ISO International Organization for Standardization, Soil Quality - Effects of pollutants on Enchytraeidae (*Enchytraeus* sp.). Determination of effects on reproduction and survival. Guideline 16387, Geneva, Switzerland (2005).
- [29] OECD Organization for Economic Cooperation and Development, Guidelines for the testing of chemicals No. 220. Enchytraeid Reproduction Test. Paris (2004).
- [30] M.J.B. Amorim, J. Rombke, A.M.V.M. Soares, Avoidance behaviour of *Enchytraeus albidus*: Effects of Benomyl, Carbendazim, phenmedipham and different soil types, *Chemosphere*, 59 (2005) 501-510.
- [31] M.J.B. Amorim, S.C. Novais, K. Van der Ven, T. Vandenbrouck, A.M.V.M. Soares, W. De Coen, Development of a microarray in *Enchytraeus albidus* (Oligochaeta): preliminary tool with diverse applications, *Environ Toxicol Chem*, 30 (2011) 1395-1402.
- [32] S.C. Novais, J. Arrais, P. Lopes, T. Vandenbrouck, W. De Coen, D. Roelofs, A.M.V.M. Soares, M.J.B. Amorim, *Enchytraeus albidus* Microarray: Enrichment, Design, Annotation and Database (EnchyBASE), *Plos One*, 7 (2012).
- [33] F.G.J. Henle, Ueber *Enchytraeus*, eine neue Anneliden-Gattung, *Archiv für Anatomie, Physiologie und wissenschaftliche Medicin*, (1837) 74-90.
- [34] M. Amorim, J. Scott-Fordsmand, Toxicity of Copper nanoparticles and CuCl₂ salt to *Enchytraeus albidus* worms: survival, reproduction and avoidance responses, *Environ Pollut*, 164 (2012) 164-168.

- [35] A. Conesa, S. Gotz, J.M. Garcia-Gomez, J. Terol, M. Talon, M. Robles, Blast2GO: a universal tool for annotation, visualization and analysis in functional genomics research, *Bioinformatics*, 21 (2005) 3674-3676.
- [36] A. Alexa, J. Rahnenfuhrer, T. Lengauer, Improved scoring of functional groups from gene expression data by decorrelating GO graph structure, *Bioinformatics*, 22 (2006) 1600-1607.
- [37] S.W. Kim, S.H. Nam, Y.J. An, Interaction of Silver Nanoparticles with Biological Surfaces of *Caenorhabditis elegans*, *Ecotox Environ Safe*, 77 (2012) 64-70.
- [38] X.Y. Yang, A.P. Gondikas, S.M. Marinakos, M. Auffan, J. Liu, H. Hsu-Kim, J.N. Meyer, Mechanism of Silver Nanoparticle Toxicity Is Dependent on Dissolved Silver and Surface Coating in *Caenorhabditis elegans*, *Environ Sci Technol*, 46 (2012) 1119-1127.
- [39] M.J. McLaughlin, R.E. Hamon, D.R. Parker, G.M. Pierzynski, E. Smolders, I. Thornton, G. Welp, Test methods to determine hazards of sparingly soluble metal compounds in soils., in: A. Fairbrother, G. Ethier, J.V. Tarazona, H. Waeterschoot (Eds.) *Test Methods to Determine Hazards of Sparingly Soluble Metal Compounds in Soils*, Society of Environmental Toxicology and Chemistry (SETAC), 2002, pp. 5-85.
- [40] B. Nota, M. Bosse, B. Ylstra, N.M. van Straalen, D. Roelofs, Transcriptomics reveals extensive inducible biotransformation in the soil-dwelling invertebrate *Folsomia candida* exposed to phenanthrene, *Bmc Genomics*, 10:236 (2009).
- [41] S.I.L. Gomes, S.C. Novais, J.J. Scott-Fordsmand, W.D. Coen, A.M.V.M. Soares, M.J.B. Amorim, Effect of Cu-nanoparticles versus Cu-salt in *Enchytraeus albidus* (Oligochaeta): Differential gene expression through microarray analysis, *Comp Biochem Physiol, C*, 155 (2012) 219-227.
- [42] J.G. Bundy, J.K. Sidhu, F. Rana, D.J. Spurgeon, C. Svendsen, J.F. Wren, S.R. Sturzenbaum, A.J. Morgan, P. Kille, 'Systems toxicology' approach identifies coordinated metabolic responses to copper in a terrestrial non-model invertebrate, the earthworm *Lumbricus rubellus*., *Bmc Biology*, 6:25 (2008).

[43] S.C. Novais, W. De Coen, M.J.B. Amorim, Transcriptional responses in *Enchytraeus albidus* (Oligochaeta): Comparison between cadmium and zinc exposure and linkage to reproduction effects, *Environ Toxicol Chem*, 31 (2012) 2289-2299.

[44] S.C. Novais, W. De Coen, M.J.B. Amorim, Gene Expression Responses Linked to Reproduction Effect Concentrations (EC10,20,50,90) of Dimethoate, Atrazine and Carbendazim, in *Enchytraeus albidus*, *Plos One*, 7 (2012).

[45] J. Xiao, Q. Rui, Y.L. Guo, X.Y. Chang, D.Y. Wang, Prolonged manganese exposure induces severe deficits in lifespan, development and reproduction possibly by altering oxidative stress response in *Caenorhabditis elegans*, *J Environ Sci-China*, 21 (2009) 842-848.

Supplementary material

Table S1: All differentially expressed genes, with M value and Parametric p value for each treatment. The genes are identified with cluster ID from Enchybase* and sequence description (annotation).

* <http://bioinformatics.ua.pt/enchybase/>

Seq. Description	Cluster ID (EnchyBase)	AgNO3_100		AgNO3_200		Ag-NPs_100		Ag-NPs_200	
		M value	Parametric p value	M value	Parametric p value	M value	Parametric p value	M value	Parametric p value
partial	EAC00001	0.23979	> 0.05	-1.63972	0.02880	-0.04534	> 0.05	0.11986	> 0.05
	EAC00004	0.03929	> 0.05	0.94814	> 0.05	2.32315	0.03790	0.34943	> 0.05
	EAC00008	0.33868	> 0.05	-1.08863	0.04494	-0.46711	> 0.05	-0.36763	> 0.05
	EAC00013	-2.03105	0.00105	-3.51118	0.00007	-1.09638	> 0.05	-0.64783	0.01502
actin	EAC00024	-0.18206	> 0.05	-1.60725	0.02671	-0.04414	> 0.05	0.13989	> 0.05
	EAC00026	0.77664	0.03350	0.54475	> 0.05	0.17866	> 0.05	0.13529	> 0.05
	EAC00037	1.51996	0.03813	0.83253	> 0.05	-0.04700	> 0.05	0.97843	> 0.05
	EAC00044	-1.49129	> 0.05	0.98580	> 0.05	-1.68171	0.03701	-1.67619	> 0.05
scbp3 protein	EAC00045	-0.00104	> 0.05	1.94118	0.01085	0.00724	> 0.05	-0.23597	> 0.05
	EAC00046	1.11467	0.04712	-0.04636	> 0.05	0.31760	> 0.05	0.45020	> 0.05
	EAC00048	-0.32050	> 0.05	-0.23248	> 0.05	-0.68292	> 0.05	-0.95332	0.02534
	EAC00049	1.63988	0.01480	0.49200	> 0.05	0.94145	> 0.05	0.77178	> 0.05
	EAC00057	1.01979	> 0.05	-3.26813	0.02138	1.12795	> 0.05	0.46941	> 0.05
	EAC00066	-1.03653	0.02771	2.66465	> 0.05	-0.22287	> 0.05	0.06173	> 0.05
scp_pervt ame: full=sarcoplasmic calcium-binding protein short=scp	EAC00067	-0.19550	> 0.05	-1.31846	0.04578	-0.90754	> 0.05	-0.87608	> 0.05
	EAC00081	2.52340	0.04977	-0.04870	> 0.05	2.77532	0.03524	0.77908	> 0.05
	EAC00092	0.22590	> 0.05	0.91478	> 0.05	1.11172	0.02472	0.12982	> 0.05
	EAC00113	1.00843	> 0.05	-3.58145	0.01583	1.04516	> 0.05	0.40343	> 0.05
actin	EAC00139	0.58217	> 0.05	-0.38740	> 0.05	0.11278	> 0.05	0.27370	0.01377
	EAC00140	1.07302	0.04642	1.78197	> 0.05	-0.22808	> 0.05	0.01642	> 0.05
universal minicircle sequence binding protein	EAC00148	-0.19434	> 0.05	-1.59476	0.02939	-0.15251	> 0.05	0.21065	> 0.05

Supplementary material- Chapter VI

	EAC00160	1.12150	> 0.05	1.11723	> 0.05	0.56437	> 0.05	1.50736	0.00076
	EAC00166	0.43585	> 0.05	-3.29611	0.01294	-0.20015	> 0.05	-0.26140	> 0.05
alpha tubulin	EAC00175	-0.30710	> 0.05	-0.50747	> 0.05	-0.51786	> 0.05	-0.36588	0.02471
actin	EAC00183	0.75565	> 0.05	-1.27590	0.03334	0.63121	> 0.05	0.70877	> 0.05
	EAC00189	-2.61690	0.02927	-1.80220	> 0.05	-2.56975	> 0.05	-1.15048	> 0.05
	EAC00191	1.07986	0.04111	1.10732	> 0.05	0.81578	> 0.05	0.58795	> 0.05
	EAC00195	-0.68637	0.04740	-1.03334	0.03223	-0.31689	> 0.05	-0.54600	0.00578
nadh dehydrogenase subunit 5	EAC00216	0.71108	> 0.05	1.69719	0.01094	0.32977	> 0.05	0.88762	> 0.05
	EAC00217	0.41319	> 0.05	-1.50467	0.03730	-0.05826	> 0.05	0.40745	> 0.05
tropomyosin	EAC00224	0.17687	> 0.05	-0.79210	> 0.05	0.15394	> 0.05	0.25509	0.01949
40s ribosomal protein s4	EAC00226	-0.09847	> 0.05	-1.63322	0.04790	-0.20624	> 0.05	-0.16074	> 0.05
	EAC00241	0.72199	> 0.05	0.04111	> 0.05	-1.08210	0.03538	-0.31966	> 0.05
	EAC00251	-1.43700	0.03221	-1.24794	0.03541	-0.40737	> 0.05	0.10291	> 0.05
	EAC00262	0.79166	> 0.05	-2.12034	0.04422	1.37692	> 0.05	-0.43415	> 0.05
	EAC00264	1.03633	> 0.05	1.42718	0.01999	0.05185	> 0.05	0.71397	> 0.05
60s ribosomal protein l7	EAC00269	-0.11203	> 0.05	0.99284	> 0.05	0.62069	> 0.05	2.35009	0.01609
	EAC00271	-1.18380	0.00799	-1.90979	0.00542	-0.44263	> 0.05	-0.56213	> 0.05
	EAC00275	1.24806	> 0.05	0.45723	> 0.05	0.63616	> 0.05	3.33891	0.02099
10 kda heat shock mitochondrial	EAC00276	-1.03575	> 0.05	1.73534	> 0.05	-1.49446	> 0.05	-1.46100	0.03122
	EAC00292	1.17860	> 0.05	-0.01921	> 0.05	0.21536	> 0.05	2.75205	0.01189
	EAC00296	1.03161	0.00942	0.09553	> 0.05	-0.18649	> 0.05	-0.39515	> 0.05
	EAC00299	1.14781	0.02463	0.47496	> 0.05	-0.52374	> 0.05	0.48884	> 0.05
b chain structural basis for the heterotropic and homotropic interactions of invertebrate giant hemoglobin	EAC00301	-0.27620	> 0.05	-4.57776	0.00144	-0.25115	> 0.05	-0.63767	> 0.05
---NA---	EAC00305	0.85670	> 0.05	0.03583	> 0.05	0.63573	> 0.05	0.84083	0.03475
	EAC00310	0.51244	> 0.05	-1.01117	0.04780	-0.60707	> 0.05	0.39438	> 0.05
	EAC00315	2.32350	0.00462	2.81336	0.00131	0.54844	> 0.05	1.36699	0.02364
tropomyosin	EAC00327	0.12594	> 0.05	-1.38958	0.04885	0.27719	> 0.05	0.91531	0.03998
	EAC00332	0.23730	> 0.05	-1.56410	0.01843	0.37629	> 0.05	0.68551	> 0.05
	EAC00336	-0.17003	> 0.05	-1.28135	> 0.05	-1.46966	0.01892	-0.59689	> 0.05
	EAC00338	-2.85345	> 0.05	-0.04882	> 0.05	-2.85739	0.01386	-0.37405	> 0.05
	EAC00345	-1.07522	0.03889	-0.38942	> 0.05	-0.93136	> 0.05	-1.01766	> 0.05

Supplementary material- Chapter VI

	EAC00352	-1.18659	0.00974	-1.97601	0.00820	-0.39953	> 0.05	-0.62933	> 0.05
	EAC00361	1.46493	0.01309	1.84954	0.00316	0.19136	> 0.05	1.16294	0.00512
cytochrome b	EAC00364	0.05333	> 0.05	1.44091	0.02867	0.17984	> 0.05	1.01417	> 0.05
cmf receptor cmfr1	EAC00366	1.12826	0.04496	0.85897	> 0.05	0.15108	> 0.05	0.33879	> 0.05
	EAC00368	0.23890	> 0.05	0.31360	> 0.05	1.11230	> 0.05	0.44030	0.01660
	EAC00374	1.21746	0.03816	0.75664	> 0.05	0.17128	> 0.05	0.43278	> 0.05
hemoglobin c chain precursor	EAC00398	0.46351	> 0.05	-3.56539	0.02757	0.49521	> 0.05	-0.75300	> 0.05
rna-directed dna polymerase from mobile element jockey-like	EAC00403	1.74884	0.01224	2.07669	0.00248	0.19999	> 0.05	0.83066	> 0.05
actin	EAC00406	0.25273	> 0.05	0.72337	> 0.05	0.70732	> 0.05	1.53062	0.04533
	EAC00412	0.25439	> 0.05	-1.16745	0.04659	0.14259	> 0.05	-0.15489	> 0.05
von willebrand factor type c domain protein	EAC00415	1.04198	0.03539	0.21376	> 0.05	0.17879	> 0.05	-0.76553	> 0.05
	EAC00417	3.05624	0.00302	2.96654	0.00214	0.46572	> 0.05	2.07936	0.03873
	EAC00418	1.14170	0.02064	1.02436	0.03315	0.10933	> 0.05	0.27152	> 0.05
	EAC00430	0.88340	0.04794	0.08035	> 0.05	0.37911	> 0.05	0.06604	> 0.05
regeneration-upregulated protein 1	EAC00452	-3.43102	0.03914	-1.63969	> 0.05	-1.84707	> 0.05	-3.07946	> 0.05
beta-actin	EAC00455	0.37837	> 0.05	-1.70522	0.02972	0.10532	> 0.05	0.22135	> 0.05
actin	EAC00459	0.04558	> 0.05	1.13668	0.04485	0.46857	> 0.05	-0.05092	> 0.05
endonuclease-reverse transcriptase -e01- partial	EAC00471	1.84129	0.00650	2.17204	0.00188	0.10770	> 0.05	0.99033	0.02570
ribosomal protein l15	EAC00476	0.35876	> 0.05	-0.58479	> 0.05	1.33534	0.04242	0.62335	> 0.05
ribosomal protein l10ae	EAC00479	-0.81198	> 0.05	-1.75828	0.04837	-0.85864	> 0.05	-0.46524	> 0.05
actin	EAC00483	0.74745	> 0.05	-1.38968	0.03633	0.37970	> 0.05	0.83761	> 0.05
	EAC00487	0.09770	> 0.05	-1.51244	0.00920	-0.19649	> 0.05	0.11485	> 0.05
	EAC00497	1.50392	0.00963	0.44677	> 0.05	0.70182	> 0.05	0.38864	> 0.05
waprin-phi1-like isoform 2	EAC00513	-0.01730	> 0.05	4.75947	0.02171	1.65341	> 0.05	0.63864	> 0.05
	EAC00519	0.85062	> 0.05	-1.60063	0.04775	-0.16624	> 0.05	0.97636	> 0.05
beta actin	EAC00523	1.24942	0.02990	0.57335	> 0.05	0.67807	> 0.05	1.21240	0.01081
	EAC00529	-1.55826	> 0.05	-2.11009	0.04812	-1.86850	> 0.05	-1.53180	> 0.05
cysteine-rich protein 1-like	EAC00887	-0.47896	> 0.05	1.16543	> 0.05	1.40982	0.01272	-0.22825	> 0.05
mads flc-like protein 2	EAC00895	1.45537	> 0.05	-2.53167	0.04446	2.04914	> 0.05	0.26506	> 0.05
mads flc-like protein 2	EAC00896	-0.50540	> 0.05	-0.21607	> 0.05	-0.78158	> 0.05	-0.85130	0.03081
---NA---	EAC00903	0.29284	> 0.05	-0.85978	> 0.05	-0.58642	> 0.05	-0.40098	0.00069
	EAC00908	-1.18131	0.01133	-1.95137	0.00554	-0.32074	> 0.05	-0.41761	> 0.05

Supplementary material- Chapter VI

	EAC00911	-0.36651	> 0.05	-1.39922	0.04830	0.13070	> 0.05	-0.13750	> 0.05
	EAC00915	0.79453	> 0.05	-3.68082	0.02210	0.84909	> 0.05	-0.48662	> 0.05
kazal-type serine protease inhibitor domain-containing protein 1-like	EAC00920	-4.17464	0.00607	-0.42270	> 0.05	-4.05812	0.00406	-4.42286	> 0.05
mads flc-like protein 2	EAC00943	-1.71056	0.01812	-1.54056	> 0.05	-1.69117	> 0.05	-1.21543	0.03552
	EAC00947	-1.00216	0.02635	-0.88629	> 0.05	-0.55990	> 0.05	-0.57204	> 0.05
	EAC00953	-0.32910	> 0.05	-1.39937	0.02782	-0.12330	> 0.05	0.59834	> 0.05
	EAC00965	0.24959	> 0.05	0.00353	> 0.05	0.15854	> 0.05	-0.48412	0.03559
mads flc-like protein 2	EAC00975	0.07680	> 0.05	-1.64798	0.00422	-0.75196	> 0.05	-0.31241	> 0.05
	EAC00980	-0.53338	> 0.05	-0.10161	> 0.05	-0.63600	> 0.05	-0.79006	0.04822
	EAC00986	2.25141	> 0.05	-0.14389	> 0.05	2.61885	0.04398	0.81943	> 0.05
	EAC01000	-1.44113	0.01417	-0.26374	> 0.05	-1.01253	> 0.05	-1.25636	0.04312
glycine n-methyltransferase	EAC01005	-0.43093	> 0.05	5.01702	0.00424	0.23909	> 0.05	0.05227	> 0.05
myosin heavy chain	EAC01025	0.34234	> 0.05	4.01718	0.00937	-0.37151	> 0.05	0.32423	> 0.05
mads flc-like protein 2	EAC01027	-0.94700	0.02964	-0.01371	> 0.05	-0.34266	> 0.05	-0.41985	> 0.05
sarcoplasmic calcium-binding	EAC01038	-0.28410	> 0.05	-1.63008	0.01900	-0.16664	> 0.05	0.27301	> 0.05
cytochrome oxidase subunit i	EAC01043	-0.14258	> 0.05	1.44732	0.03933	0.17110	> 0.05	0.52282	> 0.05
	EAC01054	0.18218	> 0.05	1.99745	0.03679	-0.67386	> 0.05	0.17092	> 0.05
mads flc-like protein 2	EAC01083	1.27126	0.04915	1.86602	0.01022	-0.22784	> 0.05	0.81927	> 0.05
phosphoglycerate kinase	EAC01086	-0.10258	> 0.05	4.24875	0.00396	0.81042	> 0.05	0.31912	> 0.05
myosin heavy chain	EAC01089	-1.25767	> 0.05	-3.54705	0.04582	-1.39946	> 0.05	-1.69191	> 0.05
protein	EAC01090	-0.60471	> 0.05	-1.20633	0.04323	-0.82132	> 0.05	-1.03685	0.04903
myosin heavy chain	EAC01096	0.62867	> 0.05	7.88653	0.00018	1.18226	> 0.05	0.84460	> 0.05
transcription factor btf3 homolog 4	EAC01097	0.64991	> 0.05	4.08661	0.00621	-0.12965	> 0.05	0.73340	> 0.05
	EAC01103	0.26381	> 0.05	-1.18655	0.04490	0.05286	> 0.05	0.10019	> 0.05
mads flc-like protein 2	EAC01116	0.67188	0.04981	1.00656	> 0.05	1.38854	0.02598	0.03494	> 0.05
mads flc-like protein 2	EAC01118	-0.32793	> 0.05	2.42560	0.02043	-0.66712	> 0.05	-0.71100	> 0.05
	EAC00555	1.17780	0.02484	1.43877	0.01283	0.42985	> 0.05	0.41200	> 0.05
	EAC00557	0.59341	> 0.05	0.36729	> 0.05	1.94893	0.01514	0.05567	> 0.05
	EAC00561	1.09139	0.03559	-0.09168	> 0.05	1.45132	> 0.05	1.14715	0.03339
	EAC00565	0.20633	> 0.05	-1.78024	0.01146	-0.28452	> 0.05	0.41474	> 0.05
adp-ribosylation factor-like protein 2-binding protein	EAC00579	1.70408	0.02509	1.15623	> 0.05	0.28125	> 0.05	1.33893	> 0.05
	EAC00582	0.18706	> 0.05	0.61413	> 0.05	-0.07242	> 0.05	-0.40134	0.02461

Supplementary material- Chapter VI

	EAC00591	0.18265	> 0.05	7.15718	0.00141	0.91979	> 0.05	-0.25921	> 0.05
zinc finger mym-type protein 1-like	EAC00592	1.50678	0.01984	1.37850	0.02389	0.34411	> 0.05	0.71806	> 0.05
---NA---	EAC00594	2.30185	0.03582	-0.78783	> 0.05	-0.30093	> 0.05	1.32257	> 0.05
	EAC00599	1.88472	0.01769	2.24952	0.01526	0.26817	> 0.05	1.51602	> 0.05
proteasome isoform b	EAC00632	0.36079	> 0.05	-0.07648	> 0.05	1.34146	> 0.05	2.76319	0.02399
dpy-30-like protein	EAC00671	0.09707	> 0.05	2.36509	0.00316	0.14399	> 0.05	-0.28514	0.04834
	EAC00624	0.44949	> 0.05	0.89245	> 0.05	1.63931	0.04209	-0.01688	> 0.05
histone	EAC00627	-2.21607	0.00086	-2.02280	0.00782	-0.36618	> 0.05	-0.78899	> 0.05
	EAC00630	0.53932	> 0.05	-1.45053	0.03363	-0.88441	> 0.05	0.62286	> 0.05
neutral and basic amino acid transport protein rbat	EAC00636	0.38914	> 0.05	1.08964	> 0.05	0.59773	> 0.05	2.65638	0.01904
tpa: endonuclease-reverse transcriptase	EAC00638	1.13640	0.03736	1.30809	0.01670	0.57876	> 0.05	0.87702	> 0.05
	EAC00646	1.45238	0.02235	1.03362	> 0.05	0.74288	> 0.05	0.55933	> 0.05
	EAC00649	1.79637	0.01443	-0.29740	> 0.05	1.02467	> 0.05	1.16372	> 0.05
	EAC00669	-0.53693	> 0.05	1.67294	> 0.05	-0.44877	> 0.05	-0.51250	0.00343
upf0631 protein c17orf108 homolog	EAC00675	1.96055	0.01153	2.36001	0.00103	0.75826	> 0.05	1.33236	0.01493
	EAC00682	1.17122	0.03255	0.99985	> 0.05	0.02727	> 0.05	0.92966	0.03565
coiled-coil-helix-coiled-coil-helix domain-containing protein mitochondrial precursor	EAC00684	0.18149	> 0.05	-1.28371	0.04202	0.08204	> 0.05	-0.31285	> 0.05
	EAC00746	1.64727	0.00707	0.96997	> 0.05	0.14107	> 0.05	0.89875	> 0.05
	EAC00694	-4.52589	0.00191	-2.12437	> 0.05	-4.44626	0.00320	#DIV/0!	> 0.05
calcium-dependent protein kinase	EAC00697	-2.10738	0.00223	-1.48877	0.04843	-2.72036	0.00368	-1.47607	> 0.05
	EAC00701	-2.32397	0.00154	-1.27736	> 0.05	-1.04801	> 0.05	-0.87489	> 0.05
	EAC00722	2.01691	0.00608	2.23755	0.00243	0.55014	> 0.05	0.76360	0.04626
	EAC00740	0.17921	> 0.05	1.02042	> 0.05	1.68405	0.02932	0.15486	> 0.05
	EAC00741	-0.18464	> 0.05	-1.78807	0.01149	-0.24508	> 0.05	0.53689	> 0.05
atp synthase e chain	EAC00748	-0.13539	> 0.05	-0.72262	> 0.05	-0.45496	> 0.05	-0.32608	0.02161
	EAC00751	0.21256	> 0.05	-2.21537	0.00601	-0.27567	> 0.05	0.25797	> 0.05
	EAC00742	-0.04308	> 0.05	2.25394	0.04475	0.98281	> 0.05	0.48012	> 0.05
	EAC00695	-2.08701	0.00568	-1.11559	> 0.05	-1.64287	0.02570	-1.71634	> 0.05
	EAC00792	-0.93914	0.03000	-1.22252	0.04916	-1.12100	> 0.05	0.12056	> 0.05
	EAC00756	1.41573	0.01922	0.97372	> 0.05	0.41645	> 0.05	0.78260	> 0.05
	EAC00765	-0.30458	> 0.05	-1.68366	0.04017	0.40232	> 0.05	0.30924	> 0.05

Supplementary material- Chapter VI

	EAC00767	-1.79559	0.03716	0.95326	> 0.05	-1.27281	> 0.05	-0.27054	> 0.05
	EAC00773	-1.89987	0.00181	-1.79051	0.00459	-0.50366	> 0.05	-1.10091	> 0.05
	EAC00780	1.08385	0.02063	0.33671	> 0.05	-0.26582	> 0.05	0.46306	0.01915
	EAC00784	-0.06725	> 0.05	-1.29015	> 0.05	0.10290	> 0.05	0.55030	0.03206
	EAC00785	-0.24703	> 0.05	-1.99147	0.01947	-1.07389	> 0.05	0.15866	> 0.05
	EAC00796	-0.60112	> 0.05	0.04973	> 0.05	-0.89858	0.04536	-0.89671	0.04112
	EAC00800	1.29892	0.00734	1.60195	0.00465	-0.05251	> 0.05	0.51315	0.02122
	EAC00806	0.49685	> 0.05	0.21451	> 0.05	2.05733	> 0.05	0.44491	0.01440
tpa: endonuclease-reverse transcriptase	EAC00816	2.17867	0.02309	1.93233	0.04264	0.99828	> 0.05	1.12265	> 0.05
	EAC00820	-0.10018	> 0.05	-1.49711	0.02655	-0.52331	> 0.05	0.08775	> 0.05
	EAC00821	1.03570	0.02406	1.49618	0.00624	0.49579	> 0.05	0.71851	0.00500
	EAC00824	-0.92720	0.04859	0.31156	> 0.05	-0.70031	> 0.05	-1.13843	> 0.05
	EAC00827	-0.18790	> 0.05	-1.62316	0.02641	-0.80618	> 0.05	-0.19785	> 0.05
elongation factor 1 alpha	EAC00829	2.06057	0.00436	2.63952	0.00187	1.15485	> 0.05	1.84155	0.00232
	EAC00830	1.57660	0.00387	0.36085	> 0.05	1.33040	0.01365	0.52703	> 0.05
	EAC00840	1.88075	0.01289	1.51547	0.04308	0.52899	> 0.05	1.09132	> 0.05
	EAC00846	-3.15572	0.00021	-2.87426	0.00348	-0.42265	> 0.05	-1.28230	> 0.05
	EAC00848	-2.73888	0.02455	-0.67286	> 0.05	-0.61621	> 0.05	-3.04093	> 0.05
	EAC00852	-0.97497	> 0.05	-1.72443	0.02331	-1.60725	0.02443	-1.15219	> 0.05
	EAC00862	1.61523	0.00287	1.93762	0.00195	0.38209	> 0.05	0.94894	0.01261
	EAC00870	0.04888	> 0.05	3.71329	0.00058	0.54209	> 0.05	0.14881	> 0.05
	EAC00875	-0.89225	> 0.05	-1.40737	0.04526	-1.25651	0.03714	-0.53660	> 0.05
btb poz domain-containing protein	EAC00881	-0.10152	> 0.05	2.26505	0.00463	0.36022	> 0.05	1.46872	> 0.05

Figure S1: Heat map of genes affected by AgNO₃ treatments, with gene annotation.

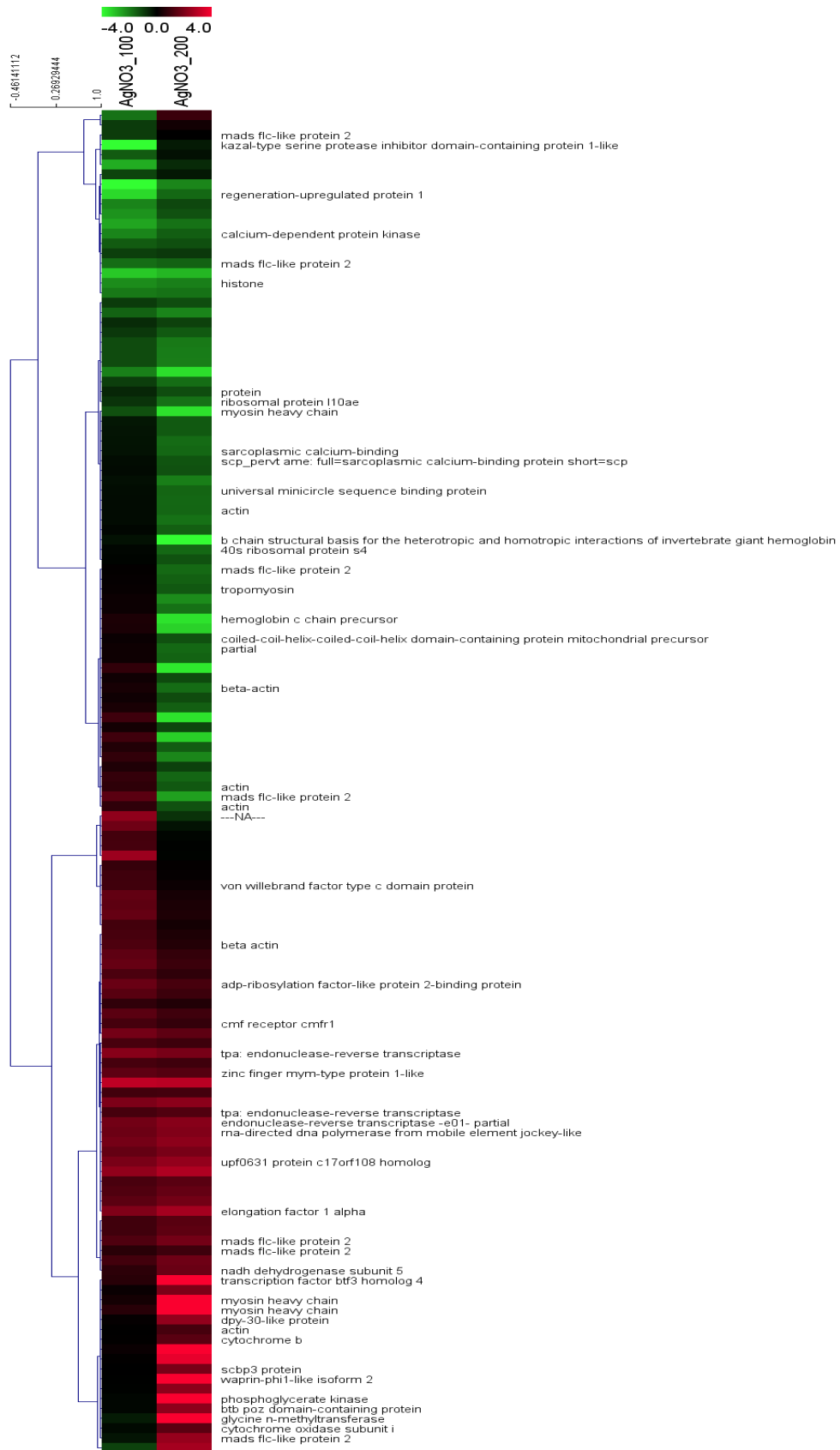
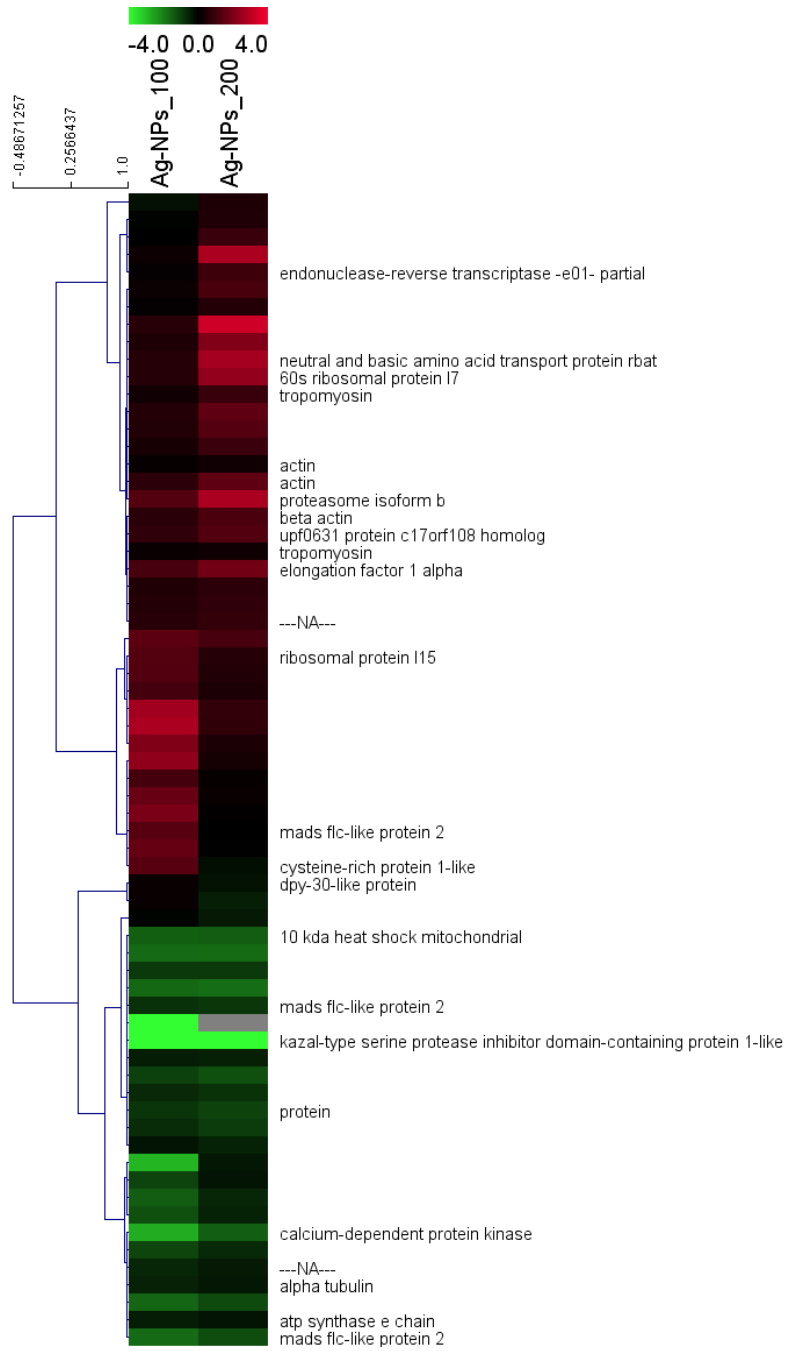


Figure S2: Heat map of genes affected by Ag-NPs treatments, with gene annotation.



Chapter VII

**Effects of silver nanoparticles to soil invertebrates:
oxidative stress biomarkers in *Eisenia fetida***

VII - Effects of silver nanoparticles to soil invertebrates: oxidative stress biomarkers in *Eisenia fetida*

Susana I.L. Gomes^a, Ditte Hansen^b, Janeck J. Scott-Fordsmand^b and

Mónica J.B. Amorim^a

^aDepartment of Biology & CESAM, University of Aveiro, 3810-193 Aveiro, Portugal

^bDepartment of Bioscience, Aarhus University, Vejlsovej 25, PO BOX 314, DK-8600 Silkeborg, Denmark

Abstract

Silver nanoparticles (Ag-NPs) are among the most produced NPs worldwide having several applications in consumer products. Ag-NPs are known to cause oxidative stress in several organisms and cell lines, however little information is available regarding their effects on soil invertebrates. The purpose of this study was to investigate if Ag-NPs cause oxidative stress on soil invertebrates. The model soil species *Eisenia fetida* was used. Our results showed that glutathione is the first mechanism triggered by Ag-NPs, followed by CAT, GPx and GR, however oxidative damage was observed for higher doses and exposure time (increased LPO). AgNO₃ exposure caused impairment in GPx and GST, probably as result of the higher bioavailability of Ag in the salt-form. The current results indicate that effects are partly caused by Ag ions released from Ag-NPs, but NPs specific effects cannot be excluded.

Keywords: earthworms; soil; nanomaterials; Reactive Oxygen Species (ROS)

1. Introduction

Exposure to silver nanomaterials (Ag-NPs) is known to induce the production of Reactive Oxygen Species (ROS) as reported in several studies (e.g. (Ahamed et al., 2010; Hayashi et al., 2012; Levard et al., 2012; Piao et al., 2011; Tsyusko et al., 2012)). That Ag-NPs are oxidized to Ag⁺ is known, however, it is still not fully clear if the ROS effects can be attributed to the Ag⁺ released from the Ag-NPs or to which extent the NPs form plays a role (e.g. (Fabrega et al., 2009; Miao et al., 2009; Sotiriou and Pratsinis, 2010)). The induction of oxidative stress following Ag-NPs is the main focus of the following study. That such responses are time dependent is well known see e.g. by (Gomes et al., 2012; Novais et al., 2011; Tsyusko et al., 2012), hence two different exposure durations (within the limits of standard ecotox soils tests) were included in this study.

Most living organisms have developed antioxidant defense mechanisms, aiming to balance the naturally formed ROS (Valavanidis et al., 2006). This mechanism includes enzymes such as superoxide dismutase (SOD), catalase (CAT), and glutathione peroxidase (GPx) which are directly involved in ROS removal; the glutathione-S-transferase (GST) and glutathione reductase (GR) participate in the glutathione antioxidant activity through conjugation with xenobiotics (GST) and through its recycling process (GR). Additional protective mechanisms include the metallothioneins (MT), metal binding proteins, which act as a chelating agent for the excess of metals and hence help to prevent oxidative stress in cells (Andrews, 2000).

The above described mechanisms are present in *Eisenia* earthworms species (e.g. Saint-Denis et al., 1998; Saint-Denis et al., 2001). *Eisenia fetida* are present in a variety of soils worldwide (Rombke et al., 2005) and have been used for long in ecotoxicology

studies (OCDE, 1984; OECD, 2004) constituting an excellent model to study NPs exposure (Gottschalk et al., 2009) .

In the present study we aimed to investigate the oxidative stress effect of Ag-NPs on the earthworm *Eisenia fetida*. The Ag-salt AgNO₃ was used for comparison purposes, two exposure durations were used: 4 and 28 days. The evaluated markers were: lipid peroxidation (LPO), total glutathione (TG), SOD, CAT, GPx, GST, GR and MT.

2. Materials and methods

2.1. Test species

The test organism was *Eisenia fetida* (Savigny, 1826), a soil earthworm. The cultures were obtained from ECT Oekotoxikologie GmbH, Germany, with a density of 500 adult worms per 5 kg of soil. Prior to the test start the worms were acclimated during one week in a mixture of garden soil and the test soil (Organization for Economic Cooperation and Development – OECD artificial soil) in equal parts, and then transferred to test soil for four weeks. Culture and test were kept at 20±1 °C with a 12h light:dark cycle. Cultures were fed on cow manure. The initial mass of the test individuals' ranged from 300 to 600 mg (OECD, 2004) ensuring similar average weight for all replicates.

2.2. Test soil and spiking procedure

OECD artificial soil (OCDE, 1984) was used, using 7% sphagnum peat (dried at 105 °C), 20% kaolin clay (Borup Kemi IS), 72.725% sand (sand n. 13, Dansand) and 0.275% CaCO₃ (99% purity, Merck) was used to adjust pH to 6 ±0.5.

Spiking of the soil with Ag-NPs followed the OECD recommendation for testing of insoluble substances (OECD, 2004). In short, 10 g of sand per replicate were mixed with the corresponding amount of Ag-NPs (as dry powder) to obtain the final

concentration range. The spiked sand was added to the remaining pre-moistened soil (540 g moist with 12.5% v/w distilled water) and homogeneously mixed. After that 12.5 % (v/w) of distilled water was added to each replicate, to reach the 50% of the WHC (Water Holding Capacity).

AgNO₃ was spiked to pre-moistened soil (540 g moist with 12.5% v/w distilled water) as aqueous solution and homogeneously mixed.

The spiking of the soil was done individually per replicate, for both Ag-NPs and AgNO₃ to ensure equal total amounts per replicate.

2.3. Experimental setup

Soil was spiked to obtain the following concentration range for AgNO₃: 0, 25, 50, 75, 100 and 200 mg Ag/kg soil (DW – dry weight) and for Ag-NPs: 0, 100, 300, 600, 900 and 1500 mg Ag/kg soil (DW). The concentrations range was based on effects on survival and reproductive output i.e. (i) for AgNO₃ the LC₅₀ was 65 mg Ag/Kg dry soil and for Ag-NPs the LC₅₀ was above 1500 mg Ag/kg dry soil, and (ii) for AgNO₃ the EC₅₀ was 15 mg Ag/kg dry soil and for the Ag-NPs was 1012 mg Ag/kg dry soil (Hansen, 2010).

The concentrations were selected based on previous range-finding results. Four replicates were used. Each replicate consisted of 10 adult worms per test containers (11cm ø x 12cm, covered with perforated lid) with in 500g test soil (white plastic buckets with a. Weekly, food was supplied (cow manure, 13 g/rep) and water loss was replenished.

For biochemical analysis, 2 organisms from each replicate were collected after 4 and 28 days of exposure. Worms were rinsed in distilled water to remove soil particles and snap frozen in liquid nitrogen as individual organisms, resulting in 8 replicates per test condition. Samples were stored at -80 °C until further analysis.

2.4. Test chemicals and characterization

The uncoated silver nanoparticles were purchased from NanoAmor, in house measurements showed a TEM (n=100) size of 49 ± 8 nm (with a tendency to agglomeration), a DLS of 155 nm, 120 nm as z-average, with PDI of 0.4, and a purity of 99.9%. The silver nitrate (crystalline extra pure) was purchased from Fluka.

2.5. Biochemical analysis

Each sample (individual organisms) was homogenized in 0.1 M K-Phosphate buffer, pH 7.4 in a proportion of 1:15 (mass:volume). Part of the tissue homogenate (150 μ L) was separated into a microtube with 2.5 μ L BHT (2,6-di-tert-butyl-4-methylphenol) 4% in methanol for lipid peroxidation (LPO) determination. The remaining tissue homogenate of each sample was centrifuged at 10000g during 20 min at 4°C, to isolate the Post-Mitochondrial Supernatant (PMS). The PMS was divided into several microtubes and stored at -80°C, for posterior analysis of biomarkers and protein quantification.

The extent of LPO was measured as thiobarbituric acid-reactive substances (TBARS) at 535nm (Bird and Draper, 1984; Ohkawa et al., 1979). In short, the sample separated for LPO measurement was incubated in 0.23 M TCA (Trichloroacetic acid), 16 mM Tris-HCl with 26 μ M DTPA (diethylene triamine pentaacetic acid), and 16mM TBA (thiobarbituric acid), at 100 °C during 60 min. The samples were centrifuged during 5 min at 115000 rpm, and the supernatant absorbance read at 535 nm.

Superoxide Dismutase (SOD) activity was determined by the photochemical inhibition of NBT (nitroblue tetrazolium) measured at 560nm (Giannopolitis and Ries, 1977). The reaction mixture consists of enzyme extracts (PMS), 50 mM K-Phosphate pH 7.8, 0.1 M EDTA (ethylenediaminetetraacetic acid disodium salt), 13 mM L-methionine, 50 mM sodium carbonate, 63 μ M NBT and 2 μ M riboflavin.

Catalase (CAT) activity was measured following the decrease in absorbance at 240nm due to H₂O₂ (substrate) decomposition (Clairborne, 1985). The reaction mixture consists of enzyme extracts (PMS), 50 mM K-Phosphate pH 7.0 and 15 mM H₂O₂.

Glutathione Peroxidase (GPx) activity was determined following the oxidation of NADPH (β -Nicotinamide adenine dinucleotide 2'-phosphate reduced tetrasodium salt), at 340nm, when GSSG (oxidized glutathione) is reduced back to GSH (reduced glutathione) by glutathione reductase (GR), using H₂O₂ as substrate (Mohandas et al., 1984). The reaction mixture consists of PMS, 50 mM K-Phosphate pH 7.0, 0.8 mM EDTA, 0.8 mM sodium azide, 0.13 U/ml GR (50 μ l per sample), 0.2 M GSH, 40 μ M NADPH and 5 μ M H₂O₂.

Glutathione Reductase (GR) activity was measured assessing the decrease of NADPH level, at 340nm (Cribb et al., 1989). The reaction mixture contains PMS, 50 mM K-Phosphate pH 7.0, 0.2 mM NADPH, 0.1 mM GSSG and 0.5 M DTPA.

Glutathione S-Transferase (GST) activity was measured at 340nm, following the conjugation of GSH with CDNB (2,4-dinitrochlorobenzene) (the substrate with the broadest range of GST isozymes detectability) (Habig et al., 1974). The reaction mixture consists of 0.7 mg/ml protein (PMS), 0.1M K-Phosphate pH 6.5, 1 mM GSH and 170 μ M CDNB.

Total glutathione (TG) was measured at 412 nm, using the recycling reaction of reduced glutathione (GSH) with DTNB in the presence of GR excess (Baker et al., 1990; Tietze, 1969), 200 μ l of PMS was incubated with 200 μ l of 12% TCA (1 hour at 4°C) and centrifuged 10000 g during 5 min to precipitate macromolecules (e.g. proteins, DNA and RNA). The resulting supernatant was used in the reaction mixture, with 0.1 M Na-K-Phosphate pH 8.0, 0.1 mM NADPH, 2 mM DTNB and 2.4 U/ml GR (15 μ l per sample).

The activity of metallothionein (MT) was measured by the method described by Viarengo et al. (1997). 95% of ethanol containing 8% chloroform was added to the 500 μ l of PMS, followed by a centrifugation step at 6000 g during 10 min at 4 °C. To 500 μ l of the supernatant obtained, the following was added: 50 μ l RNA, 10 ml hydrogen chloride (6 M HCl) and 1.2 ml of cold ethanol and frozen for 25 min at -80 °C. After centrifuging at 6000 g during 1 min., the pellet was re-suspended with 300 ml 87% ethanol and 1% chloroform. After new centrifugation step (6000 g for 1 min) the supernatant was removed and the pellet was re-suspended in 150 μ l 0.25 M NaCl and 150 μ l 0.2 M HCl containing 4 mM EDTA. Ellman's reagent (containing 0.4 mM DTNB, 2 M HCl and 0.2 M K-Phosphate pH 8.0) was added and absorbance read at 412 nm after 5 min. 1mM of GSH in 0.1 M HCl was used as standard and the amount of MT was calculated as GSH equivalent in nmol/mg protein.

Protein concentration was assayed using the Bradford method (Bradford, 1976), adapted from BioRad's Bradford micro-assay set up in a 96 well flat bottom plate, using bovine γ -globuline as a standard.

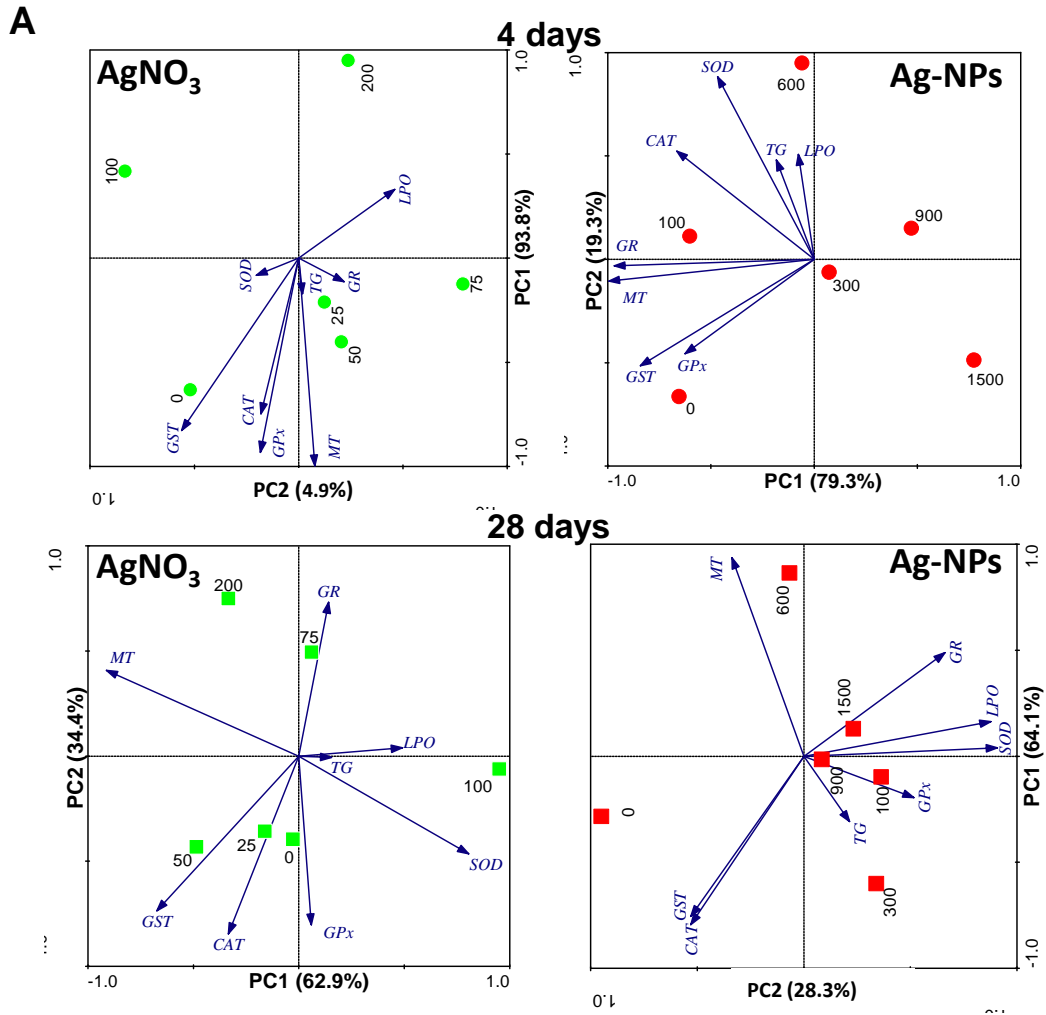
1.6. Data analysis

Univariate one-way ANOVA was used to compare means between treatments followed by Dunnett's test ($p < 0.05$) to discriminate differences from the control group. The analysis was done individually for each chemical (AgNO_3 or Ag-NPs) and time of exposure (4 days or 4 weeks) using SigmaPlot 11.0 (Systat Software, San Jose, CA).

Multivariate Principal Component Analysis (PCA) was performed to include all treatments and explore the relationship between them. To identify the general patterns, the PCA was applied on the average of each biochemical parameter for each treatment, using the covariance matrix [Using individual replicates (as oppose to averages) yielded similar results]. The analysis was performed using the software CANOCO 4.5.

3. Results

Results from the PCA are displayed in figure 1 (A-E), depending on which variables were included.



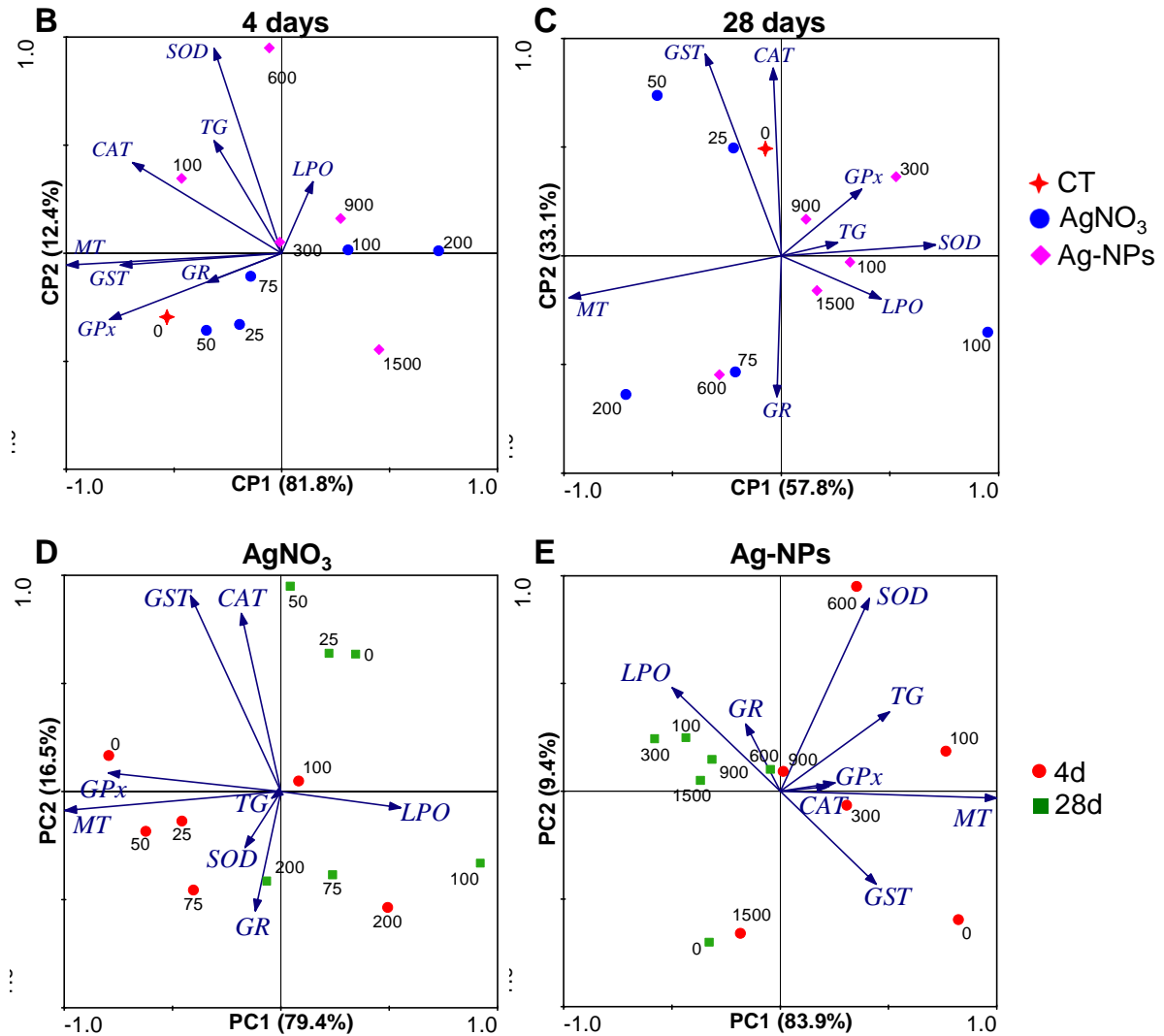
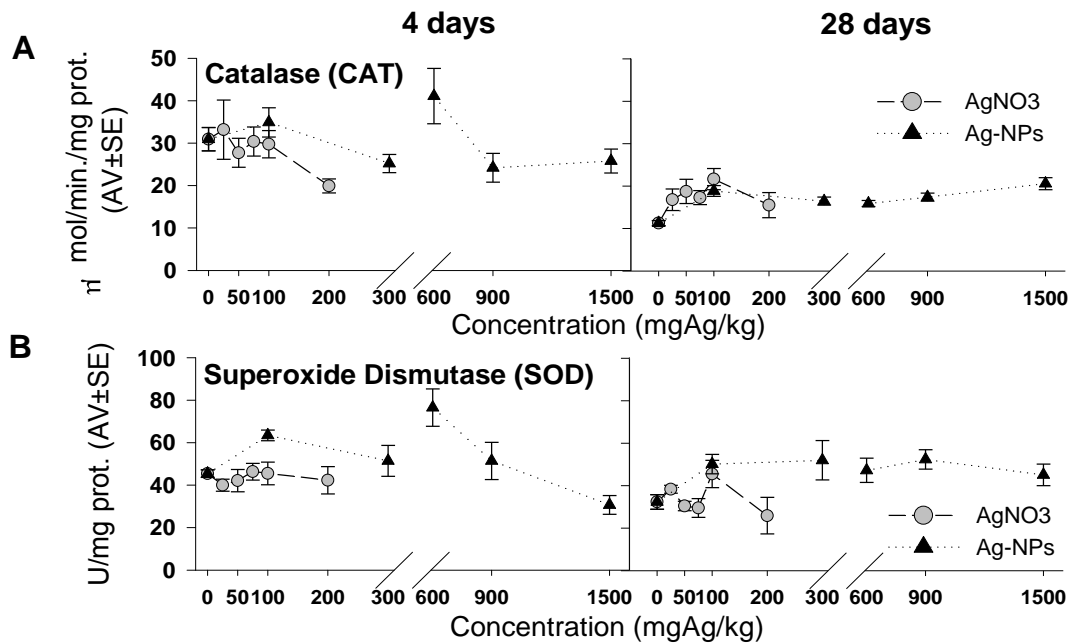


Figure 1: Biplot of the first two components of Principal Component Analysis (PCA) including all measured markers (CAT, SOD, GPx, GST, GR, TG, MT and LPO) for *Eisenia fetida* exposed to Ag (AgNO₃: 0-25-50-75-100-200 mg/kg and Ag-NPs: 0-100-300-600-1000-1500 mg/kg) during 4 and 28 days. A) All treatments, B) 4 days (4d) of exposure and C) 28 days (28d) of exposure D) AgNO₃ treatments, E) Ag-NPs treatments.

Results showed that response varied with exposure duration, mainly for CAT, GR, GPx and MT. Figure 1A shows that LPO increase is related to the highest exposure concentrations for both AgNO₃ and Ag-NPs at longer exposure time of 28 days, whereas for the 4 day exposure this is mainly the case for AgNO₃. GR is also changing

with time, from being mainly related to lower concentrations after 4 days to being associated with higher concentrations after 4 weeks. When analysing data per exposure time (fig. 1 B and C), the 28 days exposure no longer shows LPO as the single effect and indicates the important contribution of SOD, CAT, GST, MT and GR. No full discrimination between the two Ag forms, although Ag-NPs seem to be less scattered. PCA per Ag form (fig. 1 D and E) show commonalities, e.g., increased LPO levels associated with the higher concentrations and exposure time. Distinct patterns can also be seen, for instance GST and CAT increases are associated with the lower concentrations of AgNO₃ at 28 days of exposure, and to 4 days of exposure in Ag-NPs exposure. Results obtained for each measured marker can be depicted in figure 2, showing the comparison between Ag forms at each exposure time. Please note that the x axis was broke to visualise differences between concentration ranges.



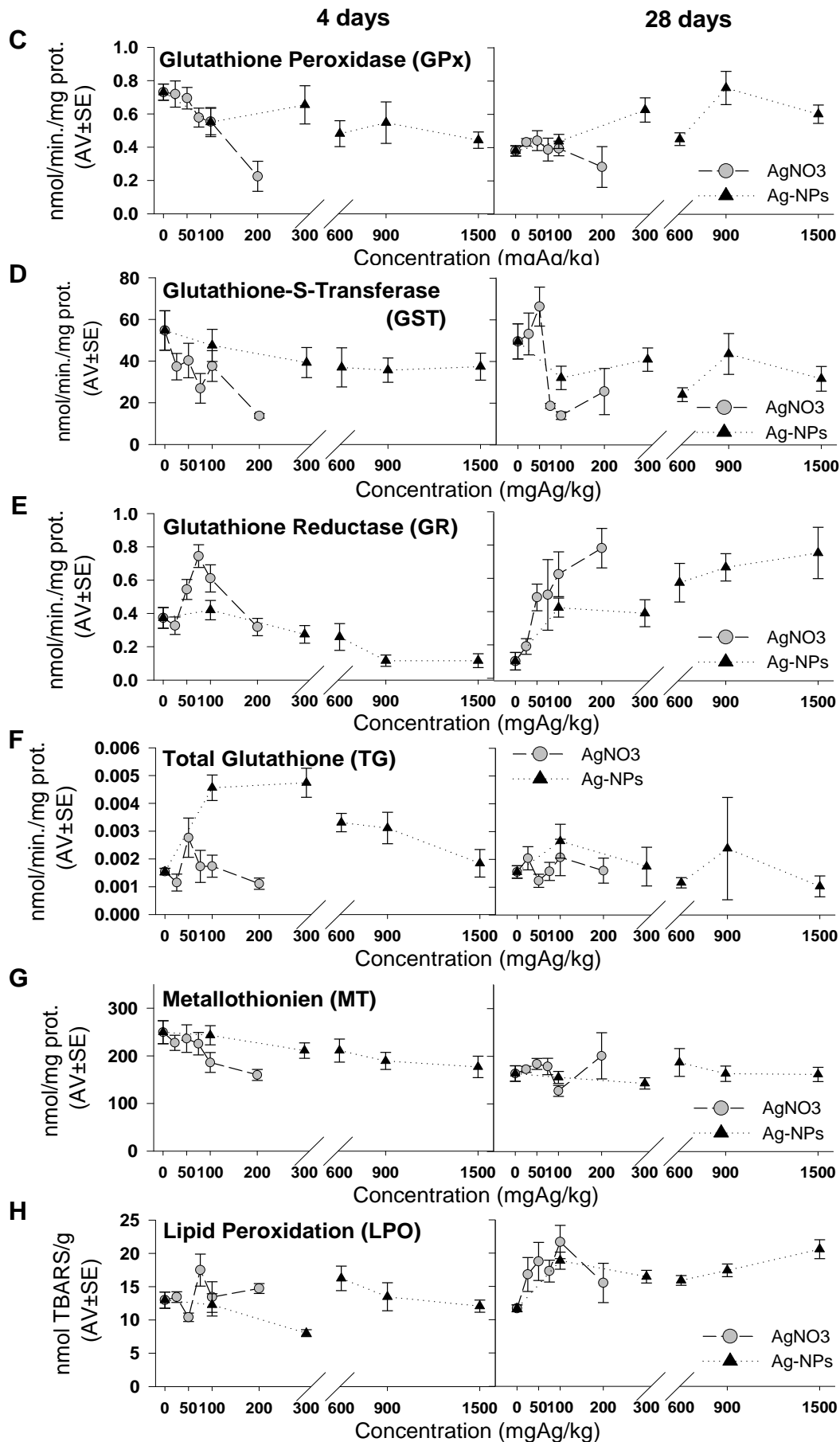


Figure 2: Results of Catalase (A), Superoxide Dismutase (B), Glutathione Peroxidase (C), Glutathione-S-Transferase (D), Glutathione Reductase (E), Total Glutathione (F), Metallothionein (G) and Lipid Peroxidation (H) levels, measured in *Eisenia fetida* after exposure to the respective concentration range of silver nitrate (AgNO₃) and silver nanoparticles (Ag-NPs), during 4 and 28 days. Data are expressed as mean values ± standard error (AV±SE).

In terms of individual results, for Ag-NPs, 4 days of exposure caused an increase in TG levels in the lower concentrations tested (100, 300 and 600 mg/kg) and the inhibition of GR activity in the higher concentrations (900 and 1500 mg/kg). For longer term exposure (28 days) CAT, GPx and GR activities were induced (fig. 2 A, C and E). Further, LPO levels were increased in all tested concentrations. GST, SOD and MT levels were not significantly affected by Ag-NPs exposure.

For AgNO₃ exposure (4 days), effects were more pronounced by an increase in GR activity in the intermediate concentrations (75 and 100 mg/kg), and seemed dose-related at 28 days, with significant increase above 75 mg/kg. Both GST and GPx were inhibited at the highest concentration (200 mg/kg). CAT, SOD, TG and MT levels were not significantly affected by AgNO₃ exposure. LPO levels increased (not significantly).

4. Discussion

In general it seems that response to AgNO₃ start earlier than to Ag-NPs, which could be related to oxidation time. The toxicity of Ag-NPs as caused by Ag⁺ released has been proposed by some authors (e.g. (Miao et al., 2009; Xiu et al., 2012)), however Ag-NPs specific effects have also been described (e.g. (Fabrega et al., 2009)). Shoults-Wilson and co-authors (2011) reported a 11-14% Ag oxidation from Ag-NPs in OECD soil. If we assume that would be the case here, then 11-14% of Ag⁺ are released from Ag-NPs, hence the effects observed at 900 mg Ag-NPs/kg should correlate to the effects

observed between 100 and 200 mg Ag⁺/kg. However, for e.g. TG, GST and GPx this was not the case, indicating NPs specific effects. This paper will not venture further into the measures of potential release of Ag ions, since although relevant this is at present not possible to sufficiently detailed level in soils or soil organisms, nor is it known how this changes over time.

For short term Ag-NPs exposure (4 days), the changes in the TG (total glutathione) suggests that the earthworms are responding to the increased levels of ROS by glutathione antioxidant activity or by its role as co-factor for GST and GPx (Lushchak, 2012; Pompella et al., 2003). This indicates that glutathione can be the starting response mechanism to be activated by Ag-NPs. The increase in glutathione levels, following Ag-NPs exposure, was already observed in primary mouse fibroblast and liver cells (Arora et al., 2009) and in zebrafish liver (Choi et al., 2010)..

Comparatively, for AgNO₃ short term exposure, the inhibition of GPx and GST activities (at 200 mg/kg) and the increase in GR activity (at 75 and 100 mg/kg) were the most significant changes. This inhibition of GPx in response to silver ions was similar to observed direct interaction of silver ion on GPx as described by Splittgerber and Tappel (1979). Further, it is also similar to in vivo responses observed in several rat organs exposed to silver via food (Black et al., 1979). Hence, the high affinity of silver ions for thiol groups (e.g. (Levard et al., 2012)) inactivating the GPx and GST (cysteine rich proteins/enzymes) could explain our observations. Glutathione is also a cysteine rich protein which participates in metals chelation (Jozefczak et al., 2012); oxidized glutathione is reduced by GR (as previously explained), which activity was increased after AgNO₃ exposure. Hence, our results suggest that a fraction of the released Ag⁺ were chelated by glutathione and the remaining fraction caused the inhibition of antioxidant enzymes. This again means that lipid peroxidation may not be prevented.

Since a similar pattern for GPx and GST (after 4 days) was observed, this indicates that either Ag ions were released from the particles in sufficient amount to inhibit the proteins or that the Ag-NPs inhibited the enzymes directly e.g. by surface reactions.

After longer exposure period (28 days) the Ag-NPs caused an increase in CAT, GPx and GR activities. Both CAT and GPx participate in hydrogen peroxide (H₂O₂) removal; as GPx use glutathione as co-factor, the increase in GR activity is consistent with increase in glutathione recycling (GPx activity oxidizes glutathione which is reduced back by GR) which is an essential mechanism to keep normal glutathione levels in cells and in consequence to keep cell homeostasis (Jozefczak et al., 2012; Lushchak, 2012). CAT activity increase was observed in *Drosophila melanogaster* exposed to Ag-NPs through food (Ahamed et al., 2010) and together with increased SOD and lipid peroxidation, oxidative stress was suggested as mechanism of Ag-NPs toxicity. On the other hand Choi and co-authors (2010) propose that the decrease in CAT and GPx in the liver of zebra fish exposed to Ag-NPs end up in the accumulation of ROS and then causing lipid peroxidation. Our results indicate that CAT and GPx are responding to an increase in H₂O₂ production, however their activities were not enough to prevent oxidative damage (observed in increased LPO levels) (Fig. 1 H).

The longer exposure to AgNO₃ caused less change in the antioxidant enzymes. The reason for this might be related with the high level of stress/damage caused by the concentrations tested which could lead to the collapse/impairment of the antioxidant defense mechanism (note that AgNO₃ EC₅₀≈15 and LC₅₀≈65 mg Ag/kg (Hansen, 2010). Similar to observations by e.g. Park and co-authors (2009) who observed an induction of ROS at lower (0.01-0.1 mg Ag⁺/L) exposure concentration but none at higher (0.05 mg Ag⁺/L) Ag⁺ exposure concentrations (measured through superoxide-sensor protein

in reporter strains of bacteria). Furthermore, they also observed, as we did in our study, that the ROS activity was higher for the shorter tested period (50 min.) compared longer periods (100 min.).

Overall, LPO occurred for longer exposure (28 days) to similar extent for AgNO₃ and Ag-NPs, at 100mg/kg and 1500/kg respectively, but was already occurring after 4 days for AgNO₃ exposure.

Overall our results are in agreement with current literature, which propose oxidative stress as a mechanism of toxicity of Ag-NPs and Ag-salt (e.g. (Choi et al., 2010; Hussain et al., 2005; Tsyusko et al., 2012) found for other organisms. A direct comparison with other soil invertebrates cannot be made since our study seems to be the first performed in soil invertebrates. In our study, we observed that total glutathione rapidly respond (at 4 days of exposure) to Ag-NPs, followed by CAT, GPx and GR (at 28 days). AgNO₃ exposure causes the depletion of GPx and GST indicating an impairment of the antioxidant defense system. Both Ag forms cause an increase in LPO after 28 days of exposure, showing that oxidative damage is occurring.

5. Conclusions

Both Ag forms induced significant changes in the anti-oxidant response system of the worm *Eisenia fetida* being time dependent. For Ag-NPs total glutathione was the first defense mechanism to be activated (at 4 days), followed by CAT, GPx and GR (at 28 days). For AgNO₃ GPx and GST were first inhibited, indicating the impairment of the anti-oxidant defense system in a shorter-time of exposure, probably due to the high effect on survival and reproduction of the concentrations. Even though anti-oxidant system was activated, it was not enough to prevent oxidative damage (LPO).

Overall our results indicate that Ag ions as released from Ag-NPs cannot fully explain the results obtained, indicating NPs specific effects.

Acknowledgements

This work was supported by funding FEDER through COMPETE Programa Operacional Factores de Competitividade, and by National funding through FCT-Fundac, ão para a Ciênciã e Tecnologia, within the research project NANOkA FCOMP-01-0124- FEDER-008944 (Ref. FCT PTDC/BIA-BEC/103716/2008), through an FCT PhD grant to Susana Gomes (SFRH/BD/63261/2009) and by the EU-FP7 MARINA (Ref. 263215). The authors thank Wiebke Schmidt and Rhaul de Oliveira for the help provided in the optimization of MT and SOD protocols, respectively.

References

- Ahamed, M., Posgai, R., Gorey, T.J., Nielsen, M., Hussain, S.M., Rowe, J.J., 2010. Silver nanoparticles induced heat shock protein 70, oxidative stress and apoptosis in *Drosophila melanogaster*. *Toxicology and Applied Pharmacology* 242, 263-269.
- Andrews, G.K., 2000. Regulation of metallothionein gene expression by oxidative stress and metal ions. *Biochemical Pharmacology* 59, 95-104.
- Arora, S., Jain, J., Rajwade, J.M., Paknikar, K.M., 2009. Interactions of silver nanoparticles with primary mouse fibroblasts and liver cells. *Toxicology and Applied Pharmacology* 236, 310-318.
- Baker, M.A., Cerniglia, G.J., Zaman, A., 1990. Microtiter Plate Assay for the Measurement of Glutathione and Glutathione Disulfide in Large Numbers of Biological Samples. *Analytical Biochemistry* 190, 360-365.
- Bird, R.P., Draper, H.H., 1984. Comparative Studies on Different Methods of Malonaldehyde Determination. *Methods in Enzymology* 105, 299-305.

- Black, R.S., Whanger, P.D., Tripp, M.J., 1979. Influence of silver, mercury, lead, cadmium, and selenium on glutathione peroxidase and transferase activities in rats. *Biol Trace Elem Res* 1, 313-324.
- Bradford, M.M., 1976. Rapid and Sensitive Method for Quantitation of Microgram Quantities of Protein Utilizing Principle of Protein-Dye Binding. *Analytical Biochemistry* 72, 248-254.
- Choi, J.E., Kim, S., Ahn, J.H., Youn, P., Kang, J.S., Park, K., Yi, J., Ryu, D.Y., 2010. Induction of oxidative stress and apoptosis by silver nanoparticles in the liver of adult zebrafish. *Aquatic Toxicology* 100, 151-159.
- Clairborne, A., 1985. Catalase activity, Greenwald RA, editor. *CRC handbook of methods in oxygen radical research*. Boca Raton, FL: CRC press, 283-284.
- Cribb, A.E., Leeder, J.S., Spielberg, S.P., 1989. Use of a Microplate Reader in an Assay of Glutathione-Reductase Using 5,5'-Dithiobis(2-Nitrobenzoic Acid). *Analytical Biochemistry* 183, 195-196.
- Fabrega, J., Fawcett, S.R., Renshaw, J.C., Lead, J.R., 2009. Silver nanoparticle impact on bacterial growth: effect of pH, concentration, and organic matter. *Environmental Science & Technology* 43, 7285-7290.
- Giannopolitis, C.N., Ries, S.K., 1977. Superoxide Dismutases .1. Occurrence in Higher-Plants. *Plant Physiol* 59, 309-314.
- Gomes, S.I.L., Novais, S.C., Gravato, C., Guilhermino, L., Scott-Fordsmand, J.J., Soares, A.M.V.M., Amorim, M.J.B., 2012. Effect of Cu-nanoparticles versus one Cu-salt: analysis of stress and neuromuscular biomarkers response in *Enchytraeus albidus* (Oligochaeta). *Nanotoxicology* 6, 134-143.
- Gottschalk, F., Sonderer, T., Scholz, R.W., Nowack, B., 2009. Modeled Environmental Concentrations of Engineered Nanomaterials (TiO₂, ZnO, Ag, CNT, Fullerenes) for Different Regions. *Environmental Science & Technology* 43, 9216-9222.

- Habig, W.H., Pabst, M.J., Jakoby, W.B., 1974. Glutathione S-Transferases - First Enzymatic Step in Mercapturic Acid Formation. *Journal of Biological Chemistry* 249, 7130-7139.
- Hansen, D., 2010. Uptake, distribution and effects of silver nanoparticles on the earthworm *Eisenia fetida*. Master thesis supervised by Janeck J. Scott-Fordsmand and Bernd Nowack. DMU, Silkeborg, Denmark.
- Hayashi, Y., Engelmann, P., Foldbjerg, R., Szabo, M., Somogyi, I., Pollak, E., Molnar, L., Autrup, H., Sutherland, D.S., Scott-Fordsmand, J., Heckmann, L.H., 2012. Earthworms and Humans in Vitro: Characterizing Evolutionarily Conserved Stress and Immune Responses to Silver Nanoparticles. *Environmental Science & Technology* 46, 4166-4173.
- Hussain, S.M., Hess, K.L., Gearhart, J.M., Geiss, K.T., Schlager, J.J., 2005. In vitro toxicity of nanoparticles in BRL 3A rat liver cells. *Toxicology in Vitro* 19, 975-983.
- Jozefczak, M., Remans, T., Vangronsveld, J., Cuypers, A., 2012. Glutathione Is a Key Player in Metal-Induced Oxidative Stress Defenses. *Int J Mol Sci* 13, 3145-3175.
- Levard, C., Hotze, E.M., Lowry, G.V., Brown, G.E., 2012. Environmental Transformations of Silver Nanoparticles: Impact on Stability and Toxicity. *Environmental Science & Technology* 46, 6900-6914.
- Lushchak, V.I., 2012. Glutathione homeostasis and functions: potential targets for medical interventions. *J Amino Acids* 2012, 736837.
- Miao, A.J., Schwehr, K.A., Xu, C., Zhang, S.J., Luo, Z., Quigg, A., Santschi, P.H., 2009. The algal toxicity of silver engineered nanoparticles and detoxification by exopolymeric substances. *Environmental Pollution* 157, 3034-3041.
- Mohandas, J., Marshall, J.J., Duggin, G.G., Horvath, J.S., Tiller, D.J., 1984. Differential Distribution of Glutathione and Glutathione-Related Enzymes in Rabbit Kidney - Possible Implications in Analgesic Nephropathy. *Biochemical Pharmacology* 33, 1801-1807.

- Novais, S.C., Gomes, S.I.L., Gravato, C., Guilhermino, L., De Coen, W., Soares, A.M.V.M., Amorim, M.J.B., 2011. Reproduction and biochemical responses in *Enchytraeus albidus* (Oligochaeta) to zinc or cadmium exposures. *Environmental Pollution* 159, 1836-1843.
- OECD, 1984. Guideline for Testing Chemicals. Earthworm, acute toxicity tests, No.207, OCDE (Organization for Economic Cooperation and Development). Paris, France.
- OECD, 2004. Guidelines for the testing of chemicals No. 222. Earthworm Reproduction Test (*Eisenia fetida/ Eisenia andrei*). Organization for Economic Cooperation and Development. Paris.
- Ohkawa, H., Ohishi, N., Yagi, K., 1979. Assay for Lipid Peroxides in Animal-Tissues by Thiobarbituric Acid Reaction. *Analytical Biochemistry* 95, 351-358.
- Park, H.J., Kim, J.Y., Kim, J., Lee, J.H., Hahn, J.S., Gu, M.B., Yoon, J., 2009. Silver-ion-mediated reactive oxygen species generation affecting bactericidal activity. *Water Res* 43, 1027-1032.
- Piao, M.J., Kang, K.A., Lee, I.K., Kim, H.S., Kim, S., Choi, J.Y., Choi, J., Hyun, J.W., 2011. Silver nanoparticles induce oxidative cell damage in human liver cells through inhibition of reduced glutathione and induction of mitochondria-involved apoptosis. *Toxicology Letters* 201, 92-100.
- Pompella, A., Visvikis, A., Paolicchi, A., De Tata, V., Casini, A.F., 2003. The changing faces of glutathione, a cellular protagonist. *Biochemical Pharmacology* 66, 1499-1503.
- Rombke, J., Jansch, S., Didden, W., 2005. The use of earthworms in ecological soil classification and assessment concepts. *Ecotoxicology and Environmental Safety* 62, 249-265.
- Saint-Denis, M., Labrot, F., Narbonne, J.F., Ribera, D., 1998. Glutathione, glutathione-related enzymes, and catalase activities in the earthworm *Eisenia fetida andrei*. *Archives of Environmental Contamination and Toxicology* 35, 602-614.

- Saint-Denis, M., Narbonne, J.F., Arnaud, C., Ribera, D., 2001. Biochemical responses of the earthworm *Eisenia fetida andrei* exposed to contaminated artificial soil: effects of lead acetate. *Soil Biology & Biochemistry* 33, 395-404.
- Shoults-Wilson, W.A., Reinsch, B.C., Tsyusko, O.V., Bertsch, P.M., Lowry, G.V., Unrine, J.M., 2011. Effect of silver nanoparticle surface coating on bioaccumulation and reproductive toxicity in earthworms (*Eisenia fetida*). *Nanotoxicology* 5, 432-444.
- SigmaPlot11.0, Copyright © 2009 Systat Software Inc.
- Sotiriou, G.A., Pratsinis, S.E., 2010. Antibacterial Activity of Nanosilver Ions and Particles. *Environmental Science & Technology* 44, 5649-5654.
- Splittgerber, A.G., Tappel, A.L., 1979. Inhibition of glutathione peroxidase by cadmium and other metal ions. *Arch Biochem Biophys* 197, 534-542.
- Tietze, F., 1969. Enzymic Method for Quantitative Determination of Nanogram Amounts of Total and Oxidized Glutathione - Applications to Mammalian Blood and Other Tissues. *Analytical Biochemistry* 27, 502-522.
- Tsyusko, O.V., Hardas, S.S., Shoults-Wilson, W.A., Starnes, C.P., Joice, G., Butterfield, D.A., Unrine, J.M., 2012. Short-term molecular-level effects of silver nanoparticle exposure on the earthworm, *Eisenia fetida*. *Environmental Pollution* 171, 249-255.
- Valavanidis, A., Vlahogianni, T., Dassenakis, M., Scoullou, M., 2006. Molecular biomarkers of oxidative stress in aquatic organisms in relation to toxic environmental pollutants. *Ecotoxicology and Environmental Safety* 64, 178-189.
- Viarengo, A., Ponzano, E., Dondero, F., Fabbri, R., 1997. A simple spectrophotometric method for metallothionein evaluation in marine organisms: An application to Mediterranean and Antarctic molluscs. *Marine Environmental Research* 44, 69-84.
- Xiu, Z.M., Zhang, Q.B., Puppala, H.L., Colvin, V.L., Alvarez, P.J.J., 2012. Negligible Particle-Specific Antibacterial Activity of Silver Nanoparticles. *Nano Letters* 12, 4271-4275.

Chapter VIII

**Exposure to different silver nanoparticles forms and
silver salt: gene expression profile in
*Enchytraeus crypticus***

VIII - Exposure to different silver nanoparticles forms and silver salt: gene expression profile in *Enchytraeus crypticus*

Susana I.L. Gomes^a, Janeck J. Scott-Fordsmand^b and Mónica J.B. Amorim^a

^aDepartment of Biology & CESAM, University of Aveiro, 3810-193 Aveiro, Portugal

^bDepartment of Bioscience, Aarhus University, Vejlsovej 25, PO BOX 314, DK-8600 Silkeborg, Denmark

Abstract

The effect of nanomaterials (NMs) is less understood in light of the implemented and existing methodologies for regular chemicals. To understand the mode of action of NMs is one of the alternatives to improve predictions and environmental risk assessment (ERA). In the present work the high-throughput gene expression tool (4x44K microarray for *Enchytraeus crypticus*) was used to investigate the mechanisms activated by Ag NMs exposure. Three NMs (PVP coated, non-coated and dispersed 300K) were investigated together with AgNO₃. Overall the results showed that Ag 300K caused the most differentiated transcriptomic profile, whereas PVP-coated and non-coated Ag NMs were similar. Commonly affected across all Ag forms were the effects on cell cycle control associated with impairment of DNA repair mechanism. Evidences are that the mechanisms of response to Ag were different between materials; the differences in properties such as the dispersion rate of the materials seem to be of high importance.

Keywords: high-throughput; mechanisms of response; nanomaterials; soil; enchytraeids

1. Introduction

Silver nanoparticles (Ag-NPs) are among the most used nanomaterials (NMs) worldwide, with a median production of 55 tons/year (ranging from 5 to 1000 tons/year according to producers and downstream users) (Piccinno et al., 2012). Among the most explored applications of Ag-NMs are conductivity and antimicrobial activity (Piccinno et al., 2012), however, e.g. the properties that make Ag-NPs so effective as bactericides also cause toxicity to non-target organisms. Based on EC values (effect concentration) for several aquatic organisms (crustaceans, algae, fish), Ag-NPs were classified as extremely toxic to aquatic organisms and bacteria (Kahru and Dubourguier, 2010). Studies on soil invertebrates showed that Ag-NPs inhibit *Enchytraeus abidus* reproduction ($EC_{50} = 225$ mg/kg) (Gomes et al., 2013) and induce apoptosis in *Lumbricus terrestris* (effect at 100mg/kg for powder dispersed in water by sonication and 4 mg/kg for colloidal) (Lapied et al., 2010). For *Eisenia fetida* Heckman et al. (2011) showed that 1000 mg/kg caused no mortality, but caused 100% effect on reproduction, similar to Shoults-Wilson et al. (2011) who observed a significant reduction in reproduction at 770 mg/kg.

To understand the mechanisms that underlie the effects is important to ensure NMs environmental safety and sustainability. Studies using high-throughput tools such as gene expression microarray analysis can provide high content and quality information, exactly useful for identifying the mechanism of action. For example, the use of cellular/molecular techniques provided evidences that oxidative stress is a mechanism of Ag-NPs toxicity, i.e. inducing ROS (reactive oxygen species) formation (e.g. Chae et al., 2009; Hayashi et al., 2012; Piao et al., 2011). Gu et al. (2011) found that short exposure (120 min.) to Ag-NPs cause damage to membrane proteins and cell wall of *Saccharomyces cerevisiae*, and Gou et al. (Gou et al., 2010) reported oxidative stress,

cell membrane, and transportation damage in *Escherichia coli*. Several authors (Guo et al., 2013; 2009; Navarro et al., 2008; Sotiriou and Pratsinis, 2010) suggest that it is the Ag^+ released fraction that causes Ag-NPs cytotoxicity.

The aim of the present study is to investigate the toxicity mechanisms of Ag-NPs, using the available high-throughput tool for *Enchytraeus crypticus*, a 4x44K custom Agilent microarray (based on Castro-Ferreira et al., 2013). To do this a set of Ag materials was studied: 3 Ag-NPs (PVP coated, non-coated and Ag 300K being dispersed) and a silver salt (AgNO_3). For that, organisms were exposed to relevant reproduction effect concentrations (EC_{20} and EC_{50}) for 3 and 7 days.

2. Materials and Methods

2.1. Test organism

The test species *Enchytraeus crypticus* (Westheide and Graefe, 1992) was used. Individuals are cultured in Petri dishes containing agar medium, consisting of a sterilized mixture of four different salt solutions ($\text{CaCl}_2 \cdot 2\text{H}_2\text{O}$; MgSO_4 ; KCl ; NaHCO_3) and a Bacti-Agar medium (Oxoid, Agar No. 1). The cultures are kept under controlled conditions, at 19°C and photoperiod 16:8 hours light:dark. Animals are feed on ground and autoclaved oats twice a week.

2.2. Test materials and characterization

The Silver (Ag) tested, representing a set of varying properties, included one Ag-salt (AgNO_3) and three Ag nanomaterials (NMs), i.e. non-coated Ag-NPs (further referred as AgNC), PVP (Polyvinylpyrrolidone)-coated Ag-NPs (further referred as AgCoated) and dispersed Ag-NPs (Ag 300K). In addition, the dispersant was tested alone, the dispersant being 4% Polyoxyethylene Glycerol Triolaete and Polyoxyethylene (20 orbitan mono-Laurat (Tween 20), see Table 1.

Table 1: Summary information of the characteristics of the tested materials in terms of supplier, state, solubility, coating, nominal size (according to the supplier), size according to TEM (Transmission electron microscopy) measurements, purity and morphology. PVP: polyvinylpyrrolidone, w/w: wet weight.

	AgNO ₃	Ag-Nanomaterials			Dispersant
		Ag NC	Ag Coated	Ag 300K	
supplier	ACS (Merck)	AG-M-03M-NP.020N (American Elements)	AG-M-03M-NPCP.020N (American Elements)	JRC repository	JRC repository
state	powder	powder	powder	liquid	liquid
solubility	Water soluble	Not dispersed	Not dispersed	Dispersible	Soluble
coating	-	-	0.2% w/w PVP	-	-
nominal size (nm)	-	20-30	20-30	15	-
TEM (nm) (n=50)	-	26±4	25±5	17±8	-
purity	99.9%	99%	99%	10.2% w/w Ag	-
morphology		Spherical*	Spherical*	Spherical	-

*Agglomerates observed

2.3. Test soil and spiking procedure

The natural standard soil LUFA 2.2 (LUFA Speyer, Germany) was used. The main characteristics can be described as follows: pH (0.01 M CaCl₂) = 5.5, organic matter = 1.77%, CEC (cation exchange capacity) = 10.1%, WHC (water holding capacity) = 41.8% grain size distribution of 7.3% clay, 13.8% silt, and 78.9% sand.

Ag-NPs-NC and Ag-NPs-C were added to the soil as powder, following the OECD recommendations for the testing of non-soluble compounds (OECD, 2004). In short, the equivalent of 2 g of dry soil per test vessel was mixed with the quantity of the NMs, as dry powders, to obtain the corresponding concentration range. This fraction of spiked soil was added to the remaining pre-moistened soil and mixed manually during 10 min, being left to equilibrate for 3 days; after that deionised water was added to reach 50% of the soil WHC. The procedure was repeated for each replicate individually. AgNO₃ and Ag-NPs 300K, being soluble or dispersed respectively, were added to the pre moistened soil as aqueous dispersions and followed the same procedure as described. The concentrations tested were selected based on the reproduction effect concentrations EC₂₀ and EC₅₀ (see Table 2).

Table 2: Tested concentrations (values in mg/kg), based on the reproduction effect concentrations (within the confidence intervals (CI) for EC₂₀ and EC₅₀ estimates) (unpublished data). The dispersant was added to resemble the volume added with the Ag-NPs 300k spiking.

	control	EC ₂₀	EC ₅₀
AgNO ₃	0	45	60
Ag-NPs non-coated	0	380	430
Ag-NPs coated	0	380	550
Ag-NPs 300K	0	60	170
dispersant	0.6% v:v	-	-

A positive control was performed with the Ag 300K dispersant. The dispersant was added to resemble the volume added with the Ag 300K spiking. Four replicates per treatment were performed.

2.4. Exposure details

For the gene expression assay, exposure followed the same procedures as the standard ERT (OECD, 2004) with adaptations as follows: twenty adults with well-developed clitellum were introduced in each test vessel, containing 20g of moist soil (control or spiked). The organisms were exposed for 3 and 7 days under controlled conditions of photoperiod (16:8h light:dark) and temperature ($20\pm 1^\circ\text{C}$) without food. After the exposure period, the organisms were carefully removed from the soil, rinsed in deionised water and frozen in liquid nitrogen. The samples were stored at -80°C , until analysis.

2.5. RNA extraction, labelling and hybridizations

RNA was extracted from each replicate containing a pool of 20 animals. Three biological replicates per test treatment (including controls) were used. Total RNA was extracted using SV Total RNA Isolation System (Promega). The quantity and purity of the isolated RNA were measured spectrophotometrically with a nanodrop (NanoDrop ND-1000 Spectrophotometer) and its quality was checked on a denaturing formaldehyde agarose gel electrophoresis.

A single-colour design was used. In brief, 500 ng of total RNA was amplified and labelled with Agilent Low Input Quick Amp Labelling Kit (Agilent Technologies, Palo Alto, CA, USA). Positive controls were added with the Agilent one-colour RNA Spike-In Kit (Agilent Technologies, Palo Alto, CA, USA). Purification of the amplified and labelled cRNA was performed with the RNeasy columns (Qiagen, Valencia, CA, USA). The cRNA samples were hybridized on the Custom Gene Expression Agilent Microarrays (4 x 44k format) developed for this species (Castro-Ferreira et al., 2013). Hybridizations were performed using the Agilent Gene Expression Hybridization Kit

(Agilent Technologies, Palo Alto, CA, USA) and each biological replicate was individually hybridized on one array. The arrays were hybridized at 65°C with a rotation of 10 rpm, during 17h. After that the microarrays were washed using Agilent Gene Expression Wash Buffer Kit (Agilent Technologies, Palo Alto, CA, USA) and scanned with the Agilent DNA microarray scanner G2505B (Agilent Technologies).

2.6.Acquisition and microarray data analysis

Fluorescence intensity data was obtained with Feature Extraction (10.5.1.1) Software (Agilent Technologies). Quality control was done by inspecting the reports on the Agilent Spike-in control probes and by making box plots of each array. Processing of the data and statistical analysis were performed using RobiNA (v 1.2.4) (Lohse et al., 2012; Lohse et al., 2010) in the R environment (<http://www.R-project.org>). After background subtraction, data was normalized between arrays using Quantile normalization. Differential expression between control and treated samples was assessed using linear models and Benjamini–Hochberg's (BH) method to correct for multiple testing (Benjamini and Hochberg, 1995) (adjusted $p < 0.05$ was considered significant). Note that for the case of the Ag-NPs 300K the dispersant control was used to obtain the relative expressions, hence normalizing for the effect of the dispersant itself. The Minimum Information About a Microarray Experiment (MIAME) compliant data from this experiment will be submitted to the Gene Expression Omnibus (GEO) at the National Center for Biotechnology Information (NCBI) website.

Cluster analysis and PCA (principal component analysis) on differentially expressed genes was performed using MultiExperiment Viewer (MeV, TIGR). The differentially expressed genes for each treatment were analysed separately for GO (Gene Ontology) term enrichment analysis (Alexa et al., 2006) using the Blast2GO software.

3. Results

Exposure to the different Ag materials for 3 and 7 days resulted in a total of 3608 differentially expressed genes (DEGs) (out of 43750) in at least one test condition, see figure 1 (note the y scale was broke from 550 to 900 to improve visualization).

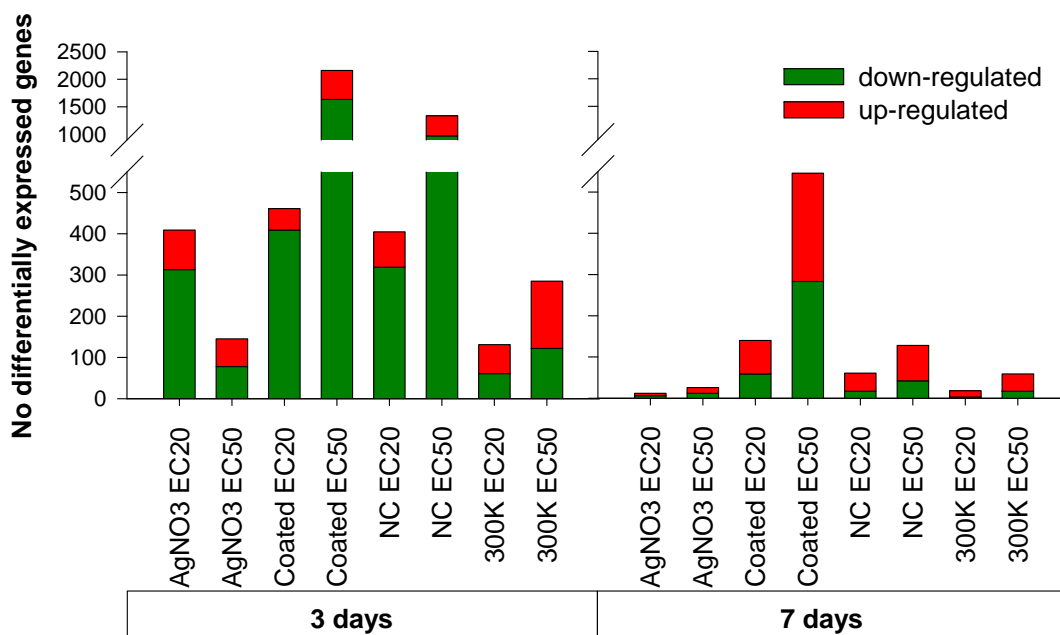
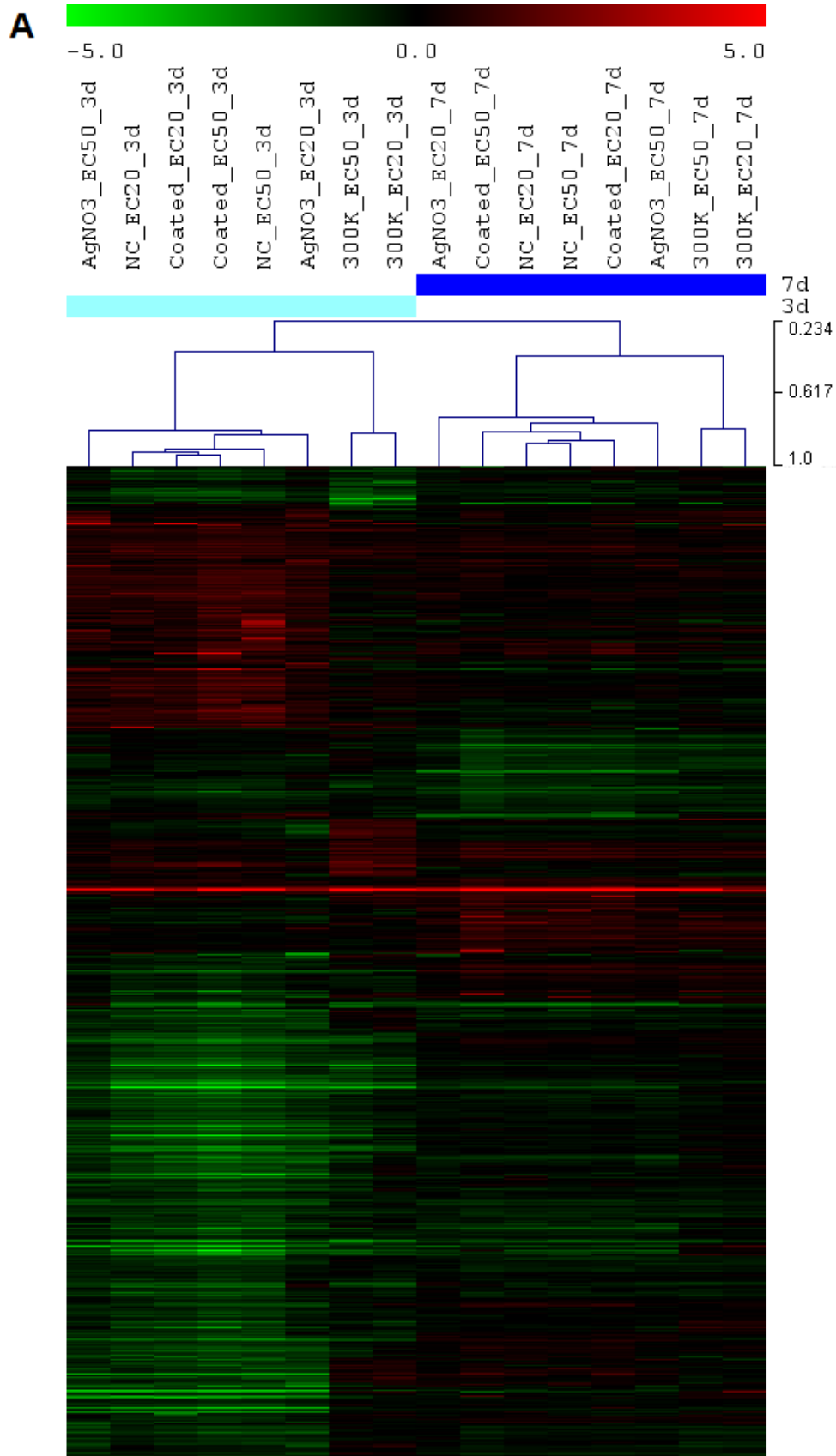


Figure 1: Results in terms of number of differentially expressed genes affected by exposure to the EC₂₀ and EC₅₀ (reproduction effect concentrations) of silver nitrate (AgNO₃) and silver nanoparticles: Coated, Non-coated (NC) and 300K, for 3 and 7 days.

The exposure for 3 days captured a higher number of DEGs (differentially expressed genes) compared to 7 days (3065 and 666 DEGs respectively) being consistent for all treatments. In general, there was more down- than up-regulated DEGs. In the Ag-NPs treatments the number of transcripts affected is increasing with the dose (i.e. EC₅₀ triggers more DEGs than EC₂₀) for 3 and 7 days. The opposite occurred for AgNO₃ where most was differentially expressed at the lower concentration, at 3 days of exposure. The Coated Ag-NPs treatment caused the highest number of DEGs.

Clustering analysis (Pearson's uncentered with average linkage) was performed on genes and samples (dendrogram on genes not shown), based on all the DEGs (Fig. 2 A). Because of the clear separation by time of exposure observed, the same analysis was done for each time individually based on the 3065 and 666 DEGs affected at 3 and 7 days, respectively (Fig. 2 B and C).



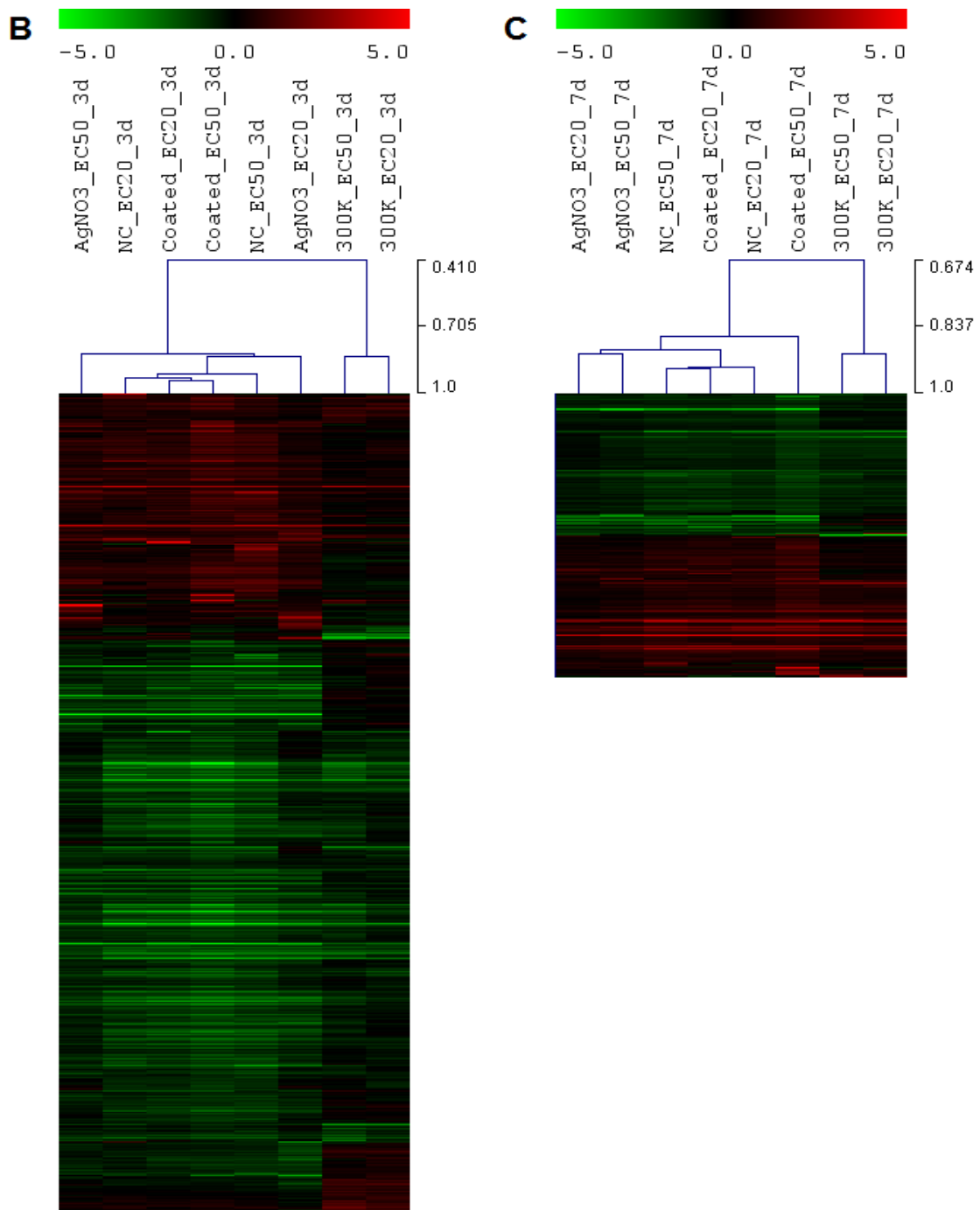


Figure 2: Expression heat map (green: down-regulated, red: up-regulated black: not differentially expressed) of differentially expressed genes (adjusted $p < 0.05$) after exposure to silver treatments- AgNO_3 : silver nitrate, NC: Ag-NPs non-coated, Coated: Ag-NPs coated, 300K: Ag-NPs 300K, and the EC20,50: reproduction effect concentration of 20% and 50%. Genes and samples (treatments) are hierarchically clustered using Pearson' Uncentered and

average linkage (dendrogram on genes not shown). (A) All treatments and exposure periods(3 and 7 days) to silver treatments. (B) 3 days of exposure. (C) 7 days of exposure.

There is a separation of Ag-NPs 300K treatments from the remaining test conditions. AgNO₃ treatments are clustered together with Ag-NPs coated and non-coated (NC), but the two Ag-NPs are closer than within any other treatments (note that Coated and NC are separated at a level of correlation around 0.9 at 3 days of exposure, see fig.2B). At 7 days of exposure (fig.2C), the Ag-NPs 300K is separated, and Coated_EC₅₀ is separated from the remaining treatments. The results from the PCA analysis are illustrated in fig.

3.

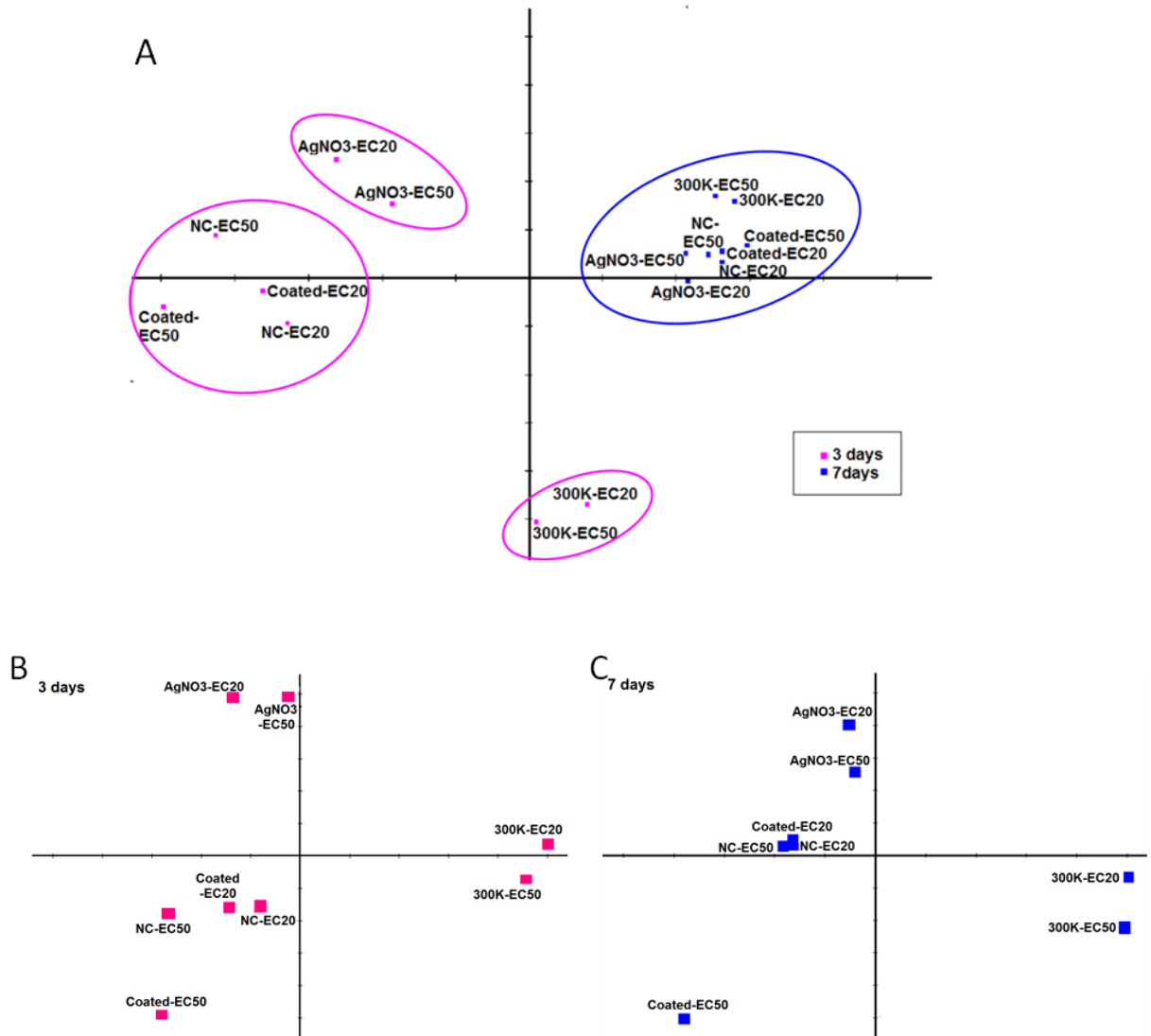


Figure 3: Principal component analysis of the samples (treatments) based on (A) all the DEGs (adjusted $p < 0.05$) for 3 and 7 days of exposure. The first two component presented explain 70.752% of the data variance (PC1-x axis = 56.991%, PC2-y axis = 13.761%). (B) 3065 DEGs for 3 days (PC1=56.724%; PC2=17.663%) (C) 666 DEGs for 7 days (PC1=47.785%, PC2=23.538%). AgNO₃: silver nitrate, NC: Ag-NPs non-coated, Coated: Ag-NPs coated, 300K: Ag-NPs 300K, EC₂₀, EC₅₀: reproduction effect concentration of 20%, 50%.

PCA analysis basically confirmed the previous clustering information, showing a separation of 3 main groups (following three days exposure): 1) Ag-NPs 300K, 2) AgNO₃ and 3) Ag-NPs (C & NC). Although it also showed that EC₂₀ and EC₅₀ for all Ag were closely related, except for the Ag-NPs coated EC₅₀.

The Venn diagrams show the results in terms of number of DEGs shared among test conditions (independently of the concentration tested), for each exposure time (fig. 4). Overall results show substantial overlap of genes (e.g. AgNO₃ and NC have more genes in common with other treatments than specifically affected, and between Coated and 300K about half of them are affected in other treatments). Results show, that coated and non-coated Ag-NPs share a higher number of DEGs.

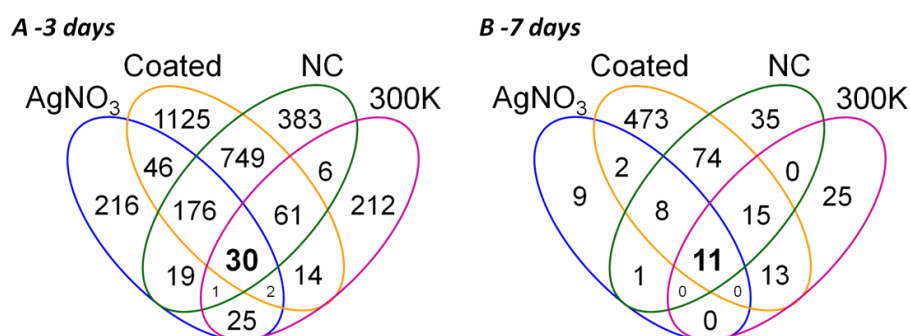


Figure 4: Venn diagram representation of the differentially expressed genes (adjusted $p < 0.05$) after exposure to the several silver treatments, silver nitrate (AgNO_3) and three silver nanoparticles: coated, non-coated (NC) and 300K for 3 days (A) and 7 days (B).

Gene set enrichment analysis on GO terms was performed to identify biological processes significantly affected by each Ag treatment. For that, 4 gene lists which include the annotated transcripts affected by each silver form (independently of the effect concentration – EC) were analysed versus the entire gene library (annotated transcripts present in the microarray). The analysis was not performed for the 7 days of exposure due to the comparatively lower number of DEGs affected and the reduced power. The GO terms significantly affected in each gene list are shown on Table S1 (Supplementary information).

4. Discussion

The differently expressed gene (DEG) response following 3 and 7 days were different for the 4 treatments and also differed for the EC_{20} or EC_{50} . Similar differences in gene expression between different days of exposure have been observed before for other stressors (e.g. Novais et al., 2011; Reynders et al., 2006) and with similar patterns of change as observed for *E. crypticus* to copper and zinc.

The discussion will be focused on the 3 days results given the comparatively higher analysis power. Across all Ag treatments, based on the gene set enrichment analysis, one common processes affected was related with cell cycle control (e.g. negative regulation of meiotic cell cycle by AgNO₃; cytokinesis, initiation of separation by Coated Ag-NPs; regulation of mitotic centrosome separation by NC Ag-NPs; cyclin catabolic process by Ag-NPs 300K). Interference with cell cycle control processes has been observed (in human cells) in response to metals (nickel, copper, cadmium and cobalt) (Hartwig et al., 2002) and in response to Ag-NPs (AshaRani et al., 2012). Often associated with impairments in cell cycle control is the breakdown of DNA repair system (AshaRani et al., 2012; Hartwig et al., 2002). Even AgNO₃ was the only treatment triggering a function directly connected with DNA repair (mitotic G2 DNA damage checkpoint), the transcripts associated with DNA repair such as several zinc-finger proteins were found down-regulated in response to all forms of Ag tested and indicating that exposure to Ag is affecting DNA repair mechanisms. The down-regulation of transcripts involved in DNA repair was also observed in another enchytraeid species (*E. albidus*) to AgNO₃ (Gomes et al., 2013), although not to Ag-NPs . The ubiquitin-related processes triggered by AgNO₃, Ag-NPs NC and 300K, are also associated with impairment of cell cycle control (Hershko, 1997). Processes related with inflammatory response, phagocytosis, and neurotransmission were triggered by AgNO₃, Coated and NC Ag-NPs (and not by Ag-NPs 300K). Unlike our results, where a down-regulation was observed for transcripts related with inflammatory response and phagocytosis, in *Eisenia fetida*' coelomocytes (*in vitro*) the induction of inflammatory processes with increased phagocytic activity in response to Ag-NPs was observed (Hayashi et al., 2012). Additionally, increased inflammatory response in the immune system cells of mussels (hemocytes) was reported for other NPs (TiO₂, SiO₂ and C60

fullerenes) (Canesi et al., 2010) suggesting a common mechanism to NMs. One obvious difference between these studies are the *in vivo* versus *in vitro* exposures - *in vivo* exposure requires longer exposure time to activate cell processes than the direct cell exposure – but also the whole organism is known to have additional cell types and routes for excretion, etc., benefiting from a multiple system of response. Neurotransmission was negatively affected by the down-regulation of several genes. These results are in agreement with those from Xu and co-authors (2013) which exposed rat cortical cells to Ag-NPs and found perturbations in pre- and post-synaptic proteins. Negative effects on neurons have been associated with calcium homeostasis disturbance and inhibition of sodium and potassium currents (Xu et al., 2013). In our study several transcripts coding for potassium channel and sodium transporter proteins were found down-regulated as well as calcium binding proteins and calcium transporters. All together these results indicate that neurotransmission of *E. crypticus* is being negatively affected when exposed to Ag.

In regard to the different treatments, the Ag-NPs 300K showed pattern distinct for the other NPs, whereas coated and non-coated (NC) Ag-NPs were more closely corresponding. The AgNO₃ treatment was somewhat different from the rest also. The effect concentrations tested were not causing large differences in the gene regulation. Although, the absolute number of genes affected was substantially higher with the increase in dose.

Uniquely affected by Ag-NPs 300k is glutathione conjugation reaction associated with the up-regulation of a transcript coding glutathione-S-transferase (GST). GSTs genes are known to respond to several kinds of stressors (including chemical); its expression was investigated (by PCR) in *Caenorhabditis elegans* in response to AgNO₃ and Ag-

NPs (dispersed by sonication in water) with 100nm (Roh et al., 2009) without showing changes in gene expression. Also exclusively activated by 300K is the process detection of bacterium (also, response to peptidoglycan). It is unclear how this bacteria recognition process is being affected by Ag-NPs 300K exposure, unless there is some kind of interference with the recognition system of the organism's cells. A more speculative idea could be that the Ag-NPs 300k was of a size that was easily taken by organisms, hence causing a stronger response than the other NPs.

PVP coated and non-coated Ag-NPs (20-30 nm) caused a similar gene expression profile indicating that the mechanisms seem to be similar, despite the higher number of DEGs on coated compared to NC. Affected by both were the processes related with energy metabolism (e.g. glucose-6-phosphate transport, long-chain fatty acid metabolic process, one-carbon metabolic process, ATP transport) of both lipids and carbohydrates. Several other metals (other metallic NPs included) affect the expression of energy related transcripts (e.g. Gomes et al., 2012; Gomes et al., 2013; Novais et al., 2012) and that seems to be associated with energy costs of detoxifying processes. In this case, carbohydrate metabolism was activated indicating a high energy use, but in regard to the lipids metabolism the response is unclear (given that transcripts are both up- and down-regulated). This may indicate that the PVP coating of the Ag particles was not important following a soil exposure.

The observed differences in response highlight the importance of supporting the biological observations with detailed studies on physicochemical fate/exposure issues e.g. the dispersion or dissolution rate in soils.

5. Conclusions

Analysis of gene expression profile of *E. crypticus* pointed differences between the different forms of silver tested. Ag-NPs 300K was the most dissimilar. Several processes related with cell cycle control were commonly affected by Ag, which can also be associated with impairment in DNA repair, hence a mechanism of toxicity. Common to AgNO₃ and NPs (Coated and non-coated) are the effects on neurotransmission. Coated and non-coated Ag-NPs showed a very similar gene expression profile.

Evidences are that the mechanisms of response to Ag were different between materials; the differences in properties such as the dispersion rate of the materials seem to be of high importance.

Acknowledgments

This study was supported by funding FEDER through COMPETE Programa Operacional Factores de Competitividade, and by National funding through FCT-Fundação para a Ciência e Tecnologia, within the research project NANOkA FCOMP-01-0124- FEDER-008944 (Ref. FCT PTDC/BIA-BEC/103716/2008), through an FCT PhD grant to Susana Gomes (SFRH/BD/63261/2009) and by the EU-FP7 MARINA (Ref. 263215).

References

- Alexa, A., Rahnenfuhrer, J., Lengauer, T., 2006. Improved scoring of functional groups from gene expression data by decorrelating GO graph structure. *Bioinformatics* 22, 1600-1607.
- AshaRani, P., Sethu, S., Lim, H., Balaji, G., Valiyaveetil, S., Hande, M.P., 2012. Differential regulation of intracellular factors mediating cell cycle, DNA repair and inflammation following exposure to silver nanoparticles in human cells. *Genome Integrity* 3, 2.

- Benjamini, Y., Hochberg, Y., 1995. Controlling the False Discovery Rate: A Practical and Powerful Approach to Multiple Testing. *Journal of the Royal Statistical Society* 57, 289-300.
- Canesi, L., Ciacci, C., Vallotto, D., Gallo, G., Marcomini, A., Pojana, G., 2010. In vitro effects of suspensions of selected nanoparticles (C60 fullerene, TiO₂, SiO₂) on *Mytilus* hemocytes. *Aquatic Toxicology* 96, 151-158.
- Castro-Ferreira, M.P., de Boer, T.E., Colbourne, J.K., Vooijs, R., van Gestel, C.A.M., van Straalen, N.M., Soares, A.M.V.M., Amorim, M.J.B., Roelofs, D., 2013. Transcriptome assembly and microarray construction for *Enchytraeus crypticus*, a model oligochaete to assess stress response mechanisms and soil quality. *Submitted*.
- Chae, Y.J., Pham, C.H., Lee, J., Bae, E., Yi, J., Gu, M.B., 2009. Evaluation of the toxic impact of silver nanoparticles on Japanese medaka (*Oryzias latipes*). *Aquatic Toxicology* 94, 320-327.
- Gomes, S.I.L., Novais, S.C., Scott-Fordsmand, J.J., Coen, W.D., Soares, A.M.V.M., Amorim, M.J.B., 2012. Effect of Cu-nanoparticles versus Cu-salt in *Enchytraeus albidus* (Oligochaeta): Differential gene expression through microarray analysis. *Comparative Biochemistry and Physiology, Part C* 155, 219-227.
- Gomes, S.I.L., Soares, A.M.V.M., Scott-Fordsmand, J.J., Amorim, M.J.B., 2013. Mechanisms of response to silver nanoparticles on *Enchytraeus albidus* (Oligochaeta): Survival, reproduction and gene expression profile. *Journal of Hazardous Materials* 254–255, 336-344.
- Gou, N., Onnis-Hayden, A., Gu, A.Z., 2010. Mechanistic Toxicity Assessment of Nanomaterials by Whole-Cell-Array Stress Genes Expression Analysis. *Environmental Science & Technology* 44, 5964-5970.
- Gu, M.B., Niazi, J.H., Sang, B.I., Kim, Y.S., 2011. Global Gene Response in *Saccharomyces cerevisiae* Exposed to Silver Nanoparticles. *Applied Biochemistry and Biotechnology* 164, 1278-1291.

- Guo, D., Zhu, L., Huang, Z., Zhou, H., Ge, Y., Ma, W., Wu, J., Zhang, X., Zhou, X., Zhang, Y., Zhao, Y., Gu, N., 2013. Anti-leukemia activity of PVP-coated silver nanoparticles via generation of reactive oxygen species and release of silver ions. *Biomaterials* 34, 7884-7894.
- Hartwig, A., Asmuss, M., Ehleben, I., Herzer, U., Kostelac, D., Pelzer, A., Schwerdtle, T., Burkle, A., 2002. Interference by toxic metal ions with DNA repair processes and cell cycle control: molecular mechanisms. *Environmental Health Perspectives* 110 Suppl 5, 797-799.
- Hayashi, Y., Engelmann, P., Foldbjerg, R., Szabo, M., Somogyi, I., Pollak, E., Molnar, L., Autrup, H., Sutherland, D.S., Scott-Fordsmand, J., Heckmann, L.H., 2012. Earthworms and Humans in Vitro: Characterizing Evolutionarily Conserved Stress and Immune Responses to Silver Nanoparticles. *Environmental Science & Technology* 46, 4166-4173.
- Heckmann, L.-H., Hovgaard, M.B., Sutherland, D.S., Autrup, H., Besenbacher, F., Scott-Fordsmand, J.J., 2011. Limit-test toxicity screening of selected inorganic nanoparticles to the earthworm *Eisenia fetida*. *Ecotoxicology* 20(1), 226-233.
- Hershko, A., 1997. Roles of ubiquitin-mediated proteolysis in cell cycle control. *Current Opinion in Cell Biology* 9, 788-799.
- Kahru, A., Dubourguier, H.C., 2010. From ecotoxicology to nanoecotoxicology. *Toxicology* 269, 105-119.
- Lapied, E., Moudilou, E., Exbrayat, J.M., Oughton, D.H., Joner, E.J., 2010. Silver nanoparticle exposure causes apoptotic response in the earthworm *Lumbricus terrestris* (Oligochaeta). *Nanomedicine* 5, 975-984.
- Lohse, M., Bolger, A.M., Nagel, A., Fernie, A.R., Lunn, J.E., Stitt, M., Usadel, B., 2012. RobiNA: a user-friendly, integrated software solution for RNA-Seq-based transcriptomics. *Nucleic Acids Res* 40, W622-W627.
- Lohse, M., Nunes-Nesi, A., Kruger, P., Nagel, A., Hannemann, J., Giorgi, F.M., Childs, L., Osorio, S., Walther, D., Selbig, J., Sreenivasulu, N., Stitt, M., Fernie, A.R., Usadel, B.,

2010. Robin: An Intuitive Wizard Application for R-Based Expression Microarray Quality Assessment and Analysis. *Plant Physiology* 153, 642-651.
- Miao, A.J., Schwehr, K.A., Xu, C., Zhang, S.J., Luo, Z., Quigg, A., Santschi, P.H., 2009. The algal toxicity of silver engineered nanoparticles and detoxification by exopolymeric substances. *Environmental Pollution* 157, 3034-3041.
- Navarro, E., Piccapietra, F., Wagner, B., Marconi, F., Kaegi, R., Odzak, N., Sigg, L., Behra, R., 2008. Toxicity of Silver Nanoparticles to *Chlamydomonas reinhardtii*. *Environmental Science & Technology* 42, 8959-8964.
- Novais, S.C., De Coen, W., Amorim, M.J.B., 2012. Transcriptional responses in *Enchytraeus albidus* (Oligochaeta): Comparison between cadmium and zinc exposure and linkage to reproduction effects. *Environmental Toxicology and Chemistry* 31, 2289-2299.
- Novais, S.C., Howcroft, C.F., Carreto, L., Pereira, P.M., Santos, M.A., De Coen, W., Soares, A.M.V.M., Amorim, M.J.B., 2011. Differential gene expression analysis in *Enchytraeus albidus* exposed to natural and chemical stressors: effect of different exposure periods. *Ecotoxicology*, 213-224.
- OECD, 2004. Guidelines for the testing of chemicals No. 220. Enchytraeid Reproduction Test. Organization for Economic Cooperation and Development. Paris.
- Piao, M.J., Kang, K.A., Lee, I.K., Kim, H.S., Kim, S., Choi, J.Y., Choi, J., Hyun, J.W., 2011. Silver nanoparticles induce oxidative cell damage in human liver cells through inhibition of reduced glutathione and induction of mitochondria-involved apoptosis. *Toxicology Letters* 201, 92-100.
- Piccinno, F., Gottschalk, F., Seeger, S., Nowack, B., 2012. Industrial production quantities and uses of ten engineered nanomaterials in Europe and the world. *Journal of Nanoparticle Research* 14.
- Reynders, H., van der Ven, K., Moens, L.N., van Remortel, P., De Coen, W.M., Blust, R., 2006. Patterns of gene expression in carp liver after exposure to a mixture of waterborne and dietary cadmium using a custom-made microarray. *Aquatic Toxicology* 80, 180-193.

- Roh, J.Y., Sim, S.J., Yi, J., Park, K., Chung, K.H., Ryu, D.Y., Choi, J., 2009. Ecotoxicity of Silver Nanoparticles on the Soil Nematode *Caenorhabditis elegans* Using Functional Ecotoxicogenomics. *Environmental Science & Technology* 43, 3933-3940.
- Shoults-Wilson, W.A., Reinsch, B.C., Tsyusko, O.V., Bertsch, P.M., Lowry, G.V., Unrine, J.M., 2011. Effect of silver nanoparticle surface coating on bioaccumulation and reproductive toxicity in earthworms (*Eisenia fetida*). *Nanotoxicology* 5, 432-444.
- Sotiriou, G.A., Pratsinis, S.E., 2010. Antibacterial Activity of Nanosilver Ions and Particles. *Environmental Science & Technology* 44, 5649-5654.
- Westheide, W., Graefe, U., 1992. Two new terrestrial *Enchytraeus* species (Oligochaeta, Annelida). *Journal of Natural History* 26, 479-488.
- Xu, F., Piatt, C., Farkas, S., Qazzaz, M., Syed, N., 2013. Silver nanoparticles (AgNPs) cause degeneration of cytoskeleton and disrupt synaptic machinery of cultured cortical neurons. *Molecular Brain* 6, 1-15.

Supplementary material

Table S1: List of Biological processes (GO terms) significantly affected by exposure to AgNO₃ and Ag-NPs: Coated, NC (non-coated) and 300K for 3 days. a: number of annotated transcripts in the gene library. b: number of genes found for this GO term in the significant gene list and c: P value calculated by the Fisher exact test.

AgNO ₃					
GO-ID	Term (Biological process)	Annotated ^a	Sig. Annotated ^b	P-Value ^c	
GO:0002862	negative regulation of inflammatory response to antigenic stimulus	2	2	0.0001	contig10645, contig08003
GO:0060027	convergent extension involved in gastrulation	15	3	0.0006	contig19303, contig17895, contig12104
GO:0042376	phyloquinone catabolic process -->vitamine K	4	2	0.0007	contig18190, contig18023
GO:0031145	anaphase-promoting complex-dependent proteasomal ubiquitin-dependent protein catabolic process	55	4	0.0033	GYUW2K402JTAGL, contig10645, contig09609, contig10894
GO:0046827	positive regulation of protein export from nucleus	8	2	0.0033	GYUW2K401B29P3, contig03170
GO:0051437	positive regulation of ubiquitin-protein ligase activity involved in mitotic cell cycle	64	4	0.0057	GYUW2K402JTAGL, contig10645, contig09609, contig10894
GO:0001707	mesoderm formation	34	3	0.0064	GYUW2K401B29P3, contig03170, contig12104
GO:0050918	positive chemotaxis	11	2	0.0064	contig17895, contig03170
GO:0048205	COPI coating of Golgi vesicle --> vesicle mediated transport	11	2	0.0064	contig03760, contig15025
GO:0006691	leukotriene metabolic process --> inflammatory mediator	14	2	0.0104	contig18190, contig18023
GO:0007438	oocyte development	1	1	0.0112	contig03329
GO:0007432	salivary gland boundary specification	1	1	0.0112	contig03329
GO:0007374	posterior midgut invagination	1	1	0.0112	contig03329

Supplementary material – Chapter VIII

GO:0007174	epidermal growth factor catabolic process	1	1	0.0112	contig03329
GO:0006597	spermine biosynthetic process	1	1	0.0112	contig24735
GO:0035311	wing cell fate specification	1	1	0.0112	contig03329
GO:0042443	phenylethylamine metabolic process --> neurotransmissor	1	1	0.0112	GYUW2K401D3B4G
GO:0030327	prenylated protein catabolic process	1	1	0.0112	contig09619
GO:0060691	epithelial cell maturation involved in salivary gland development	1	1	0.0112	contig24318
GO:0031017	exocrine pancreas development	15	2	0.0119	contig24318, contig10934
GO:0045471	response to ethanol	43	3	0.0123	GYUW2K402JTAGL, contig03170, contig03329
GO:0006911	phagocytosis, engulfment	44	3	0.0131	contig18539, GYUW2K401AZURM, contig08546
GO:0017148	negative regulation of translation	19	2	0.0188	contig02617, contig03170
GO:0008593	regulation of Notch signaling pathway	19	2	0.0188	GYUW2K401BQR16, GYUW2K402JPFI
GO:0051436	negative regulation of ubiquitin-protein ligase activity involved in mitotic cell cycle	52	3	0.0204	contig10645, contig09609, contig10894
GO:0006693	prostaglandin metabolic process --> compostos lipidicos derivas dos ácidos gordos	20	2	0.0207	contig18190, contig18023
GO:0060125	negative regulation of growth hormone secretion	2	1	0.0223	contig19303
GO:0018095	protein polyglutamylation	2	1	0.0223	contig12307
GO:0051463	negative regulation of cortisol secretion	2	1	0.0223	contig19303
GO:0043519	regulation of myosin II filament organization	2	1	0.0223	GYUW2K401C23XH
GO:0043457	regulation of cellular respiration	2	1	0.0223	contig03170
GO:0030589	pseudocleavage involved in syncytial blastoderm formation	2	1	0.0223	contig03329
GO:0009047	dosage compensation by hyperactivation of X chromosome	2	1	0.0223	contig02617
GO:0046886	positive regulation of hormone biosynthetic process	2	1	0.0223	GYUW2K402I2UB6

Supplementary material – Chapter VIII

GO:0046845	branched duct epithelial cell fate determination, open tracheal system	2	1	0.0223	contig03329
GO:0035298	regulation of Malpighian tubule size	2	1	0.0223	contig03329
GO:0035202	tracheal pit formation in open tracheal system	2	1	0.0223	contig03329
GO:0019747	regulation of isoprenoid metabolic process	2	1	0.0223	contig09967
GO:0021854	hypothalamus development	2	1	0.0223	GYUW2K402HKK11
GO:0046324	regulation of glucose import	21	2	0.0228	contig03170, GYUW2K402F231X
GO:0046686	response to cadmium ion	23	2	0.0270	GYUW2K402JTAGL, contig09837
GO:0006936	muscle contraction	106	4	0.0313	contig03170, contig15001, contig13305, GYUW2K402I94X7
GO:0046677	response to antibiotic	25	2	0.0316	GYUW2K401C23XH, contig03170
GO:0045742	positive regulation of epidermal growth factor receptor signaling pathway	3	1	0.0332	contig03329
GO:0007479	leg disc proximal/distal pattern formation	3	1	0.0332	contig03329
GO:0007370	ventral furrow formation	3	1	0.0332	contig03329
GO:0071445	cellular response to protein stimulus	3	1	0.0332	GYUW2K402JTAGL
GO:0051447	negative regulation of meiotic cell cycle	3	1	0.0332	contig03170
GO:0042420	dopamine catabolic process --> neurotransmitter	3	1	0.0332	GYUW2K401D3B4G
GO:0035225	determination of genital disc primordium	3	1	0.0332	contig03329
GO:0008295	spermidine biosynthetic process	3	1	0.0332	contig24735
GO:0006890	retrograde vesicle-mediated transport, Golgi to ER	26	2	0.0340	contig03760, contig15025
GO:0007269	neurotransmitter secretion	64	3	0.0349	contig17895, GYUW2K401BPDJS, contig03760
GO:0006887	exocytosis	112	4	0.0371	contig11524, contig17895, contig03170, contig16585
GO:0035317	imaginal disc-derived wing hair organization	28	2	0.0389	contig08546, contig03329
GO:0007095	mitotic G2 DNA damage checkpoint	4	1	0.0440	GYUW2K402JTAGL
GO:0060045	positive regulation of cardiac muscle cell proliferation	4	1	0.0440	GYUW2K402JTAGL
GO:0033169	histone H3-K9 demethylation	4	1	0.0440	GYUW2K402I2UB6

Supplementary material – Chapter VIII

GO:0033160	positive regulation of protein import into nucleus, translocation	4	1	0.0440	GYUW2K402JTAGL
GO:0043615	astrocyte cell migration	4	1	0.0440	contig17895
GO:0008586	imaginal disc-derived wing vein morphogenesis	4	1	0.0440	contig03329
GO:0035149	lumen formation, open tracheal system	4	1	0.0440	contig03329
GO:0046671	negative regulation of retinal cell programmed cell death	4	1	0.0440	contig08220
GO:0060872	semicircular canal development	4	1	0.0440	contig03760
GO:0034339	regulation of transcription from RNA polymerase II promoter by nuclear hormone receptor	4	1	0.0440	GYUW2K402I2UB6
GO:0007525	somatic muscle development	4	1	0.0440	contig14253

Coated					
GO-ID	Term	Annotated ^a	Sig. Annotated ^b	P-Value ^c	TestSeqs
GO:0030433	ER-associated protein catabolic process	19	5	0.001807	GYUW2K401C3TYB, GYUW2K401CH8BU, GYUW2K402HD98T, contig03466, contig12534
GO:0008089	anterograde axon cargo transport	6	3	0.002083	contig12041, contig06005, contig04507
GO:0002862	negative regulation of inflammatory response to antigenic stimulus	2	2	0.0023871	contig10645, contig08003
GO:0007270	neuron-neuron synaptic transmission	49	8	0.002393	contig17387, GYUW2K401EDXYI, contig21765, contig03170, GYUW2K402ICSLI, GYUW2K402G855S, GYUW2K402IZBWQ, contig04816
GO:0035099	hemocyte migration --> cell from invertebrates immune system	15	4	0.0050209	GYUW2K401AO5ZN, contig03329, GYUW2K402GCEB2, contig03703
GO:0006911	phagocytosis, engulfment	44	7	0.0051242	contig08546, contig18022, GYUW2K402F74UG, GYUW2K401DGBEB, GYUW2K401AZURM, contig03703, contig22765
GO:0006825	copper ion transport	16	4	0.0064389	GYUW2K401CUYJS, contig09599, GYUW2K402ILEPJ, contig11932
GO:0034447	very-low-density lipoprotein particle clearance	3	2	0.0069285	contig05743, contig02050
GO:0001676	long-chain fatty acid metabolic process	17	4	0.0080991	contig21490, contig03502, contig13092, GYUW2K401C1QNZ
GO:0060218	hematopoietic stem cell differentiation	10	3	0.010788	contig01815, contig09748, contig08604
GO:0034214	protein hexamerization	4	2	0.0134082	GYUW2K401BAIXC, contig12534

Supplementary material – Chapter VIII

GO:0007108	cytokinesis, initiation of separation	4	2	0.0134082	contig12156, contig07597
GO:0070723	response to cholesterol	4	2	0.0134082	contig14559, contig16815
GO:0006122	mitochondrial electron transport, ubiquinol to cytochrome c	4	2	0.0134082	contig11406, contig09555
GO:0009253	peptidoglycan catabolic process	11	3	0.0143011	contig17026, contig12756, contig16451
GO:0000038	very long-chain fatty acid metabolic process	20	4	0.0146793	contig21490, contig03502, contig13092, contig12579
GO:0009086	methionine biosynthetic process	20	4	0.0146793	contig01815, contig01813, contig01812, contig14659
GO:0043171	peptide catabolic process	12	3	0.0183858	contig12958, contig09748, contig08604
GO:0007601	visual perception	44	6	0.0193829	contig16580, GYUW2K401AML0R, GYUW2K402G855S, contig03742, GYUW2K401C1QNZ, GYUW2K401B9VZQ
GO:0002019	regulation of renal output by angiotensin	5	2	0.0216265	contig09748, contig08604
GO:0002005	angiotensin catabolic process in blood	5	2	0.0216265	contig09748, contig08604
GO:0043124	negative regulation of I-kappaB kinase/NF-kappaB cascade	5	2	0.0216265	contig24724, GYUW2K401AYGYU
GO:0001707	mesoderm formation	34	5	0.0236542	GYUW2K401B29P3, contig16815, contig12104, contig03170, contig22418
GO:0042632	cholesterol homeostasis	34	5	0.0236542	contig09967, GYUW2K401EEE9N, contig07387, contig06593, GYUW2K401DGBEB
GO:0006730	one-carbon metabolic process	35	5	0.0265214	contig25354, contig04109, contig04108, contig07897, contig16306
GO:0007492	endoderm development	14	3	0.0282902	GYUW2K402F17UV, contig16815, GYUW2K401EW1AW
GO:0046500	S-adenosylmethionine metabolic process	14	3	0.0282902	contig10402, contig07897, GYUW2K402FSF7J
GO:0019464	glycine decarboxylation via glycine cleavage system	6	2	0.0313982	contig26967, GYUW2K401DC691
GO:0050482	arachidonic acid secretion--> ácido gordo não saturado precursor de prostagandinas	6	2	0.0313982	contig09748, contig08604
GO:0046836	glycolipid transport	6	2	0.0313982	contig09967, GYUW2K402FJUME
GO:0035160	maintenance of epithelial integrity, open tracheal system	6	2	0.0313982	GYUW2K401AO5ZN, contig03329
GO:0016998	cell wall macromolecule catabolic process	26	4	0.0359794	GYUW2K402G7VDL, GYUW2K401DG1YA, GYUW2K401BS3PY, contig12282
GO:0001575	globoside metabolic process	16	3	0.0404926	contig07661, contig12551, contig04360
GO:0030593	neutrophil chemotaxis	7	2	0.0425523	contig03170, contig06593

Supplementary material – Chapter VIII

GO:0030512	negative regulation of transforming growth factor beta receptor signaling pathway	7	2	0.0425523	GYUW2K401CH8BU, contig08131
GO:0046626	regulation of insulin receptor signaling pathway	17	3	0.0474341	contig03170, GYUW2K401D4627, contig18022
GO:0045745	positive regulation of G-protein coupled receptor protein signaling pathway	1	1	0.0488867	contig04816
GO:0007438	oocyte development	1	1	0.0488867	contig03329
GO:0007432	salivary gland boundary specification	1	1	0.0488867	contig03329
GO:0010164	response to cesium ion	1	1	0.0488867	contig07222
GO:0007374	posterior midgut invagination	1	1	0.0488867	contig03329
GO:0002318	myeloid progenitor cell differentiation	1	1	0.0488867	contig06593
GO:0033488	cholesterol biosynthetic process via 24,25-dihydrolanosterol	1	1	0.0488867	contig08818
GO:0001878	response to yeast	1	1	0.0488867	GYUW2K402F74UG
GO:0007174	epidermal growth factor catabolic process	1	1	0.0488867	contig03329
GO:0006600	creatine metabolic process	1	1	0.0488867	GYUW2K402H12ZE
GO:0001780	neutrophil homeostasis	1	1	0.0488867	contig06593
GO:0060074	synapse maturation	1	1	0.0488867	contig17387
GO:0045299	otolith mineralization	1	1	0.0488867	contig20705
GO:0032682	negative regulation of chemokine production	1	1	0.0488867	contig06593
GO:0032425	positive regulation of mismatch repair	1	1	0.0488867	contig06913
GO:0006043	glucosamine catabolic process --> precursor na sintese de preotinas e lipidos	1	1	0.0488867	GYUW2K402G7RXR
GO:0032275	lutinizing hormone secretion	1	1	0.0488867	GYUW2K401DJ3LF
GO:0090070	positive regulation of ribosome biogenesis	1	1	0.0488867	GYUW2K402IER1W
GO:0009594	detection of nutrient	1	1	0.0488867	GYUW2K402IER1W
GO:0043129	surfactant homeostasis	1	1	0.0488867	contig17387
GO:0015760	glucose-6-phosphate transport	1	1	0.0488867	contig06593

Supplementary material – Chapter VIII

GO:0035321	maintenance of imaginal disc-derived wing hair orientation	1	1	0.0488867	contig02291
GO:0035311	wing cell fate specification	1	1	0.0488867	contig03329
GO:0046884	follicle-stimulating hormone secretion	1	1	0.0488867	GYUW2K401DJ3LF
GO:0042443	phenylethylamine metabolic process	1	1	0.0488867	GYUW2K401D3B4G
GO:0030327	prenylated protein catabolic process	1	1	0.0488867	contig09619
GO:0010747	positive regulation of plasma membrane long-chain fatty acid transport	1	1	0.0488867	contig14559
GO:0019805	quinolinate biosynthetic process	1	1	0.0488867	contig05204
GO:0060596	mammary placode formation	1	1	0.0488867	GYUW2K401DJ3LF
GO:0007510	cardioblast cell fate determination	1	1	0.0488867	GYUW2K401EDXYI
GO:0051969	regulation of transmission of nerve impulse	83	8	0.0496432	contig17387, contig18292, contig21765, contig03170, GYUW2K402JLP9T, GYUW2K402ICSLI, GYUW2K402G855S, contig20705

NC					
GO-ID	Term	Annotated ^a	Sig. Annotated ^b	P-Value ^c	TestSeqs
GO:0001707	mesoderm formation	34	6	6.75E-04	contig22418, GYUW2K401B29P3, contig18722, GYUW2K402HNIYP, contig03170, contig12104
GO:0002862	negative regulation of inflammatory response to antigenic stimulus	2	2	0.0010342	contig10645, contig08003
GO:0046827	positive regulation of protein export from nucleus	8	3	0.0016455	GYUW2K401B29P3, contig03170, GYUW2K401AWM6X
GO:0007584	response to nutrient	73	8	0.0023418	contig02050, contig02048, contig09837, contig06593, contig26942, GYUW2K401ES0R6, contig21490, contig09890
GO:0034447	very-low-density lipoprotein particle clearance	3	2	0.0030362	contig02050, contig05743
GO:0018105	peptidyl-serine phosphorylation	35	5	0.0049536	GYUW2K401EE3T7, contig16483, GYUW2K402I55X8, contig03170, GYUW2K401AWM6X
GO:0042493	response to drug	183	13	0.006386	contig02050, contig02048, contig09837, contig26942, GYUW2K402I189L, contig11208, GYUW2K401ERQX3, contig10430, contig17387, contig07387, GYUW2K401AWM6X, contig09890, GYUW2K401DBPGU
GO:0046500	S-adenosylmethionine metabolic process	14	3	0.009261	GYUW2K402FSF7J, contig15679, contig10402
GO:0006027	glycosaminoglycan catabolic process	28	4	0.0117695	contig07661, contig04360, contig16451, GYUW2K402G397J

Supplementary material – Chapter VIII

GO:0006983	ER overload response	6	2	0.0142329	GYUW2K401CH8BU, GYUW2K401AWM6X
GO:0032212	positive regulation of telomere maintenance via telomerase	6	2	0.0142329	contig01815, GYUW2K402I55X8
GO:0043392	negative regulation of DNA binding	6	2	0.0142329	GYUW2K402I55X8, contig10430
GO:0001676	long-chain fatty acid metabolic process	17	3	0.0161077	contig03502, contig21490, GYUW2K401C1QNZ
GO:0033993	response to lipid	209	13	0.0180037	contig02050, contig02048, contig09837, contig18722, contig26942, GYUW2K401ES0R6, GYUW2K401EDXYI, GYUW2K401DABYI, contig10430, contig03170, contig17387, contig07387, contig09890
GO:0042476	odontogenesis	18	3	0.0188759	contig02048, GYUW2K401C1QNZ, contig17387
GO:0050774	negative regulation of dendrite morphogenesis	7	2	0.0195046	contig22418, GYUW2K401AWM6X
GO:0030593	neutrophil chemotaxis	7	2	0.0195046	contig06593, contig03170
GO:0007270	neuron-neuron synaptic transmission	49	5	0.020183	GYUW2K402IZBWQ, GYUW2K401EDXYI, GYUW2K401BJ25D, contig03170, contig17387
GO:0046683	response to organophosphorus	34	4	0.0229293	GYUW2K401AQUCF, contig10430, GYUW2K401C8PXB, contig09890
GO:0001952	regulation of cell-matrix adhesion	8	2	0.0254576	contig21101, contig09890
GO:0014070	response to organic cyclic compound	267	15	0.0264756	contig09837, contig06593, contig18722, contig26942, GYUW2K401ES0R6, GYUW2K401AQUCF, GYUW2K401EDXYI, contig11208, GYUW2K401DABYI, contig02573, contig10430, contig03170, contig17387, contig07387, contig09890
GO:0009743	response to carbohydrate stimulus	36	4	0.0277044	contig06593, contig18722, GYUW2K402GVO4G, contig09890
GO:0001990	regulation of systemic arterial blood pressure by hormone	9	2	0.0320428	contig02048, contig09748
GO:0050830	defense response to Gram-positive bacterium	9	2	0.0320428	GYUW2K402FQD1W, contig20840
GO:0050729	positive regulation of inflammatory response	9	2	0.0320428	contig03170, contig07387
GO:0010164	response to cesium ion	1	1	0.0321878	contig07222
GO:0045657	positive regulation of monocyte differentiation	1	1	0.0321878	contig10430
GO:0002318	myeloid progenitor cell differentiation	1	1	0.0321878	contig06593
GO:0001878	response to yeast	1	1	0.0321878	GYUW2K402F74UG
GO:0007144	female meiosis I	1	1	0.0321878	contig15579

Supplementary material – Chapter VIII

GO:0032909	regulation of transforming growth factor beta2 production	1	1	0.0321878	contig18722
GO:0006600	creatine metabolic process --> helps to supply energy to cells	1	1	0.0321878	GYUW2K402H12ZE
GO:0001780	neutrophil homeostasis	1	1	0.0321878	contig06593
GO:0019049	evasion or tolerance of host defenses by virus	1	1	0.0321878	contig18722
GO:0060074	synapse maturation	1	1	0.0321878	contig17387
GO:0006590	thyroid hormone generation	1	1	0.0321878	GYUW2K401AQUCF
GO:0032682	negative regulation of chemokine production	1	1	0.0321878	contig06593
GO:0051365	cellular response to potassium ion starvation	1	1	0.0321878	contig10430
GO:0050765	negative regulation of phagocytosis	1	1	0.0321878	contig09890
GO:0032060	bleb assembly	1	1	0.0321878	contig08182
GO:0043129	surfactant homeostasis	1	1	0.0321878	contig17387
GO:0015867	ATP transport	1	1	0.0321878	GYUW2K402IXGOU
GO:0015866	ADP transport	1	1	0.0321878	GYUW2K402IXGOU
GO:0015760	glucose-6-phosphate transport	1	1	0.0321878	contig06593
GO:0042443	phenylethylamine metabolic process	1	1	0.0321878	GYUW2K401D3B4G
GO:0030327	prenylated protein catabolic process	1	1	0.0321878	contig09619
GO:0046602	regulation of mitotic centrosome separation	1	1	0.0321878	contig15579
GO:0060691	epithelial cell maturation involved in salivary gland development	1	1	0.0321878	contig24318
GO:0007510	cardioblast cell fate determination	1	1	0.0321878	GYUW2K401EDXYI
GO:0006406	mRNA export from nucleus	38	4	0.0330292	contig03927, contig12744, contig15124, GYUW2K402I3A9U
GO:0031398	positive regulation of protein ubiquitination	75	6	0.0336148	contig04952, contig10645, GYUW2K401CH8BU, GYUW2K402JDXQC, contig10487, GYUW2K401CLX00
GO:0043085	positive regulation of catalytic activity	255	14	0.0369413	contig02050, contig02048, contig04952, contig10645, GYUW2K401EE3T7, contig06593, GYUW2K401CH8BU, contig18722, GYUW2K402JDXQC, contig10487, GYUW2K401CLX00, contig03703, contig05743, contig03170
GO:0060218	hematopoietic stem cell differentiation	10	2	0.0392135	contig01815, contig09748
GO:0030850	prostate gland development	10	2	0.0392135	contig09599, contig09890

Supplementary material – Chapter VIII

GO:0009219	pyrimidine deoxyribonucleotide metabolic process	10	2	0.0392135	contig17953, GYUW2K401C8PXB
GO:0007586	digestion	24	3	0.0406419	contig09748, contig03714, contig03712
GO:0050804	regulation of synaptic transmission	79	6	0.0417573	GYUW2K402JLP9T, GYUW2K401BJ25D, contig05339, contig03170, contig17387, GYUW2K401AWM6X
GO:0007610	behavior	335	17	0.0438409	GYUW2K401EMA8V, GYUW2K401COLHN, contig21261, contig04784, GYUW2K402JLP9T, contig15008, contig10430, GYUW2K401BJ25D, GYUW2K401C095C, contig06031, contig10025, GYUW2K401C1QNZ, contig05339, contig03170, GYUW2K401D3B4G, GYUW2K402IXGOU, contig09890
GO:0031334	positive regulation of protein complex assembly	25	3	0.0451143	GYUW2K401AYGYU, GYUW2K402GVO4G, GYUW2K401AWM6X
GO:0046677	response to antibiotic	25	3	0.0451143	GYUW2K401ES0R6, GYUW2K402GVO4G, contig03170
GO:0010226	response to lithium ion	11	2	0.0469252	contig11208, GYUW2K401AWM6X
GO:0048205	COPI coating of Golgi vesicle	11	2	0.0469252	contig03760, contig15025
GO:0030878	thyroid gland development	11	2	0.0469252	contig18722, GYUW2K401AQUCF
GO:0055085	transmembrane transport	649	29	0.0471813	GYUW2K402HELGW, contig23021, contig09837, contig06593, contig09422, GYUW2K401C90RT, contig09369, GYUW2K402HU5GR, GYUW2K402I189L, contig25393, GYUW2K401CZFEM, GYUW2K401C5MMA, GYUW2K401ERQX3, GYUW2K402JLP9T, GYUW2K402I55X8, GYUW2K401BEBSE, contig14277, GYUW2K402IROV7, GYUW2K401C8IT7, contig04318, GYUW2K401C1QNZ, contig24190, contig03179, contig19147, GYUW2K402GSWXN, contig14186, contig07828, GYUW2K402IXGOU, GYUW2K401CCKSW
GO:0007179	transforming growth factor beta receptor signaling pathway	43	4	0.0487807	GYUW2K401CH8BU, contig18722, contig03703, contig10430
GO:0043065	positive regulation of apoptotic process	125	8	0.0489393	contig18722, GYUW2K401AXI1M, GYUW2K401AYGYU, contig10430, contig01903, contig12470, GYUW2K401AWM6X, contig09890

300K					
GO-ID	Term	Annotated ^a	Sig. Annotated ^b	P-Value ^c	TestSeqs
GO:0008054	cyclin catabolic process -->control of cell cycle	8	2	0.0018484	GYUW2K402FYQVG, contig20085
GO:0008272	sulfate transport	13	2	0.0050111	contig09306, contig25393

Supplementary material – Chapter VIII

GO:0046653	tetrahydrofolate metabolic process	14	2	0.0058147	contig01815, contig08098
GO:0002561	basophil degranulation	1	1	0.008289	contig14264
GO:0001878	response to yeast	1	1	0.008289	GYUW2K402F74UG
GO:0019064	viral entry into host cell via membrane fusion with the plasma membrane	1	1	0.008289	contig13680
GO:0033274	response to vitamin B2	1	1	0.008289	contig08098
GO:0006803	glutathione conjugation reaction	18	2	0.009567	contig00461, contig12382
GO:0009086	methionine biosynthetic process	20	2	0.0117529	contig01815, contig08098
GO:0006965	positive regulation of biosynthetic process of antibacterial peptides active against Gram-positive bacteria	2	1	0.0165097	GYUW2K402JKJ5T
GO:0001954	positive regulation of cell-matrix adhesion	2	1	0.0165097	contig21101
GO:0071679	commissural neuron axon guidance	2	1	0.0165097	contig17315
GO:0071529	cementum mineralization	2	1	0.0165097	contig03259
GO:0032494	response to peptidoglycan	2	1	0.0165097	GYUW2K402JKJ5T
GO:0030710	regulation of border follicle cell delamination	2	1	0.0165097	GYUW2K401CUIY1N
GO:0046956	positive phototaxis	2	1	0.0165097	GYUW2K401CUIY1N
GO:0016045	detection of bacterium	2	1	0.0165097	GYUW2K402JKJ5T
GO:0043200	response to amino acid stimulus	24	2	0.0167083	contig08098, contig23139
GO:0009396	folic acid-containing compound biosynthetic process	27	2	0.0209085	contig01815, contig03259
GO:0001831	trophectodermal cellular morphogenesis	3	1	0.0246628	contig20085
GO:0051974	negative regulation of telomerase activity	3	1	0.0246628	contig02986
GO:0002076	osteoblast development	3	1	0.0246628	contig02986
GO:0002051	osteoblast fate commitment	3	1	0.0246628	contig02986
GO:0035090	maintenance of apical/basal cell polarity	3	1	0.0246628	GYUW2K402HL65M
GO:0000209	protein polyubiquitination	31	2	0.027111	GYUW2K402GDRFE, GYUW2K402FYQVG
GO:0045175	basal protein localization	4	1	0.0327488	GYUW2K401CUIY1N
GO:0048843	negative regulation of axon extension involved in axon guidance	4	1	0.0327488	contig17315

Supplementary material – Chapter VIII

GO:0043619	regulation of transcription from RNA polymerase II promoter in response to oxidative stress	4	1	0.0327488	GYUW2K402FRN6L
GO:0031062	positive regulation of histone methylation	4	1	0.0327488	contig02986
GO:0008592	regulation of Toll signaling pathway	4	1	0.0327488	GYUW2K402JKJ5T
GO:0046618	drug export	4	1	0.0327488	contig23139
GO:0001738	morphogenesis of a polarized epithelium	36	2	0.0357615	GYUW2K401CUY1N, GYUW2K401BYUUJ
GO:0043650	dicarboxylic acid biosynthetic process	36	2	0.0357615	contig09978, contig03259
GO:0060136	embryonic process involved in female pregnancy	5	1	0.0407683	contig23139
GO:0051781	positive regulation of cell division	5	1	0.0407683	contig02986
GO:0016336	establishment or maintenance of polarity of larval imaginal disc epithelium	5	1	0.0407683	GYUW2K401CUY1N
GO:0010842	retina layer formation	5	1	0.0407683	contig13749
GO:0015695	organic cation transport	5	1	0.0407683	GYUW2K401B4IEE
GO:0042127	regulation of cell proliferation	310	6	0.0444784	contig01815, GYUW2K401D0REA, GYUW2K401CUY1N, contig20085, GYUW2K401CVAXG, contig02986
GO:0000079	regulation of cyclin-dependent protein serine/threonine kinase activity	41	2	0.0453222	GYUW2K402FYQVG, contig02986
GO:0060287	epithelial cilium movement involved in determination of left/right asymmetry	6	1	0.0487217	contig13749
GO:0006428	isoleucyl-tRNA aminoacylation	6	1	0.0487217	GYUW2K402JSOYD
GO:0045167	asymmetric protein localization involved in cell fate determination	6	1	0.0487217	GYUW2K401CUY1N
GO:0050919	negative chemotaxis	6	1	0.0487217	contig17315
GO:0032212	positive regulation of telomere maintenance via telomerase	6	1	0.0487217	contig01815
GO:0030511	positive regulation of transforming growth factor beta receptor signaling pathway	6	1	0.0487217	contig02986
GO:0046621	negative regulation of organ growth	6	1	0.0487217	contig02986
GO:0007567	parturition	6	1	0.0487217	contig15972

Chapter IX

**Effect of 10 different TiO₂ and ZrO₂ (nano)particles on
the soil invertebrate *Enchytraeus crypticus***

IX - Effect of 10 different TiO₂ and ZrO₂ (nano)particles on the soil invertebrate *Enchytraeus crypticus*

Department of Biology & CESAM, University of Aveiro, 3810-193 Aveiro, Portugal

Department of Chemistry & CICECO, University of Aveiro, 3810-193 Aveiro, Portugal

Department of Bioscience, Aarhus University, Vejlsovej 25, PO BOX 314, DK-8600
Silkeborg, Denmark

Abstract

Nearly 80% of all the nano-powders produced worldwide are metal oxides, and among these materials titanium dioxide (TiO₂) is one of the most produced. TiO₂ (and ZrO₂) toxicity is estimated low to soil organisms, but studies have shown that TiO₂-NPs cause oxidative stress. Additionally, it is known that TiO₂ undergoes photocatalysis under UV irradiation, which is often not taken into account in toxicity testing. In this study we investigated the effects of different TiO₂ and ZrO₂ materials on the soil oligochaete *Enchytraeus crypticus* using two ways of exposure (soil versus water) and studied the effects of UV irradiation on TiO₂ toxicity. Our results showed that ZrO₂ (bulk and nano) were not toxic, while ZrCl₄ reduced the reproduction. TiO₂ materials were also not toxic via soil exposure, neither under UV irradiation. However when UV light was included in the water tests, the UV-exposed organisms reproduce less when transferred to clean soil and the effect of TiO₂ was potentiated.

Keywords: UV light; titanium dioxide; zirconium dioxide; enchytraeids;

1. Introduction

Titanium dioxide nanoparticles (TiO₂-NPs) are among the most used nanoscaled materials, given their incorporation in many consumer products (e.g. sunscreens and toothpastes), industry (e.g. paints, paper) (Robichaud et al., 2009), and photocatalytic processes such as water treatment (e.g. Savage and Diallo, 2005). Zirconium dioxide (ZrO₂), another metal oxide, is less applied mostly used in ceramics (including medical devices (Manicone et al., 2007)), and catalysis (Yamaguchi, 1994), and ZrO₂-NPs can be additionally used in optical and electronic applications (Channu et al., 2011).

Recent estimates suggest that by 2015, 10% of the TiO₂ production in the world (i.e. 10% of 1,400,000 tons) is in the nano-form (Robichaud et al., 2009). Gottschalk and co-authors (2009) had predicted that by 2012, TiO₂-NPs concentration in sludge treated soil (in US) could reach 0.47 mg/kg, no similar figures are available for ZrO₂.

TiO₂-NPs can cause toxicity is well known from both in vitro and in vivo studies, although studies also report absence of effects at “high” concentrations.

In vitro studies using various types of cell lines (mostly mammalian) show that TiO₂-NPs cause genotoxicity and cytotoxicity associated with oxidative stress (e.g. (Guichard et al., 2012; Meena et al., 2012; Setyawati et al., 2013; Srivastava et al., 2013; Zhang et al., 2011)). For soil invertebrates, an in vitro study using *E. fetida* coelomocytes showed that TiO₂-NPs were taken up by the cells, but did not affect the anti-oxidative stress levels or cell viability (Bigorgne et al., 2012). The absence of cytotoxicity of TiO₂-NPs was also observed in two cell lines of human lymphocytes (Andersson-Willman et al., 2012) indicating differences in sensitivity between cell types.

In vivo data, using various types of TiO₂-NPs tested in soil dwelling organisms showed accumulation but little effect. Hu and co-authors (2010) reported that TiO₂-NPs accumulated in *E. fetida* tissues following 7 days of exposure. Further, studies on the

effects on earthworms using up to 1g/kg (Heckmann et al., 2011) and 10g/kg (McShane et al., 2012) caused no mortality but decreased reproduction (Heckman et al., 2001). Schlich and co-authors (2012) observed an increase in reproductive output following TiO₂-NPs exposure, but only in worms exposed during the winter. Hu et al (2010) observed that the NPs caused DNA damage in worms exposed to 1 and 5 mg/kg, and mitochondrial damage and peroxidation products accumulation at 5 mg/kg. Aslund et al. (2012) showed that *E. fetida* exposed to nano or bulk (micro sized) TiO₂ forms had similar metabolomic profile, consistent with oxidative stress.

For ZrO₂-NPs, little is known about soil organism toxicity, one study reported (Heckmann et al., 2011) that 1g/kg (in nano and bulk form) caused no effects on survival or reproduction for *E. fetida*. An *in vitro* study revealed that ZrO₂-NPs cause cytotoxicity - EC₅₀ ≈ 5µg/ml - to various cell lines (Soto et al., 2007).

Apart from direct interaction with tissue, both Ti and Zr oxides are photoactive (Carp et al., 2004; Sayama and Arakawa, 1993) and can in this way cause oxidative effects. TiO₂ is activated at around 3.20 eV for anatase and 3.02 eV for rutile (corresponding to 384 and 410 nm wavelengths, respectively) and ZrO₂ is activated at 5.2 eV (corresponding to 239 nm). The effect of TiO₂ photocatalytic activity has been largely explored for environmental remediation (Chen et al., 2003; Chien et al., 2011; Savage and Diallo, 2005; Zhang et al., 2010; Zhang et al., 2008). Despite the knowledge on the photoactivation mechanism (Carp et al., 2004)) which leads to the formation of Reactive Oxygen Species (ROS), studies focusing on the effects of UV on TiO₂ toxicity to the living organisms have only recently been addressed in aquatic organisms (Bar-Ilan et al., 2012; Ma et al., 2012; Miller et al., 2012; Yeo and Kang, 2010). These studies showed that UV irradiation potentiates TiO₂-NPs toxicity, e.g. *Danio rerio* (Bar-

Ilan et al., 2012), *Oryzias latipes* and *Daphnia magna* (Ma et al., 2012), marine phytoplankton (Ma et al., 2012) and *Hydra magnipapillata* (Yeo and Kang, 2010).

In the present study we aimed to assess the effects of TiO₂ and ZrO₂ in soil organisms. The choice of the materials was related to their environmental relevance and comparison between two similar systems (Zr and Ti); *cf.* for example the Organization for Economic Cooperation and Development (OECD) Working Party on Nanomaterials. The effects were assessed using 3 exposure media (soil, soil:water extracts, and water). The UV-light exposure was mimicking “realistic” daily doses of UV irradiation. The soil invertebrate model species *Enchytraeus crypticus* was used, assessing its survival and reproduction. The list of 10 different materials studied included various nano, bulk and salt-forms. The following hypotheses were tested: (H1) the different tested materials can cause different toxicity; (H2) the decreased complexity of the exposure matrix (from soil to water) can help to elucidate toxicity; (H3) UV-light exposure (and photoactivation of TiO₂) leads to an increase of the toxicity.

2. Materials and methods

2.1. Test materials

Ten different materials were used: six TiO₂ and four Zr-based materials (see Table 1). The TiO₂ and ZrO₂ nanoparticles were either purchased or synthesized. The in-house synthesized and surface modified nanoparticles will be defined from here on as (IHS-powder, IHS-dispersion, ZrO₂-NPs-powder, ZrO₂-NPs-dispersion), for TiO₂ and Zr-based materials, respectively. For a details on the methods and surface modification please see the Supplementary Information.

2.2. Test species

The test organism *Enchytraeus crypticus* (Westheide and Graefe, 1992) was used. Individuals were cultured in Petri dishes containing agar medium, consisting of a sterilized mixture of four different salt solutions (CaCl₂·2H₂O; MgSO₄; KCl; NaHCO₃) and a Bacti-Agar medium (Oxoid, Agar No. 1). The cultures were kept under controlled conditions, at 19°C and photoperiod 16:8 hours light:dark, and were feed on ground and autoclaved oats.

2.3. Test media

2.3.1. ISO water

The reconstituted ISO water was used (OECD, 2004) containing: 2 mM of CaCl₂·2H₂O, 0.5 mM of MgSO₄·7H₂O, 0.77 mM of NaHCO₃ and 0.077 mM of KCl in ultra pure water.

2.3.2. OECD soil

OECD artificial soil was used according to the guideline (OECD, 1984): constituted by 75% of sea sand (VWR, technical washed with sulphuric acid), 20% of Kaolin clay (Sigma Aldrich), 5% of sphagnum peat (sieved to ≤ 2 mm) and CaCO₃ (Merk) for pH adjustment to 6 (±0.5). All the soil constituents were mixed thoroughly and let to stabilize prior the use for the tests.

2.3.3. OECD soil:water extracts

OECD soil:water extracts was obtained by mixing OECD soil and ultra pure water in a proportion of 1:2 (w/v) under orbital agitation during 1 hour. After that the soil was left to settle and the resulting suspension was filtered through a 0.5 µm glass fibre filter. The soil:water extract was stored at 4°C until use (two days maximum).

2.3.4. Spiking procedures and test concentrations

For the soil exposure, the nominal tested concentrations were 100-1000 mg/kg of all TiO₂ materials (Bulk, Degussa, NM103, NM104 and IHS-powder) and Zr materials (Bulk-ZrO₂, ZrO₂NPs-powder and ZrCl₄), plus an additional 10 mg/kg for ZrCl₄. The spiking of the soil followed the OECD guideline for testing of insoluble substances (OECD, 2004). In short, 2 g of sand per replicate were mixed with the corresponding amount of the test materials (as dry powders) to obtain the final concentration range. The spiked sand was added to the remaining pre-moistened soil (18 g of soil with 10% v/w distilled water) and homogeneously mixed. After that 12% (v/w) of distilled water was added to each replicate, to reach 50% of the Water Holding Capacity (WHC) of the soil. The spiking of the soil was done individually to ensure total raw amounts per replicate. Four replicates per treatment plus controls were prepared.

For the water tests the concentrations were 0, 1, 10 and 100 mg/L for all the TiO₂ and Zr-based materials. The suspensions were prepared using ultra pure water, which was sonicated for 30 minutes as mixed with the materials. The suspensions of TiO₂ (IHS-dispersion) and ZrO₂ (ZrO₂-NPs-dispersion) were tested as prepared (ca. 3.2 mg/L for TiO₂ and ca. 6 mg/L for ZrO₂) and 2 and 10 times diluted.

The exposure via OECD soil:water extract tests was performed for the TiO₂ materials, at the lowest concentration tested for ISO water tests (1 mg/L for Bulk, Degussa, NM103, NM104 and IHS-powder; and 0.3 mg/L for IHS-dispersion).

For all the water treatments ten replicates per treatment plus controls were prepared.

2.3.5. UV exposure procedure

For TiO₂ materials, the exposure was performed with simultaneous UV radiation.

For soil exposure, UV irradiation was performed during 30 min on a daily basis, which corresponds to the UV dose equivalent of a full day of sun light in equatorial regions, a

worst case scenario like. Ultraviolet radiation was provided by an UV lamp (Spectroline XX15F/B, Spectronics Corporation, NY, USA, peak emission at 312 nm) and a cellulose acetate sheet was coupled to the lamp to cut-off UVC range wavelengths. The daily intensity of UVA and UVB (280-400 nm) was $3676 \pm 75 \text{ mW/m}^2$, corresponding to an average daily dose of 6617 J/m^2 . Two sets of controls were performed for TiO₂ test: with and without extra UV-light exposure.

For water exposure, UV irradiation was performed during 15 min on a daily basis. The daily intensity of UVA and UVB (280-400 nm) radiations was $1735 \pm 46 \text{ mW/m}^2$, corresponding to an average daily dose of 1562 J/m^2 .

The photoactivation of ZrO₂ requires wavelengths in the range of UVC radiation (239 nm). This wavelength is absorbed by earth's atmosphere (e.g. de Gruijl 1999) and the testing would be outside of realistic scenarios, hence not pursued here.

2.4. Toxicity tests

2.4.1. Exposure via soil

Toxicity tests followed the Enchytraeid Reproduction Test (ERT) guideline (OECD, 2004). In short, ten adult organisms with well-developed *clitellum* and similar size were selected and introduced in each test vessel, containing 20 g of moist soil and 25 mg of food (finely ground and autoclaved rolled oats). The vessels were covered with a lid containing small holes and the test ran during 3 weeks, at $20 \pm 1 \text{ }^\circ\text{C}$ and 16:8 hours photoperiod. Weekly, 12.5 mg of food was supplied and soil moisture was adjusted by replenishing weight loss. At the test end adult enchytraeids were searched in the soil under a stereo microscope and counted. Juvenile enchytraeids were immobilized with ethanol and coloured with Bengal red (1% solution in ethanol). Each replicate was sieved to eliminate the kaolin clay and then juveniles were counted under a stereo microscope.

2.4.2. *Exposure via ISO water*

The test conditions were as described by Rombke and Knacker (1989) for *Enchytraeus albidus*, based on Daphnia Acute Immobilization Test (OECD, 2004). For each test condition, including controls, five adult organisms with *clitellum* and similar size were selected per replicate. The exposure is performed in 24 well plates, where each well correspond to a replicate and contain 0.5 ml of ISO test water, 0.5 ml of spiked solution and five organisms. The test duration was five days, at 20±1 °C and 16:8 hour photoperiod. Survival was evaluated and organisms were considered dead when not responding to any mechanical stimulus. Survival was assessed every 24 hours.

Ten replicates for each test condition were performed and the remaining wells of the plates were filled with controls (resulting in a total of 24 control replicates).

2.4.3. *Exposure via OECD soil:water extracts*

The test procedure is the same as described for the ISO water tests, including daily UV illumination.

2.4.4. *Post-exposure in clean soil*

The organisms were transferred from water and soil:water exposure (ISO water and OECD soil extract) to control (non-spiked) OECD soil. The procedure followed the ERT guideline (i.e. 3 weeks post-exposure). The surviving organisms for each test condition were pooled in groups of 10 and introduced on test vessels with soil. Four replicates per pre-exposure condition were performed (eight for the controls).

2.5. *Data analysis*

The concentration effects on reproduction (effect concentration that causes 50% reduction on reproduction, EC₅₀) were determined using the model threshold sigmoid two parameters (TRAP 1.21). Significant differences between the control and each

treatment were investigated based on One Way Analysis of Variance (ANOVA) with Dunnett's method for multiple comparisons (SigmaPlot 11.0). To compare the control groups (control versus control UV in the post-exposure tests) a Student's t test was performed (SigmaPlot 11.0).

3. Results

3.1. Test materials characterization

Table 1: List of characteristics of the materials tested.

	ZrO ₂			TiO ₂					
	Bulk	ZrO ₂ -NPs-powder	ZrO ₂ -NPs-dispersion	Bulk	Degussa	NM103	NM104	IHS-powder	IHS-dispersion
Supplier	Sigma Aldrich	IHS	IHS	Sigma-Aldrich	Evonik	Sachtleben	Sachtleben	IHS	IHS
Size (nm) – Scherrer	55.8	3.3		-	15-60	20	20	8.7	
TEM (nm)	> 200			400	20	20	20		9
Surface area (m²/g) – BET	8.4	36		ND	61	60	60	110	
Shape	spherical	spherical	spherical	spherical	spherical	spherical	spherical	square	square
Coating	none	none	acetic acid	none	none	hydrophobic*	hydrophilic [#]	none	acetic acid
Crystal form	monoclinic	61% cubic, 39% monoclinic	61% cubic, 39% monoclinic		86% anatase, 14% rutile	rutile	rutile	anatase	anatase
Method		benzyl alcohol route	benzyl alcohol route		gas phase hydrolysis	precipitation	precipitation	benzyl alcohol route	benzyl alcohol route

*treated by alumina dimethicone

[#] treated by alumina and glycerin

3.2. Biological characterisation

3.2.1. Exposure via soil

The tests fulfilled the validity criteria as within the standard guideline (OECD, 2004), with controls' mortality lower than 20% and number of juveniles higher than 25 with respective coefficient of variation below 50%. The pH before the test was 6.6 ± 0.1 and

6.6 ± 0.05 for TiO₂ and Zr tests respectively, and after the test was 6.2 ± 0.1 and 6.6 ± 0.1 for TiO₂ and Zr tests, respectively (average ± standard deviation).

There were no effects on adult survival for any of the tested materials. For effects on reproduction, the results on the number of juveniles produced can be observed in Table 2.

Table 2: Results in terms of number of juveniles produced for *Enchytraeus crypticus* after exposure via soil spiked to 0-100-1000 mg/kg under daily UV irradiation (+UV) of TiO₂ materials and 0-10-100-1000 mg/kg of Zr materials. For TiO₂ materials, a control was performed under standard laboratory illumination (0). Results are expressed as average ± standard error (AV±SE), not tested: n.t., * p<0.05, Dunnett’s test.

TiO ₂ materials	concentration (mg/kg)			
	0	0 + UV	100 + UV	1000+ UV
Bulk			434.0 ±26	471.8 ±38
Degussa			346.5 ±64	455.8 ±32
NPs	383.2±59	447.0 ±30	405.0 ±40	323.8 ±46
			405.5 ±51	401.8 ±12
			386.8 ±41	324.5 ±46
IHS-powder				
Zr materials	0	10	100	1000
ZrO ₂ -NPs-powder		n.t.	229.5 ±16	241.3 ±15
Bulk ZrO ₂	272.0 ±11	n.t.	242.0 ±11	255.3 ±11
ZrCl ₄		242.3 ±17	248.8 ±7	11.3 ±2*

Results showed that the UV-irradiation had no toxic effects on *E. crypticus* (no significant differences between controls with and without UV) and had no effects on TiO₂ materials toxicity.

Concerning Zr-based materials, only ZrCl₄ caused toxicity at 1000 mg/kg (estimated EC₅₀=502 mg/Kg).

3.2.2. Exposure via ISO water

The exposure in ISO water, in controls had a survival >90%. The pH at the beginning of the tests was 6.4 ± 0.3 for TiO₂ and 5.7 ± 1 for Zr suspensions (average ± standard deviation), respectively. There were no effects on survival except for ZrCl₄ (pH=2.7) and TiO₂ HIS-dispersion (pH=5.5). Figure 1 shows the results for survival along the 5 days of exposure to TiO₂ materials (with and without UV) and Zr materials.

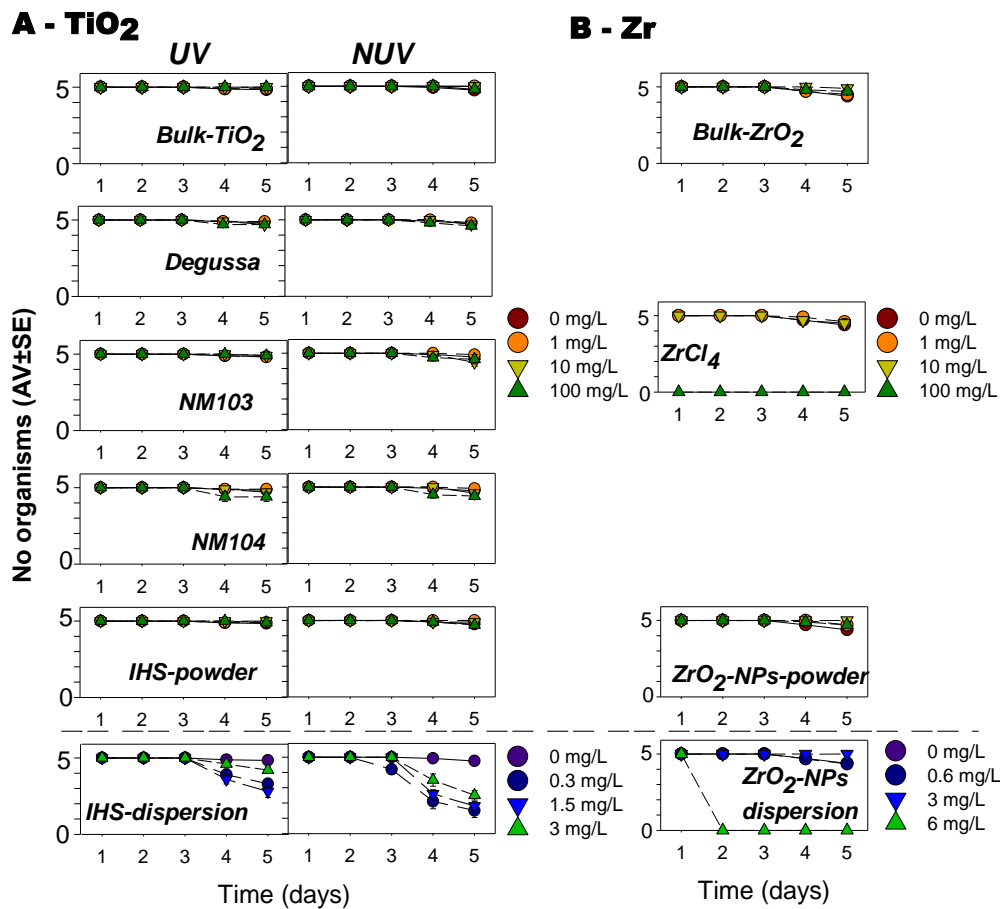


Figure 1: (A) Effects of Bulk-TiO₂ and TiO₂-nanoparticles (Degussa, NM103, NM104, IHS-powder and IHS-dispersion) on *Enchytraeus crypticus* survival, when exposed via water along 5 days of exposure (daily monitor), with (UV) and without UV radiation (NUV). (B) Effects of Bulk-ZrO₂, ZrCl₄, ZrO₂-NPs-powder and ZrO₂NPs-dispersion on *Enchytraeus crypticus*, when exposed via water for 5 days. Data are expressed as average of living organisms ± standard error (AV±SE) (n=24 for control and n=10 for treatments).

Within the set of TiO₂ materials tested, the IHS-dispersion was affecting survival, causing significant reduction already at day 4, for all the NUV and in the two lowest concentrations UV (Fig.1 A). It has been noted that aggregation was visible in the IHS-dispersion NPs (surface modified nanoparticles) (pH=5.5). This apparently inhibited *E. crypticus* movements.

Figure 1B shows the number of surviving organisms following exposure to the respective Zr-materials as a function of the exposure time. For the Zr-materials tested, there was no effect on survival except for 100mg ZrCl₄/L (pH=2.7) and 6mg/L ZrO₂NPs-dispersion (pH=5.3).

Ti and Zr IHS-dispersed represent the nanoparticles coated with acetic acid (and sodium acetate was used to increase the pH of the suspension), which may have caused the effect. Hence, the organisms were exposed to acetate alone (i.e. no particles), this caused mortality in the same range. Despite the similarities, we are not entirely sure that the acetate concentration used in this exposure is the same for the particles, since the ration between released and NPs-bound acetate is unknown.

3.2.3. exposure via OECD soil:water extract

All organisms survived in controls. No significant effects on survival were observed for any of the treatments.

3.2.4. Post-exposure in clean soil

Following the initial water-exposure, the organisms were transferred to clean soil and kept 3 weeks in a post-exposure. There were no effects on survival, but the reproduction was affected by UV radiation alone (control conditions) and in presence of NPs. For the control conditions, the strongest inhibition was observed for the organisms pre-exposed in the water with dissolved organics matter (OECD water extract), compared to the pure ISO water (Table 3).

Table 3: Results in terms of number of juveniles produced for *Enchytraeus crypticus* transferred to clean soil after exposure via water (ISO water and OECD soil:water extract) under standard laboratory illumination (NUV) and under UV irradiation (UV). Results are expressed as average \pm standard error (AV \pm SE), ** t-test (p<0.001).

<i>ISO water</i>		
	NUV	UV
CT	408.9 ± 14	163.5** ± 10
<i>OECD soil:water extract</i>		
	NUV	UV
CT	379.6 ± 17	38.6** ± 3

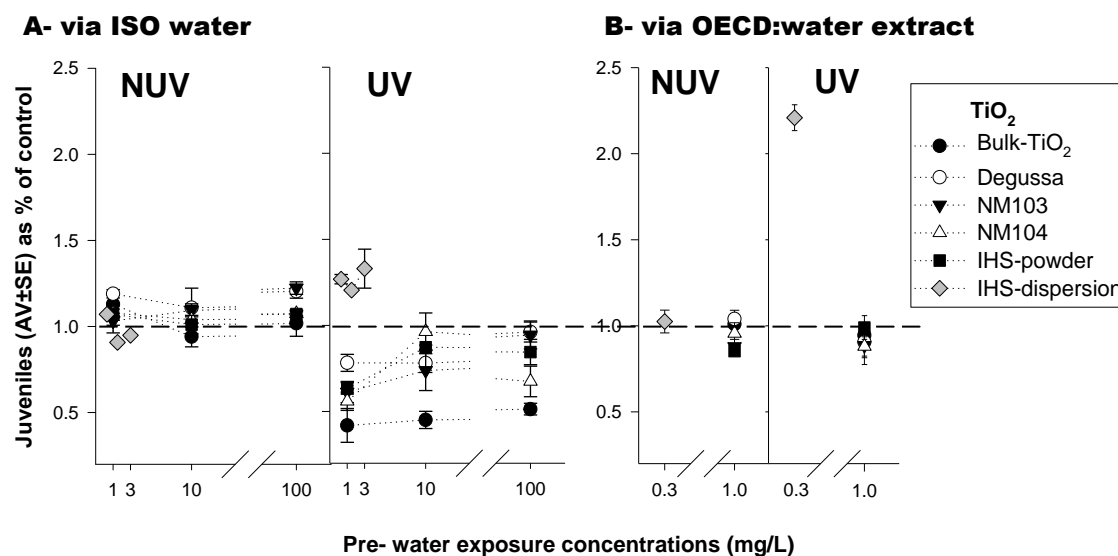


Figure 2: Results of the effect of TiO₂ on reproduction of *Enchytraeus crypticus* in terms of number of juveniles produced, when organisms were pre-exposed (A) via ISO water and (B) via OECD:water extract to Bulk-TiO₂ and five TiO₂-NPs (Degussa, NM103, NM104, IHS-powder and IHS-dispersion – with and without UV radiation – UV and NUV) and following transfer to clean OECD soil. Results are expressed as % of control (Table 3). The dashed line on 1 sets the differences to control.

Concerning the exposure to UV+TiO₂ (Fig. 2A UV), results showed that UV radiation increased the TiO₂ toxicity for all the materials, except for the IHS-dispersion where a decrease was observed. For the increased toxicity in the rest of the materials, no clear dose-response was observed: UV+Bulk-TiO₂ caused an overall reduction in reproduction independently of the concentration, whereas for TiO₂-NPs Degussa, NM103, NM104 and IHS-powder the reduction was more pronounced for the lowest concentration (1mg/L).

When the pre-exposure to the different TiO₂ materials was done in OECD soil:water extract (to the lowest concentration tested in ISO water - highest observed effect), after

transfer to clean soil there were no effects on adults' survival, except again a positive effect for the IHS dispersion (fig. 2 B).

The tests performed in OECD extract confirmed that without UV radiation (Fig 2B NUV), TiO₂ materials caused no toxicity. For Zr-based materials, results showed no effect from post exposure in clean soil (after ISO water exposure to Zr-based materials) on survival and reproduction output (Table 5).

Table 4: Results in terms of number of juveniles produced for *Enchytraeus crypticus* transferred to clean soil after exposure via ISO water to Zr-based materials. Results are expressed as average \pm standard error (AV \pm SE), X: not transferred to clean soil

Zr materials	pre-water exposure concentrations (mg/L)			
	0	1	10	100
Bulk-ZrO ₂		263.0 \pm 40	243.8 \pm 16	246.8 \pm 13
ZrCl ₄		313.8 \pm 23	309.8 \pm 8	X
ZrO ₂ -NPs-powder	279.0 \pm 24	263.0 \pm 23	304.0 \pm 24	262.8 \pm 8
		0.6	3	6
ZrO ₂ -NPs-dipersion		281.0 \pm 16	269.0 \pm 36	X

3.2.5. Toxicity modelling across all particles

It can be assumed that toxicity, as due to oxidative stress, is related to particle characteristics e.g. surface area or particle diameter, coating. Due to the observed limited effects, it was not possible to relate particle characters with expressed toxicity.

4. Discussion

Hypothesis 1: the different test materials cause different toxicity;

The tested materials, both Ti and Zr systems caused virtually no toxicity in soil up to 1000mg/kg, except for ZrCl₄ (reproduction EC₅₀=500mg/kg). It seemed neither to be a pH (stable in all the tests performed) nor a Chloride effect (to low concentrations). To our knowledge, this is the first time that a Zr-salt (ZrCl₄) is tested in soil invertebrates, and showed that the effects of ZrCl₄ are in the same range as other metal salts (e.g. EC₅₀(NiCl₂)=275mg/kg for *E. albidus* (Lock and Janssen, 2002) and EC₅₀(CuCl₂)=251 mg/Kg in a natural soil (Amorim and Scott-Fordsmand, 2012).

For ZrO₂ (bulk and nano) similar results were obtained with *Eisenia fetida* exposed to 1000mg/kg, showing no effects on survival and reproduction. However exposure to TiO₂ decreased the reproduction in 50% (Heckmann et al., 2011).

Hypothesis 2: The decreased complexity of the exposure matrix (from soil to water) can help to elucidate toxicity;

Differences between tested media indicated that the water bioavailable fraction is a main exposure route for toxicity, as visible from the highest toxicity via water exposure compared to the soil:water extracts results. Clearly the introduction of soil particles (OM, clay, etc) in the media reduced the toxic effects.

In the exposure via the ISO water the exposure to the materials was assumed maximised. For 100 mg ZrCl₄/L all organisms died within 3 hours exposure. In this particular case the mortality must be related with the low pH (≈3) of ZrCl₄ in solution. ZrCl₄ is a strong Lewis acid and in solution it tends to react forming HCl and Zr-oxy complexes. We are aware of the introduction of this confounding factor, but the pH

manipulation would further increase factors and interpretation. Despite the fact that the effect of Zr was masked by the pH in water, testing in soil (pH buffered by soil and kept at 6.6) also showed the toxicity of Zr-based materials.

In terms of ZrO₂-NPs, exposure in water showed toxicity for ZrO₂-NPs-HIS-dispersion causing 100% mortality after 24 hours. The observed effects are probably related with the concentration of acetate ions in the solution as sodium acetate was used to adjust the pH of the dispersion. All surviving organisms performed well when transferred to clean OECD soil and given time to reproduce (3 weeks), indicating that even if there was Zr uptake via water, the materials did not cause enough damage to be reflected later on.

The results from water exposure showed no effect on survival for *E. crypticus* for the Ti materials. Lapied and co-authors (2011) also exposed *Lumbricus terrestris* earthworms in water to similar concentrations of TiO₂-NPs (aluminium and polydimethyl siloxane coated) and found no mortality during 7 days. These results are in agreement with ours (except for TiO₂ IHS-dispersion for the reasons as explained above).

Hypothesis 3: UV light exposure (and photoactivation of Ti) increases toxicity

The applied UV dose of $\approx 6600\text{J/m}^2/\text{day}$ in the present study is environmentally relevant since doses of 10 kJ/m^2 can occur, e.g. in Argentina (Luccini et al., 2006) and even higher doses can be found in some regions of Africa and Australia (Ciren and Li, 2003). Nevertheless, they can also be considered worst-case scenario for European standards. Our results showed that UV exposure to the soil and soil:water extracts caused no effect. TiO₂ photocatalysis (under UV irradiation) has been applied to remove pollutants from soils (Chien et al., 2011; Quan et al., 2005; Zhang et al., 2008); however the effects of UV irradiated TiO₂ materials had not been studied before in soil organisms. The principle of photocatalytic degradation of contaminants is based on the potential of

TiO₂ to promote oxidation/reduction reactions (including ROS generation) when UV irradiated, thus the occurrence of photodegradation of contaminants in soils (Chien et al., 2011; Quan et al., 2005; Zhang et al., 2008).

However the concentrations of TiO₂ used for soil remediation were higher than those tested in the present study (our highest concentration was equivalent to 0.1% wt). Another possible explanation for the lack of negative effects on *E. crypticus* (based on survival and reproduction) is the obvious limited penetration of light into soil (maximum of 0.5 mm (Quan et al., 2005)). This could mean that the ROS generation occurred in the top layer of the soil and the burrowing behaviour of enchytraeids (test vessel ≈ 2 cm depth) would prevent them from exposure to ROS (or reduced it to a very limited extent).

On the contrary, the UV exposure alone in water media affected the organisms. The UV exposure alone causes a reduction of ca. 50% in reproduction. Disinfection (via ROS production) of water using sun light has been used since early Egyptian times and described by scientists since late 1870s (Byrne et al., 2011). The possible accumulation of ROS in our test organism did not cause mortality in the short term exposure, but was enough to cause the reduction in reproduction (long term post exposure effect). To our knowledge, this is the first time that TiO₂ materials are tested together with UV on terrestrial invertebrates. Studies on aquatic organisms showed that UV enhances TiO₂ toxicity (Ma et al., 2012; Miller et al., 2012) in short-term assays (24 to 96 hours). The fact that no increase in mortality was observed for the UV treated groups can be due to differences in UV intensities/doses applied, which were lower in our study.

The increase in toxicity of TiO₂+ UV had not been reported before for soil animals. The effects observed were not dose-related, but more pronounced in the lower concentration

(1mg/L). A possible explanation could be related to the higher aggregation of particles for higher concentrations, which would decrease exposure area of Ti compared to the lower concentration.

IHS-dispersion (TiO₂-NPs coated with acetic acid) were not more toxic than UV alone (or were less toxic in the case of OECD extract exposure) (Fig.2 UV). The use of coated TiO₂-NPs is common in sunscreens to prevent adverse effects mediated by photocatalytic redox reaction at the NPs' surface; however the coating does not guaranty the total absence of photocatalytic activity (Smijs and Pavel, 2011). Mano and co-authors (2012) found that PEG coated TiO₂-NPs (Degussa) were less toxic to human cell lines and induce less stress-related genes than the non-modified TiO₂-NPs. The role of TiO₂ coating to prevent photo-induced damage to skin cells was studied by Carlotti and co-authors (Carlotti et al., 2009) and they found that not all the coating agents effectively protect TiO₂-NPs from interaction with UV. Our results suggest that acetic acid coating persist attached to NPs and prevents the interaction of UV light with TiO₂ surface and its photocatalytic activity. On the other hand, the coating of NM103 and NM104 (alumina based) might be degraded during the tests and/or was not effective in avoiding the interaction of UV with TiO₂ surface; these results are in agreement with Carlotti and co-authors findings (2009) which show that alumina coating seems to degrade during the 24h incubation for peroxidation assay (less than our 5 days exposure period). Also in agreement with our results is that both anatase and rutile based TiO₂ can cause ROS from photocatalysis (Carlotti et al., 2009).

In presence of media containing dissolved organic matter (OECD soil:water extracts), instead of just water, the effects of UV radiation alone were more severe to *E. crypticus* (Table 3). This may be because ROS are formed by dissolved organic carbon exposed to

sunlight (Cooper et al., 1988). Curiously, the presence of TiO₂ did not increase the negative effect caused by UV alone effect. One possible explanation is related with the fact that UV irradiated TiO₂ caused the degradation of organic matter (Huang et al., 2008) and we can hypothesize that there is an equilibrium between the amount of ROS produced by the dissolved organic matter and from those produced by TiO₂ which are in part used to degrade the organic matter (hence, less TiO₂-generated ROS became available to cause damage to the organisms).

5. Conclusions

Overall, TiO₂ combined with UV light poses higher risk, in particular via water media exposure or to organisms that live/dwell on the soil surface (with direct exposure to sun light).

The ZrCl₄ was more toxic than ZrO₂-NPs or bulk-ZrO₂. The TiO₂ materials (bulk or nano) were not toxic to *E. crypticus* via soil exposure. The water exposure tests showed that UV radiation caused toxicity and increased TiO₂ toxicity.

The possibility of performing exposure using different media was an important aspect to advance the interpretation of results and is recommended by the authors.

References

- Amorim, M., Scott-Fordsmand, J., 2012. Toxicity of Copper nanoparticles and CuCl₂ salt to *Enchytraeus albidus* worms: survival, reproduction and avoidance responses. *Environmental Pollution* 164, 164-168.
- Andersson-Willman, B., Gehrman, U., Cansu, Z., Buerki-Thurnherr, T., Krug, H.F., Gabrielsson, S., Scheynius, A., 2012. Effects of subtoxic concentrations of TiO₂ and ZnO

- nanoparticles on human lymphocytes, dendritic cells and exosome production. *Toxicol Appl Pharmacol* 264, 94-103.
- Aslund, M.L.W., McShane, H., Simpson, M.J., Simpson, A.J., Whalen, J.K., Hendershot, W.H., Sunahara, G.I., 2012. Earthworm Sublethal Responses to Titanium Dioxide Nanomaterial in Soil Detected by H-1 NMR Metabolomics. *Environmental Science & Technology* 46, 1111-1118.
- Bar-Ilan, O., Louis, K.M., Yang, S.P., Pedersen, J.A., Hamers, R.J., Peterson, R.E., Heideman, W., 2012. Titanium dioxide nanoparticles produce phototoxicity in the developing zebrafish. *Nanotoxicology* 6, 670-679.
- Bigorgne, E., Foucaud, L., Caillet, C., Giamberini, L., Nahmani, J., Thomas, F., Rodius, F., 2012. Cellular and molecular responses of *E. fetida* coelomocytes exposed to TiO₂ nanoparticles. *Journal of Nanoparticle Research* 14.
- Byrne, J.A., Fernandez-Ibanez, P.A., Dunlop, P.S.M., Alrousan, D.M.A., Hamilton, J.W.J., 2011. Photocatalytic Enhancement for Solar Disinfection of Water: A Review. *Int J Photoenergy*.
- Carlotti, M.E., Ugazio, E., Sapino, S., Fenoglio, I., Greco, G., Fubini, B., 2009. Role of particle coating in controlling skin damage photoinduced by titania nanoparticles. *Free Radical Res* 43, 312-322.
- Carp, O., Huisman, C.L., Reller, A., 2004. Photoinduced reactivity of titanium dioxide. *Prog Solid State Ch* 32, 33-177.
- Channu, V.S.R., Kalluru, R.R., Schlesinger, M., Mehring, M., Holze, R., 2011. Synthesis and characterization of ZrO₂ nanoparticles for optical and electrochemical applications. *Colloid Surface A* 386, 151-157.
- Chen, J., Liu, M., Zhang, L., Zhang, J., Jin, L., 2003. Application of nano TiO₂ towards polluted water treatment combined with electro-photochemical method. *Water Res* 37, 3815-3820.

- Chien, S.W.C., Chang, C.H., Chen, S.H., Wang, M.C., Rao, M.M., Veni, S.S., 2011. Effect of sunlight irradiation on photocatalytic pyrene degradation in contaminated soils by micro-nano size TiO₂. *Science of the Total Environment* 409, 4101-4108.
- Ciren, P.B., Li, Z.Q., 2003. Long-term global earth surface ultraviolet radiation exposure derived from ISCCP and TOMS satellite measurements. *Agr Forest Meteorol* 120, 51-68.
- Cooper, W.J., Zika, R.G., Petasne, R.G., Plane, J.M.C., 1988. Photochemical formation of hydrogen peroxide in natural waters exposed to sunlight. *Environmental Science & Technology* 22, 1156-1160.
- de Gruijl, F.R., 1999. Skin cancer and solar UV radiation. *European Journal of Cancer* 35, 2003-2009.
- Gottschalk, F., Sonderer, T., Scholz, R.W., Nowack, B., 2009. Modeled Environmental Concentrations of Engineered Nanomaterials (TiO₂, ZnO, Ag, CNT, Fullerenes) for Different Regions. *Environmental Science & Technology* 43, 9216-9222.
- Guichard, Y., Schmit, J., Darne, C., Gate, L., Goutet, M., Rousset, D., Rastoix, O., Wrobel, R., Witschger, O., Martin, A., Fierro, V., Binet, S., 2012. Cytotoxicity and genotoxicity of nanosized and microsized titanium dioxide and iron oxide particles in Syrian hamster embryo cells. *Ann Occup Hyg* 56, 631-644.
- Heckmann, L.-H., Hovgaard, M.B., Sutherland, D.S., Autrup, H., Besenbacher, F., Scott-Fordsmand, J.J., 2011. Limit-test toxicity screening of selected inorganic nanoparticles to the earthworm *Eisenia fetida*. *Ecotoxicology* 20(1), 226-233.
- Hu, C.W., Li, M., Cui, Y.B., Li, D.S., Chen, J., Yang, L.Y., 2010. Toxicological effects of TiO₂ and ZnO nanoparticles in soil on earthworm *Eisenia fetida*. *Soil Biology & Biochemistry* 42, 586-591.
- Huang, X., Leal, M., Li, Q., 2008. Degradation of natural organic matter by TiO₂ photocatalytic oxidation and its effect on fouling of low-pressure membranes. *Water Res* 42, 1142-1150.
- Lapied, E., Nahmani, J.Y., Moudilou, E., Chaurand, P., Labille, J., Rose, J., Exbrayat, J.M., Oughton, D.H., Joner, E.J., 2011. Ecotoxicological effects of an aged TiO₂

- nanocomposite measured as apoptosis in the anecic earthworm *Lumbricus terrestris* after exposure through water, food and soil. *Environment International* 37, 1105-1110.
- Lock, K., Janssen, C.R., 2002. Ecotoxicity of nickel to *Eisenia fetida*, *Enchytraeus albidus* and *Folsomia candida*. *Chemosphere* 46, 197-200.
- Luccini, E., Cede, A., Piacentini, R., Villanueva, C., Canziani, P., 2006. Ultraviolet climatology over Argentina. *J Geophys Res-Atmos* 111.
- Ma, H.B., Brennan, A., Diamond, S.A., 2012. Phototoxicity of TiO₂ nanoparticles under solar radiation to two aquatic species: *Daphnia magna* and Japanese medaka. *Environmental Toxicology and Chemistry* 31, 1621-1629.
- Manicone, P.F., Iommetti, P.R., Raffaelli, L., 2007. An overview of zirconia ceramics: Basic properties and clinical applications. *J Dent* 35, 819-826.
- Mano, S.S., Kanehira, K., Sonezaki, S., Taniguchi, A., 2012. Effect of Polyethylene Glycol Modification of TiO₂ Nanoparticles on Cytotoxicity and Gene Expressions in Human Cell Lines. *Int J Mol Sci* 13, 3703-3717.
- McShane, H., Sarrazin, M., Whalen, J.K., Hendershot, W.H., Sunahara, G.I., 2012. Reproductive and behavioral responses of earthworms exposed to nano-sized titanium dioxide in soil. *Environmental toxicology and chemistry / SETAC* 31, 184-193.
- Meena, R., Rani, M., Pal, R., Rajamani, P., 2012. Nano-TiO₂-Induced Apoptosis by Oxidative Stress-Mediated DNA Damage and Activation of p53 in Human Embryonic Kidney Cells. *Appl Biochem Biotech* 167, 791-808.
- Miller, R.J., Bennett, S., Keller, A.A., Pease, S., Lenihan, H.S., 2012. TiO₂ nanoparticles are phototoxic to marine phytoplankton. *Plos One* 7, e30321.
- OECD, 1984. Guideline for Testing Chemicals. Earthworm, acute toxicity tests, No.207, OECD (Organization for Economic Cooperation and Development). Paris, France.
- OECD, 2004. Guidelines for the Testing of chemicals No 202. *Daphnia* sp. Acute Immobilization Test. Organization for Economic Cooperation and Development. Paris.

- OECD, 2004. Guidelines for the testing of chemicals No. 220. Enchytraeid Reproduction Test. Organization for Economic Cooperation and Development. Paris.
- Quan, X., Zhao, X., Chen, S., Zhao, H.M., Chen, J.W., Zhao, Y.Z., 2005. Enhancement of p,p'-DDT photodegradation on soil surfaces using TiO₂ induced by UV-light. *Chemosphere* 60, 266-273.
- Robichaud, C.O., Uyar, A.E., Darby, M.R., Zucker, L.G., Wiesner, M.R., 2009. Estimates of Upper Bounds and Trends in Nano-TiO₂ Production As a Basis for Exposure Assessment. *Environmental Science & Technology* 43, 4227-4233.
- Rombke, J., Knacker, T., 1989. Aquatic toxicity test for enchytraeids. *Hydrobiologia* 180, 235-242.
- Savage, N., Diallo, M.S., 2005. Nanomaterials and water purification: Opportunities and challenges. *Journal of Nanoparticle Research* 7, 331-342.
- Sayama, K., Arakawa, H., 1993. Photocatalytic Decomposition of Water and Photocatalytic Reduction of Carbon-Dioxide over ZrO₂ Catalyst. *J Phys Chem-US* 97, 531-533.
- Schlich, K., Terytze, K., Hund-Rinke, K., 2012. Effect of TiO₂ nanoparticles in the earthworm reproduction test. *Environ Sci Eur* 24, 1-10.
- Setyawati, M.I., Khoo, P.K.S., Eng, B.H., Xiong, S.J., Zhao, X.X., Das, G.K., Tan, T.T.Y., Loo, J.S.C., Leong, D.T., Ng, K.W., 2013. Cytotoxic and genotoxic characterization of titanium dioxide, gadolinium oxide, and poly(lactic-co-glycolic acid) nanoparticles in human fibroblasts. *J Biomed Mater Res A* 101A, 633-640.
- Smijs, T.G., Pavel, S., 2011. Titanium dioxide and zinc oxide nanoparticles in sunscreens: focus on their safety and effectiveness. *Nanotechnology, Science and Applications*, 95-112.
- Soto, K., Garza, K.M., Murr, L.E., 2007. Cytotoxic effects of aggregated nanomaterials. *Acta Biomaterialia* 3, 351-358.
- Srivastava, R.K., Rahman, Q., Kashyap, M.P., Singh, A.K., Jain, G., Jahan, S., Lohani, M., Lantow, M., Pant, A.B., 2013. Nano-titanium dioxide induces genotoxicity and apoptosis in human lung cancer cell line, A549. *Hum Exp Toxicol* 32, 153-166.

- Yamaguchi, T., 1994. Application of ZrO₂ as a Catalyst and a Catalyst Support. *Catal Today* 20, 199-218.
- Yeo, M.K., Kang, M., 2010. The effect of nano-scale Zn-doped TiO₂ and pure TiO₂ particles on *Hydra magnipapillata*. *Molecular & Cellular Toxicology* 6, 9-17.
- Zhang, D.Q., Li, G.S., Yu, J.C., 2010. Inorganic materials for photocatalytic water disinfection. *J Mater Chem* 20, 4529-4536.
- Zhang, L.H., Li, P.J., Gong, Z.Q., Li, X.M., 2008. Photocatalytic degradation of polycyclic aromatic hydrocarbons on soil surfaces using TiO₂ under UV light. *J Hazard Mater* 158, 478-484.
- Zhang, Y.L., Yu, W.Q., Jiang, X.Q., Lv, K.G., Sun, S.J., Zhang, F.Q., 2011. Analysis of the cytotoxicity of differentially sized titanium dioxide nanoparticles in murine MC3T3-E1 preosteoblasts. *J Mater Sci-Mater M* 22, 1933-1945.

Supplementary material

Experimental section

Synthesis and ligand exchange procedure

All the reagents were purchased from Sigma Aldrich and were used without further purification.

All the preparations were conducted in a glove box (H_2O and O_2 below 1 ppm). Titanium dioxide (TiO_2) and Zirconium dioxide (ZrO_2) nanoparticles have been synthesized according to the following procedure. 500 mg of Titanium (IV) isopropoxide (99.9%) and 500 mg of Zirconium (IV) isopropoxide isopropanol complex (99.9%) were added to 20 ml of benzyl alcohol (99%), respectively. The solutions were stirred and transferred to a 45 ml Teflon cup and inserted into a stainless steel autoclave and heated at 250 and 230 °C for 48 h, respectively. After the syntheses, the particles were purified by repeating three purification/centrifugation cycles with ethanol. As obtained TiO_2 and ZrO_2 nanoparticles are denoted IHS-powder and ZrO_2 -NPs-powder, respectively.

In order to ensure colloidal dispersion in water, the particles were modified with glacial acetic acid using a ligand exchange procedure. Briefly, 100 mg of preformed TiO_2 or ZrO_2 nanocrystals were dispersed in 5 ml of chloroform. Then, 200 mg of glacial acetic acid were added to the dispersion. The obtained mixtures were stirred overnight at room temperature. The particles were precipitated twice with ethanol to remove the excess of acetic acid and the supernatant was discarded. To promote dispersion in water, 1-2 mg of sodium acetate was added and a clear water suspension was obtained. The final pH of the solution was *ca.* 5. TiO_2 and ZrO_2 water dispersions are denoted HIS-dispersion and ZrO_2 -NPs-dispersion, respectively.

Characterization

Structural characterization of the nanoparticles was carried out by X-ray powder diffraction (XRD) using a Cu-K α radiation operating at 45 kV and 40 mA on an X'Pert MPD Philips diffractometer. The patterns were acquired in the 2θ range from 3 to 70° using a step size of 0.2°.

The size and shape of the particles prior and after surface modification were evaluated by transmission electron microscopy (TEM). A Hitachi-9000 TEM operating at 300 kV was used. For TEM studies one or two drops of the nanoparticle dispersions in ethanol and water solution were deposited on copper TEM grids covered with amorphous carbon.

Fourier transform infrared (FTIR) spectra were acquired between 4000-600 cm^{-1} , with a 4 cm^{-1} resolution in Attenuated Total Reflectance (ATR) mode, using a Nicolet iS5 equipment.

Discussion

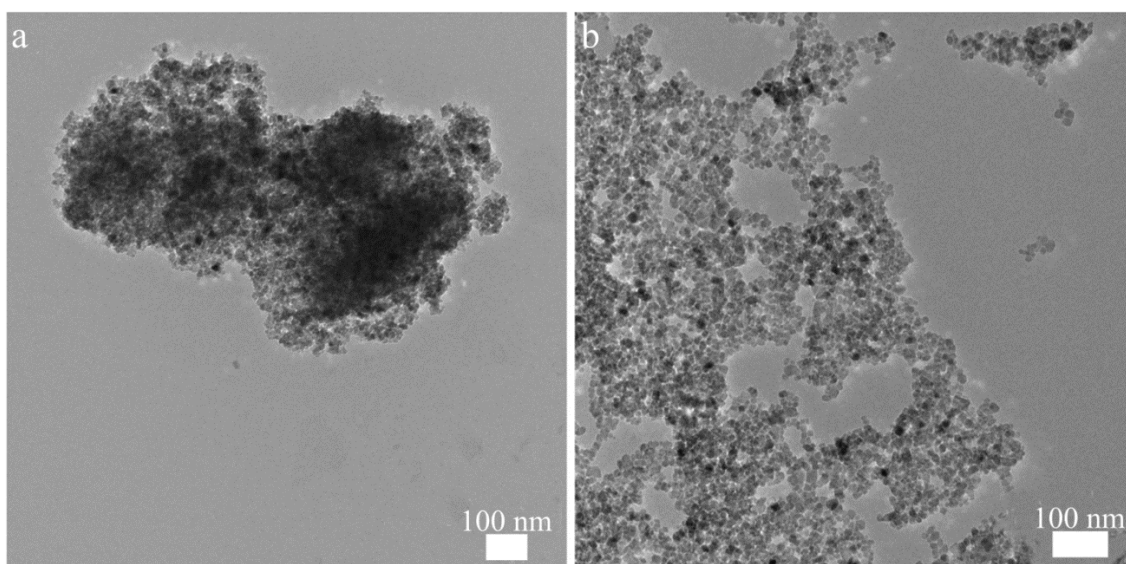


Figure S1: TEM micrographs of (a) bare and (b) surface modified TiO_2 nanoparticles.

In figure S1, two representative TEM images of TiO_2 nanocrystals before and after surface modification are shown. The nanoparticles possess a pseudo-spherical morphology. The average crystallite size, determined from the XRD patterns (see below) using the Scherrer equation, is 8.7 nm and is in good agreement with the size determined from TEM measurements. The as-synthesized nanoparticles are rather aggregated (Fig. S1a). On the other hand, after surface modification the TiO_2 nanoparticles are better dispersed on the carbon coated TEM grid (Fig. S2a).

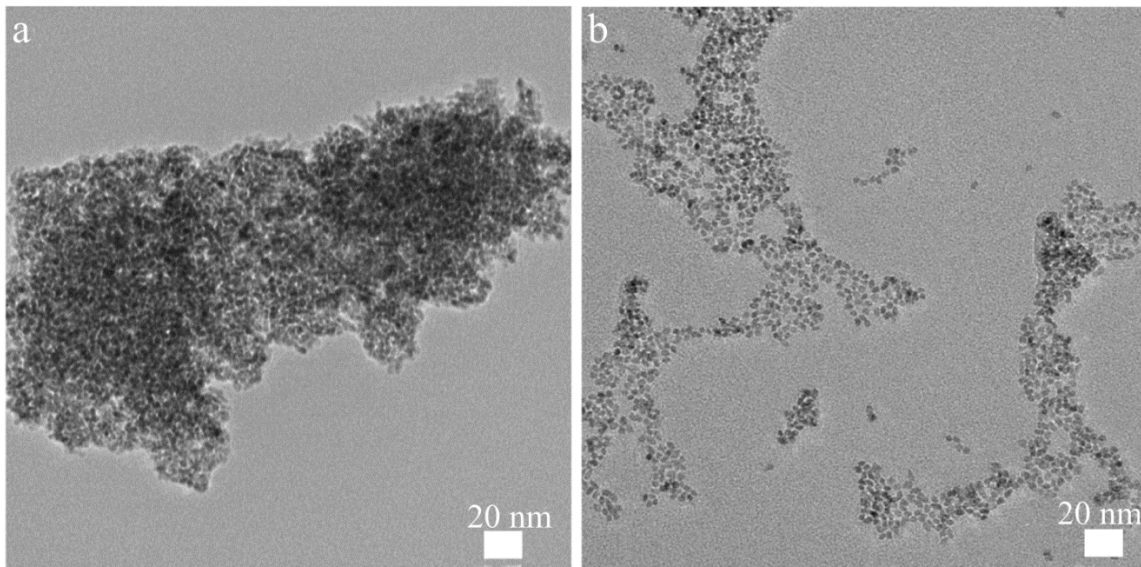


Figure S2: TEM images of (a) bare and (b) surface modified ZrO₂ nanoparticles.

In figure S2, TEM images related to ZrO₂ nanocrystals are shown. After the ligand exchange procedure (Fig. S2b), the particles show a lower degree of aggregation compared to the pristine ZrO₂ nanocrystals (Fig. S2a). The particles possess a pseudo-spherical shape. Their crystallite size, evaluated from the XRD patterns (see below) by the Scherrer equation, is 3.3 nm and is comparable to the size determined by TEM measurements.

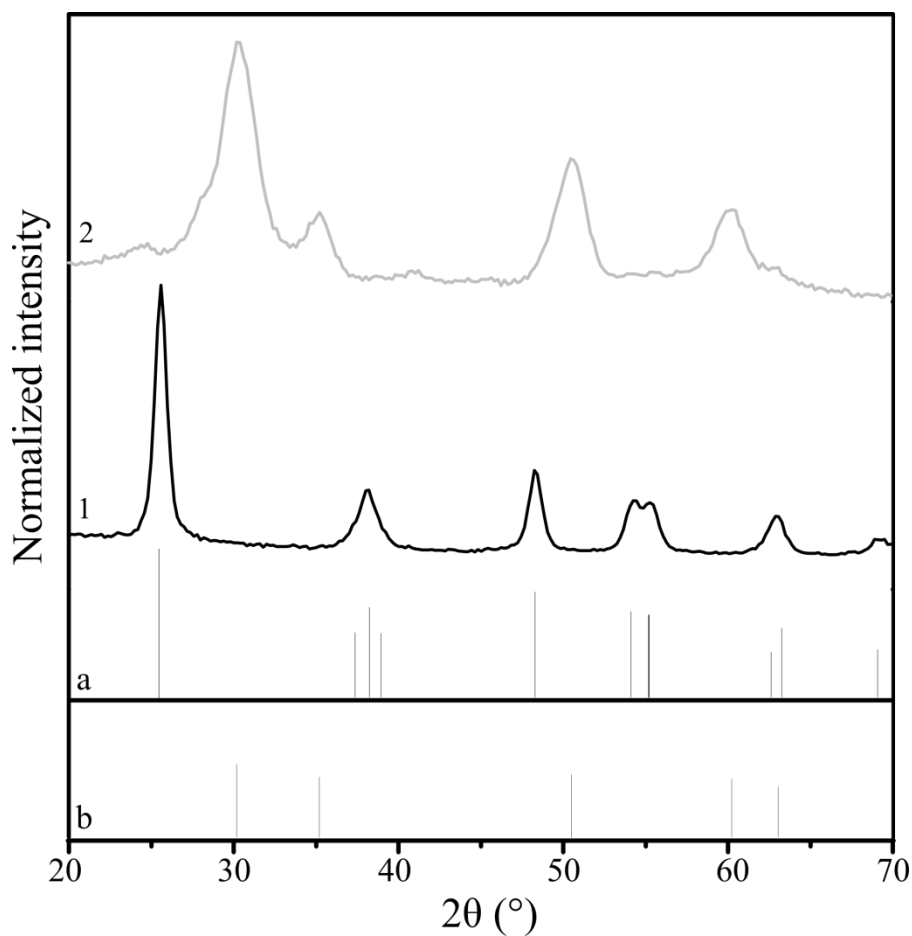


Figure S3: XRD patterns of (1) TiO_2 and (2) ZrO_2 nanoparticles and corresponding (a-b) JPCDS cards, respectively.

The powder x-ray diffractograms related to the nanoparticles used in this work are shown in figure S3. TiO_2 nanoparticles (1, a) crystallize in anatase polymorph (JPCDS card 004-0477). As-synthesized ZrO_2 nanocrystals (2, b) are present in the tetragonal modification (JPCDS card 049-1642) with a small percentage of monoclinic phase. In agreement with a structural study recently reported.^[3]

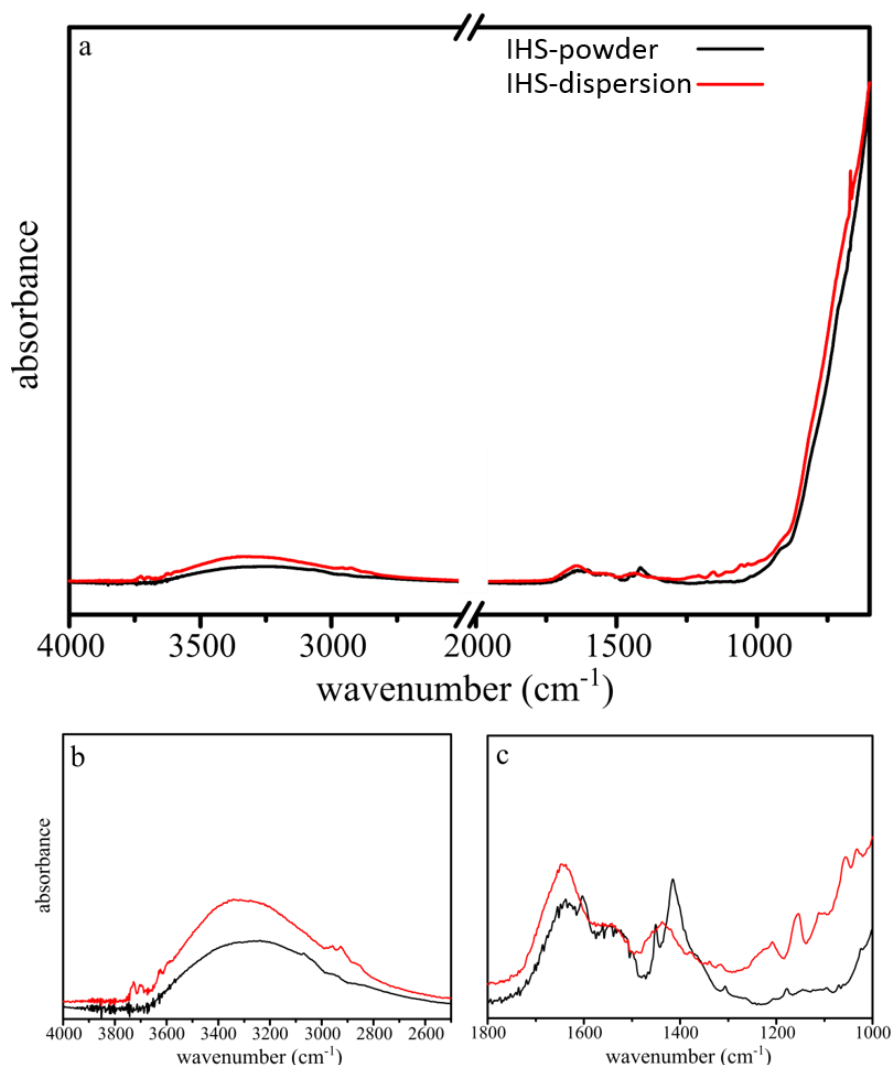


Figure S4: (a) Overall and (b-c) detailed FT-IR spectra of as-synthesized (black trace) and modified (red trace) TiO₂ nanocrystals, respectively.

The FTIR spectra of TiO₂ nanoparticles before and after surface modification are shown in figure S4. In the spectral region between 3600 and 3000 cm⁻¹, the stretching band ascribable to -OH groups bound to the nanocrystal surface is visible (Fig. S4b). This is further confirmed by the -OH bending signal situated at 1630 cm⁻¹ for the pristine and modified particles, respectively.

Moreover, a small peak due to the stretching of the -CH band of phenyl rings is detectable at 3080 cm⁻¹ (Fig. S4b, black line). This feature disappears after the ligand exchange procedure. In fact, the typical signals due the stretching vibrations of the methyl group of the acetic acid are present between 2900-3000 cm⁻¹ (Fig. S4b, red line). Interestingly, the region between 1800 and 1000 cm⁻¹ is strongly affected after the surface modification step (Fig. S4c). The presence of benzoate species can be evidenced

in the initial spectrum of the pristine nanoparticles (Fig. S4a, black trace). In fact, the asymmetric (1540 cm^{-1}) and symmetric (1420 cm^{-1}) stretching bands can be detected, in addition to the frequencies related to the C-C of the phenyl rings. The difference between the two bands is *ca.* 120 cm^{-1} . Benzoate species attached to the surface of the nanoparticles are often detected upon reaction of metal alkoxides in benzyl alcohol.^[1-3] Upon surface modification, the carboxylate symmetric band is shifted (Fig. S4, red trace) and the contribution of the phenyl rings disappear. The difference is *ca.* 110 cm^{-1} , pointing out the presence of a bidentate coordination of the surface acetate species.^[4] Below 1000 cm^{-1} , very intense absorption tails due to the stretching of Ti-O bonds are present.

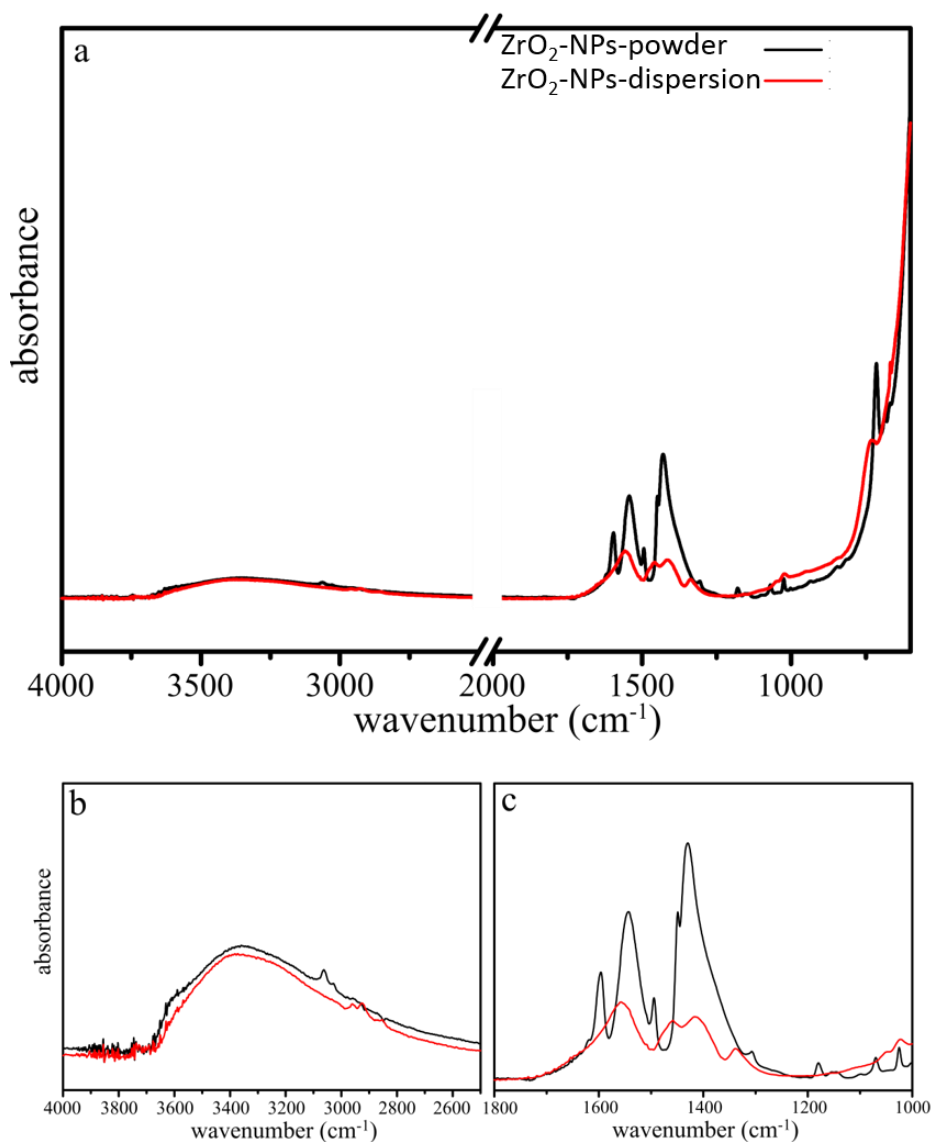


Figure S5: (a) Overall and (b-c) detailed FT-IR spectra of as-synthesized (black trace) and modified (red trace) ZrO₂ nanocrystals, respectively.

In figure S5, the FTIR spectra of ZrO₂ nanoparticles before and after the surface modification procedure are shown.

Similarly to TiO₂ spectra (*cf.* Fig. S4), the signals in the region between 4000 and 2500 cm⁻¹ are modified (Fig. S5b). It can be noted the presence of the typical –CH₃ stretching bands and the absence of the –CH vibrations of the phenyl rings after the treatment with acetic acid. This is confirmed by the lack of features between 1200 and 1000 cm⁻¹ ascribable to the bending vibrations of the –CH bonds and to the stretching vibrations of the C-C bonds in the phenyl ring at 1600 cm⁻¹ (Fig. S5c). This proves that the benzoate species at the surface of the pristine nanoparticles are removed after ligand exchange process.^[1-3] The carboxylate vibrations of the acetate species have a different signature compared to the ones of the benzoates. Indeed, the asymmetric and symmetric vibrations for the as-synthesized ZrO₂ nanoparticles are found at 1545 cm⁻¹ and 1430 cm⁻¹, respectively. After the treatment with acetic acid they are centered at 1560 cm⁻¹ and 1410 cm⁻¹ (Fig. S5c, red trace). The calculated difference between these two bands is *ca.* 150 cm⁻¹, revealing the possible presence of a bridging coordination.^[4] The sharp absorption features below 1000 cm⁻¹ can be attributed to the stretching of the Zr-O bonds.

References

1. X. Bai, A. Pucci, V. T. Freitas, R. A. S. Ferreira, N. Pinna, *Adv. Funct. Mater.* **2012**, 22, 4275-4283.
2. A. Pucci, M.-G. Willinger, F. Liu, X. Zeng, V. Rebutini, G. Clavel, X. Bai, G. Ungar, N. Pinna, *ACS Nano*, **2012**, 6, 4382.
3. L. Saviot, D. B. Murray, G. Caputo, M. C. Marco De Lucas, N. Pinna, *J. Mater. Chem. C*, **2013**, 1, 8108-8116.
4. G. B. Deacon, R. J. Philips, *Coord. Chem. Rev.* **1980**, 33, 227-250.

Chapter X

General discussion

X – General discussion

In the present PhD thesis I focussed on identifying the responses and mechanisms of response which precede the phenotypical effects; this was investigated for four different NMs. Below is a summary of the responses indentified following the exposure to these NMs.

Copper nanoparticles (Cu-NPs) toxicity at survival and reproduction level, was similar to Cu historical field contamination (aged 80 years) and lower than for copper salt, which seems to relate with the corresponding similar and higher bioavailable fraction of Cu^+ [Chapter IV]. X-ray absorption near-edge spectroscopy (XANES) analysis showed partial oxidation of the Cu-NPs in soil (around 40%), indicating that the toxicity exhibited by Cu-NPs can only partly be related with Cu^{2+} release. In terms of gene responses, in the first gene expression (microarray) study [Chapter III] similar nominal concentrations of Cu-salt and Cu-NPs were compared. Transcription and translation processes were negatively affected by both copper forms, but the most prominent effect was noticed at the level of energy metabolism, at which the same genes were differently affected by the two copper forms (nano and salt). The results indicate mitochondrial disruption, which can cause and/or be a result of ROS (reactive oxygen species) formation, a known mechanism involved in copper toxicity. The analysis of oxidative stress related biomarkers [Chapter II] confirmed that exposure to Cu-NPs and Cu-salt induce significant effects on antioxidant defence machinery and those effects were Cu-form and time dependent. Induction of GPx activity along with a GSH depletion and GSSG increase is a common response to both copper forms, however, the activation of SOD and CAT by Cu-NPs prevented the oxidative damage (increase in LPO levels) observed for Cu-salt exposure.

Following this the effects of NMs shape was analysed: the spherical Cu-NPs (discussed above) were compared with wired shape Cu-NMs (Cu-Nwires). For these similar EC values were obtained in terms of survival and reproduction [Chapter V]. Now a more advanced tool was available, the high-throughput gene expression 4x44K microarray (for *Enchytraeus crypticus*) was used to assess the gene expression profile in response to the various copper forms (the two NMs and two salt forms) [Chapter V]. The transcriptomic profile showed that the Cu form used was more important for discrimination of exposure than the concentration i.e. 20 and 50% effect concentrations on reproduction); this indicated a Cu-form specific effects. Some of the mechanisms revealed in the first microarray study (Chapter III) were concurrently identified using the upgraded microarray (for instance, regulation of transcription and mitochondrial related genes). Few transcripts were commonly affected by all the copper-forms, however those commonly affected by Cu-salt treatments (CuNO₃ and Cu-salt historical contamination) reveal that Cu²⁺ affects calcium ion regulation and activates the chemosensory system of the enchytraeids. The identification of functions commonly affected by Cu-salt historical contamination and the two NMs tested is consistent with partial oxidation of the NMs with Cu²⁺ release. However NPs specific effects were also identified, namely negative effects on histone modification and DNA repair processes. Despite the high number of transcripts commonly affected by both NMs, it was also possible to identify processes uniquely affected by Cu-NPs (apoptosis regulation) and Cu-Nwires (locomotion behaviour).

The studies performed at gene level [Chapters III and V] revealed a consistent response between the two enchytraeid species (and two gene libraries) to similar materials, confirming the success of the molecular techniques in identifying materials' signatures.

There are indications of the contribution of Cu^{2+} to the Cu-NPs toxicity, however NPs specific effects were clearly identified.

In Figure 1, the integration of results between the various endpoints obtained for copper exposure was attempted within the AOPs (Adverse Outcome Pathways) concept.

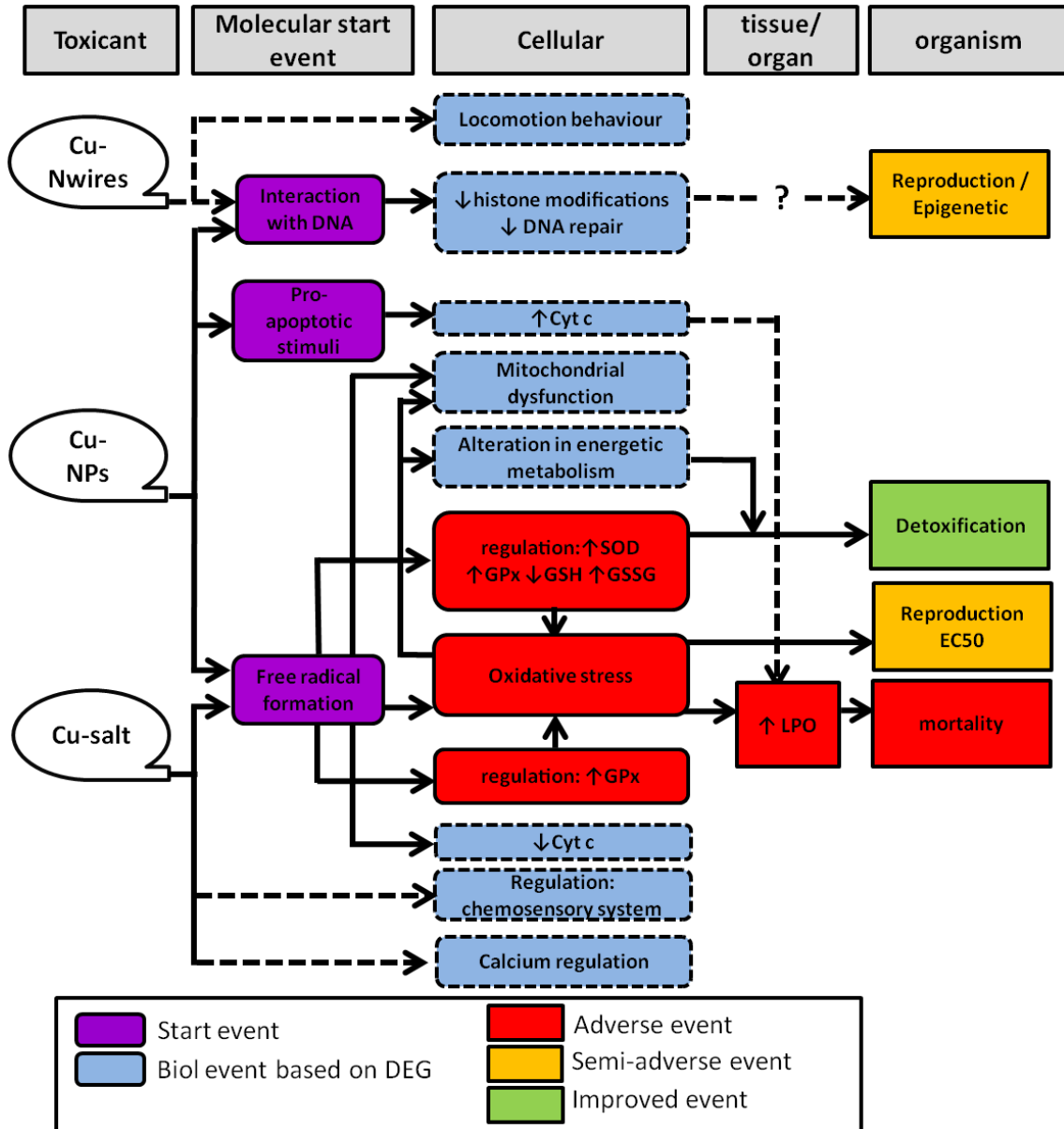


Figure 1: Adverse Outcome Pathways (AOP) to copper exposure for a soil invertebrate. Conceptualisation is based on results using *Enchytraeus crypticus* and *Enchytraeus albidus* as model species for data from transcription (gene expression), oxidative stress markers, survival,

reproduction and avoidance. Multiple adverse outcomes are integrated in this conceptualization where the various end-states are influenced by the relative tolerance and/or effectiveness of Cu-detoxification strategies of the organisms. Square boxes represent final states for the organism, whereas rounded boxes represent intermediate states. Solid lines indicate relationships previously observed, whereas dashed lines represent relationships hypothesized in this study. Cu-NPs: copper nanoparticles; Cu-Nwires: copper nanowires; CuNO₃: copper nitrate.

Silver nanoparticles (Ag-NPs) were less toxic than silver salt in terms of survival and reproduction [Chapter VI] and biochemical and molecular techniques were applied to investigate the mechanisms of response underlying the observed toxicity.

At first, the effects of similar nominal concentrations of Ag-NPs and Ag-salt were investigated using microarray technology [Chapter VI]. The results indicate the responses to Ag-NPs reflect an effect of Ag⁺, but we also found biological processes specifically affected by Ag-NPs such as developmental processes and regulation of locomotion. Even though genes involved in the antioxidant defence machinery were not significantly extracted within the microarray analysis, ROS formation and oxidative damage are often associated with silver toxicity, thus the effects of silver exposure on oxidative stress biomarkers were investigated [Chapter VII]. Increased lipid peroxidation was observed for both Ag forms exposure, indicating oxidative damage to the cells. Glutathione is the first mechanisms activated by Ag-NPs exposure, followed by CAT, GPx and GR; however the oxidative damage was not prevented at higher exposure periods. In the case of Ag-salt, the increase of LPO levels might be related with the impairment of the antioxidant defence enzymes (GPx and GST) at early exposure periods. The time dependent response observed corroborated the higher toxicity of Ag-salt even at shorter exposure time, nevertheless Ag-NPs activate

antioxidant defence mechanisms, which were not enough to prevent oxidative damage latter on.

A new transcriptomic study was performed to investigate gene expression profile in response to silver [Chapter VIII], at this stage comparing similar effect concentrations on reproduction (EC_{20} and EC_{50}). Three different NPs (PVP coated, non-coated and dispersed) and $AgNO_3$ were compared, and results showed (similarly to what was observed for Cu treatments) that materials signature was more important for the differentiation than these tested concentrations. The most similar materials (PVP coated and non-coated NPs) were grouped closely together which provide a good indication on the power of discrimination that can be achieved using high throughput molecular techniques. Dispersed Ag-NPs triggered the most dissimilar expression profile, being the only one affecting for instance glutathione-s-transferase (by up-regulation). Oxidation with consequent Ag^+ release of PVP and non-coated Ag-NPs (even if to a short extent) might be responsible for the closer transcriptomic profile between these two NPs and $AgNO_3$.

In Figure 2, the integration of results between the various endpoints obtained for silver exposure was attempted within the AOPs concept.

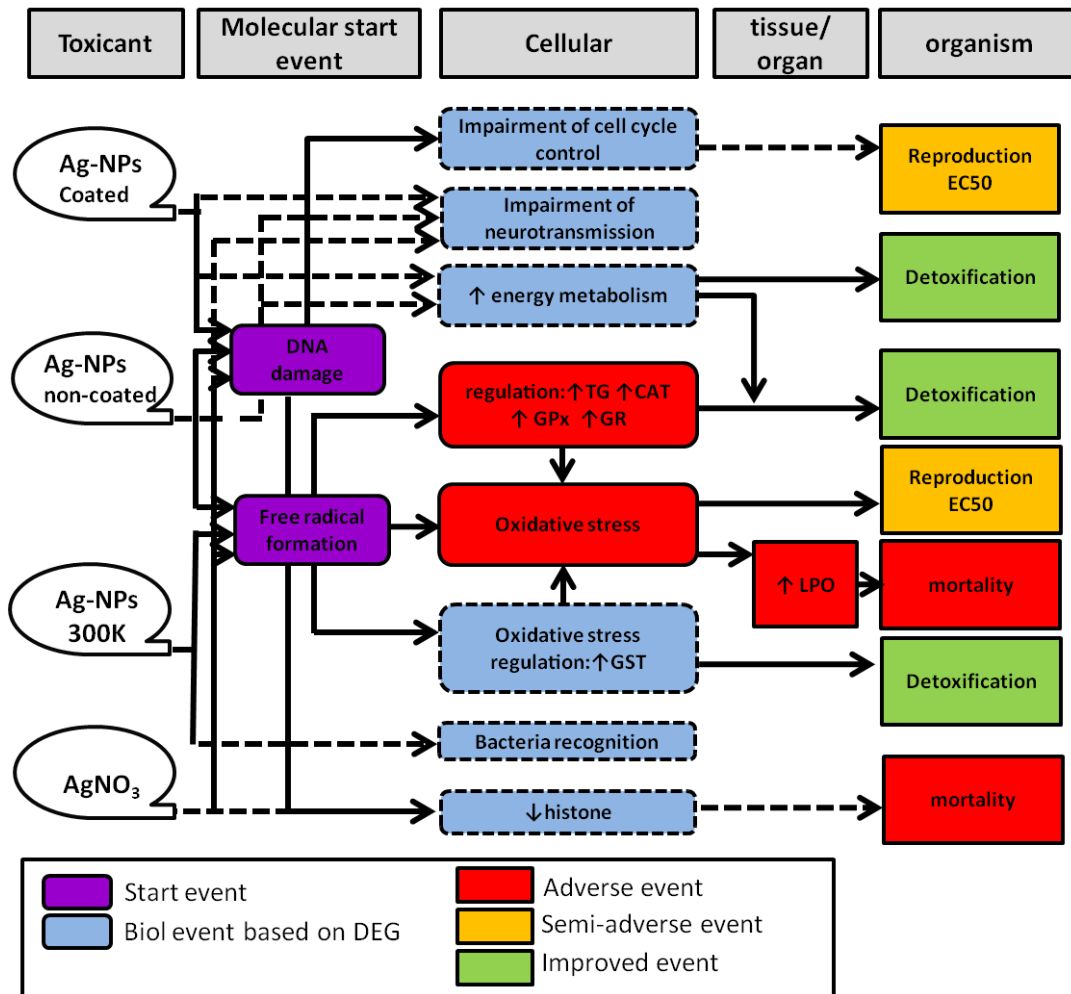


Figure 2: Adverse Outcome Pathways to silver exposure for a soil invertebrate. Conceptualisation is based on results using *Enchytraeus crypticus*, *Enchytraeus albidus* and *Eisenia fetida* as model species for data from transcription (gene expression) oxidative stress markers, survival, reproduction and avoidance. Multiple adverse outcomes are integrated in this conceptualization where the various end-states are influenced by the relative tolerance and/or effectiveness of Ag-detoxification strategies of the organisms. Square boxes represent final states for the organism, whereas rounded boxes represent intermediate states. Solid lines indicate relationships previously observed, whereas dashed lines represent relationships hypothesized in this study. (PVP coated silver nanoparticles: Ag-NPs Coated; non coated silver nanoparticles: Ag-NPs non-coated; dispersed silver nanoparticles: Ag-NPs 300K; AgNO₃: silver nitrate.

Titanium and Zirconium dioxide nanoparticles (TiO₂ and ZrO₂-NPs) effects were investigated at organism level (survival and reproduction) [Chapter IX] and the results showed that both were non toxic. TiO₂ undergoes photocatalysis under UV irradiation, but realistic UV daily doses showed not to increase TiO₂ toxicity to enchytraeids exposed in soil. However, if the exposure was done via the water, UV radiation was toxic and increased TiO₂ toxicity. The possibility of performing studies with enchytraeids, using different exposure media was a very important advantage which was positively explored for NMs effect discrimination.

Conclusion

In summary, the present thesis highlights the successful application of cellular and molecular techniques to detect effects at short periods of exposure which could be anchored to long term effects (e.g. reproduction). Further, because the same effect concentrations were used for the transcriptomic (sub-lethal concentrations of NMs) the discrimination obtained between materials is an actual “material signature” and not a concentration variation related signature.

Study recommendations

There are obviously many factors that were not possible to assess (in one PhD thesis) and that could be suggested to address. Nevertheless, if a study prioritisation would be required from the present experience, the following priority list is suggested for guidance:

1. To test further highly characterised materials that cover a wide range in properties with overlapping sets (specially designed nanomaterials libraries).

2. Long term testing using the multi-endpoint approach at a series of time points. The aims are:

1.1 - to investigate the potential link between short and long term effects;

1.2 - to investigate the potential longer-term effects of NMs.

3. To invest on genome sequencing of ecotoxicity relevant species.